Bond Activation by Unconventional Lewis Pairs

by

Jacob Geri

A dissertation submitted in partial fulfillment
of the requirements for the degree of
Doctor of Philosophy
(Chemistry)
in the University of Michigan
2018

Doctoral Committee:

Associate Professor Nathaniel Szymczak, Chair
Professor Richard Laine
Professor Melanie Sanford
Professor John Wolfe

Jacob B. Geri

jbgeri@umich.edu

ORCID iD: 0000-0002-9215-5610

Dedication

This thesis is dedicated to my family: inherited, given, and chosen.
But most importantly, my mother.

Acknowledgements

Nathaniel Szymczak has been an ideal PhD supervisor. He provides a high degree of freedom to his students, which forces them to take responsibility for the success or failure of fundamental project hypotheses from their first days in the lab. With Nate as a guide, I learned essential scientific skills: how to formulate testable hypotheses, how to recognize and escape from intractable approaches to chemical problems, and how to design robust experiments which provide definitive yes/no answers. In other words, Nate taught me a language in which one can ask Nature questions and get answers back. He also made me a better scientific communicator, and I tried to follow his example when mentoring undergraduate and graduate students later in my graduate career. He put an extraordinary amount of effort into my training; I estimate that he has spent between five and seven hundred hours teaching me how to be a good scientist. He always supported my work, always believed in my projects and dreams, never gave me an order, and never told me "no". His integrity, intelligence, sensitivity, and idealism will inspire me for the rest of my life.

I appreciate the helpful advice and suggestions of PhD committee members Richard Laine, John Wolf, and Melanie Sanford. I am especially thankful to Melanie Sanford, who gave me very insightful professional advice and excellent training while I worked in her lab during a first-year lab rotation. I also need to thank Vincent Pecoraro, who gave me my first lab experiences in graduate school while I was an entirely inexperienced synthetic chemist, and Nicolai Lehnert, who was very patient with my questions in his Advanced Inorganic Spectroscopy course. Corinna Schindler also provided essential experimental assistance. Much of my PhD work would not have been possible without the tireless work of Jeff Kampf, who provided crystal data for numerous difficult and unstable molecules. I would also like to thank Paul Lennon, James Windak, Eugenio Alvarado, and Chris Kojiro, who provided instrumental support and training, and Gunther Kellner for his help with equipment.

The members of the Szymczak Lab have been wonderful comrades and friends. I am grateful for their patience with my idiosyncrasies and excesses over the last five years; without

their support, scientific conversations, and frequent rebuttals to my crazier ideas I think I would still be deep in the scientific wilderness. Eric Dahl was an especially helpful; we worked well together and helped each other reach many crucial realizations and invent new research directions. Grayson Ritch has been a close personal friend, and has never hesitated to call me out on my excesses. Lily Hale's piercing intelligence, indefatigable work ethic, idealism, and illuminating scientific conversations have always inspired me to be better and never accept failure. James Shanahan has been a close collaborator and friend, and his careful work and depth of vision have provided much needed perspective at crucial junctures. The five of us have been close, and I look forward to seeing what new directions our lives will take.

In my early years in the lab, I was still quite inexperienced in the lab and benefited greatly from the mentorship of Dr. Cameron Moore at an important and precarious time. Oscar Tutusaus and Laura Essex also provided important support and validation at this time. Tyler Carter, another early Szymczak lab member, unknowingly enabled most of my later work by leaving behind a very consequential vial full of extra hexamethylborazine when he graduated.

I had the pleasure of working with three very talented undergraduate students: Justin Wang, Tyler Lopez, and Joanna Ciatti. Tyler and Joanna were amazingly hard-working members of the lab, and impressed me with their drive and ambition. I am especially happy that I was able to see Joanna develop into an independent scientist over the course of her long tenure in the Szymczak lab, transitioning from working on an established project to leading a new effort, and am excited to see how her bright future unfolds. I have enjoyed watching Michael Wade Wolfe's synthetic skills, knowledge, and scientific thinking develop over the past two years while pursuing independent work relating to our borazine fluoroalkylation reagents. I am especially happy that unfinished aspects of my project can continue in the hands of such an excellent colleague.

Lastly, I need to thank all of my wonderful friends and family members for their love and support. Matthew Wolfe, Isaac Roles, Martin Hurtado, Claire Radigan, Julian Hurtado, Philip and Vicki Kiser, Jefferson Clayton, Raymond Rivera, Justin Straughan, Robert Campana, Alonso Arguelles, Aaron Proctor, Michael Robo, Michael Carnegie, Roland Philbin, Ethan Preston, Ryan Pool, and Noah Allington are wonderful friends who gave me perspective on life beyond the laboratory. I thank my family, but especially Lisa Geri, Barry Stipe, Carol Cushing, and Monica Stipe. Most importantly, I need to thank Jihkai Yeh for all of the love, energy, and happiness he has given me in our time together.

Table of Contents

List of Figures

Abstract

Frustrated Lewis pairs are powerful tools for bond heterolysis in organic and inorganic chemistry. In these systems, an electron-deficient Lewis acid and an electron-rich Lewis base synergistically polarize strong bonds in substrate molecules, forming electrophilic and nucleophilic fragments that can be used in subsequent reactions. However, synergistic bond heterolysis is only possible when reactive Lewis acids and bases are unable to form inert Lewis acid/base adducts with each other. In this monograph, I used a broad definition of what constitutes Lewis acids and bases to design unconventional frustrated Lewis pairs that address significant challenges in catalysis, bioinorganic chemistry, and organofluorine chemistry. First, transition metal catalysts incorporating pendent oxyanion bases were prepared that mediate metal/ligand cooperative H_2 and HBPin heterolysis, followed by transfer of electrophilic proton or boryl equivalents and nucleophilic hydrides to nitriles, carbonyl compounds, or carbon dioxide. Next, a reduced Fe(0) center was used as a Lewis base in combination with triorganoborane and alkali cation Lewis acids to synergistically weaken and polarize the N-N triple bond in N_2. Polarization of N_2 was then exploited in selective -*N*, rather than -*Fe*, protonation reactions. Finally, a weak borazine-based Lewis acid was used in combination with strong bases to deprotonate HCF_3 and HCF_2R. The incipient CF_3^- and CF_2R^- anions, typically highly unstable, were captured and stabilized by borazine to form stable fluoroalkylation reagents, which react like traditional Grignard reagents. Overall, these systems demonstrate the generality and utility of the frustrated Lewis pair concept.

Chapter 1. Introduction

Reactions between electrophilic and nucleophilic species underpin a large part of synthetic organic chemistry. These reactions frequently depend on heterolytic bond cleavage (deprotonation, hydride transfer, C-X dissociation in SN1 reactions, etc.) to expose reactive species, and can be mediated by compatible pairs of Lewis acids and bases. The scope of what constitutes a Lewis acid or base is very broad; any molecule with a lone pair of electrons, and even solvated electrons themselves, can react as a Lewis base, while any molecule capable of accepting a lone pair can react as a Lewis acid.[1] Conventional Lewis acids such as trialkylboranes (BR_3) and alkali cations (Li^+)[2] and Lewis bases such as amines (NR_3) and halide anions (F^-)[3] are commonly used as catalysts in organic methodology through formation of reversible adducts with complementary Lewis basic (nucleophilic) and acidic (electrophilic) sites in organic molecules. My PhD work has focused on using less conventional Lewis acids (borazines, pendent boranes) and bases (toluide, Fe^0) in combination to effect previously unknown types of small molecule activation/transfer and address problems in catalysis, bioinorganic chemistry, and the development of green chemical processes.

1.1 The Frustrated Lewis Pair (FLP) Concept

Bond heterolysis is a fundamental process in which a Lewis acid, which accepts electrons, or a Lewis base, which donates electrons, splits a neutral molecule into two fragments of opposite charge by providing stability to the less stable fragment. The liberated fragments may subsequently react as nucleophiles and electrophiles with organic and inorganic substrates. This mechanistic paradigm includes many of the most common reactions (deprotonation, hydride transfer, C-X dissociation, etc.) (Figure **1-1**). Highly polarized bonds such as O-H or C-F can be heterolyzed by strong Lewis acids and bases with release of free, charged electrophiles or nucleophiles, but less polar substrates such as dihydrogen and dinitrogen cannot. Only the combined presence of both Lewis acids *and* bases can enable the heterolysis or polarization of such species.[4]

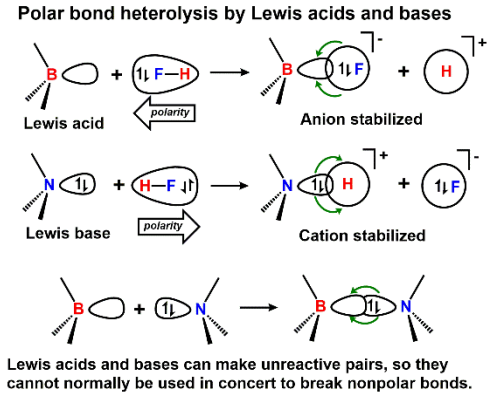

Figure 1-1 Polar bond heterolysis

Normally, Lewis acids and bases will react to produce neutralized species in which the reactivity of the free acids and bases are attenuated, precluding their combined use.[5] However, it is possible to design compatible pairs of organic Lewis acids and bases that retain their individual reactivity while coexisting in solution, enabling synergistic activation of typically inert molecules. In these molecules, steric repulsion, geometric constraints, and electronic tuning are exploited to maintain compatibility between free Lewis acidic and basic moieties, "frustrating" their natural tendency to react with each other.[6] Due to the very broad definition of Lewis acids and bases, "frustrated Lewis pairs" (FLP)s can be designed that incorporate a wide variety of inorganic, main group, and organic nucleophiles and electrophiles as acidic or basic partners.[7] A defining feature of such systems is their unique ability to activate diatomic molecules with no net dipolar moment (H_2) and promote their functionalization (Figure **1-2**).[8]

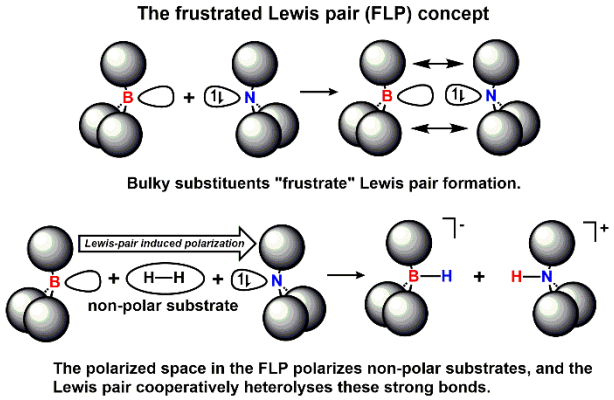

Figure 1-2 The FLP concept

While organic FLPs capable of activating nonpolar bonds have been recently introduced by Stephan and Erker, the FLP concept has a long history in inorganic chemistry. The homogeneous catalysts used for selective polar bond hydrogenation use compatible Lewis acidic

transition metal / base pairs to heterolyze H_2,[9] alkanes can be activated through transition-metal assisted deprotonation of C-H σ adducts with Lewis acidic transition metals in the concerted cyclometallation/deprotonation (CMD) pathway[10], and exogenous bases play a key role in mediating B-C bond polarization in the Suzuki reaction.[11]

Of special interest in this monograph are three classes of unconventional Frustrated Lewis pairs: 1) intramolecular FLPs using pendent bases attached to Lewis acidic transition metal centers, 2) FLPs using low-valent transition metal centers as Lewis bases and free organic and inorganic Lewis acids, and 3) FLPs using electronically mismatched Bronsted superbases and weak organoboron Lewis acids (Figure **1-3**).

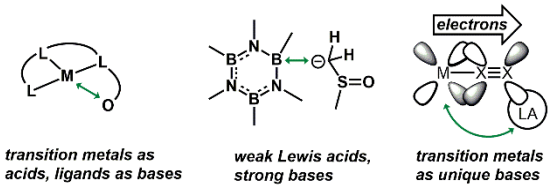

Figure 1-3 Example systems used in Chapters 2-7

1.2 Intermolecular Transition-Metal Based FLPs

Transition metals are potent Lewis acids in bond heterolysis reactions due their ability to form σ-adducts with a variety of traditionally inert substrates (H_2,[12] R_2B-H,[13] R_3Si-H,[14] R_3C-H).[15] These adducts form through interactions similar to those found in metal olefin complexes: empty metal orbitals accept electron density from filled σ-bonding orbitals in the substrate, while filled metal d-orbitals donate electron density to the empty σ* antibonding orbital in the substrate as described by the Dewar Chatt Duncanson bonding model.[16] The presence of both interactions can lead to strong and highly tunable bonding interactions in metal σ-complexes that can be modulated through ligand geometric and electronic properties, metal oxidation state, and metal identity.[17]

Transition metal / base FLPs were the first molecular systems known to promote heterolytic cleavage of H_2 and other inert species. When substrate-to-metal charge transfer dominates, each atom of the σ-bond becomes more electrophilic.[18] In E-H σ-adducts, this manifests as a dramatic decrease in the pKa of an E-H bond when coordinated to the metal center, permitting facile deprotonation of otherwise weak acids including dihydrogen and hydrocarbons by using bases that do not irreversibly displace the E-H σ-adduct from the metal center.[19]

Dihydrogen ligands provide easily quantified examples of this effect, with coordinated H_2 molecules at Ru(II) centers exhibiting pK_a values ranging from -5 to 42.[19] Free H_2 has a pKa of

approximately 50[20]. Deprotonation reveals a metal hydride or metal aryl species that can act as a nucleophile in subsequent reactions, as seen in examples with Mo[21] and W[22] (Figure **1-4**). This approach to σ-bond activation has enabled the design of widely used transition metal / base pairs that catalyze selective hydrogenation of unsaturated polar bonds (C=O, C=S, C=N, C≡N),[23] an important methodology that complements the selectivity of heterogeneous hydrogenation catalysts (Pd/C) for unsaturated non-polar bonds (alkenes, alkynes, arenes).

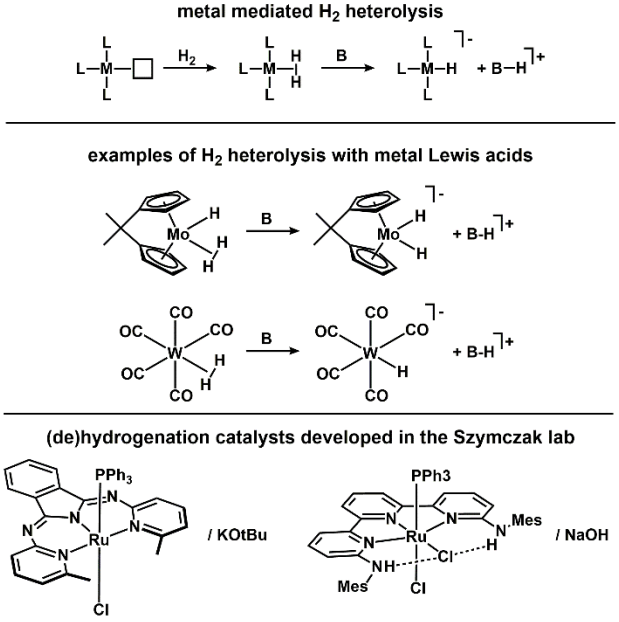

Figure 1-4 Intermolecular transition metal-based FLPs

The Szymczak lab has extensively studied Ru(II) complexes supported by bispyridylisoindolinate (BPI) and terpyridine (TPY) pincer ligands in combination with alkoxide bases as reversible hydrogenation catalysts.[24] In hydrogenation reactions, Ru(II) and Ir(III) pincer complexes are widely used as hydrogenation catalysts due to their advantageous hydride affinity relative to other elements, that enables tolerance of acidic functional groups and selective hydride delivery to polar bonds in carbonyl, imine, and nitrile functional groups.[25] BPI is a rigid ancillary pincer ligand which provides a strong σ-donor trans to an empty equatorial coordination site at Ru(II), allowing for enhanced Ru-H nucleophilicity and enabling the first selective dehydrogenative oxidation of amines to nitriles.[26] This work was carried out by previous Szymczak members Tim Tseng and Lilian Hale. A thorough mechanistic study implicated amine deprotonation by the Ru-H unit as the rate determining step in nitrile hydrogenation and amine

dehydrogenation, highlighting the importance of the trans σ-donor presented by the ancillary BPI ligand.[27]

1.3 Intramolecular Transition-Metal Based FLPs

Intramolecular FLPs using transition metal Lewis acids covalently tethered to Lewis bases present significant advantages over intermolecular FLPs as catalysts. First, and most significantly, intramolecular FLPs eliminate a significant part of the entropic penalty suffered by intermolecular systems by preorganizing the Lewis acids and bases for substrate capture/activation.[24b] Secondly, the combination of adjacent electrophilic and nucleophilic centers resulting from bond heterolysis can significantly enhance selectivity in their reactivity with unsaturated, polar substrates such as carbonyls and imines over nonpolar alkenes.[28]

Two limiting approaches to the design of intramolecular inorganic FLPs have been pursued. In the first, a metal-coordinated Lewis base can present a free lone pair that can act as a basic center (Figure **1-5**).[29] Metal amidos are the most common primary coordination sphere intramolecular bases, but phosphides,[30] oxoanions,[24c,31] and carbenes[32] have all been used as well. These systems have been extensively exploited as enantioselective hydrogenation catalysts. While such systems are efficient in H_2 activation, the congested steric environment at the metal hydride that enables highly enantioselective hydrogenation reactions prevents applications requiring other E-H activations (B-H, Si-H, etc.).

Alternatively, Lewis bases can be positioned in the secondary sphere of the metal center (Figure **1-6**). This approach offers a high degree of design freedom, allowing chemists to target ideal metal-base distances and independently tune the Lewis acidity and Lewis basicity of the FLP without coupled effects resulting from metal-base bonds.[33] Designing catalysts with tethered "pendent" bases is challenging, due to the ease with which they can irreversibly bind to the Lewis acidic metal center. This self-quenching process can be prevented through imposition of steric and geometric constraints through rational ligand design and selection of metal and pendent base elements with reduced mutual binding affinity.[34]

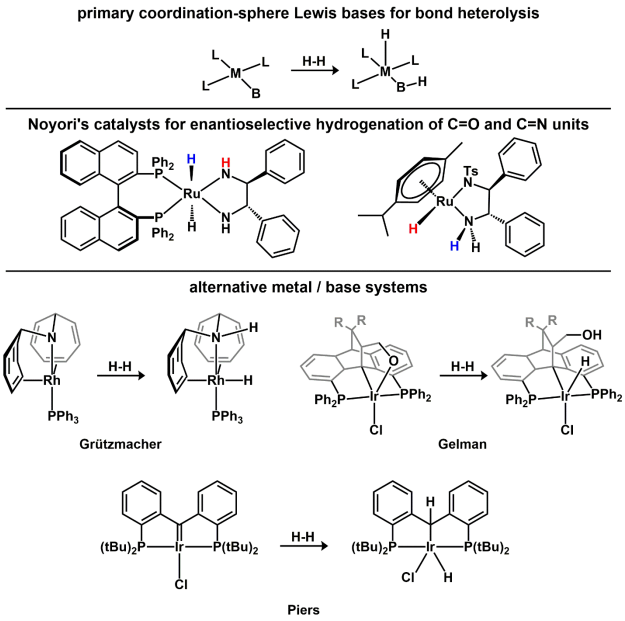

Figure 1-5 Intramolecular transition-metal based FLPs with primary coordination-sphere bound bases

The enzyme [Fe]-hydrogenase, a metalloenzyme that catalyzes H_2 heterolysis and the reduction of methenyltetrahydromethanopterin cation (MTP^+), represents an excellent example of this approach.[35] In the active site, an Fe(II) metal center is bound to a multidentate ligand that includes a 2-hydroxy pyridine fragment that binds through the nitrogen atom, providing a basic oxoanionic center upon deprotonation in the secondary coordination sphere that is incapable of binding to the metal center. Mechanistic studies suggest that this oxoanionic species is key to H_2 heterolysis at the Fe(II) center.[36] Since the Fe-hydrogenase active site was structurally characterized, 2-hydroxypyridine has been extensively exploited in the design of ligands for intramolecular transition metal FLPs.[33b] In these complexes, linear binding at the *N*- atom of 2-hydroxypyridine units prevents efficient binding with the -O atom, enabling E-H bond heterolysis reactions and hydrofunctionalization catalysis.[24b,e,37]

Intramolecular FLPs using Ir(III) centers as Lewis acids and 2-hydroxybipyridine and related 2-hydroxybipyrimidine ligands as pendent bases reported by Himeda, and Fujita are highly efficient hydrogenation catalysts.[33a,38] Their catalytic reactions follow a well-defined mechanism in which the pendent oxoanion bases facilitate efficient deprotonation of metal-H_2 σ-adduct intermediates to expose nucleophilic Ir(III) hydrides, which then insert into CO_2 and other polar electrophiles.[39] Sequential deprotonation of multiple -OH groups in related complexes modulates

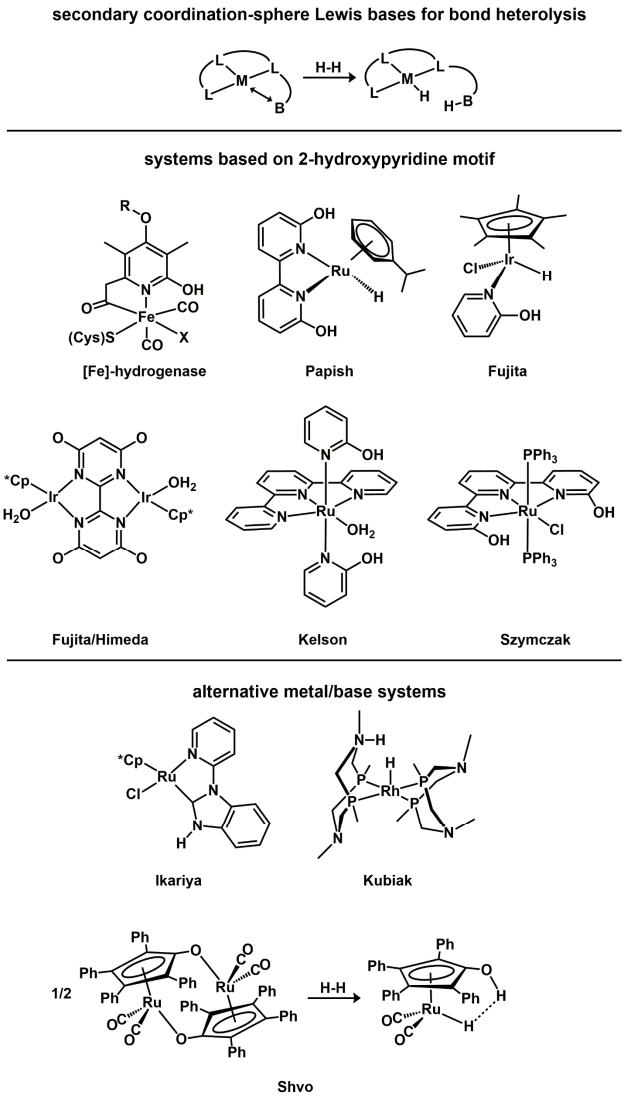

Figure 1-6 Intramolecular transition-metal based FLPs with secondary coordination-sphere tethered bases

ancillary ligand electron-donor strength, permitting regulation of electron density and Ir-H hydricity at the Ir center.

Other previously described systems exploiting 2-hydroxypyridine units as basic partners in intramolecular transition metal FLPs include Ru(tpy)(2-OHpy)$_2$[40] and Ru(dihydroxybipy)(cymene)Cl,[41] which are active catalysts for transfer hydrogenation of carbonyl compounds using isopropanol as a source of H_2. The Szymczak lab introduced dihydroxyterpyridine as a pincer ligand scaffold offering two 2-hydroxypyridine units positioned to provide pendent bases under basic conditions and act as cooperative hydrogen bond

donors/acceptors.[24e] The derived Ru(II) complexes were efficient and highly selective catalysts for alcohol dehydrogenation and ketone hydrogenation.

In addition to inorganic FLP systems based on transition metals supported by 2-hydroxypyridine ligands, many other pendent bases have been successfully exploited in catalyst design. These include pendent N-heterocyclic functionality,[42] tertiary amine groups,[31] and cyclopentadienyl-coordinated oxoanions.[33d] However, some of the most successful secondary sphere bases are carbanion equivalents generated from deprotonation of methylene linkages in pincer ligand scaffolds pioneered by Milstein et. al (Figure **1-7**).[33f] The carbon centered bases are located in the pincer ligand backbone and are stabilized by conjugation with metal-bound heterocyclic nitrogen atoms. The lone-pair orientation of the carbanionic tautomer enables facile six-membered transition states for E-H activation. The derived catalysts are structurally diverse and have been applied to many difficult hydrogen-borrowing functionalizations including the dehydrogenative, aqueous conversion of alcohols to carboxylic acids,[43] ester, amide, and nitrile hydrogenation,[44] and extremely efficient reversible CO_2 hydrogenation.[45]

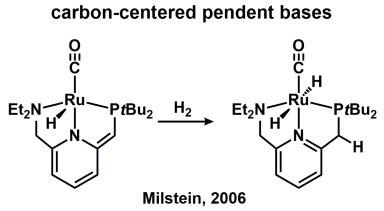

Figure 1-7 Carbon-centered tethered bases

In this thesis (Chapter 2), we developed intramolecular and intermolecular FLP systems using Ru(II)-pincer scaffolds.[46] First, a bispyridylisoindolinate pincer ligand was prepared in which both pyridines bore 2-hydroxy substituents, synthesized its Ru(II) complexes in a variety of protonation states, and investigated its ability to mediate B-H and H-H heterolysis reactions through an intramolecular FLP manifold. Next, we applied the complexes as catalysts to reactions in which E-H bond heterolysis represents a key step: polar bond hydrogenation and hydroboration. Later, in collaboration with an undergraduate student (Joanna Ciatti), we investigated ligand design principals for reversible CO_2 hydrogenation catalysis using modular Ru(II)BPI and Ru(II)TPY pincer complexes. This work showed that increasingly electrophilic pincer ligands led to significantly improved catalytic activity for *both* hydrogenation and dehydrogenation of CO_2.

1.4 FLPs Using Reduced Transition Metals as Lewis Bases

In addition to typical transition metal FLP systems, in which an electrophilic metal center acts as a Lewis acid and an organic compound with unengaged lone pairs acts as a base, it is possible to design FLPs in which an electron rich, low-valent metal center can act as a Lewis base while an organic compound with empty p- or s- orbitals can act as a Lewis acid.[47] These systems offer distinct reactivity from traditional FLP systems due to the π, rather than σ, character of the Lewis base. If metal-to-substrate charge transfer dominates in a σ or π-adduct with a substrate, each atom comprising the bond in the substrate becomes more nucleophilic. This effect is magnified in the presence of a free Lewis acid, as was demonstrated by Braunschweig et. al. using Pt(0) / borane Lewis pairs.[48] Additionally, the Mankad group has reported several examples of H-H activation using Lewis-basic metal based FLPs, including a Ag/Ru system (Figure **1-8**).[49]

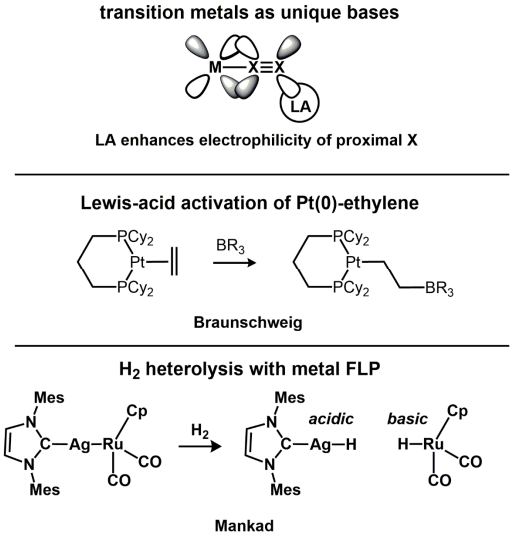

Figure 1-8 Metals as Lewis Bases in FLPs

Exogeneous Lewis acids can be used to enhance the electrophilicity of ligands bound to reduced metal complexes, increasing the rate of nucleophilic insertion reactions. A common example in organic methodology is the activation of organocuprate complexes for conjugate alkylation of α, ß-unsaturated ketones with Lewis acids.[2] In these reactions, an electron-rich Cu(I) center bound to two strong σ-donor alkyl anions forms a π-adduct with the alkene unit in a α, ß-unsaturated ketone. Coordination of BF_3 or Li^+ to the oxygen atom of the ketone functional group dramatically increases the electrophilicity of the ß-carbon atom,[50] facilitating selective alkyl insertion at this position (Figure **1-9**).

In related reactions, insertion of alkyl anion ligands into carbon monoxide is accelerated upon addition of exogenous Lewis acids. Added Lewis acids can coordinate to the oxygen atom of the carbonyl ligand, greatly enhancing its electrophilicity and facilitating nucleophilic alkyl insertion to form metalloacyl products.[51] This was conclusively demonstrated in the seminal work by Shriver et. al., who showed that $W(CO)_5Ph^-$ reacts with $AlPh_3$ to form an alane-stabilized metallobenzoyl ligand.[52]

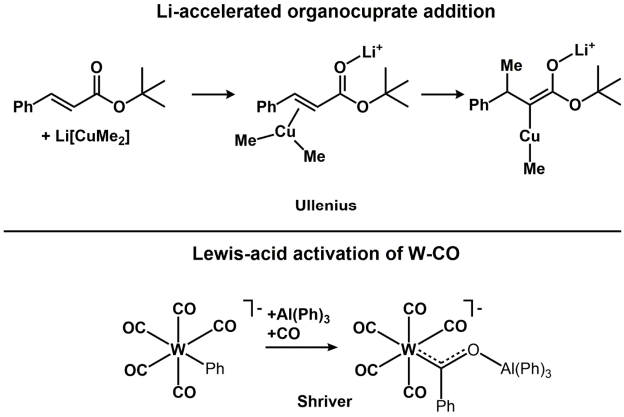

Figure 1-9 Activation of carbonyl groups with transition metal bases and exogeneous Lewis acids

Similarly, there are scattered reports of dinitrogen ligands bound to π-basic reduced metal centers acting as nucleophiles in reactions with Lewis acids (Figure **1-10**). Rhenium, osmium,[53] tungsten, and molybdenum-N_2 adducts[54] have been reported to react with $SiMe_3^+$ and $AlMe_3$,[55] in addition to H^+,[56] Lewis acids to form M-N_2-LA adducts. With reduced Fe(0) complexes, crystallographic and spectroscopic evidence suggests that lithium and magnesium cations[57] can interact with nucleophilic N_2 ligands and decrease the strength of the N-N bond.

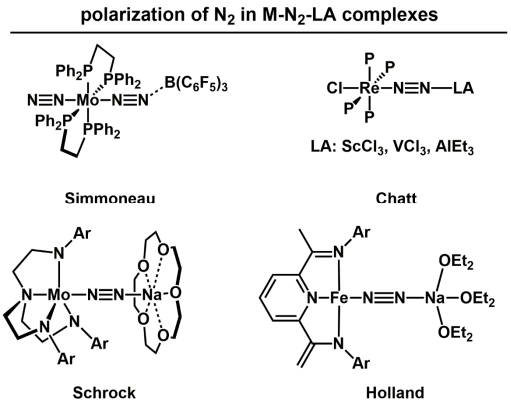

Figure 1-10 M-N_2-LA adducts

Intramolecular systems are more uncommon, despite their use by metalloenzymes that activate O_2 and N_2 (where the Lewis acidic component is a network of electrophilic hydrogen bonds).[58] Bercaw and coworkers reported the first example of a synthetic system (2008),[59] in which a Re(0) tetracarbonyl diphosphine complex bearing two pendent borane units undergo boron-mediated hydride attack at the carbonyl carbon, forming a Lewis acid-stabilized metalloformyl ligand. This seminal work demonstrated that carbon monoxide could undergo cooperative activation by a strongly π-basic, low valent metal center and a tethered boron Lewis acid; in the presence of exogeneous borane, no reaction was observed (Figure **1-11**).

In 2013, Szymczak, Tutusaus, and Ni developed an intramolecular Lewis acid/base triad system for cooperative hydrazine binding and cleavage.[60] In the reported complex, a reduced V(III) metal center engages a hydrazine ligand in an unusual η-2 binding mode assisted by both N-coordination to a pendent boron Lewis acid and hydrogen bonding with a pendent morpholine Lewis base. This work was expanded upon by Szymczak and Kiernicki, who reported that a Fe(II) complex supported by a tridentate ligand with two tethered boranes in the secondary coordination sphere captured hydrazine using both boron Lewis acids, then mediate N-N cleavage to form a rare $Fe(NH_2)_2$ complex upon addition of a strong reductant.[61] Control reactions with a Zn(II) complex, the ligand alone, and no additive suggested the possible role of a pendent borane-mediated oxidative addition reaction.

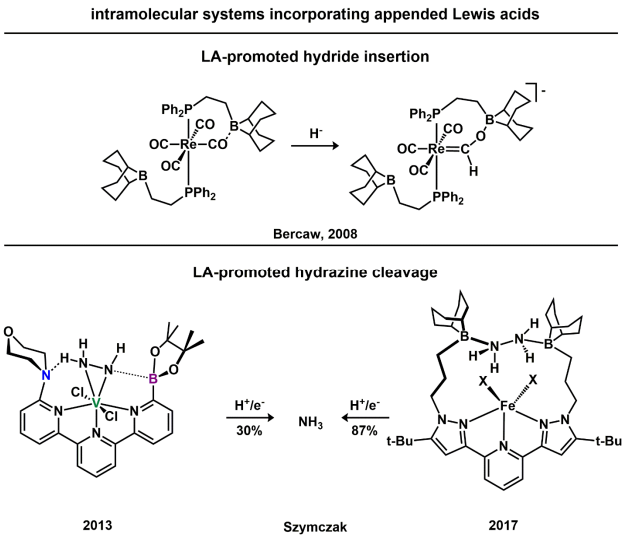

Figure 1-11 Intramolecular FLPs using transition metal Lewis bases

We applied an intermolecular FLP system using $Fe(0)DEPE_2$ as a Lewis basic unit and a variety of alkali metal and organic Lewis acids to N_2 activation and functionalization (Chapter

3).[62] In this work, we used exogeneous Lewis acids as models for hydrogen bond donors in the active site of nitrogenase. Exogeneous Lewis acids were found to cooperatively activate N_2, lengthening the N-N bond and weakening the bond strength as assessed by X-Ray crystallography, IR spectroscopy, and density functional theory calculations. The added Lewis acids led to localization of electron density at the distal nitrogen atom, which enabled selective protonation of a dinitrogen ligand.

1.5 Organic electronically frustrated Lewis pairs

While several examples of small molecule activation mediated by organic Lewis acid/base pairs sporadically appeared in the literature by Brown (lutidine/$B(Me)_3$)[63] and Wittig (CPh_3^-/BPh_3),[64] their potential went unrecognized for decades. Lewis pairs that exploit steric bulk to maintain compatibility were the first entirely organic FLPs to appear in the literature (Figure **1-12**). In 2006, the Stephan group at the University of Toronto reported that 1-dimesitylphosphine-4-bis(pentafluorophenylborane-tetrafluorobenzene mediated H_2 heterolysis,[65] a reaction previously thought to require the participation of a metal center. Intramolecular FLPs that activate H_2 in concert were later prepared by Erker et. al..[66] In addition, it was shown that intermolecular systems comprising mixtures of various bulky organoborane and organoalane Lewis acids and bulky phosphine and amine bases are capable of similar reactions with H_2.[7] Organic FLP systems based on steric bulk were quickly applied as hydrogenation catalysts.

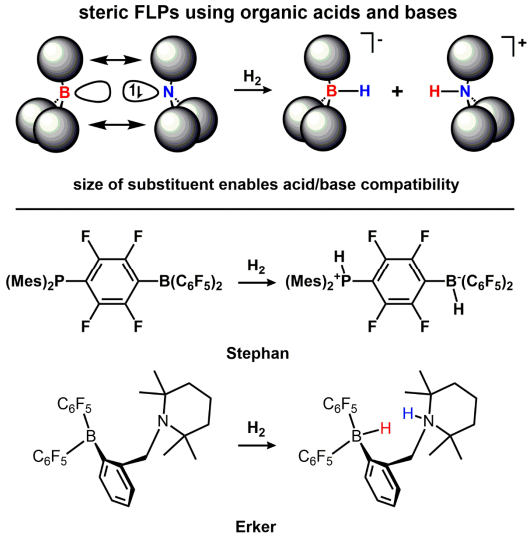

Figure 1-12 Organic FLPs

Frustrated Lewis pairs that exploit mismatched strength (electronic FLPs), rather than steric bulk, are more uncommon. However, the bond heterolysis reactions they promote yield more reactive nucleophiles or electrophiles (Figure **1-13**). The combination of the strong Lewis acid $B(C_6F_5)_3$ with a very weak Lewis base diethyl ether is an illustrative example of this class of FLP. Adduct formation is reversible, enabling small concentrations of the free Lewis acid and base to coexist in solution despite the bulk of the Lewis pair existing as less reactive adducts. This small concentration of free Lewis acid / base can form $H(OEt_2)_2^+/HB(C_6F_5)_2^-$ under catalytic conditions.[67] This transient superacidic species is proposed to protonate olefins, generating reactive carbocationic intermediates that abstract hydride from $HB(C_6F_5)_3^-$. The same system can be used to hydrogenate aryl aldehydes and ketones.[68] In these reactions, carbonyl groups are protonated to form reactive oxocarbenium cations that abstract hydride from $HB(C_6F_5)_3^-$ to form alcohols. This reactivity is distinct from traditional steric FLP catalysis in that stronger sterically protected bases such as phosphines are insufficiently acidic to generate the required oxocarbenium intermediate through carbonyl protonation.[69]

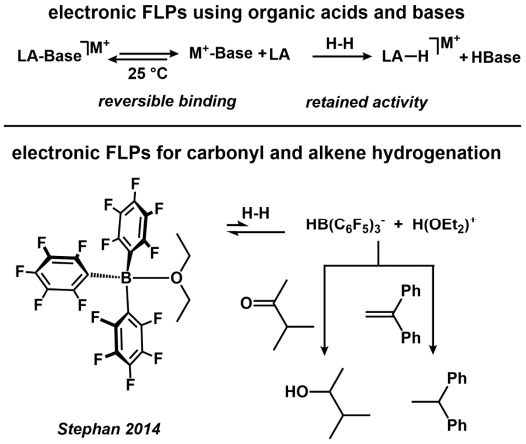

Figure 1-13 Organic FLPs using electronically mismatched Lewis acids and bases

In contrast to electronic FLPs that use strong Lewis acids and weak Lewis bases, FLPs that use strong Lewis bases and weak Lewis acids are rarely encountered. Generally, they are not active as catalysts, with neither the Lewis acid or base being recoverable after bond heterolysis/transfer reactions, and are generally used for C-H bond deprotonation / carbanion capture in cases of high carbanion instability. Their applications are limited to the generation / capture / transfer of highly unstable carbanion synthons, because more stable carbanionic species can be easily handled as organolithium, magnesium, or zinc reagents. Traditional Lewis acidic partners such as boranes typically react with carbanionic equivalents irreversibly, and are incapable of promoting desirable

carbanion transfer reactions. Strong and irreversible superbase coordination is typical unless bulky bases are employed; for this reason, P_4-tBu phosphazene / electron-deficient arnenes,[70] $KN(SiMe_3)_2$ / $SiMe_3Cl$,[71] and $KN(SiMe_3)_2$ / $B(OMe)_3$[71] are representative examples of this class of FLP.

We developed electronic FLP systems that use weak Lewis acids and dimsyl anion, toluide, and diisopropylamide superbases to promote fluoroalkyl C-H bond heterolysis.[72] The borazine-stabilized fluoroalkyl anions thus generated were highly reactive nucleophilic synthons, and after fluoroalkyl transfer the borazine Lewis acid was quantitatively regenerated. The fluoroalkyl-borazine adducts had reactivity profiles mimicking alkyl Grignard reagents, enabling a wide variety of previously unknown C-C bond disconnections. Our initial work focused on HCF_3 activation / CF_3^- stabilization/ CF_3^- transfer using hexamethylborazine as a weak Lewis acid, but later expanded the scope of this chemistry to the conversion of other 1-H fluoroalkyl groups into reactive fluoroalkyl nucleophiles. The scope of C-H bond heterolysis / fluoroalkyl transfer reactions include HCF_3, H_2CF_2, HCF_2CF_3, and generalized HCF_2Ar difluoromethyl(hetero)arenes.

Chapter 2. A Proton-Switchable Nitrile Hydroboration Catalyst

Portions of this chapter have been published:

Geri, J. B.; Szymczak, N. K.; A Proton-Switchable Bifunctional Ruthenium Complex That Catalyzes Nitrile Hydroboration.

J. Am. Chem. Soc. 2015, 137, 12808-12814.

2.1 Abstract

A new bifunctional pincer ligand framework bearing pendent proton-responsive hydroxyl groups was prepared and metalated with Ru(II) and subsequently isolated in four discrete protonation states. Stoichiometric reactions with H_2 and HBPin showed facile E–H (E = H or BPin) activation across a Ru(II)–O bond, providing access to unusual Ru–H species with strong interactions with neighboring proton and boron atoms. These complexes were found to promote the catalytic hydroboration of ketones and nitriles under mild conditions, and the activity was highly dependent on the ligand's protonation state. Mechanistic experiments revealed a crucial role of the pendent hydroxyl groups for catalytic activity.

2.2 Introduction

Proton-switchable catalysis is widely used in biological systems as a means to gate reactivity and facilitate otherwise incompatible reaction sequences.[58a,73] Modification of a given proton gradient can be used to induce reversible geometric changes[74] and modulate electronic density at a metal site[38a,75], and collectively, these can be used as a switch for catalytic activity. To mimic such function, metal complexes containing proton responsive ligands have recently been shown to exhibit pH dependent activity that enables on/off switching.[38b,41,76] Such bifunctional metal complexes have emerged as efficient catalysts for (transfer)hydrogenation[23,77] and hydrofunctionalization[33c,78] reactions. These transformations rely on the cooperative activation of E-H bonds (E= H, BR_2, SiR_3) and subsequent transfer of reactive electrophilic and nucleophilic moieties to polar substrates.

Metal-ligand constructs with multiple accessible protonation states can impart a high level of control over reaction initiation as well as activity.[24b,33b] However, the regulation of activity between three or more discrete protonation states is underdeveloped. While there are several examples of catalytic systems that respond to protonation/deprotonation, they are usually limited to two isolable species, and characterization of multiple (>2) protonation states is rare.[38b,41,76,79] In addition to a "base activation" strategy whereby a single proton transfer event turns on catalysis, further modulation of a catalyst's protonation state can also dramatically tune nucleophilicity at a metal site[33e,75a,80] and allow further control over catalytic activity. Our group is working to evaluate how the precise structural, electronic, and cooperative modes of a metal's secondary coordination sphere can be used to regulate reactivity, and have developed ligands with appended polar groups to assess their ability to influence subsequent reactivity.[24e,37a,60,81]

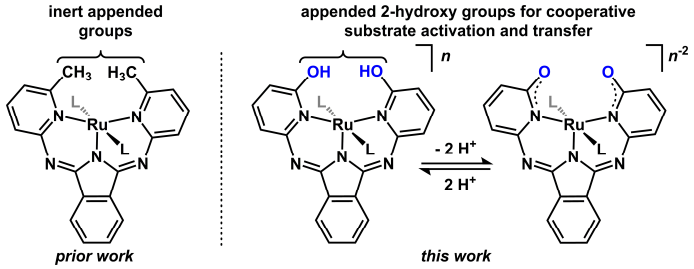

Figure 2-1 Conceptual development of bis(2'-hydroxy-6'-iminopyridyl)isoindolene (BH3PI)

In contrast to the intense attention paid to the development of proton-responsive hydrogenation catalysts, cooperative activation of weakly-nucleophilic B-H bonds to effect polar bond reduction remains relatively unexplored.[33c,78b,8283] Despite significant advances in the reduction of nitriles over the last three decades, there remain challenging selectivity problems.[84] For instance, harsh reductants such as main group hydrides show poor selectivity for nitriles in the presence of carbonyl-containing functional groups,[8586] while heterogeneous hydrogenation of nitriles is incompatible with functional groups susceptible to hydrogenolysis.[87] Due to the problems associated with regent compatibility, investigations into catalysts that promote nitrile hydroboration are under active investigation[82b,88] and bifunctional complexes are uniquely situated for this purpose.

We recently reported a series of ruthenium complexes containing an *N,N,N*-bMepi pincer ligand (bMepi = 1,3-bis(6'-methyl-2'-pyridylimino)isoindolinate), which are highly active precatalysts for the dehydrogenation of alcohols and amines.[24a,26] We hypothesized that by modifying the *ortho* substituents from inert -CH_3 to reactive -*OH* groups, we could bias the system

for bifunctional E-H activation pathways and also provide access to protonation state dependent catalysis (Figure **2-1**).[24b,33b,89] In this chapter, we report the development of a new ligand platform, bis(2'-hydroxy-6'-iminopyridyl)isoindolene (BH_3PI; H_x denotes the available proton inventory of the ligand framework), its associated ruthenium complexes in four protonation states, and showcase the ability of these complexes to promote extremely rapid, proton-switchable and responsive catalysis for ketone and nitrile hydroboration.

2.3 Synthesis, Characterization, and Structural Features of Designed Complexes

We prepared BH_3PI by a three-step synthetic protocol from commercially available reagents (Figure **2-2**). Condensation of 2-bromo-6-aminopyridine and phthalonitrile afforded bis(2'-bromo-6'-iminopyridyl)isoindoline in 73% yield. Nucleophilic substitution with sodium benzyl oxide proceeded in 71% yield, and the resulting benzyl ether was deprotected in neat BBr_3 to provide the ligand (BH_3PI) in 74% yield as a red powder; the preparation can be scaled to gram quantities.

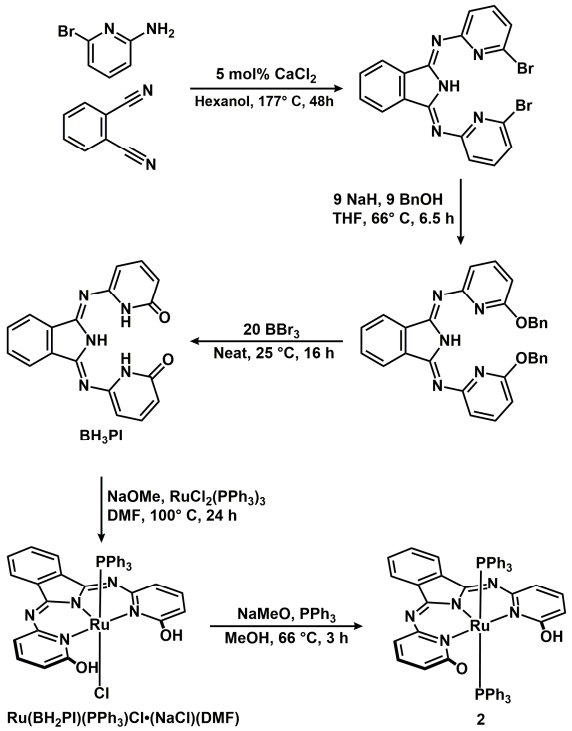

Figure 2-2 Synthesis of BH3PI and Ru(BHPI)$(PPh_3)_2$.

We assessed whether a metal-BH_3PI complex was able to accommodate multiple protonation states (of use for the cooperative activation of small molecules) by examining its

ruthenium(II) complexes. $Ru(BH_2PI)(PPh_3)Cl•(NaCl)(DMF)$ was prepared by treating $Ru(PPh_3)_3Cl_2$ with BH_3PI in the presence of 1 equiv. $NaOCH_3$ in DMF solvent. Following dehydrohalogenation with another equiv. of $NaOCH_3$ in the presence of PPh_3, $RuBH_1PI(PPh_3)_2$ (**2**) was obtained in 85% yield. NMR spectroscopic analysis revealed a C_2-symmetric set of ligand resonances, consistent with fast exchange of the single acidic proton, and the ^{31}P NMR spectrum revealed a singlet at δ 33.6, consistent with *trans*-disposed PPh_3 ligands.

This complex was a useful synthon for further proton transfer reactivity. For instance, addition of one equiv. trifluoroacetic acid (CF_3COOH) afforded $RuBH_2PI(PPh_3)_2(CF_3CO_2)$ (**3**) in quantitative yield, as noted by the appearance of a new resonance at δ 32.0 in the ^{31}P NMR spectrum. Further protonation of **3** using two equiv. CF_3COOH afforded **4**. NMR spectroscopy revealed that protons in the complex were in rapid exchange, reflected in the observation of one acidic proton resonance at δ 13.84. Alternatively, the addition of one equiv. potassium bis(trimethylsilyl)amide ($KN(Me_3Si)_2$) to **2** in the presence of 18-crown-6 afforded the deprotonated complex, $[Ru(BH_0PI)(PPh_3)_2][K(18\text{-crown-6})]$ (**1**), as noted by the disappearance of the OH resonances in the ^1H NMR spectrum.

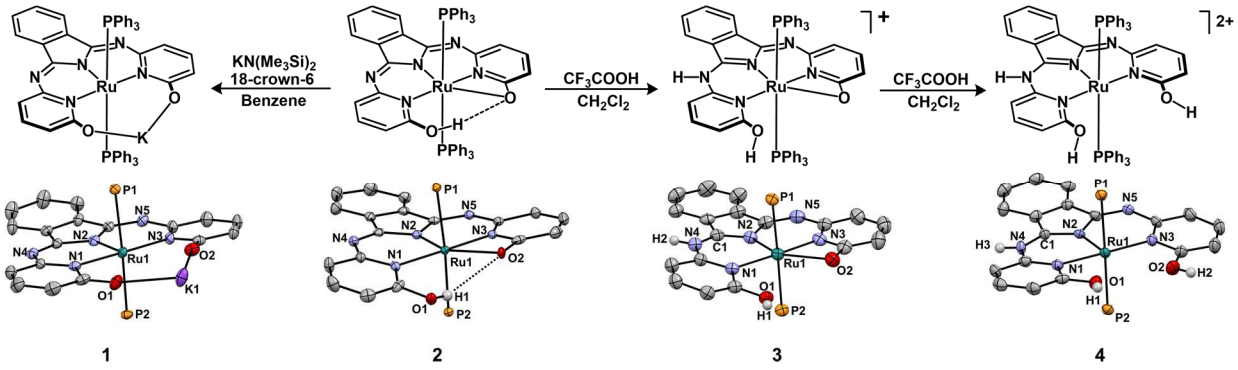

Figure 2-3 Synthesis of metal complexes in different protonation states.

The series of homologous complexes that differ by stepwise protonation provided a unique opportunity to examine the metal's protonation-state dependent electronic environment and catalytic activity. Crystals suitable for X-Ray diffraction were obtained for **1**-**4**, and the solid-state structures confirm similar primary coordination environments at ruthenium. Fully deprotonated complex **1** adopts C_s symmetry, in which BH_3PI coordinates as a trianionic ligand and a potassium ion is coordinated to both pendent aryloxide bases, and capped by an 18-crown-6 unit. Protonation induces the formation of a Ru–O bond in $RuBH_1PI(PPh_3)_2$ (**2**), with the ligand framework enforcing a distorted $\kappa^2(N,O)$ binding mode of one pyridonate arm and a weak hydrogen bond[90]

between the OH–O units (O1-O2 = 3.28 Å). The $\kappa^2(N,O)$ coordination is preserved upon additional protonation in **3**, which occurs at the imine nitrogen N4. The lengthening of the C1–N4 bond (0.03 Å) and shortening of the C1–N2 bond (0.05 Å) clearly reflects the change in ligand donor properties of the indole nitrogen (N2) upon protonation. Further protonation affords a neutral ligand in complex **4**, with no Ru–O bond.

The electronic environment at Ru imparted by each protonation state of the BH_3PI ligand was quantified in **1**-**3**. In addition to the structural metrics, differential pulse voltammetry (DPV) experiments were used to assess electronic differences at the Ru center imposed by each protonation state of BH_3PI in **1**-**3**. The potentials for the first oxidative event undergo an anodic shift with increasing protonation state (E_{Ox}: -660, -460 and 195 mV, vs. Fc/Fc^+, for **1**, **2**, and **3** in propylene carbonate/0.1 M [^{n}Bu$_4$][PF_6]), which is consistent with a more electron-rich metal center imparted by each successive deprotonation.

2.4 E-H Heterolysis: Reactions and Kinetics

We evaluated the cooperative ability of the charge-disparate OH/O^- moieties and ruthenium in **2** to promote heterolytic H-E (E = H, BR_2) bond activation. When treated with H_2 (30 psig) at room temperature, a reaction occurred. The ^{1}H NMR spectrum (-80 °C) revealed a new hydride resonance (δ -10.5) and an acidic proton peak at δ +13.5 that integrated in a 1:2 ratio, consistent with H_2 heterolysis across the metal-ligand framework to form hydride complex **5** in 91% yield. These resonances broadened as the temperature was raised, suggesting a dynamic exchange process. Analysis of the minimum spin-lattice relaxation times, T_1(min), confirmed that the *OH* and hydride peaks undergo chemical exchange and are in close proximity, as noted by their similar short T_1(min) values (76 and 72 ms; -15 °C, 500 MHz). While short T_1 values are often associated with metal η^2-H_2 complexes, they may also reflect unusually short H-H distances in metal hydride complexes engaged in dihydrogen bonds through dipole-dipole relaxation.[91] The unusually short T_1 values in **5** are likely a consequence of close H-H contacts to both of the appended OH groups through bifurcated dihydrogen bonds. Proton/hydride exchange likely proceeds through a transient rotating η^2-H_2 intermediate, which was not observed (Figure **2-4**b).[92] The exchange rate was measured *via* spin-saturation transfer[93] from -75 to -15 °C, which provided a $\Delta H^‡$ and $\Delta S^‡$ for the H^+/H^- exchange process of 7.7(2) kcal/mol and -20(1) e.u. (corresponding to an extrapolated rate of 519 s^{-1} at 25 °C)[94, 95] through analysis of an Eyring plot.[93c,95a,96]

The solid state structure of **5** (Figure **2-4**) reveals a Ru-H unit engaged in highly unusual bifurcated dihydrogen bonds with both appended OH groups.[97,98] The Ru-H and both OH protons are clearly distinguishable, and located from the difference map. H-H contacts between H1 and H(2,3) of 1.29 and 1.51 Å (average: 1.40 Å) reflect strong and extremely short dihydrogen bonds (typical values range from 1.7-2.0 Å).[99] As X-Ray diffraction data do not provide precise measurements of H-H distances, we evaluated the M-H---HO distance using through-space dipole-dipole induced nuclear spin relaxation, which afforded an average H-H distance of 1.51 Å at -35° C.[91] These two measurements, taken through dissimilar methods, showcase the highly coupled proton/hydride environment imposed by the rigid isoindoline ligand, and establish the dihydrogen bonds in **5** as among the shortest yet reported.[95a,100]

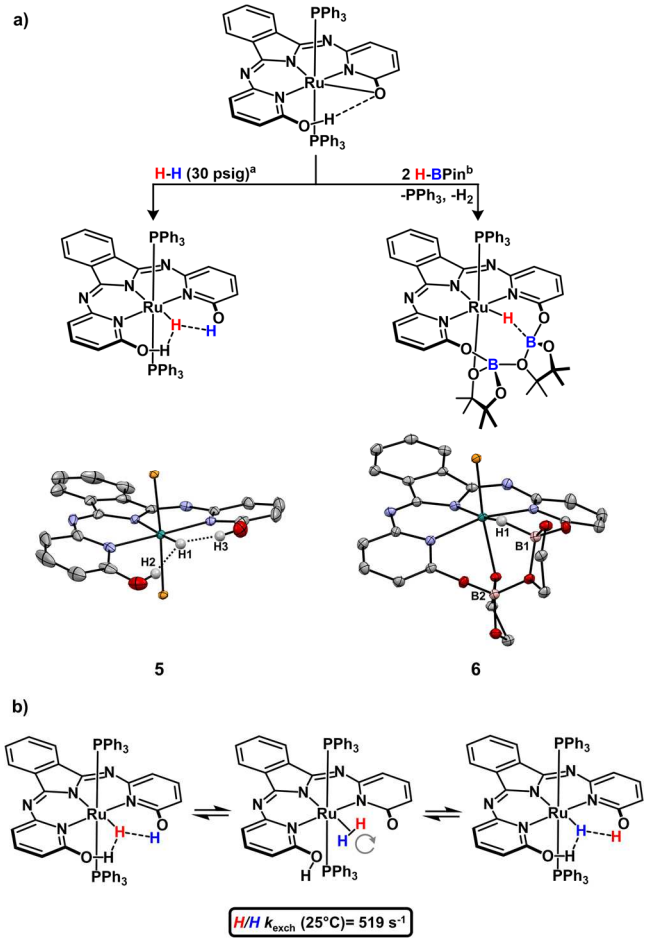

Figure 2-4 a) H_2 and HBPin heterolysis. b) Proposed mechanism for H/H exchange.

Following the demonstration of **2** mediating heterolytic cleavage of H_2, we explored similar reactivity with the B-H bond in pinacolborane (HBPin). When **2** was combined with 2 equiv. HBPin in methylcyclohexane, complex **6** was obtained in 87% yield, and was characterized by ^{1}H,

^{31}P, and ^{11}B NMR spectroscopy. The ^{1}H NMR spectrum revealed a hydride signal at δ -11.0 (J_{HB}: 20 Hz), while the ^{31}P and ^{11}B NMR spectra revealed singlets at δ 69.6 and δ 6.0, respectively, consistent with a single phosphorus-containing compound with a tetrahedral boron unit.

Slow cooling of a solution of 6 in methylcyclohexane afforded crystals suitable for single crystal X-Ray diffraction. The solid-state structure is analogous to 5 and similar B-H activation occurs across the Ru-O bond, with the BPin boron (B1) positioned in close proximity to the resulting hydride. The ruthenium hydride (H1) was located from the difference map and freely refined. The B1-H1 contact (1.39 Å) in 6 contact reflects a weak B-H interaction (*cf.* B-H in $LiBH_4$: 1.10 Å)[101] and is similar to a previously reported Ru-H-HBPin coordination complex (1.39 Å).[102] Although bond distances to hydrogen cannot be accurately obtained from typical X-Ray data, the low J_{HB} coupling constant (20 Hz; typical B-H single bond coupling is 140 Hz)[103] further supports a weak B-H interaction, indicating that 6 may represent an arrested state of B-H heterolysis. In addition to the HBPin activation across the Ru-O unit, the other appended OH group was transformed into an OBPin, with the OBPin unit also participating as a ligand to complete an octahedral geometry about Ru.

2.5 Catalytic Hydroboration of Polar Bonds

Based on the rapid H-E activation and exchange rates noted above, we hypothesized that the low kinetic barrier should translate into rapid catalysis. We investigated the catalytic competence of the bifunctional complexes **1**, **2**, and **3** for polar bond hydroboration using ketone and nitrile substrates. When HBPin was introduced to a vial containing 1 equiv. acetophenone and 4 mol% **2** in C_6D_6, 3% conversion to pinacolborato 1-phenylethanol occurred in 20 minutes at 25 °C. Catalysis was significantly improved for the deprotonated complex, **1**, while fully protonated **3** showed only trace activity. For instance, when using identical reaction conditions with 100-fold less catalyst loading (0.04 mol% **1**), 54% conversion to borylated 1-phenylethanol occurred (quantitative conversion after 1 h; (initial TOF = 1.2(3) s^{-1})).[104] The catalytic activity of **1** is one of the fastest reported for ketone hydroboration at room temperature.[33c,88b,105] For comparison, the unfunctionalized complex ($HRu(bMepi)(PPh_3)_2$, **7**, Figure **2-5**), was significantly slower (initial TOF = 0.037(4) s^{-1}) than **1** under identical conditions. Thus, we found a dramatic effect on catalysis enabled by substituting inert -*CH₃* groups with polar, reactive -*OH* groups.

Due to the ability of the bifunctional complexes **1**-**3** to promote rapid ketone hydroboration, we targeted the more challenging hydroboration of nitriles.[82b,88b] Using 5 mol% complex **2** in the presence of 4.5 equiv. HBPin, benzonitrile was converted to the borylated primary amine as the sole product in very low yield (0.05%) after 13 min at 25 °C in C_6D_6 solvent; complex **1** promoted the hydroboration reaction in a much higher yield (66%) after 13 min.[106] Because the electronic environment at ruthenium is regulated by the ligand protonation state, we hypothesized that the strong proton-responsive effect would translate into distinct catalytic rates dependent on protonation state. Initial TOFs for complexes **1-3** were determined *via in-situ* NMR spectroscopy (Figure **2-5**) and compared with **1**. Complex **3** was inactive for nitrile hydroboration (no product detected). In contrast, catalysis was *turned on* using complex **2** (initial TOF = 2.7(3) x 10^{-4} s^{-1}), and the rate was further accelerated using complex **1** (initial TOF = 1.19(2) x 10^{-2} s^{-1}). We note that single proton transfer events of the appended OH groups promote dramatic changes in reaction rate for **1**-**3**, which serve to both gate and accelerate the nitrile hydroboration reaction.

Catalytic nitrile hydroboration with **1** was general to several *p*-substituted aryl nitriles in moderate to excellent yields (Table 1). The reaction is tolerant to several functional groups, leaving methyl esters (**10m**, 95%), additional nitriles (**10j**, 89%), benzyl ethers (**10c**, 79%), free amines (**10i**, 78%), trifluoromethyl (**10d**, *p*-88%; **10e**, *o*-50%), 2-furyl (**10l**, 96%) and 2-pyridyl (**10k**, 76%) functionality intact. These results suggest that the catalytic hydroboration reaction shows selectivity that is distinct from previously reported heterogeneous and homogeneous reductions; heterogeneous systems cleave benzyl ethers in the presence of nitriles,[87] and homogeneous catalytic systems have not shown selectivity for nitriles over esters.[82b,88b,105a,107]

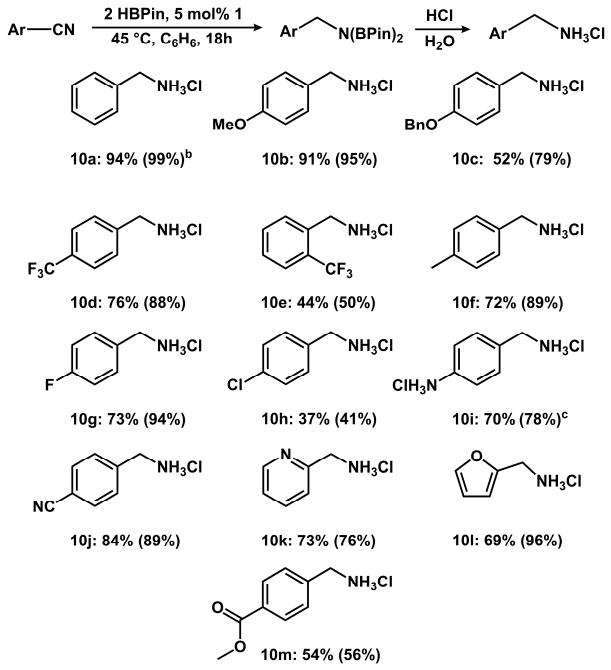

Figure 2-5 Nitrile Hydroboration Scope

2.6 Mechanistic Analysis

Many reduction reactions involving platinum-group metals have recently been shown to promote the formation of catalytically active nanosized clusters.[108] In order to interrogate the form of the active catalyst (homogeneous or heterogeneous) in the current system, we undertook selective poisoning experiments. The addition of Hg(0) (~800 equiv), which was added after catalysis was initiated, did not appreciably change the overall reaction profile. In addition, we performed substoichiometric ligand poisoning experiments, which are a simple and effective means of assessing whether a given precatalyst forms a catalyst of higher nuclearity. No change in the reaction profile was noted with 0.5 equiv. PMe_3, while complete poisoning required 2 equiv. PMe_3, inconsistent with a heterogeneous system, where low surface area aggregates are typically poisoned by ≪1 equiv of added ligand poison. Finally, in the absence of any poisoning reagent, highly reproducible (nonsigmoidal) reaction kinetic profiles were observed. The combined results of these tests suggest that the active catalytic species is indeed a homogeneous ruthenium complex.

The protonation-state dependent rate acceleration for **1**-**3** may be due to regulation of either the metal's electronic environment by changes in the protonation state, or alternatively, by general base catalysis. To test the efficiency of transition metal-free base catalyzed nitrile hydroboration, we first assessed the pK_a and of the monoprotonated complex, **2**, (pK_a (**2**)= between 9.5 and 10.8)

and selected (K(18-crown-6)(*p*-cresolate) (**9**: pK_a=10.2)) as a suitable model base to evaluate general base catalysis.[109] Using identical reaction conditions as described above for nitrile hydroboration, **9** effected the hydroboration reaction with modest efficiency (1.8% conversion in 13 min; initial TOF=1.4(2) x 10^{-4} s^{-1}), which is two orders of magnitude lower than **1**. Activity did not improve in the presence of an equimolar mixture of **7** and **9**, indicating that nitrile activation by coordination to ruthenium is not responsible (or required) for promoting the reduction reaction. The low catalytic activity of a base with a similar pK_b to **1** indicates that the change in the overall protonation state at the metal serves to regulate reactivity at the metal site, rather than to promote general base catalysis.[88a,110]

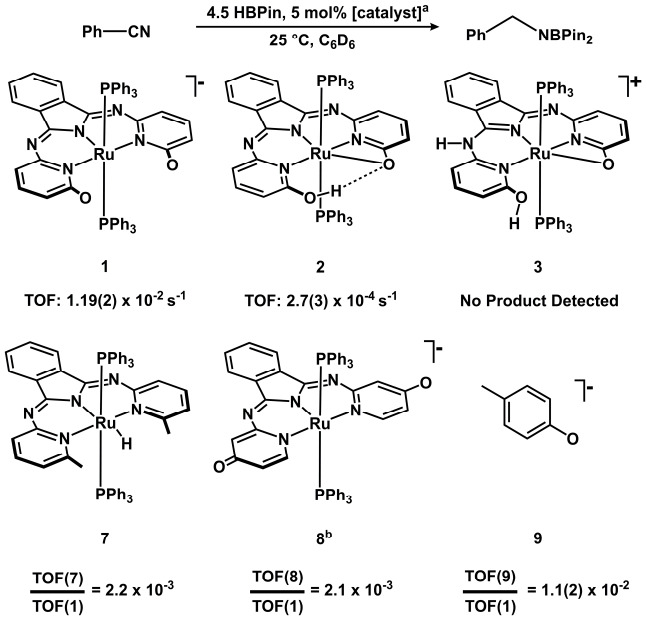

Figure 2-6 Benzonitrile hydroboration using 1-3, 7-9.

To evaluate the importance of bifunctional E-H activation, we conducted the benzonitrile hydroboration reaction using complex **7**, a variant with inert -*CH₃* groups rather than -*OH* groups; this complex had minimal activity (relative TOF to **1** = 2.2 x 10^{-3} at 25 °C). To examine whether catalysis was due to electronic differences imparted by the -*OH* groups, a variant that moves the -*OH* groups from the *ortho* to the *para* position (complex **8**) was assessed. **8** presents an electronically similar ligand field, yet maintains a distinct spatial orientation of the -*OH* groups, which is directed *away* from the Ru center. Under identical reaction conditions, **8** was significantly slower than **1** (relative TOF to **1** = 2.1 x 10^{-3}), which suggests that the position of the -*OH* groups play a key role to impart hydroboration reactivity. Collectively, the very low catalytic activities of

7, **8**, and **9** indicate that the identity and position of the *–OH* groups in **1** is essential for catalytic activity, and strongly implicate a crucial role of metal-ligand cooperativity for the B-H heterolysis and transfer steps in nitrile hydroboration.

The above evidence indicates that a cooperative mechanism is operative. At high PhCN (0.2 M) and HBPin (0.5 M) concentrations, present under standard conditions, the reaction is first order in **1** and zero order in both HBPin and benzonitrile,[111] consistent with a mononuclear bifunctional mechanism where H-B activation across the Ru-O unit and ligand substitution/precoordination are *not* rate limiting. Instead, an intramolecular transformation is implicated in the rate determining step. To distinguish between a limiting outer-sphere or inner-sphere type pathway, we evaluated catalytic reactions *in situ*.

In order to identify potential catalytic intermediates, stoichiometric reactions between **1** and either HBPin or PhCN were analyzed by NMR spectroscopy. Under conditions of excess PhCN similar to those used in catalysis, one equiv. free PPh_3 was observed. Alternatively, in the presence of excess HBPin, conversion to a mixture of hydride containing species was observed in addition to a single phosphorus resonance at δ 39.6. Two of the hydride resonances (δ -5.95 and -10.44) were affected upon selective ^{31}P decoupling, which confirms that both hydrides reside on the same complex as a phosphine ligand. Their $^{2}J_{HP}$ coupling constants of 103 and 12 Hz are consistent with hydride ligands that are *trans* and *cis* to a phosphine ligand, respectively. We tentatively assign this species as **11**, which we note is coordinatively saturated.

In-situ ^{1}H NMR spectra revealed that **11** is also present *during* catalysis, and importantly, its concentration tracked with the consumption of nitrile substrate.[112] In addition to observing catalytically relevant intermediates, a species at δ 8.78 was observed and identified as an imine by an $^{1}H/^{13}C$-gHSQC experiment. During the course of catalysis, the imine peak remained as a singlet (and did not shift its position) and its concentration was 3.5 times greater than the concentration of total ruthenium, consistent with a free, rather than coordinated, imine species. Our proposed mechanism illustrating key species in the nitrile hydroboration reaction is shown in Figure **2-7**, and features BH activation of HBPin by **1**, which can participate in an outer-sphere type transfer of the H and BPin units across the nitrile substrate.[113] We propose that the imine intermediate can dissociate, equilibrating with **11** and that the second hydride transfer is rate limiting. The catalytic hydroboration reaction was hindered in the presence of exogenous alkali metal chelators (18-crown-6 or 2,2,2-cryptand), and the alkali metal is proposed to facilitate the assembly of multiple

BPin groups, driving the equilibrium toward coordinated imine. The identification of six-coordinate Ru(II) complexes during catalysis and minimal activity observed for **7** in the presence of **9** suggest an outer sphere pathway may be more likely than an inner-sphere pathway for rate limiting hydride transfer to the observed imine intermediate. This proposed mechanism is consistent with the observed protonation-state dependent relative rates of **1**-**3**: the increase in metal electron density upon deprotonation leads to a concomitant increase in Ru-H hydricity and the number of hydride ligands, facilitating nucleophilic hydride transfer in the rate determining step.

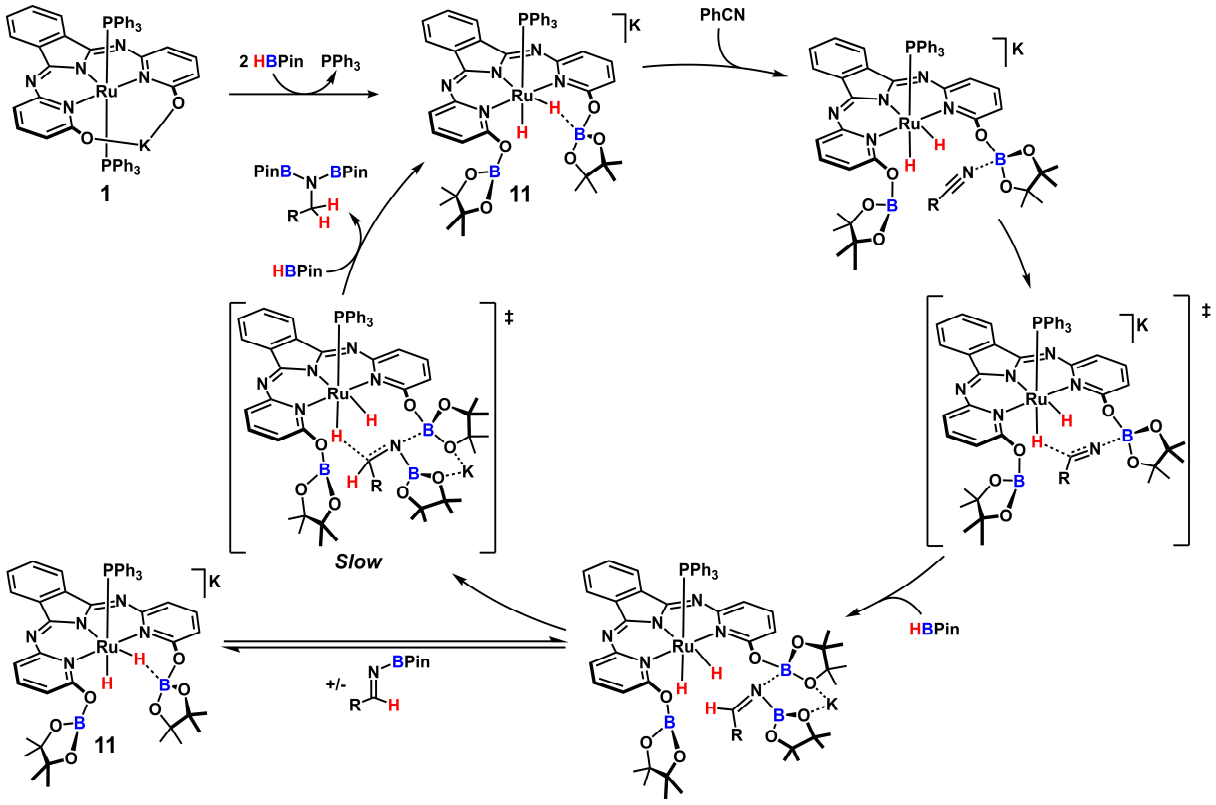

Figure 2-7 Proposed mechanism for nitrile hydroboration by **1.**

2.7 Conclusions

In summary, a proton-responsive bifunctional catalyst for nitrile hydroboration with unprecedented efficiency was developed. Nitrile hydroboration with HBPin has only been reported on one previous occasion with one substrate, and harsh conditions were required.[88a] **1** catalyzes this reaction under mild conditions with a variety of aromatic nitriles. This reaction enables the selective reduction of nitriles to produce synthetically useful diborylamines that can used as organic synthons,[114115] or be easily deprotected.[88b] The designed bifunctional ligand serves a

critical role to mediate and regulate this reaction by (1) promoting E-H bond heterolysis, (2) tethering the BPin unit for cooperative substrate interactions, and (3) facilitating proton-switchable regulation of electron density at the metal.

2.8 Experimental Details

2.8.1 Ligand Synthesis

Bis(2-bromo-6-iminopyridyl)isoindolene:

2-Bromo-6-aminopyridine (10.000 g; 57.800 mmol), phthalonitrile (3.526 g; 27.52 mmol) and $CaCl_2$ (0.301 g; 2.71 mmol) were weighed in air into a 200 mL Schlenk flask. To this was added 75 mL of hexanol and a stirbar, and the vessel was fitted with a reflux condenser equipped with a T-joint in line to the nitrogen manifold. The headspace of the flask was flushed with nitrogen, and the suspension was heated in a 170 °C oil bath for two days with vigorous stirring, which resulted in a green suspension. The suspension was then cooled to -20 °C for 16 h and filtered, affording yellow crystals. The solid was washed with water (200 mL), diethyl ether (200 mL), ethyl acetate (200 mL), and hexanes (200 mL) to afford a yellow-green solid. The filter cake was extracted into chloroform (ca. 800 mL), until complete dissolution, and the chloroform solution was concentrated to ca. 400 mL at 61 °C. 50 mL ethyl acetate was then added, and the solution was cooled to -20° C for 16 h to afford 9.22 g (73% yield) of light orange prismatic crystals. ^{1}H-NMR ($CDCl_3$): 11.88 (ζ, 1H, s), 7.99 (β, 2H (q, J_{1H-1H}=5.6, 3.1)), 7.63 (α, 2H (q, J_{1H-1H}=5.6, 3.1)), 7.56 (ε, 2H (t, J_{1H-1H}=7.8)), 7.25 (γ, 2H (d, J_{1H-1H}=12.6)), 7.24 (γ, 2H, (d, J_{1H-1H}=12.6)). ^{13}C-NMR: 160.55, 153.48, 140.34, 140.22, 135.30, 132.30, 124.37, 122.90, 120.24. HRMS: 457.9444 (M+H: 457.9444).

Bis(2-benzyloxy-6-iminopyridyl)isoindolene:

HBBrPI (3.000 g; 6.56 mmol) and NaH (1.416 g; 59.06 mmol) were weighed into a Schlenk flask and 65 mL of THF was added. After the cessation of effervescence, benzyl alcohol (5.407 mL; 52.50 mmol) was added dropwise over the course of five minutes to the solution. The suspension was then brought to reflux with vigorous stirring for 6.5 h at 66 °C. The volatiles were removed by rotary evaporation and the crude solid was dissolved in 600 mL of a mixture of CH_2Cl_2 and water (1:1); the water layer was then removed, and the deep yellow CH_2Cl_2 extract was washed with 200 mL water, 100 mL brine, dried with MgSO4, filtered, and concentrated to ca. 150 mL at 44 °C. The addition of 150 mL of methanol followed by cooling to -20 °C for 16h afforded 2.381

g (71% yield) of fine yellow needles after filtration. ^{1}H-NMR ($CDCl_3$): 11.76 (ζ, 1H, s), 8.08 (β, 2H ($J_{1H\text{-}1H}$=5.5, 3.0, q), 7.67 (α, 2H ($J_{1H\text{-}1H}$=5.5, 3.0, q)), 7.57 (ε, 2H ($J_{1H\text{-}1H}$=7.8, t)), 7.28-7.23 (η, 10H, m), 6.97 (γ, 2H ($J_{1H\text{-}1H}$=7.5, d)), 6.45 (γ, 2H, ($J_{1H\text{-}1H}$=8.1, d)), 4.97 (η, 4H, s). ^{13}C-NMR: 162.80, 158.23, 152.31, 140.74, 136.70, 135.52, 131.96, 128.47, 128.39, 128.05, 122.77, 114.34, 107.62, 68.09. HRMS: 512.2096 (M+H: 512.2096).

Bis(2-hydroxy-6-iminopyridyl)isoindolene (BH_3PI):

HBBnPI (2.041 g; 3.992 mmol) was weighed into a Teflon-capped vial with a magnetic stirbar. The solid was then combined with neat BBr_3 (7.58 mL; 79.8 mmol), resulting in a blood-red suspension, that was vigorously stirred for 16 h. The suspension was diluted with 100 mL of pentane and rapidly poured into a chilled solution of NaOH (600 mL; 1.67 M) with stirring (Note: This step must be performed in an efficient fume hood). The alkaline suspension was washed with CH_2Cl_2 (2 x 200 mL), diethyl ether (200 mL), and hexanes (200 mL), filtered through a pad of Celite and the deep red solution acidified to pH 4 using glacial acetic acid. After cooling to 5 °C, the product was obtained as a red solid after filtration. Yield: 0.986 g (74%). ^{1}H-gCOSY spectroscopy was used to assign a peak overlapping with pyridine. ^{1}H-NMR (Pyridine, d_5): 8.24 (β, 2H ($J_{1H\text{-}1H}$=4.9, 3.0, q)), 7.70 (ε, 2H ($J_{1H\text{-}1H}$=7.7, t)), 7.59 (α, overlap with pyridine (q)), 7.30 (γ, 2H ($J_{1H\text{-}1H}$=7.3, d)), 6.75 (γ, 2H ($J_{1H\text{-}1H}$=7.9, d)). ^{13}C-NMR: 163.91, 159.81, 154.87, 142.66, 137.71, 133.20, 124.17, 116.24, 108.46. HRMS: 332.1146 (M+H: 332.1147). Anal. Calcd for $C_{18}H_{13}O_2N_5$: C, 65.25; H, 3.95; N, 21.14. Found: C, 65.28; H, 3.93; N, 21.09.

2.8.2 Preparation of Complexes

Ru(BH_2PI)(PPh_3)Cl(NaCl)(DMF):

BH3PI (924 mg; 2.79 mmol), sodium methoxide (150.75 mg; 2.79 mmol), 16 mL of DMF, and $Ru(PPh_3)_3Cl_2$ (2.674 g; 2.79 mmol) were combined and sealed in a 20 mL vial with a teflon-lined screw cap. The red suspension was heated to 100 °C for 24 h with strong stirring to give a green precipitate, which was recovered by filtration through a glass fritted funnel. The green solid was washed with 150 mL DMF, 150 mL THF, 100 mL diethyl ether, and 100 mL pentane, then dried under high vacuum for 24 h to afford 1.180 g (53% yield) of Ru(BH_2PI)(PPh_3)Cl(NaCl)(DMF). Note: the product is insoluble in most solvents and has extremely low solubility in MeOH. ^{1}H-NMR (MeOH, d_4): 8.03 (β, 2H, broad), 7.68 (ε, 2H ($J_{1H\text{-}1H}$=8.0, t)), 7.59(α, 2H, broad), 7.20 (ζ, 3H ($J_{1H\text{-}1H}$=7.1, t)), 7.01 (ζ, 6H ($J_{1H\text{-}1H}$=6.9, t)) , 6.94 (ζ, 6H ($J_{1H\text{-}1H}$=9.3, t)), 6.80 (γ, 2H ($J_{1H\text{-}1H}$=8.7, d, broad)), 6.33 (2H, ($J_{1H\text{-}1H}$=7.4, d)); ^{31}P-NMR: 62.15. IR

(ATR, cm^{-1}): 3048, 2980, 2921, 1672, 1634, 1547, 1520, 1463, 1434, 1410, 1385, 1343, 1331, 1262, 1099, 1088, 793, 771, 765, 747, 704, 698, 668. LCT-MS: 694.2 (M-Cl=694.09), 432.1(M-(Cl, PPh_3)=432.00). Anal. Calcd for $C_{39}H_{34}Cl_2N_6NaO_3PRu$: C, 54.43; H, 3.98; N, 9.76. Found: C, 54.70; H, 3.80; N, 9.44.

[$Ru(BH_0PI)(PPh_3)_2$][K(18-crown-6)] (1):

$Ru(BH_1PI)(PPh_3)_2$ (2) (638.0 mg, 0.668 mmol), KHMDS (146 mg, 0.733 mmol) and 18-crown-6 (194 mg, 0.757 mmol), and 10 mL C_6H_6 were combined and sealed in a scintillation vial with a teflon-lined screw cap. The suspension was stirred for 16 h, transferred to a 100 mL flask, layered with 40 mL pentane, and sealed with a rubber septum. After 24 hours, the mixture was filtered to afford 729.2 mg (86%) of a black powder. ^{1}H-NMR (C_6D_6): 7.81 (β, 2H, broad), 7.37 (ε, 2H ($J_{1H\text{-}1H}$=7.1, t)), 7.31 (ζ, 12H ($J_{1H\text{-}1H}$=6.7, d)), 6.97 (α, 2H ($J_{1H\text{-}1H}$=4.78, 2.87, q)), 6.77 (ζ, γ, 20H, broad), 5.81 (γ, 2H, ($J_{1H\text{-}1H}$=6.0, d)), 3.17(η, 24H, broad). ^{31}P-NMR: 30.69. UV-Vis: 566nm (Benzene). IR (ATR, cm^{-1}): 3051, 2898, 1564, 1509, 1462, 1432, 1350, 1313, 1213, 1191, 1060, 1028, 1004, 960, 906, 836, 797, 770, 735, 692, 581. Anal. Calcd for $C_{66}H_{64}N_5O_8P_2Ru$: C, 63.05; H, 5.13; N, 5.57. Found: C, 63.42; H, 5.05; N, 5.59. Differential Pulse Voltammetry (0.1 M $TBAPF_6$ in propylene carbonate): E_{ox} -195 mV (mV vs. Fc/Fc^+).

$Ru(BH_1PI)(PPh_3)_2$ (2):

$Ru(BH_2PI)(PPh_3)Cl$ (898 mg; 1.23 mmol), PPh_3 (297 mg; 1.23 mmol), sodium methoxide (61.3 mg; 1.23 mmol), and 20 mL MeOH was combined and sealed in a scintillation vial with a teflon-lined screw cap. The dark suspension was stirred vigorously for 3 h at 66 °C, and volatiles then removed under vacuum. The residue was extracted with 60 mL CH_2Cl_2 and the black solution dried under vacuum. The black solid was then reconstituted in 20 mL CH_2Cl_2 and layered with 100 mL pentane. After 24 hours, the resulting mixture was filtered to afford 638 mg (54% yield) of black rhombohedral crystals. Note: In solutions of CH_2Cl_2, THF, and benzene, this compound exhibits dynamic dissociation of PPh_3 by NMR spectroscopy to give a three-component mixture. This behavior is still observed in methanol solutions, but the addition of 2 EQ. PPh_3 to NMR samples provides clean ^{1}H-NMR spectra of $Ru(BH_1PI)(PPh_3)_2$. Crystals suitable for elemental analysis were obtained after 2 successive recrystallizations from methanol. ^{1}H-NMR (MeOH, d_4): 7.76 (β, 2H ($J_{1H\text{-}1H}$=5.3, 2.9, q)), 7.40 (α, 2H ($J_{1H\text{-}1H}$=5.3, 2.9, q)), 7.07 (ζ, γ, 8H, m), 6.90 (ζ, 24 H, m), 6.27 (2H, ($J_{1H\text{-}1H}$=5.8, d)), 5.63 (2H, ($J_{1H\text{-}1H}$=8.0, d)). ^{31}P-NMR: 34.24. UV-Vis: 589 nm (Benzene). IR (ATR, cm^{-1}): 3051, 1533, 1498, 1481, 1459, 1431, 1315, 1289, 1255, 1187, 1145,

1105, 904, 793, 740, 692. Differential Pulse Voltammetry (0.1 M $TBAPF_6$ in propylene carbonate): E_{ox} 460mV (mV vs. Fc/Fc^+). Anal. Calcd for $C_{54}H_{41}N_5O_2P_2Ru$: C, 67.92; H, 4.33; N, 7.33. Found: C, 67.81; H, 4.61; N, 7.22.

$Ru(BH_2PI)(PPh_3)_2TFA$ (3):

$Ru(BH_1PI)(PPh_3)_2$ (2) (100 mg; 0.104 mmol) was dissolved in 1.5 mL CH_2Cl_2, and to this was added trifluoroacetic acid as a 1% v/v stock solution in CH_2Cl_2 (8.02 µL; 0.104 mmol). The brilliant green solution was stirred for 2 h, then layered with 15 mL pentane. After 24 hours, the mixture was filtered to afford 104 mg (94%) of black powder. ^{1}H-NMR (MeOH, d_4): 7.91 (β, 2H (J_{1H-1H}=5.0, 2.86, q)), 7.63 (α, 2H (J_{1H-1H}=5.5, 3.0, q)), 7.39 (ε, 2H (J_{1H-1H}=8.0, t)), 7.25 (ζ, 6H (J_{1H-1H}=7.3, t)), 7.03 (ζ, 12H (J_{1H-1H}=7.8, t)), 6.96 (ζ, 12H, m), 6.59 (γ, 2H, broad), 6.00 (γ, 2H (J_{1H-1H}=8.1, d)). ^{31}P-NMR (MeOH, d_4): 32.14. ^{19}F-NMR: 76.96 UV-Vis: 624 nm (Benzene) IR: 3057, 1670, 1640, 1578, 1542, 1514, 1481, 1463, 1453, 1433, 1361, 1318, 1292, 1267, 1195, 1159, 1123, 1093, 794, 771, 745, 695, 673, 655. Differential Pulse Voltammetry (0.1 M $TBAPF_6$ in propylene carbonate): E_{ox}: 660 mV (mV vs. Fc/Fc^+). Anal. Calcd for $C_{54}H_{41}N_5O_2P_2Ru$: C, 62.92; H, 3.96; N, 6.55. Found: C, 63.23; H, 4.09; N, 6.56.

$Ru(BH_3PI)(PPh_3)_2TFA_2$ (4):

$Ru(BH_1PI)(PPh_3)_2$ (2) (10.0 mg, 0.0104 mmol), trifluoracetic acid (3.2 µL, 0.042 mmol), and 600 µL CH_2Cl_2 were combined in a sealed NMR tube and spectra were recorded. Upon standing for three weeks, platelike green crystals were recovered and used for X-Ray diffractometry. ^{1}H-NMR (CH_2Cl_2): 13.84(η, 3H, broad), 8.09(β, 2H (J_{1H-1H}=5.2, 2.9, q)), 7.63(α, 2H (J_{1H-1H}=5.6, 2.9, q)), 7.56(ε, 2H (J_{1H-1H}=8.0, t)), 7.03(γ, 2H (J_{1H-1H}=8.4, d)), 7.00(ζ, 12H, (J_{1H-1H}=7.9, t)), 6.88(18H, m), 6.50(2H, (J_{1H-1H}=7.9, d)). ^{31}P-NMR: 30.48. ^{19}F-NMR: -75.00.

$RuH(BH_2PI)(PPh_3)_2$ (5):

$Ru(BH_1PI)(PPh_3)_2$ (2) (10.0 mg, 0.0104 mmol) was dissolved in 600 µL CH_2Cl_2 in a J-Young NMR tube and the headspace pressurized with 30 psig H_2. The tube was then shaken vigorously, and allowed to stand for four hours; 91% conversion was observed via NMR spectroscopy. ^{1}H-NMR (C_6D_6): 13.15 (η, 2H, s), 8.15 (β, 2H (J_{1H-1H}=5.4, 3.1, q)), 7.26 (ζ, ε, α, 16H, m), 6.93 (γ, 2H (J_{1H-1H}=7.7, d)), 6.81(ζ, 18H, m), 6.08(γ, 2H (J_{1H-1H}=7.7, d)), -10.53 (θ, 1H (J_{31P-1H}=15, t)). ^{31}P-NMR: 43.59. UV-Vis: 566 nm (Benzene). IR: 3050.88, 1636.70, 1578.13,1528.79, 1431.80, 1383.95, 1318.65, 1292.97, 1265.63, 1185.20, 1149.57, 1108.77, 1089.41, 998.24, 797.91, 742.68, 695.35, 517.58.

RuH(B(OBPin)$_2$PI)(PPh$_3$) (6):

RuBHPI(PPh$_3$)$_2$ (2) (10.0 mg, 0.0104 mmol) was suspended in 0.5 mL methylcyclohexane. HBPin (3.0 µL, 0.0208 mmol) was then added, and the mixture stirred for one hour. This was then filtered, and the volatiles removed under vacuum. The resulting purple solid was dissolved in C_6D_6 and used for NMR characterization (87% chemical yield based on integration vs. PhSiMe$_3$). ^{1}H-gCOSY was used for the assignment of resonances. ^{1}H-NMR: 8.20 (β, 1H, (J_{1H-1H}=7.3, d)), 7.80 (β*, 1H, (J_{1H-1H}=7.3, d)), 7.36 (γ*, 1H, (J_{1H-1H}=7.3, d)), 7.35 (ζ, 6H, (J_{1H-1H}=7.5, t)), 7.14 (α, 1H, (J_{1H-1H}=7.3, t)), 7.09 (ε, 1H, (J_{1H-1H}=7.6, t)), 7.07 (ε*, 1H, (J_{1H-1H}=7.7, t)), 7.04 (α*, 1H, (J_{1H-1H}=7.3, t)), 7.01 (γ, 1H, d, overlap), 7.00 (ζ, 9H, m), 6.49 (γ*, 1H, (J_{1H-1H}=7.7, d)), 6.37 (γ, 1H, (J_{1H-1H}=7.6, d)), 1.82 (η, 3H, s), 1.70 (η, 3H, s), 1.65 (η, 3H, s), 1.20 (η, 3H, s), 0.99 (η, 3H, s), 0.69 (η, 3H, s), 0.30 (η, 3H, s), 0.29 (η, 3H, s), -10.99 (θ, 1H, d (J_{1H-11B}=20, d)). ^{31}P-NMR: 69.61. ^{11}B-NMR: 6.08.

2.8.3 General Procedure for Catalytic Nitrile Hydroboration

Benzonitrile (32.8 mg; 0.318 mmol), trimethylphenylsilane (10.0 µL; 0.058 mmol) internal standard, 1.2 mL C_6H_6, and [Ru(BH$_0$PI)(PPh$_3$)$_2$][K(18-crown-6)] (**1**) (20.0 mg; 15 µmol) were sealed at 25° C in a screw-cap 8 mL vial, and stirred for 5 minutes. Pinacolborane (92 µL; 0.636 mmol) was added, and the solution stirred at 45° C for 18h, at which time a 40 µL sample was taken for NMR analysis (used for determination of chemical yields, calculated by integration of ArC*H*$_2$N(BPin)$_2$). Volatiles were then removed under vacuum, and the residue stirred in 5 mL aqueous HCl (0.05 M) at room temperature for two hours. After this time, a green precipitate was removed with filtration through a celite pad. The resulting light-yellow solution was lyophilized and then dissolved in 1.5 mL 0.05 M HCl and subjected to flash reverse-phase chromatography with water as the eluent (Biotage SNAP KP-C18-HS, 30g). Benzylammonium chloride eluted within the first three column volumes, and the combined fractions were lyophilized to give a fine white powder. Chemical yield: 99%. Isolated yield: 94%.

2.8.4 Electrochemical Characterization

Differential pulse voltammetric oxidation of **1-3** in propylene carbonate/0.1 M tetrabutylammonium hexafluorophosphate. DPV parameters: 50 mV pulse height, 10 mV pulse width, 100 ms period, 10 mV increment. A three-electrode setup employing a glassy carbon working electrode, Ag wire reference electrode, and Pt wire counter electrode was used for

differential pulse voltammetry; at the end of the experiments, ferrocene was added as an internal reference. First oxidative events (vs. $Fc^{0/+}$): (**1**) -660 mV; (**2**) -460 mV; (**3**) 0.195 mV.

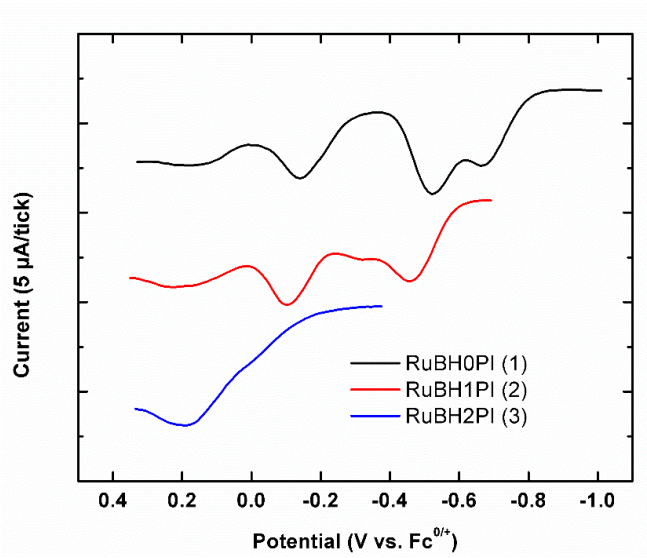

Figure 2-8 Differential Pulse Voltammetry for **1-3**

2.8.5 Spin Saturation Transfer Kinetics with Ru(H)(BH2PI)(PPh3)2

An NMR tube charged with 10 mg of $Ru(HBH_2PI)(PPh_3)_2$ and 600 µL CD_2Cl_2 was cooled to the desired temperature (-74, -55, -35, -15 °C, 5 °C, 25°C) and a spin-saturation transfer experiment was conducted. The hydride resonance was irradiated with a two second pulse. The delay between successive data acquisitions was 10 seconds. T_1 values were determined at each temperature for both the Ru-H and OH resonances through standard inversion recovery experiments. The difference in integrated signal for the OH resonance between such experiments with and without Ru-H saturation, against the solvent as an internal standard, was then used along with the respective T_1 value in the following equation to determine the rate constant k of H^+/H^- exchange at each temperature. These values are plotted below as k vs. $\ln(k)/T$, allowing for the determination of $\Delta H^{\ddagger}$ and $\Delta S^{\ddagger}$ using the Eyring equation.[93a]

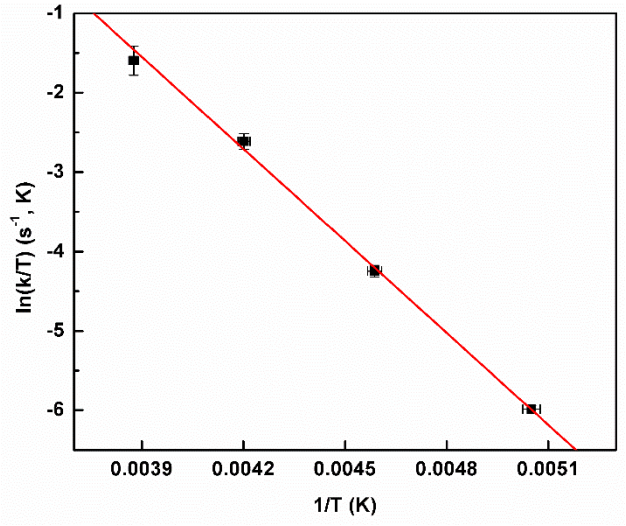

$$k = \frac{1}{T_{OH}}\left(\frac{I(OH)_0}{I(OH)_{saturated}} - 1\right)$$

R^2=0.99782

$\Delta H^{\ddagger}$=7.6(2) kcal/mol $\Delta S^{\ddagger}$=-20.3(9) EU

Figure 2-9 Eyring Plot for H-H Exchange in **5**

2.8.6 H-H Distance Measurement in $Ru(HBH_2PI)(PPh_3)_2$ via Dipole-Dipole Relaxation

The average distance between the acidic protons and hydride in solvated $Ru(HBH_2PI)(PPh_3)_2$ was determined through dipole-dipole relaxation calculations[6]. First, the T_1(min) was determined through a plot of the T_1 value at various temperatures. The T_1(min) is useful because at this temperature, the rotational correlation time at a given field strength is a constant value, allowing for practical, quantitative analysis of the relationship between interatomic distance and dipole-dipole relaxation time through the following equation:

$$\frac{1}{T_1} = \frac{2\gamma_H{}^2\gamma_x{}^2\hbar^2}{15r^6}S(S+1)\left(\frac{\tau_c}{1+\tau_c{}^2\omega_-{}^2} + \frac{3\tau_c}{1+\tau_c{}^2\omega_H{}^2} + \frac{6\tau_c}{1+\tau_c{}^2\omega_+{}^2}\right)$$

T_1 is the spin-lattice relaxation time, γ is the gyromagnetic ratio of the proton (H) or heteroatom (X), $\hbar$ is Planck's constant divided by 2π, r is the interatomic distance between a given pair of atoms, S is the nuclear spin of the heteroatom or hydrogen atom influencing the ^{1}H T_1 value, τ_c is the rotational correlation time, ω_H is the Larmor frequency of the hydrogen atom, $\omega_- = \omega_H + \omega_X$ $\omega_- = \omega_H - \omega_X$, and ω_X is the Larmor frequency of the heteroatom or hydrogen atom influencing the ^{1}H T_1 value. Substituting T_1(min) and τ_c(min), the following equation is obtained:

$$\frac{1}{T_1(\text{min})} = \frac{2\gamma_H{}^2\gamma_x{}^2\hbar^2}{15r^6}S(S+1)\left(\frac{\tau_c(\text{min})}{1+\tau_c(\text{min})^2\omega_-{}^2} + \frac{3\tau_c(\text{min})}{1+\tau_c(\text{min})^2\omega_H{}^2} + \frac{6\tau_c(\text{min})}{1+\tau_c(\text{min})^2\omega_+{}^2}\right)$$

As all the above terms are now constants except for T_1(min) and r, the above equation can be simplified:

$$\frac{1}{T_1(\text{min})} = \frac{K_x}{r^6}$$

K_x can be readily determined for all elements.

The experimental T_1(min) was determined through plotting the T_1 value across a range of temperatures using calibrated pulse widths. Below is a plot of the T_1 value against temperature and an example determination of the T_1 value using exponential regression of pulse-width calibrated data.

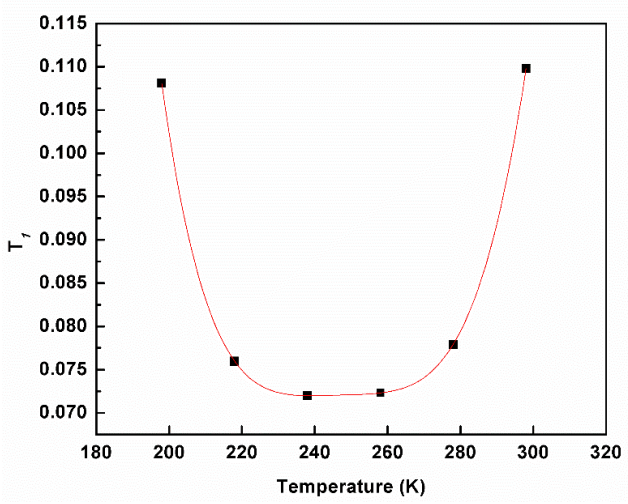

Figure 2-10 T_1(Min) Determination for H^- Ligand in **5**

The application of the above equations to this empirical T_1(min), 0.07138(8) s, is inappropriate due to the net contribution of remote atoms in $Ru(HBH_2PI)(PPh_3)_2$. Using the crystal structure, distances between *all* atoms aside from the acidic OH protons and the ruthenium hydride were determined. K_x was then calculated for ^{1}H, ^{13}C, ^{17}O, ^{15}N, ^{14}N, ^{101}Ru, and ^{31}P, and the total contribution from these atoms calculated and subtracted from the empirical value to give the T_1(min) as it would be if there were no atoms in the molecule aside from the three hydrogen atoms in question. This was then used to calculate the average H-H distance.

Interaction	$\frac{1}{T_1(\text{min})}$
^{1}H-H1	0.8945
^{13}C-H1	0.00003595
^{14,15}N-H1	0.007361
^{17}O-H1	0.0001025
^{31}P-H1	0.04459
^{101}Ru-H1	0.02294

$$\frac{1}{T_1(\text{min})} = \sum_{H(2,3)} \frac{K_H}{r^6} + \sum_{\substack{Other \\ Atoms}} \frac{K_x}{r^6}$$

$$\frac{1}{0.07138} = \frac{155.02}{r(average)^6} + 0.9695$$

$$r(average) = 1.511 \text{ Å}$$

2.8.7 Hydroboration Kinetics

NMR analysis of kinetics experiments was performed using VNMRj 4.0 with a total interpulse delay of 10 seconds.

Example Procedure for Ketone Hydroboration Initial Rate Experiments: Acetophenone (18.6 µL; 0.159 mmol), trimethyl phenylsilane (5.0 µL; 0.029 mmol) (internal standard), 630 µL C_6D_6, and $[Ru(BH_0PI)(PPh_3)_2][K(18\text{-crown-6})]$ (0.080 mg; 63.7 nmol) were sealed in a screw-cap NMR tube at 25° C, inverted twice, and vortexed for ten seconds at 2000 rpm. After standing for 10 minutes, pinacolborane (23.1 µL; 0.159 mmol) was added, the NMR tube inverted twice, and vortexed for ten seconds at 2000 rpm. After standing for four minutes, ^1H NMR spectra were collected every minute for 20 minutes. Integration of product peaks compared to the methyl proton resonances of the trimethyl phenylsilane internal standard was used to determine the concentration of product as a function of time. The initial reaction rate was determined through linear regression.

Example Procedure for Nitrile Hydroboration Initial Rate Experiments:

Benzonitrile (16.4 µL, 0.159 mmol), trimethyl phenylsilane (5.0 µL, 0.029 mmol), 600 µL C_6D_6, and $[Ru(BH_0PI)(PPh_3)_2][K(18\text{-crown-6})]$ (2.0 mg, 1.5 µmol) were sealed at 25° C in a screw-cap NMR tube, inverted twice, and vortexed for ten seconds at 2000 rpm. Pinacolborane (104 µL, 0.716 mmol) was then added, the NMR tube resealed, inverted twice, and vortexed for ten seconds at 2000 rpm. After standing for six minutes, NMR spectra were collected every minute for 8 minutes. Integration of product peaks was used to determine the concentration of product as a function of time, and the initial reaction rate was determined through linear regression.

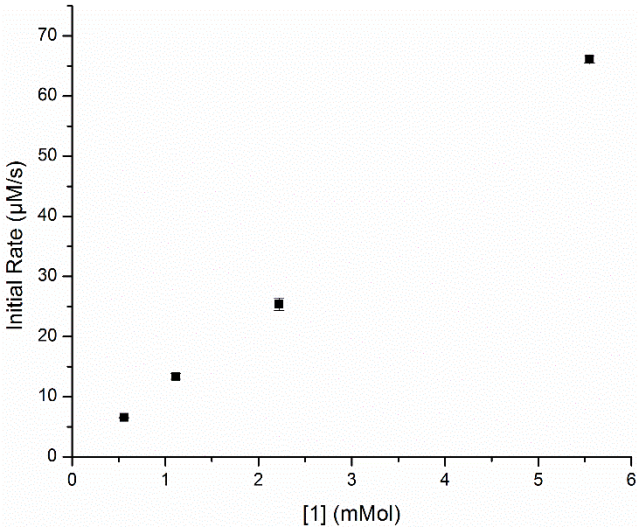

Figure 2-11 Order Determination in **1** for Nitrile Hydroboration

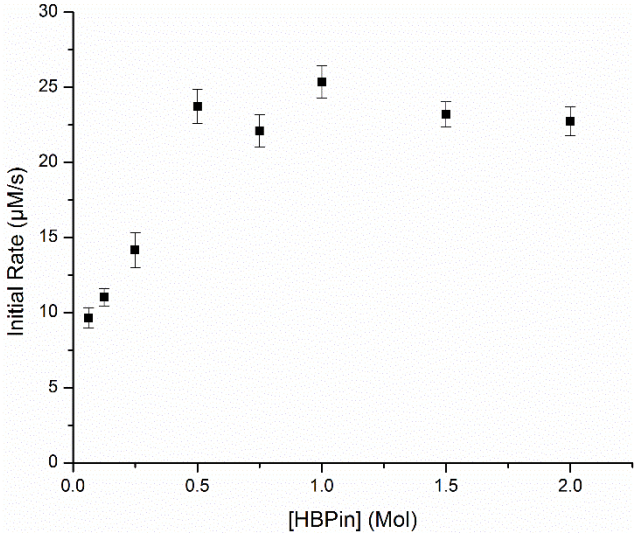

Figure 2-12 Order Determination in HBPin for Nitrile Hydroboration

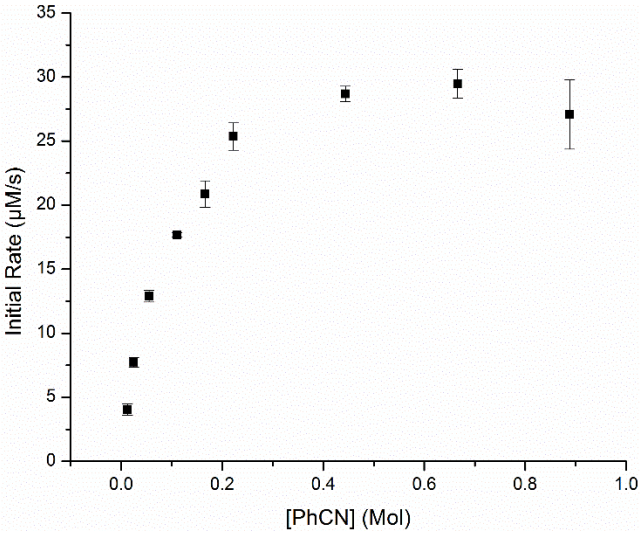

Figure 2-13 Order Determination in PhCN for Nitrile Hydroboration

2.8.8 Tests for Homogeneity:

Hg(0) Poisoning Experiment:

The addition of liquid Hg(0) to an ongoing reaction is a well-known test for the homogeneity of an active catalytic species. To test whether or not 1 is a precatalyst which forms catalytically active metal nanoparticles, a reaction was performed using standard conditions and product formation was followed for 90 minutes via NMR spectroscopy to establish a kinetic profile. An identical experiment was then run, and NMR spectra were collected for the first 20 minutes. Then, the sealed sample was returned to the glovebox and a drop of Hg(0) was carefully added at 30 minutes after reaction initiation. The NMR tube was then resealed, shaken vigorously,

and returned to the NMR spectrometer where data collection was resumed 6 minutes after Hg(0) addition. The addition of Hg(0) had no significant impact on the reaction rate.

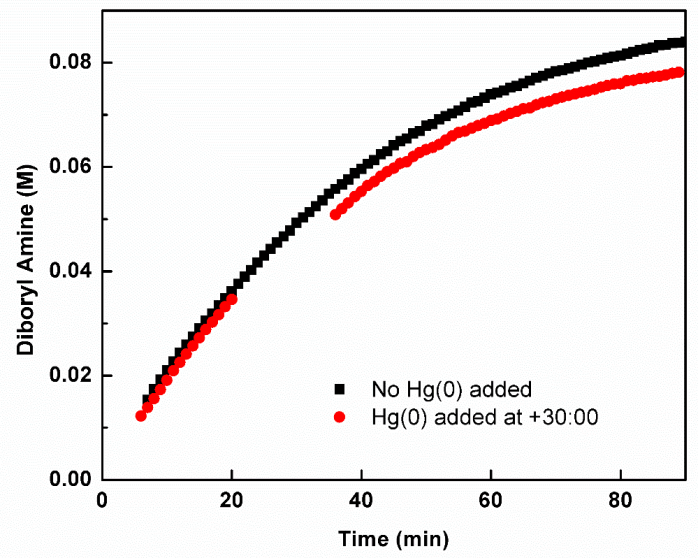

Figure 2-14 Hg(0) Poisoning Experiment with **1**

PMe_3 Poisoning Experiments:

While the Hg(0) test can be an effective diagnostic tool for determining whether or not a catalytic species is homogeneous or heterogeneous, substoichiometric poisoning experiments are a complementary test of homogeneity. If low surface area metal particles are operative catalysts, very small quantities of ligand relative to the molar concentration of metal atoms (<<1 equivalent) are able to completely eliminate catalytic activity[7]. These experiments were conducted exactly as the Hg(0) poisoning experiment described *vide supra*, except instead of adding Hg(0) 2, 1, 0.5, and 0 equivalents of PMe_3 relative to the concentration of 1 were added to ongoing catalytic reactions. The reaction was completely inhibited with the addition of 2 EQ PMe_3.

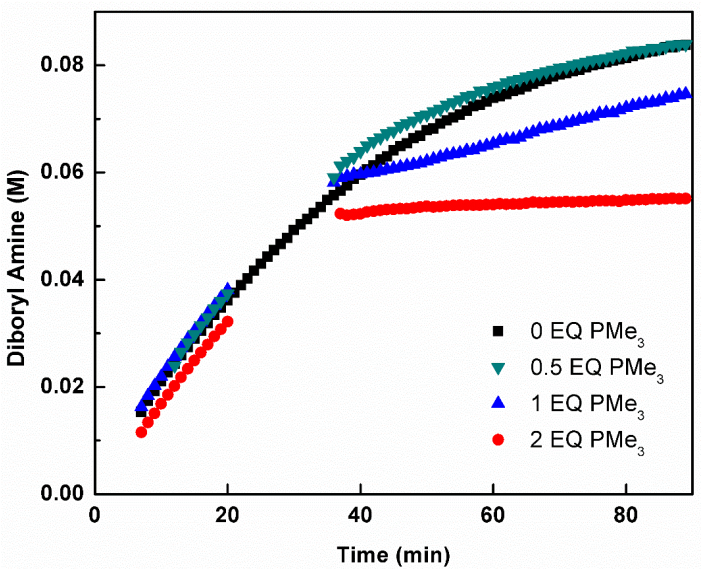

Figure 2-15 PMe_3 Poisoning Experiment with **1**

2.8.9 Stoichiometric Experiments with 1

Reaction of (1) with Excess HBPin

$[Ru(BH_0PI)(PPh_3)_2][K(18\text{-crown-}6)]$ (1): (13.8 mg, 0.011 mmol) was dissolved in a mixture of 500 µL HBPin and 100 µL C_6D_6 in a NMR tube. The tube was vigorously shaken and then vortexed for 30 seconds at 2000 rpm. Immediately upon shaking the tube, a dark purple color was observed. After standing at room temperature for 10 minutes, NMR spectra were recorded at -25 °C.

^1H coupled ^{31}P spectra showed a doublet with $J_{1H\text{-}31P}$ of 103 Hz, identical to the coupling constant of a doublet seen at δ -5.95 in the ^{31}P coupled ^1H spectrum. ^1H-NMR spectra were then collected with selective decoupling of the ^{31}P resonance at δ 39.57, showing that the ^1H signal at δ -5.95 ($J_{31P\text{-}1H}$ = 103 Hz), a signal at δ -10.44 ($J_{1H\text{-}31P}$= 12 Hz), and the ^{31}P resonance at δ 39.57 are in the same spin system. A 1d NOESY experiment confirms that the hydride signals at δ -5.95 and δ -10.44 correspond to hydrides in close proximity, providing further evidence that the three resonances are covalently connected through a Ru(II) center (11).

In addition, an additional pair of signals at δ -1.95 and -12.98 were observed which, in a ^1H-COSY experiment, show strong coupling. Importantly, their linewidths were unaffected by broadband ^{31}P decoupling, and in the absence of additional ligands in solution corresponds to 12.

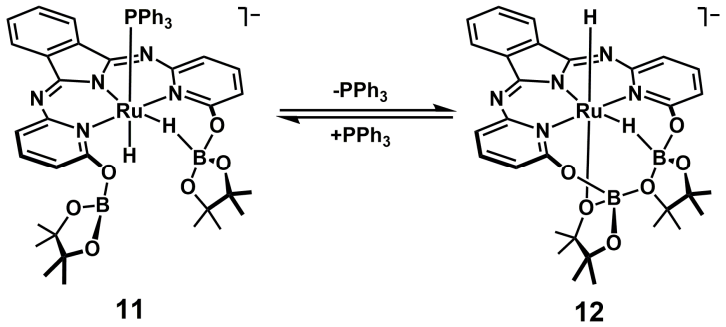

Figure 2-16 Equilibrium between **11** and **12**

2.8.10 p*K*a Determination for 1

The pK_a of **2** was determined in benzene by allowing **1** to react with one equiv. of various phenols. *p*-phenyl phenol generated **2** as observed by UV-Vis spectroscopy, whereas mesitol did not. This shows that the pK_a must lie between 9.5 and 10.8, and as cresol has an intermediate pK_a value relative to these two phenols (pK_a (H_2O)=9.5 (*p*-phenyl phenol), 10.8 (mesitol), 10.2 (cresol)[8]) the conjugate base of cresol (**7**) was selected as an appropriate base control.

Chapter 3. Charge Effects Regulate Reversible CO_2 Reduction Catalysis

This chapter contains work done in collaboration with Joanna Ciatti, and will soon be submitted to a peer-reviewed journal for publication.

3.1 Abstract

Modular but geometrically constrained ligands were used to investigate the impact of key ligand design parameters (charge, steric bulk, and bite angle) on CO_2 hydrogenation / formic acid dehydrogenation activity. A highly active, optimized catalyst was applied in multiple cycles of hydrogen storage/release, generated high pressure H_2/CO_2 from formic acid, and achieved over 118,000 turnovers in CO_2 hydrogenation.

3.2 Introduction

Hydrogen is an excellent energy storage medium through electrochemical proton reduction (energy storage)[116] / hydrogen oxidation (energy release),[117] but is difficult to transport as a compressed gas. Reversible hydrogenation of CO_2 to formic acid (FA) is a desirable chemical strategy for H_2 storage/release.[118] FA prepared from CO_2 also has practical utility as a carbon-negative feedstock in organic synthesis and as a source of high-pressure CO_2/H_2 gas.[119]

An ideal system for hydrogen storage using CO_2 would require only pressure/temperature changes to switch between storage and release (Figure **3-1**). While heterogeneous catalysts can mediate reversible CO_2 (de)hydrogenation, they generate CO as an unwanted byproduct during FA dehydrogenation.[120] Mechanism-guided[121] design of homogeneous Ru(II) and Ir(III) complexes supported by pincer ligands has led to efficient catalytic systems for selective CO_2 (de)hydrogenation[122] and reversible CO_2 hydrogenation has been demonstrated. However, pH cycling[123] is required by most systems for storage/release cycles because catalyst activity for hydrogenation and dehydrogenation is high at different pH values. Several Ru(II) catalysts supported by ancillary pincer ligands promote efficient, switchable CO_2 hydrogenation/dehydrogenation without chemical input,[120] but significant structural differences

between the handful of reported catalysts and a lack of systematic structure/activity relationship studies precludes formulation of general ligand design principles.[45,124]

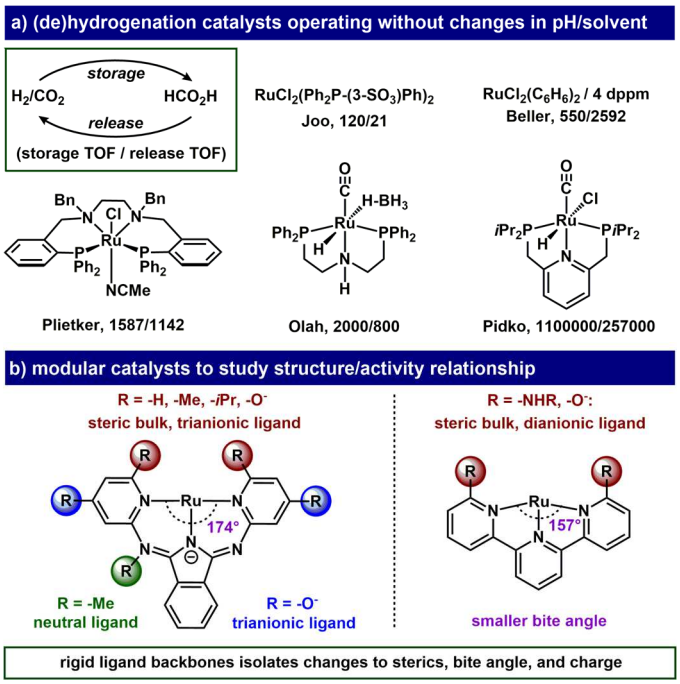

Figure 3-1 a) Previously reported catalysts for CO_2 hydrogenation; b) modular approach to elucidate ligand design principals for reversible CO_2 hydrogenation

In this work, we compare the CO_2 (de)hydrogenation activity of a series of Ru(II) complexes supported by modular N,N,N-pincer ligands and evaluate the impact of ligand charge, steric bulk, and bite angle on catalytic activity to establish ligand design guidelines for switchable CO_2 hydrogenation. Previous catalyst structure/activity relationship studies have generally focused on optimizing either hydrogenation or dehydrogenation, and have not identified ligand design parameters capable of promoting high activity for *both* reactions under one set of solution conditions.[33a] Using a set of pincer ligands with systematically varied properties, we designed a catalyst which promotes highly efficient CO_2 hydrogenation and dehydrogenation under a single set of optimized reaction conditions.

3.3 Reaction Optimization

Bispyridylisoindolinate (BPI) and terpyridine (tpy) ligands provide substitutional modularity in rigid frameworks (Figure **3-1**), and Ru(II) complexes supported by these ligands catalyze CO_2,[125] carbonyl[24a,e], and nitrile hydrogenation.[24d] Therefore, we selected a series of Ru(II)-BPI and Ru(II)-tpy complexes to study the impact of ligand bulk, bite angle, and charge on

catalytic activity for both CO_2 hydrogenation and FA dehydrogenation (**1-9**). CO_2 hydrogenation reactions were run in a sealed Parr bomb, while FA dehydrogenation reactions were run in vented reactors under conditions mirroring complete hydrogenation.

Hydrogenation conditions were optimized with **4** as a catalyst: solvent (dioxane, DMF, MeCN, 2-MeTHF, toluene, *o*-dichlorobenzene, NEt_3), base (0.4 M K_2CO_3, Cs_2CO_3, KOtBu, $K(N(SiMe_3)_2)$, KOH, 1,8-diazabicyclo(5.4.0)undec-7-ene (DBU), NEt_3), catalyst loading, temperature, and CO_2/H_2 pressure were systematically screened.[‡] This established DBU/DMF as a suitable base/solvent pair, and optimized conditions for hydrogenation were set at 120 °C, 7:70 bar CO_2:H_2. While **1-9** were stable under hydrogenation conditions (3 hours, 0.005%: 2491 h^{-1}; 16 hours, 0.001%: 2440 h^{-1}), decomposition was observed during FA dehydrogenation (3 hours, 0.005%: 3752 h^{-1}; 16 hours, 0.001%: 529 h^{-1}). Therefore, comparisons between catalysts were made at 18 hours / 0.001% loading and 3 hours / 0.005% loading for hydrogenation and dehydrogenation, respectively (Figure **3-2**).

3.4 Effect of Ligand Design Parameters on Catalytic Activity

The impact of ligand charge on (de)hydrogenation activity was investigated through comparison of complexes **1**-**3**. Complex **1** should be in a fully deprotonated state during hydrogenation and dehydrogenation catalysis due to the low pK_a of the pendent -OH groups (~8) vs. the high pK_a of HDBU (12), providing a trianionic ligand. **2** contains a monoanionic ligand, while imine methylation affords the neutral ligand in **3**. Modulated pincer ligand charge is expected to translate to changes in the net charge of complexes during catalysis. Laurenczy et. al. reported that cationic Ru-phosphine complexes accelerate FA dehydrogenation, proposing that coulombic attraction between Ru(II) and anionic H^- and FA^- was responsible,[126] while Himeda et. al. demonstrated that anionic iridium hydride complexes exhibit accelerated CO_2 hydrogenation, and proposed that enhanced hydricity was responsible.[33a] Increasing pincer ligand charge from -3 to 0 afforded increased dehydrogenation activity (TON: 5840 (**1**), 7630 (**2**), 13800 (**3**)). However, **3** *also* promoted faster hydrogenation than **1** and **2** (TON: 28200 (**1**), 14500 (**2**), 44000 (**3**)). Together these data suggest that increasingly cationic ligand charge can improve CO_2 hydrogenation *and* FA hydrogenation activity, which may be a useful ligand design principal for switchable H_2 storage catalysts.

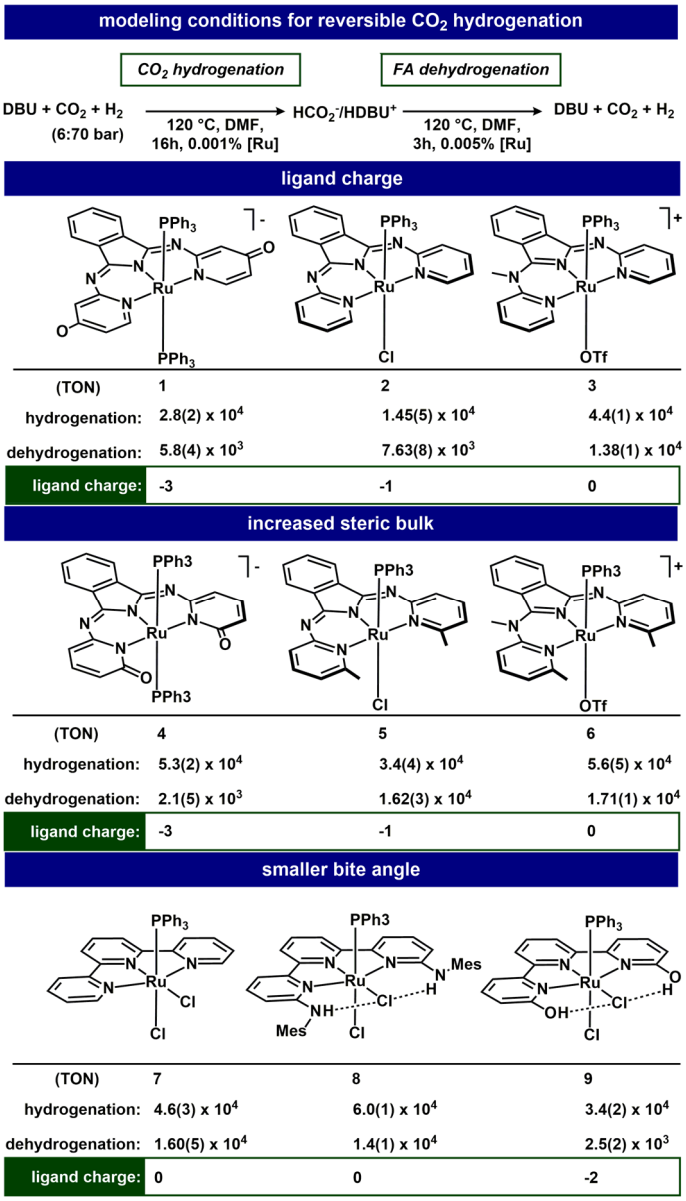

Figure 3-2 Relative Rates for Reversible CO2 Hydrogenation

The impact of steric bulk near a labile coordination site on catalytic activity was investigated through comparison of **1-3** and **4-6**. These complexes were selected because the presence of -Me and -O^- groups, which present similar steric bulk, at the -*o* position of BPI pyridine arms has been shown to increase catalytic activity for amine dehydrogenation. Catalytic activity increased significantly upon replacement of -H (**1-3**, hydrogenation TON: 28200, 14500, 44000, dehydrogenation TON: 5840, 7630, 13800) with -Me or -O^- groups (**1-4**, hydrogenation TON: 53200, 34400, 56500, dehydrogenation TON: 2100, 16200, 17100) **6** is the second-fastest catalyst capable of mediating reversible CO_2 hydrogenation without changes to solution pH; in addition to

high turnover frequencies, **6** can achieve high turnover numbers (118,000) at high dilution (1.2 ppm). Importantly, these data also suggest that the high activity of **4**, in which cooperative H_2 activation pathways are possible, in comparison to **1**, in which these activation pathways are *not* possible (due to rotation of the pendent $-O^-$ bases to the -4 position of the pyridine arms), may largely result from steric bulk. This is illustrated by the similar ratio of activity between **1** and **4** (0.52) and **2** and **5** (0.42), in which steric bulk alone is altered.

Terpyridine ligands are isoelectronic with neutral BPI derivatives, but provide a smaller bite angle (157 degrees[127] vs. 174 degrees).[24c] In comparison with **7**, **8** provided similar activity in CO_2 hydrogenation and FA dehydrogenation (TON: 44887 vs. 46853; 13826 vs. 16080), indicating that bite angle may have a small impact on catalytic activity. As with the BPI scaffold, tpy ligands can be substituted at the -2 positions of the pyridine arms to modulate the performance of metal catalysts. We previously reported that substitution at these positions has a significant impact on alcohol dehydrogenation activity; -OH groups (**9**) significantly reduced stability, while bulky -NHMes groups (**8**) increased stability.[27,28] We found that these same trends held in CO_2 hydrogenation and FA dehydrogenation: **8** (with -NHMes groups) afforded increased stability during hydrogenation (TON: 60567 vs. 46853 at 16h, 0.001% [Ru]; 9093 vs. 7093 at 3h, 0.005% [Ru]), and introduction of -OH groups in **10** led to a marked reduction in TON.

3.5 Preliminary Mechanistic Analysis

To explore a mechanistic rationale for the impact of ligand charge on FA dehydrogenation, we compared the activity of **1-3** under standard conditions with activity under conditions in which the concentration of individual reactants was changed (Figure **3-3**). Under 7 bar H_2, TON is lowered by 19% relative to standard conditions (0 bar). Under 7 bar CO_2, TON was reduced by 89%. Added tetrabutylammonium formate lowered catalytic activity with increasingly cationic ligand charge, suggesting that formate coordination can prevent metal-based reactions by blocking an empty coordination site. The addition of metallic mercury to catalytic CO_2 hydrogenation reactions using **6** did not impact the yield of formate. These data suggest that hydride elimination (and loss of CO_2) from a mono-formate complex is rate determining in FA dehydrogenation, and enhanced hydride affinity at the Ru(II) center imparted by more cationic BPI ligands may be responsible for the observed ligand charge effect in **1**-**3**.

In contrast to FA dehydrogenation, which displayed a consistent trend between ligand charge and catalytic activity, the CO_2 hydrogenation activity of trianionic **5** and neutral **7** is higher than monoanionic **6**. Himeda et. al. suggested that anionic ligands can accelerate catalysis by increasing Ru-H hydricity, but we found that reduced H_2 pressure inhibited catalysis more than reduced CO_2 pressure (49% vs. 113% in comparison to standard conditions). This may suggest that H_2 activation is slower than H^- insertion into CO_2. Overall, varied effects on TON from added TBA formate, DBU, and $HDBU^+/CF_3CO_2^-$ indicate that in contrast to FA dehydrogenation, where ligand charge appears to impact relative activity within a single mechanistic regime, ligand charge may dictate different rate-determining steps for H_2 activation.

percent change in TON under altered initial conditions for 1-3							
CO_2 hydrogenation				FA dehydrogenation			
standard initial conditions: 70 bar H_2, 6 bar CO_2, 0.4 mmol DBU				standard initial conditions: 0 bar H_2, 0 bar CO_2, 0.4 mmol HDBU+/FA-			
	1	2	3		1	2	3
35 bar H_2	34%	65%	49%	6 bar H_2	78%	81%	83%
3 bar CO_2	86%	132%	122%	6 bar CO_2	12%	8%	13%
0.2 mmol NBu_4^+/FA^-	66%	56%	124%	0.2 mmol NBu_4^+/FA^-	103%	86%	73%
0.6 mmol DBU	101%	166%	95%	0.6 mmol DBU	94%	99%	79%
0.2 mmol $HDBU^+/TFA^-$	64%	47%	81%	0.2 mmol $HDBU^+/TFA^-$	90%	90%	93%

Figure 3-3 Impact of varied initial conditions on CO_2 hydrogenation and FA dehydrogenation

We used **6** to generate high pressure H_2/CO_2 gas from excess formic acid in a sealed vessel. While our mechanistic studies indicated that excess H_2 and CO_2 impeded FA dehydrogenation under conditions containing free base in solution, when excess free formic acid is present FA dehydrogenation can proceed under high H_2/CO_2 pressure. Upon heating a 1.3 molar DMF solution of FA containing 5% DBU and 0.004% **6** for 3 hours at 120 °C in a sealed Parr reactor with 40 mL headspace, we observed a pressure of 190 bar. Capture of the evolved gas afforded a 94% yield of 1:1 CO_2/H_2 gas. The maximum pressure we could measure was limited by the mechanical strength of our reactor; we expect that higher pressures can likely be attained.

Finally, we applied the exceptional catalytic activity of **6** in a chemical H_2 storage device which required no chemical input (pH swings, catalyst addition, solvent changes) to switch between H_2 storage and H_2/CO_2 release. Using 0.1% **4** under standard reaction conditions, CO_2 was hydrogenated to FA over the course of 30 minutes at 120 °C. The reactor was then cooled, depressurized, and heated at 120 °C for 30 minutes to release stored H_2/CO_2 gas at ambient

pressure. The cycle was repeated six times, with a gradual reduction in evolved H_2/CO_2 caused by catalyst decomposition during H_2 release. Notably, the H_2/CO_2 mixture generated during FA dehydrogenation was extremely pure (GC-TCD: 99.9999%, CO:H_2 basis).

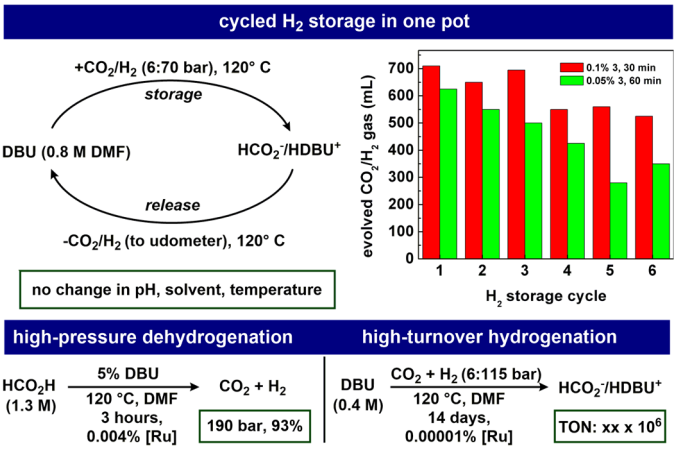

Figure 3-4 H_2 storage cycles, high pressure dehydrogenation, and high-turnover hydrogenation

3.6 Conclusions

We have used a series of Ru(II) complexes bearing systematically varied N,N,N- pincer ligands to evaluate the effect of ligand charge, bite angle, and cooperative ligand functionality in reversible CO_2 hydrogenation. Unlike previous mechanism-guided studies, which have identified ligand design strategies to maximize *either* CO_2 hydrogenation activity *or* FA dehydrogenation activity, we have identified increased ligand charge and modest steric bulk as ligand properties that can increase catalytic activity for both reactions. We then used an optimized complex for reversible, one-pot storage of H_2, high turnover CO_2 hydrogenation, and dehydrogenation of formic acid to generate high pressure H_2/CO_2. We hope that these findings will be useful in the design of improved catalysts for reversible CO_2 hydrogenation.

3.7 Experimental Details

3.7.1 Synthesis of 7:

$Ru(BPI^{Me})PPh_3OTf_2$ (7):

$Ru(BPI)(PPh_3)_2Cl$ (6, 0.103 mmol, 100 mg) was dissolved in 0.5 mL DCM and 10 equiv. MeOTf (1.03 mmol, 116 µL) added. The solution was allowed to stand for 16 hours, then the reaction solution cooled to -80 °C for 1 hour to precipitate the product. The solvent was decanted, and the crystals washed with pentane to give the product (52.4 mg) as large, blue crystals (52%).

^{1}H-NMR (CD_2Cl_2): 9.97 (α, 1H, (d, J_{1H-1H}=5.6)), 9.07 (π, 1H, (d, J_{1H-1H}=5.9)), 8.23 (ψ, 1H, (d, J_{1H-1H}=7.3)), 7.99 (γ, 1H, (t, J_{1H-1H}=8.1)), 7.82 (ι, 1H, (t, J_{1H-1H}=7.4)), 7.80 (υ, 1H, (d, J_{1H-1H}=6.1)), 7.64 (ρ, 1H, (t, J_{1H-1H}=7.7)), 7.57 (ζ, 1H, (d, J_{1H-1H}=6.7)), 7.56 (η, 1H, m (overlap)), 7.34 (β, 1H, (t, J_{1H-1H}=6.6)), 7.30 (δ, 1H, (d, J_{1H-1H}=8.4)), 7.22 (φ, 3H, (t, J_{1H-1H}=7.4)), 7.07 (κ, 6H, (t, J_{1H-1H}=6.8)), 6.96 (λ, 6H, (dd, *J*=8.2, 9.1)), 6.94 (ο, 1H, (t, J_{1H-1H}=6.1)), 3.47 (ε, 3H, s). ^{13}C-NMR: 163.74 (7), 157.19 (19), 157.16 (1), 154.60 (15), 152.88 (5), 146.93 (14), 140.84 (13), 138.44 (3), 137.43 (17), 134.34 (8), 132.88 (21 (d, $J_{13C-31P}$=42)), 131.61 (20 (d, $J_{13C-31P}$=196)), 131.28 (11), 131.11 (10), 130.43 (16), 129.80 (23 (d, $J_{13C-31P}$=14)), 128.25 (trace benzene), 128.03 (22 (d, $J_{13C-31P}$=49)), 123.67 (12), 122.67 (9), 121.07 (18), 119.41 (2), 118.83 (24, 25) 114.23 (4), 42.19 (6). ^{31}P-NMR: 59.10. ^{19}F-NMR: -79.15, -79.26. Note: Shorter reaction time gives incomplete conversion, longer reaction time decomposes product.

3.7.2 Optimization of CO_2 Hydrogenation Reaction Conditions Using 1

Conditions and set-up for optimization reactions were similar to those used for the "small-scale CO_2 hydrogenation" experiments. Base (0.400 mmol), 1 mL solvent, and 0.0625mol% **4** (dispensed as a 4 mM stock solution in DMF) were combined under N_2 in 8 mL scintillation vials equipped with a stirbar and topped with an open-top septum screwcap with inner PTFE liner. The septum was pierced with a 0.25-inch, 27-gauge needle, and the vials loaded into a stainless-steel reactor and CO_2 (6 bar) and H_2 (35 bar) were added to the headspace. The reactor was then heated

Solvent	**K_2CO_3**	**KO^{t}Bu**	**K(N(SiMe$_3$)$_2$)**	**Cs_2CO_3**	**KOH**	**DBU**	**NEt_3**
Dioxane							
TON	136	150	8	9.6	3.2	138	73.6
DMF							
TON	--	--	--	1424	--	1216	--
MeCN							
TON	539	68.8	510	512	14.4	877	17.6
2-MeTHF							
TON	104	163	8	240	6.4	606	1.6
Toluene							
TON	0	52.8	3.2	28.8	4.8	253	1.6
***o*-dichlorobenzene**							
TON	214	448	6.4	62.4	4.8	642	0
DMF (air)							
TON	92.8	722	258	54.4	114	1090	4.8

NEt$_3$

Figure 3-5 Tabulated Turnover Numbers for Initial Optimization

to 80 °C in a large, machined aluminum heating block for 16 hours with stirring at 600 rpm. At the end of the reaction the reactor was allowed to cool in an ice bath to 25 °C (as measured through changes in the internal pressure), and slowly vented to atmospheric pressure and analyzed for formate content. Formate was quantified by first evaporating DMF solvent from vials in vacuum chamber, then adding a stock solution of sodium acetate internal standard in D_2O for ^1H NMR.

3.7.3 Reaction Temperature Optimization

Cs_2CO_3 base (0.400 mmol), 1 mL solvent, and 0.0625mol% **4** (dispensed as a 4 mM stock solution in DMF) were combined under N_2 in 8 mL scintillation vials equipped with a stirbar and topped with an open-top septum screwcap with inner PTFE liner. The septum was pierced with a 0.25-inch, 27-gauge needle, and the vials loaded into a stainless-steel reactor and CO_2 (6 bar) and H_2 (35 bar) were added to the headspace. The reactor was then heated in a large, machined aluminum heating block for 1 or 16 hours, dependent on experiment, with stirring at 600 rpm. At the end of the reaction the reactor was allowed to cool in an ice bath to 25 °C (as measured through changes in the internal pressure), and slowly vented to atmospheric pressure and analyzed for formate content. Formate was quantified by first evaporating DMF solvent from vials in vacuum chamber, then adding a stock solution of sodium acetate internal standard in D_2O for ^1H NMR. Reactions were completed in triplicate at each temperature and time point.

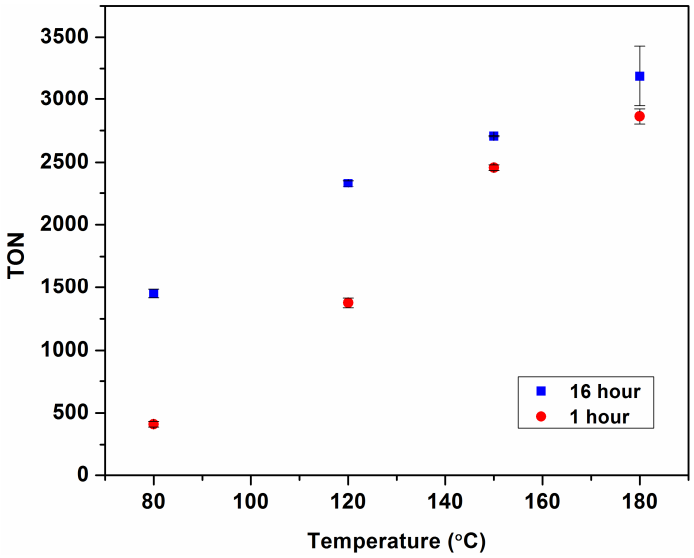

Figure 3-6 Reaction Temperature Optimization

3.7.4 High Turnover Experiment

DBU (0.400 mmol), 1 mL DMF, and **3** or **4** (dispensed as a 5 mM stock solution in DMF) were combined under N_2 in 8 mL scintillation vials equipped with a stirbar and topped with an open-top septum screwcap with inner PTFE liner. Identical vials were prepared within the same experiment for error estimation. The septum was pierced with a 0.25-inch, 27-gauge needle, and the vials loaded into a stainless-steel reactor and CO_2 (6 bar) and H_2 (35 bar) were added to the headspace. The reactor was then heated to 80 °C in a large, machined aluminum heating block for 7 days, with stirring at 600 rpm. At the end of the reaction the reactor was allowed to cool in an ice bath to 25 °C (as measured through changes in the internal pressure), and slowly vented to atmospheric pressure and analyzed for formate content. Formate was quantified by first evaporating DMF solvent from vials in vacuum chamber; then 6 mL DMSO, 1 mL D_2O, and benzaldehyde (0.400 mmol) internal standard were added to each reaction and stirred at 900 rpm for 30 minutes before collecting ^1H NMR.

3.7.5 General Protocols for CO_2 Hydrogenation and Formate Dehydrogenation:

Description of apparatus for pressurized reactions:

Catalyst	Loading (mol%)	Loading (μmol)	Base	TON
3	0.0053	2.12×10^{-2}	DBU	$2.5(1) \times 10^4$
4	0.0053	2.12×10^{-2}	DBU	$2.3(1) \times 10^4$
--	--	--	DBU	3.84×10^2
3	0.0018	7.07×10^{-3}	DBU	$6.51(7) \times 10^4$
4	0.0018	7.07×10^{-3}	DBU	$5.84(9) \times 10^4$
3	0.0018	7.07×10^{-3}	--	4.48×10^2
3*	0.00009	3.50×10^{-3}	DBU	$2.03(4) \times 10^5$
4*	0.00009	3.50×10^{-3}	DBU	$2.01(2) \times 10^5$
--*	--	--	DBU	8.49×10^4

Figure 3-7 Long Duration, High Turnover CO_2 Hydrogenation Experiments

All reactions were run in 300 or 130 mL stainless steel Parr reactors equipped with a pressure gauge, burst disc, and inlet/outlet needle valve. Small-scale reactions were conducted in 8 mL scintillation vials that were loaded into an aluminum block machined to hold seven vials and fit with 1 mm tolerance into a 300 mL cylindrical Parr reactor. Large-scale reactions were conducted in a c.a. 130 mL volume glass liner loaded into either a 130 mL or 300 mL Parr reactor.

Between used this liner was soaked in a base bath for 24 hours to remove trace contaminants. To exclude air from the reactions, the volume contained in the connection between the tank and the reactor was purged with ultra-high-purity reactant gas (CO_2 or H_2) 10 times at 100 psi.

General conditions for small-scale CO_2 hydrogenation reactions:

Base (0.400 mmol), 1 mL solvent, and 1-10 (dispensed as a 2.0 mM stock solution in matching solvent) were combined in 8 mL scintillation vials equipped with a stirbar and topped with an open-top septum screwcap with inner PTFE liner. The septum was pierced with a 0.25-inch, 27-gauge needle, and the vials loaded into a stainless-steel reactor and CO_2 and H_2 were added to the headspace to obtain the desired gas partial pressures. The reactor was then heated to the desired temperature in a large, machined aluminum heating block for the desired reaction time with stirring at 660 rpm. At the end of the reaction the reactor was cooled in an ice bath until the internal temperature dropped below 25 °C (as measured through changes in the internal pressure, ca. 10 min), and slowly vented to atmospheric pressure and analyzed for formate content.

General conditions for small-scale formate dehydrogenation reactions:

1-10 (dispensed as a 2.0 mM stock solution in DMF) were combined with DBU (0.400 mmol) and formic acid (0.400 mmol) in 1 mL DMF in 8 mL scintillation vials equipped with a stirbar and topped with an open-top septum screwcap with inner PTFE liner. The septum was pierced with a 0.25-inch, 27-gauge needle, and the vials loaded into an aluminum heating block and heated in the glovebox as open systems for the desired reaction time and with 660 rpm stirring to permit continuous release of CO_2/H_2 gas. At the end of the reaction the vials were cooled to room temperature and analyzed for remaining formate content. Control reactions were carried out in the absence of catalyst to measure the rate of the background formate decomposition reaction, allowing for accurate determination of the turnover number.

Formate Quantification:

^{1}H-NMR spectroscopy was used to quantify formate in the reaction mixtures. With DBU as base and DMF as the solvent for CO_2 hydrogenation and in all FA dehydrogenation experiments, 0.400 mmol $PhSiMe_3$ internal standard was added to the reaction mixture, the mixture vortexed for 10 seconds at 2000 rpm, and then the homogeneous solution sampled for ^{1}H-NMR in DMSO-d_6. With all other solvents and bases, solvent and other volatiles were removed from the reaction mixture under vacuum. The resulting solid was dissolved in D_2O along with 0.400 mmol sodium

acetate internal standard to afford a homogeneous solution for ^{1}H NMR integration. NMR acquisition parameters: d1=40 seconds, total interpulse delay: 45 seconds.

3.7.6 **Reversible H_2 Storage**

DBU (11.2 mmol, 1.67 mL) and **3** (0.05%, 5.6 μmol, 5.6 mg) were dissolved in 14 mL DMF in a glass-lined, 300 mL stainless steel reactor along with a PTFE stirbar. The reactor was then charged to 7 bars CO_2 / 70 bar H_2 and stirred at 660 rpm at 120 °C for one hour (*H_2 storage*). At the end of this time the reactor was cooled in a stirred water bath to 30 °C (10 min.), and pressure inside the reactor vented through an oil bubbler. After venting for 15 minutes, the reactor was heated to 120 °C for one hour (*H_2 release*). In this time, evolved gas was collected and measured in a 600 mL gas burette submerged in 10 liters of pH 1.0 water (acidified to eliminate CO_2 solubility). Thermal gas expansion in the headspace was measured to be 103 mL (from 30 °C to 120 °C), and this volume was subtracted from the collected gas volume to accurately measure the molar quantity of CO_2:H_2 evolved during FA dehydrogenation. At the end of this time, the reactor was cooled to 25 °C in a water bath, charged with 7 bar CO_2 / 70 bar H_2, and stirred at 660 rpm at 120 °C to begin a new H_2 storage cycle. During the sixth cycle, the evolved gas was analyzed by GC-TCD: 46.9% CO_2, 43.2% H_2, and 0.0056% CO (99.987% selectivity for H_2/CO_2 vs. H_2O/CO). Six cycles were performed. An additional set of reactions were performed as described above, but at 0.1% **3** and using only 30-minute reaction times for CO_2 hydrogenation and FA dehydrogenation.

	1h, 0.05% **3**		18h, 0.001% **3**	
Cycle	Gas Evolved (mL)	% Yield (vs. DBU)	18h, 0.001%	% Yield (vs. DBU)
1	622	113%	707	129%
2	547	99%	647	117%
3	497	90%	692	125%
4	422	76%	547	99%
5	277	50%	557	101%
6	347	63%	522	94%

Figure 3-8 Cycled H_2 storage in CO_2

3.7.7 Generation of High Pressure Gas Through Formic Acid Dehydrogenation

Formic acid (160 mmol, 6.000 mL), DBU (7.47 mmol, 1.117 mL), and **3** (0.00038%, 6.0 mg, 5.9 μmol) were dissolved in DMF (120 mL) with a PTFE stirbar in a 150 mL glass-lined stainless-steel reactor under nitrogen at ambient pressure. The headspace volume was approximately 40 mL. The reactor was sealed and heated to 120 °C for three hours, at which time the pressure had increased to 190 bar. The evolved gas was measured using a gas burette, showing that the reaction evolved 7275 mL gas (93% vs. starting formic acid, 247,000 turnovers). The reactor's safety burst disc pressure, 210 bar, limited our ability to investigate catalysis at higher pressures. The evolved gas was analyzed by GC-TCD: 46.9% CO_2, 43.2% H_2, and 0.0056% CO (99.987% selectivity for H_2/CO_2 vs. H_2O/CO).

Chapter 4. Testing the Push-Pull Hypothesis: Lewis-Acid Augmented N_2 Activation

Portions of this chapter have been published:

Geri, J. B.; Shanahan, J. P., Szymczak, N. K.; Testing the Push-Pull Hypothesis: Lewis-Acid Augmented N_2 Activation at Iron

J. Am. Chem. Soc. 2017, 139, 5952–5956.

4.1 Abstract

We present a systematic investigation of the structural and electronic changes that occur in an Fe(0)-N_2 unit (Fe(depe)$_2$(N_2); depe = 1,2-bis(diethylphosphino)ethane) upon the addition of exogenous Lewis acids. Addition of neutral boranes, alkali metal cations, and an Fe^{2+} complex increases the N-N bond activation ($\Delta\ \nu_{NN}$ up to 172 cm^{-1}), decreases the Fe(0)-N_2 redox potential, polarizes the N-N bond, and enables *–N* protonation at uncommonly anodic potentials. These effects were rationalized using combined experimental and theoretical studies.

4.2 Introduction

The reduction of dinitrogen to ammonia is one of the most important, yet challenging, chemical transformations. While the currently used industrial process for nitrogen fixation requires forcing temperature and pressure (~1000 °C and > 100 atm), nitrogen fixation by nitrogenases operates under ambient conditions.[57,128] Nitrogenases use a multi-metallic active site contained within a network of amino acid residues that are essential in orchestrating a series of multi-proton, multi-electron transfers to N_2. Although this strategy may ultimately provide a low energy/carbon route to ammonia, the discrete mechanistic steps in the biological reduction sequence are largely unknown.[129]

A key step in the proposed mechanism of nitrogenase is the coordination and activation of a classically inert dinitrogen ligand at a reduced iron center.[129a] The high π-basicity, and highly

negative reduction potentials, required of the metal center have led to a primary coordination sphere-focused design strategy in the development of model complexes.[56,130] This requirement contrasts with the low operating potential required for N_2 fixation by nitrogenases, which suggests that additional design principles may be required.[131] In particular, the role of acidic sites in the secondary-sphere of nitrogenase (highly conserved α-195^{His}, α-191^{Gln}, arginine residues and adjacent S-H and Fe centers)[58b,132] has been relatively unexamined in synthetic systems.[133] These sites are required for nitrogenase activity, as demonstrated by mutation studies,[134] and may play a crucial role in enabling nitrogenase's low overpotential and high selectivity (Figure **4-1**).

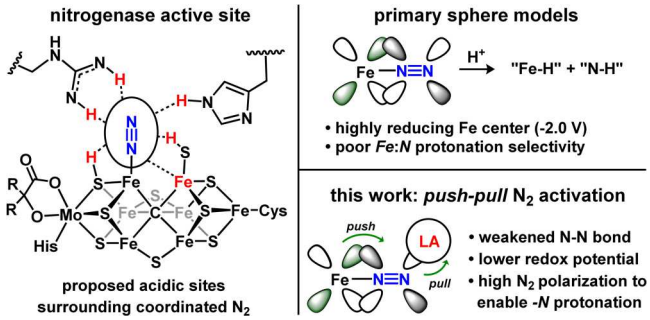

Figure 4-1 FeMo-co active site with proposed interactions of acidic groups (left), and conceptual framework illustrating the use of Lewis acids to test the push-pull hypothesis (right).

Hydrogen bonding groups and Lewis acidic sites are commonly used in metalloenzymes to modulate substrate binding and activation.[135] In nitrogenase, this concept has been used to formulate the so called "push-pull" hypothesis, in which electron density is "pushed" from a reduced iron center and "pulled" into the N_2 unit by adjacent Lewis acidic sites.[129a,b] These interactions lead to polarization of N_2 and enhanced charge transfer from the iron center; the two effects may contribute to the low overpotential and high protonation selectivity observed in the enzyme. The push-pull approach is an intriguing concept for understanding N_2 activation in nitrogenase and may also provide a general strategy that could be used in the design of synthetic nitrogenases. However, this concept has not been experimentally tested, which may be due to the synthetic challenges inherent in combining highly acidic and reducing centers in a single molecule.[133] Herein we report an experimental test of the push-pull hypothesis through a systematic investigation of the ability of *exogenous* Lewis acids to activate a reduced Fe-N_2 complex.

4.3 Preparation and Characterization of Fe-N_2-LA Adducts

$Fe(depe)_2(N_2)$ (**1**) was selected as a model Fe(0)-N_2 unit for our investigation because it provides a sterically-accessible, nucleophilic N_2 ligand and was recently shown to catalyze N_2 reduction.[136] While Lewis acids (LAs) such as $SiMe_3^+$ and H^+ have been reported to react with structural analogues of **1** to provide ill-defined mixtures,[137] their excessive electrophilicity and strong coulombic effects make them inadequate models for non-covalent interactions in the secondary-sphere of nitrogenase. In contrast, neutral boranes are a highly electronically and sterically tunable class of LAs[138] that are ideal for modeling these interactions. $B(C_6F_5)_3$, a powerful yet reductively stable borane, was initially selected to interrogate the push-pull hypothesis via adduct formation with **1**.

When $B(C_6F_5)_3$ was combined with **1**, a LA/base adduct (**2**) was formed in quantitative yield as assessed by IR and NMR spectroscopy (Figure **4-2**). The IR spectrum revealed that the N-N bond was significantly weakened by the addition of $B(C_6F_5)_3$, noted by the 129 cm^{-1} shift of the ν_{NN} stretch (**1**: 1959 cm^{-1} **2**: 1830 cm^{-1}). The formation of **2** was general in a variety of nonpolar solvents (pentane, C_6D_6, toluene, PhF, MTBE, THF) allowing for analysis by ^1H, ^{11}B, ^{15}N, ^{19}F, and ^{31}P NMR spectroscopy, which supported a persistent borane-N_2 interaction in solution and a highly activated N_2 unit. NMR spectra of **2** at room temperature contain a sharp ^{11}B resonance at -10 ppm, consistent with a tetrahedral boron center. The ^{15}N NMR spectrum suggests significant polarization of the N_2 unit induced by the LA: the $\Delta\delta$ for the iron-bound and terminal N-atoms increases from 5 to 109 ppm (**1**: N_α -45.2, N_β -40.5;[139] **2**: N_α -10.5, N_β -119.8 ppm). The significant upfield shift of $N_ß$ (-74.6 ppm), as opposed to the downfield shift N_α (+30.0 ppm), suggests increased localization of electron density at the terminal nitrogen atom.[140]

A single crystal of **2** was grown from toluene/pentane and analyzed by an X-ray diffraction experiment. The N-N bond length is elongated by 0.04(1) Å (**1**: 1.142(7); **2**: 1.186(3)), reflecting the significant N-N activation apparent in the IR and ^{15}N NMR spectra.[136b] An important structural detail is the bent N1-N2-B1 geometry, with a bond angle of 137.0(3)°.[141] This bond angle suggests strong interaction between the empty boron *p*-orbital and the N_2 π^* orbital. To the best of our knowledge, this type of N_2 activation has not been observed with other neutral LAs.[142]

To evaluate the generality of enhanced N_2 activation by LAs and the influence of Lewis acidity, we selected a set of borane and alkali metal LAs of varying strength (BR_3 (R = 2,6-F_2-Ph,

2,4,6-F_3-Ph, C_6F_5, OC_6F_5, F); Li [$B(C_6F_5)_4$], Na^+, K^+, Rb^+, Cs^+ [$BAr^F{}_4$ = $B(3,5\text{-}(CF_3)_2C_6H_3)_4$)]. Although select examples of alkali metal–N_2 interactions have been reported, these complexes are often further supported by intramolecular cation-π interactions and charge pairing, making efforts to systematically evaluate the role of the alkali metal LAs in N_2 activation highly challenging.[57,143]

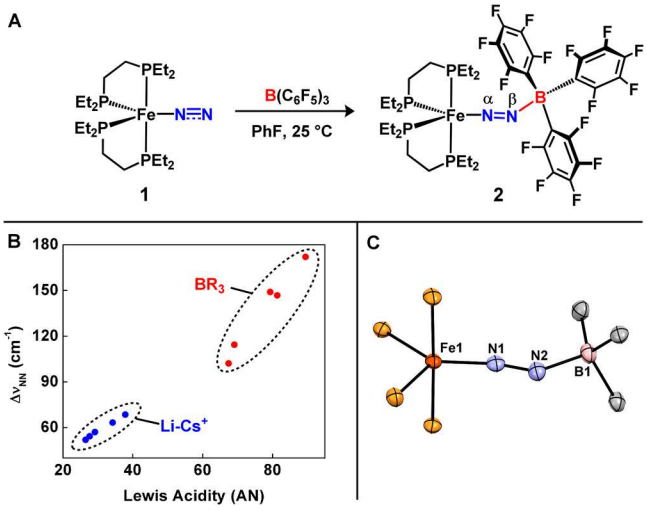

Figure 4-2 A: Synthesis of **2**. B: Generality of N_2 activation using a variety of Lewis acids (Li, Na, K, Rb, Cs; BR_3 (R = F, OC_6F_5, C_6F_5, $C_6F_3H_2$, $C_6F_2H_3$)). C: Crystal structure of **2**.

The availability of a broad set of LA-N_2 adducts enabled an investigation of the relationship between Lewis acidity, N-N bond strength, and N_2 binding affinity. The ν_{NN} undergoes a smooth bathochromic shift as a function of LA strength, as quantified by the Acceptor Number (AN).[144] As the LA strength increases from Cs^+ (AN: 26) to $B(OC_6F_5)_3$ (AN: 89), the N-N bond is weakened as shown by a lowering of the ν_{NN} from 1920 to 1787 cm^{-1} (Figure **4-2**). Within the series of alkali metal cations, the association constant (measured in Et_2O) varies between 94(5) and 430(80) M^{-1} and stronger binding is correlated with increasing Lewis acidity. The same trend holds within the series of fluorinated triphenylboron LAs (measured in PhF, BR_3; R = 2,6-F_2-Ph, 2,4,6-F_3-Ph, C_6F_5), whose association constants increase from 4.6 x 10^3 to 7.9 x 10^4 M^{-1}.[145] The shift of the ν_{NN} and binding affinity clearly illustrates that the strength of the N-N and LA-N_2 bonds can be dramatically tuned by the LA.

4.4 Computational Analysis of Fe-N_2-LA Adducts

The ability to finely tune the strength of boron-based LAs in **1**-BR_3 adducts presents a unique opportunity to explore the impact of exogenous LAs on the electronic structure of a Fe-N_2 unit. Using DFT methods, we interrogated the molecular orbitals of **1** and **2** to provide quantitative

orbital mixing coefficients between neutral $Fe(depe)_2$ and LA-N_2 fragments (Figure **4-3**A) as well as natural bonding orbital (NBO) populations and net atomic charges.

In complex **1**, the combination of the empty, high-lying N_2 π* orbital with the filled $Fe(depe)_2$ d_{xy} orbital leads to a high-energy HOMO with a small contribution from unfilled N_2 π* orbitals (Figure **4-3**A). Upon introduction of $B(C_6F_5)_3$ to the N_2 fragment, the empty boron *p* orbital mixes with the N_2 π* orbital, which lowers its energy from -1.18 to -4.60 eV. The resulting LA-N_2 π* orbital can then better interact with the filled $Fe(depe)_2$ d_{xy} orbital, leading to stabilization of the HOMO (-3.73 to -4.60 eV) and an increase in its N_2 π* character from 18% to 39%; these effects track closely with increasing Lewis acidity (Figure **4-3**B). The increase in π* character in the HOMO equates to greater charge transfer (*via* π -backbonding) from $Fe(depe)_2$ to the N_2 unit. The relationship between the N-N-B angle and orbital energies of a N_2-BF_3 fragment was probed through a Walsh-type analysis. In contrast to the free N_2-BF_3 fragment, in which a linear geometry is favored by 21 kcal/mol, population of the N_2 π* orbitals upon Fe(0) coordination leads to a net stabilization of the bent 120° geometry by 13 kcal/mol, compared to a linear (180°) geometry. These orbital considerations provide a rationale for the experimentally observed weakening of the N-N bond and bent activation in **1** upon *N*- coordination with a simple Lewis acid.

Crucially, the LA induced increase in N_2 activation is not provided at the expense of N_2 polarization or basicity, even though a LA might be expected to quench the Lewis basic terminal nitrogen atom. The difference in NBO charge between the nitrogen atoms in **1** ($\Delta = 0.32$) increases upon coordination of $B(C_6F_5)_3$ ($\Delta = 0.39$ in **2**), indicating enhanced N_2 polarization. Importantly, the negative charge of the terminal nitrogen atom *increases* from -0.22 in **1** to -0.30 in **2**. Increasing Lewis acidity from $B(C_6F_2H_3)_3$ to $B(OC_6F_5)_3$ further populates the N_2 π* orbitals (0.217 to 0.228 e^-) and the negative charge at the terminal nitrogen (-0.25 to -0.37), suggesting that the *basicity* of the terminal nitrogen atom is enhanced upon LA coordination.

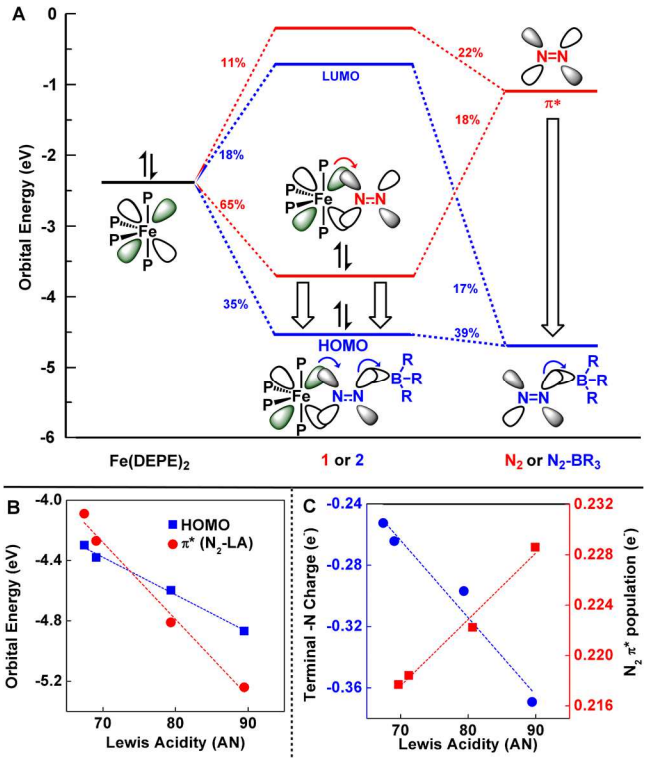

Figure 4-3 Computational analysis of Fe-N_2-LA adducts. A: MO diagram for $Fe(depe)_2N_2B(C_6F_5)_3$. B: Orbital energies vs. LA strength. C: Terminal -N charge and N_2 π^* population vs. Lewis acid strength.

4.5 Electrochemical Characterization of Fe-N_2-LA Adducts

The addition of $B(C_6F_5)_3$ to **1** lowers the HOMO energy by 0.9 volts (Figure **4-3**B), indicating that **2** and related LA activated N_2 adducts should exhibit significantly lower redox potentials than **1**. Electrochemical experiments were used to test this prediction. The cyclic voltammogram of **1** featured a reversible redox event at -2.17 V (0.1 M [^{n}Bu$_4$N][BAr$^F{}_4$],[146] PhF, vs Fc^+/Fc, at -45 °C).[147] Upon addition of $B(C_6F_5)_3$, the redox couple undergoes an anodic shift to -1.15 V, as assessed by DPV (differential pulse voltammetry) and becomes irreversible by cyclic voltammetry (Figure **4-4**). The imparted irreversibility is consistent with the absence of reactivity between LAs with the corresponding Fe(I)-N_2 complex, $[Fe(depe)_2(N_2)]^+$. The *1.0-volt difference* from **1** is consistent with the predicted 0.9 V shift from DFT calculations. The shift in the redox couple is a general effect, and tracks closely with Lewis acidity (Figure **4-4** right). Overall, the significantly lower HOMO energies in the **1**-LA adducts afford a significant anodic shift of the Fe-N_2 unit, and validates the conceptual foundation of the push-pull hypothesis.

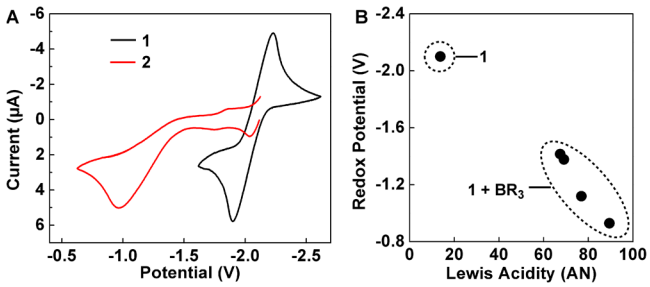

Figure 4-4 A: Cyclic voltammetry of **1** and **2**; B: Onset of oxidation vs. Lewis acidity (vs. Fc/Fc^+)

4.6 Selective -*N* Protonation of N_2

An important prediction of our theoretical analysis is that Lewis acidic centers can bias the Fe-N_2 unit toward *–N* protonation rather than *–Fe* protonation. The reactivity of H^+ with **1** has been extensively investigated, but no protonated Fe-N_2H_x adducts have been observed from these reactions.[128a] Furthermore, the electron yield for N_2 reduction products is low upon addition of acid, indicating preferential protonation at iron.[136c] In contrast to these systems, where a highly reducing iron center favors *–Fe* protonation, LA coordination to the terminal nitrogen atom in **2** shifts electron density from the metal center to the terminal nitrogen atom.[148] We experimentally probed the impact of this effect on protonation selectivity in N_2 complexes activated with LAs.

Multinuclear NMR spectroscopy was used to assess protonation selectivity for **1** vs. **2**. When **2** was combined with $HBAr^F{}_4{\cdot}(OEt_2)_2$ (PhF, -45 °C), a new complex, **3**, formed in 91% yield (^{31}P integration) (Figure **4-5**). The ^{15}N NMR spectra revealed further separation between the iron-bound and terminal nitrogen resonances than either **1** or **2** and exhibited one-bond ^{15}N-^{1}H coupling (**3**: N_α -49.3, N_β -140.7 ppm ($^1J_{15N\text{-}1H}$ = 80.7 Hz)), consistent with *–N* protonation of the N-N unit. The protonation reaction is >95% selective; only a 4% yield of *trans*-Fe(H)(depe)$_2$(N_2) is observed by ^{31}P and ^{15}N NMR spectroscopy.[139,149] In contrast, subjection of **1** to identical reaction conditions in the *absence* of $B(C_6F_5)_3$ affords a mixture of *–cis* and *–trans* Fe(H)(N_2)(depe)$_2$, indicating that protonation occurs exclusively at the iron center.[150] The monoprotonated product (**3**) contains a structurally unique Fe-NN(B)H unit and was characterized by X-ray crystallography, NMR, and IR spectroscopy.

Comparison between ^{14}N- and ^{15}N-labeled **3** allowed identification of the ^{14}N-H (3259 cm^{-1}) and ^{14}N-^{14}N (1519 cm^{-1}) stretches, the latter of which indicates a significant weakening of the N-N bond. The solid-state structure of **3** revealed an N1-N2 bond length that is elongated by 0.12(1) Å (vs. **1**) to 1.252(8) Å, consistent with further weakening of the N-N bond. H1 was located

from the difference map and indicates protonation of the terminal nitrogen atom (N2), a conclusion reinforced by contraction of the N-N-B angle to 130.6(6)°. Furthermore, the Fe1-N1 bond length is shortened by 0.07(1) Å, and consistent with an iron hydrazido formulation.[151] The N-N bond length of **3** is longer than **2** and slightly shorter than the related iron hydrazido ([(SiP$^{iPr}_3$)Fe=N-N(Me)H]$^+$: 1.284(4) Å) complex recently reported by Peters and Rittle.[151a] Progressive elongation of the N-N bond in **1**, **2**, and **3** is reflected in progressively lower Wiberg bond orders (2.5, 2.0, and 1.7), further highlighting the comparable impact of protons and neutral LAs on N-N bond strength. Collectively, these data demonstrate that *–N* coordination of a LA can simultaneously lower the redox potential of an Fe-N_2 unit while enabling selective terminal *–N* protonation, potentially offering an explanation for the low overpotential of nitrogenase.[152]

4.7 Synthesis of Push-Pull Bimetallic N_2 Complexes

In principal, the enhanced activation of N_2 upon addition of main group LAs should also translate to transition metal LAs, affording M-(μ-N_2)-M' cores.[153] Although such iron homo- and heterobimetallic units are often highly activated, their preparation commonly relies on combining two highly reduced metal fragments.[150,154] As an alternative strategy to further activate the N_2 unit, we investigated the effect of adding an *oxidized*, rather than a *reduced* iron center to an Fe(0)-N_2 unit. In this arrangement, the charge disparity between two iron sites may facilitate charge transfer to the N_2 unit, similar to main-group LAs (*vide supra*). We selected an Fe(II)(^{i}Pr$_2$Tp)Cl as a monomeric, yet sterically accessible iron center.[154b] When **1** was combined with Fe(II)(^{i}Pr$_2$Tp)Cl in the presence of NaBAr$^F_4$, a new compound Fe(depe)$_2$(μ-N_2)Fe(^{i}Pr$_2$Tp)(BAr$^F_4$) (**4**), was obtained (Figure **4-5**).

This S = 2 (μ_{eff} = 4.77μ_B) complex contains a high-energy, solvent-dependent IVCT band at 910 nm (ε=1700 M^{-1}cm^{-1}, $\Delta\nu_{½}$ = 3398 cm^{-1}) as well as structurally distinct environments for each Fe center in the X-ray structure (trigonal bipyramidal for Fe1 and tetrahedral for Fe2). These data are consistent with a Class II mixed-valence complex containing localized Fe(0)/Fe(II) centers.[155] Importantly, the IR spectrum of **4** contains an activated N-N unit (ν_{NN} = 1825 cm^{-1}), which is nearly identical to the shift found in **2** and *more* activated than the related homodimer (Fe(dmpe)$_2$)$_2$(μ-N_2) (ν_{NN} = 1933 cm^{-1}).[150] This indicates that a high spin Lewis acidic Fe(II) center induces greater activation of the N-N bond than the addition of a more reduced and Lewis-basic

Fe(0) center. The extent of N_2 activation enabled by charge disparate Fe centers may provide insights into how N_2 is activated within the multimetallic core of nitrogenase.

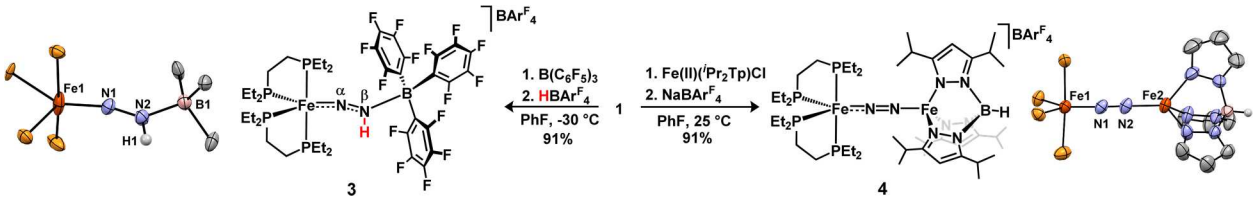

Figure 4-5 Selective Protonation of N_2, Preparation of Push-Pull Fe(0)-N_2-Fe(II) Complex

4.8 Conclusions

In contrast to the mildly reducing conditions used for N_2 reduction in nitrogenases, synthetic complexes that both bind and enable N_2 protonation require powerful reducing equivalents and possess redox potentials. In this chapter, we describe the first application of secondary sphere Lewis acids based on main group elements, alkali metal cations, and an Fe(II) center to an Fe-N_2 unit. Our study provides an alternative N_2 activation strategy that weakens the N-N bond, enables mild redox potentials, and enhances protonation selectivity through the simple addition of Lewis acids. Theoretical analysis shows that this effect is caused by efficient stabilization of the N_2 π^* orbital and polarization of the N_2 unit between the reducing and acidic fragments, much like the frustrated Lewis pair systems widely used for small molecule activation.[4] This work supports a mechanistic rationale for the conserved acidic residues in nitrogenase, and we anticipate that it may focus future efforts in the bioinorganic community towards the exploitation of Lewis acids.

4.9 Experimental Details

4.9.1 General Considerations:

Tetrakis(3,5-bistrifluoromethylphenyl)borate and tetrakis(pentafluorophenyl)borate are abbreviated as BAr^F_4 and $B(C_6F_5)_4^-$, respectively. $B(C_6F_5)$, $B(C_6H_5)_3$, $Li(Et_2O)(B(C_6F_5)_4)$, $Fe(Cp^*)_2$, BF_3•OEt_2, 1,2-bis(diethylphosphino)ethane (depe), and iron dichloride were used from commercial sources without further purification. $^{15}N_2$ (98%) was purchased from Cambridge Isotope Laboratories. Tetrahydrofuran, pentane, and diethyl ether were purified using a Glass Contour solvent purification system through percolation through a Cu catalyst, molecular sieves, and alumina and finally stored over activated molecular sieves for a minimum of 48 hours, then

stored over potassium mirrors. Toluene, benzene, and methyl tert-butyl ether were distilled from molten sodium/ketyl radical and stored over potassium mirrors. Fluorobenzene was fractionally distilled from P_2O_5 after stirring for three days. Diisopropyl ketone was distilled from calcium hydride and stored over molecular sieves. Fe(II)(^{i}Pr$_2$Tp)Cl,[156] Fe(depe)$_2$N$_2$,[157] NaBAr$^F_4$,[158] KBAr$^F_4$, RbBAr$^F_4$, CsBAr$^F_4$,[159] H(OEt$_2$)$_2$BAr$^F_4$,[160] B(C$_6$H$_3$F$_2$)$_3$, B(C$_6$H$_2$F$_3$)$_3$,[161] and B(OC$_6$F$_5$)$_3$[162] were prepared according to literature methods. Tetrabutylammonium BAr$^F_4$ was prepared according to literature methods, doubly recrystallized, then dried over P_2O_5 for three days under high vacuum.[163] Unless otherwise specified, all reactions were prepared and carried out in an anhydrous nitrogen atmosphere using standard Schlenk and/or glovebox techniques.

NMR spectra were recorded on a Varian Vnmrs 700, Varian Inova 500, or Varian MR400 spectrometer. ^{1}H, ^{13}C, ^{15}N, ^{19}F, ^{11}B, and ^{31}P shifts are reported in parts per million (ppm) relative to TMS, with the residual solvent peak used as an internal reference. ^{31}P, ^{15}N, ^{11}B, and ^{19}F NMR spectra are referenced on a unified scale, where the single primary reference is the frequency of the residual solvent peak in the ^{1}H NMR spectrum. ^{1}H and ^{13}C NMR are referenced vs. tetramethylsilane, ^{15}N is referenced vs. nitromethane, ^{31}P is referenced vs. phosphoric acid, ^{19}F is referenced vs. fluorotrichloromethane, and ^{11}B is referenced vs. BF$_3$•OEt$_2$. Multiplicities are reported as follows: singlet (s), doublet (d), triplet (t), quartet (q), and multiplet (m). Transmission IR spectra were recorded on a Nicolet iS10 using either a bolt KBr press or 0.25 mm path length KBr solution cell, and electronic absorption spectra were recorded on a Varian Cary-50 spectrophotometer. Crystals were mounted on a Rigaku AFC10K Saturn 944+ CCD-based X-ray diffractometer equipped with a low temperature device and Micromax-007HF Cu-target micro-focus rotating anode (λ = 1.54187 Å) operated at 1.2 kW power (40 kV, 30 mA). The X-ray intensities were measured at 85(1) K with the detector placed at a distance 42.00 mm from the crystal; the data were processed with CrystalClear 2.011 and corrected for absorption. The structures were solved and refined with the Olex2 software package[164] and ShelXL.[165]

Electrochemical measurements were performed on a Bio-Logic SP200 potentiostat/galvanostat with a built-in electrochemical impedance spectroscopy (EIS) analyzer. CV and DPV were measured in fluorobenzene with 0.1 M [NBu$_4$][BAr$^F_4$] as the electrolyte with a platinum working electrode (1.6 mm disk OD, 6.4 mm OD PCTFE shroud), a platinum counter electrode, and a chloridized silver wire electrode in a glass tube filled with the electrolyte solution with a CoralPor™ tip. All measurements were performed under an N_2 atmosphere in a glovebox

with electrolyte solutions that had been cooled in a -40 °C in an acetonitrile dry ice bath prior to adding the measured compound. The OCP of was made to be reproducible prior to voltammetry experiments of each analyte solution. The DPV and CV were measured with iR compensation to 85% of the solution uncompensated resistance and then corrected to Fc* and subsequently to Fc centered at 0.459 V and -0.181 V respectively vs the reference electrode. R_u values between 6.5-10 kΩ were determined for each solution by a single frequency EIS method (ZIR) for each cell. DPV were measured using a pulse amplitude to 50 mV, pulse width of 50 ms, and step time of 200 ms.

4.9.2 Synthesis of Fe-N_2-LA Adducts

$Fe(depe)_2(\mu\text{-}N_2)(B(C_6F_5)_3)$ (2):

$Fe(depe)_2N_2$ (1) (25.0 mg, 50.0 µmol) and $B(C_6F_5)_3$ (25.8 mg, 50.0 µmol) were combined in a scintillation vial. Pentane (4 mL) was then added at room temperature and the mixture stirred for three minutes, generating a dark brown precipitate. The solvent was then removed under vacuum and the residual crystals washed with pentane (1 mL). This pentane was then removed by syringe and the solid dried under vacuum for 10 minutes to afford diamagnetic $Fe(depe)_2(\mu\text{-}N_2)(B(C_6F_5)_3)$ (2) (44.3 mg, 87% yield) as black crystals. A C_6D_6 solution of 2 was used for transmission IR spectroscopy. ^{1}H-NMR (C_6D_6): 1.42 (-C*H*$_2$, 2H, m), 1.35 (-C*H*$_2$, 2H, m), 1.20 (-C*H*$_2$, 2H, m), 1.13 (-C*H*$_2$, 2H, m), 1.11 (-C*H*$_2$, 2H, m), 0.82 (-C*H*$_3$, 6H, broad), 0.75 (-C*H*$_2$, 2H, m), 0.56 (-C*H*$_3$, 6H, m). ^{19}F-NMR (C_6D_6): -131.65 (-*o* F, 6F, d ($J_{19F\text{-}19F}$=19.1)), -159.47 (-*p* F, 3F, t ($J_{19F\text{-}19F}$=20.8)), -164.83 (-*m* F, 6F, t ($J_{19F\text{-}19F}$=19.2)). ^{11}B-NMR (C_6D_6): -6.35 (s). ^{31}P-NMR (C_6D_6): 76.15 (s). ^{15}N-NMR ((C_6H_5F): -10.54 (1N, s), -119.83 (1N, s). IR (C_6D_6, cm^{-1}): ^{14}N-^{14}N: 1816.3, ^{15}N-^{15}N: 1757.9 (calc.: 1753.6). 2 can be prepared in-situ through combining a 1:1 ratio of $Fe(depe)_2N_2$ with $B(C_6F_5)_3$ in a variety of solvents (IR, cm^{-1}): C_6D_6: 1816.3, PhF: 1810.3, methyl tert-butyl ether: 1816.6, tetrahydrofuran: 1805.0.

$Fe(depe)_2(\mu\text{-}^{15}N_2)(B(C_6F_5)_3)$ (2-^{15}N):

1 (5.0 mg, 10 µmol) was dissolved in C_6D_6 (500 µL) in a screw-cap scintillation vial. 4 mL $^{15}N_2$ was sparged through the solution, and the solution allowed to stand for five days. Solid $B(C_6F_5)_3$ (5.2 mg, 10 µmol) was then added, and the resulting solution was analyzed by transmission IR spectroscopy. For ^{15}N-NMR characterization, 1 (5.0 mg, 10 µmol) was dissolved in C_6H_5F (500 µL) in a screw-cap NMR tube under an argon atmosphere. Solid $B(C_6F_5)_3$ (5.2 mg, 10 µmol) was then added, and the tube inverted until homogeneous (<1 minute). 3 mL $^{15}N_2$ was

sparged through the solution, and the solution allowed to stand for three minutes, and then immediately analyzed by ^{15}N-NMR.

Fe(depe)$_2$(μ-N$_2$H)(B(C$_6$F$_5$)$_3$)(BAr$^F_4$) (3):

A solution of 2 (50 μmol in 4.0 mL C_6H_5F, 12.5 mM) was cooled to -30 °C in a small scintillation vial containing a teflon-coated stirbar. H(OEt$_2$)$_2$BAr$^F_4$ (50.6 mg, 50 μmol) was rapidly added to 2 in one portion, and vigorously shaken for 10 seconds to provide a homogeneous solution. The deep red solution of 2 immediately changes to an intense purple. The solution was then layered with 15 mL of -30 °C pentane and allowed to stand overnight, affording large purple crystals. The solvent was decanted, the crystals washed with pentane, and finally dried under vacuum for five minutes at room temperature to afford Fe(depe)$_2$(μ-N$_2$H)(B(C$_6$F$_5$)$_3$)(BAr$^F_4$) (3) as a crystalline solid (91.9 mg, 98%). For NMR analysis, in an identical preparation the cold C_6H_5F solution of 3 was transferred to a -30 °C NMR tube, and NMR spectra recorded at -45 °C without allowing the solution to warm beyond -30 °C. A sample of the solid was used to prepare a KBr pellet in a bolt-press for transmission IR analysis. ^{31}P-NMR showed a single diamagnetic product as composing 91% of phosphorus atoms in the sample, with the remaining 9% consisting of 4% *trans*-Fe(depe)$_2$(N$_2$)H and 5% of an unknown impurity. A single crystal was prepared by allowing pentane to diffuse into a solution of 4 in C_6H_5F at -30 °C. Samples of solid 3 are stable at room temperature under nitrogen for at least 4 hours. ^{31}P-NMR (C_6H_5F, -45 °C): 90.23 (1P, dd ($J_{31P\text{-}31P}$=44.7, 39.2), 78.56 (2P, h (37.3, 36.1), 72.01 (1P, dd ($J_{31P\text{-}31P}$ =47.0, 38.4). ^{19}F-NMR (C_6H_5F, -45 °C): -60.11 (BAr$^F_4$, 24F, s), -125.3 — -138.8 (6F, m (overlapping broad signals), -150.3 — -155.7 (3F, m (overlapping broad signals), -158.1 — -163.3 (6F, m (overlapping broad signals). ^{11}B-NMR (C_6H_5F, -45 °C): -1.09. ^{15}N-NMR (C_6H_5F, -45 °C): -49.31 (proximal –*N*, 1N, s (broad)), -140.71 (terminal –*N*, 1N, d ($J_{15N\text{-}1H}$=80.7). IR (KBr, cm^{-1}): ^{14}N-^{1}H: 3259, ^{15}N-^{1}H: 3247 (calc.: 3245); ^{14}N-^{11}B: 1421, ^{15}N-^{11}B: 1406 (calc.: 1401); ^{14}N-^{14}N: 1519, ^{15}N-^{15}N: 1465 (calc.: 1467), ^{14}N-^{56}Fe: 639, ^{15}N-^{56}Fe: 618 (calc.: 621).

Fe(depe)$_2$(μ-N$_2$H)(B(C$_6$F$_5$)$_3$)(BAr$^F_4$) (3-^{15}N):

A solution of 2-^{15}N in C_6H_5F (60 μmol in 0.6 mL, 100 mM) was cooled to -30 °C in an NMR tube, under an argon atmosphere. A solution of H(OEt$_2$)$_2$BAr$^F_4$ (60 μmol in 0.2 mL C_6H_5F, 300 mM) cooled to -30 °C was rapidly added to 2 in one portion using a -30 °C syringe, and the chilled NMR tube rapidly inverted to mix the two components. NMR spectra were then recorded at -45 °C. To obtain a solid sample for KBr pellet IR spectroscopy, A solution of 2-^{15}N in C_6H_5F

(60 µmol in 0.6 mL, 100 mM) was cooled to -30 °C in scintillation vial, under an argon atmosphere. A solution of $H(OEt_2)_2BAr^F_4$ (60 µmol in 0.2 mL C_6H_5F, 300 mM) cooled to -30 °C was rapidly added to 2 in one portion using a -30 °C syringe, and the chilled vial shaken to mix the two components. The purple solution was then triturated with 6 mL -30 °C pentane, and allowed to settle for 1 hour. The pentane was decanted and the purple solid dried under vacuum for 5 minutes at room temperature. The solid was then used to prepare a KBr pellet in a bolt-press and was analyzed by transmission IR spectroscopy.

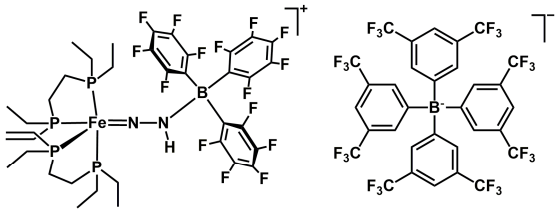

^{14}N-^{1}H: 3259; ^{15}N-^{1}H: 3247 (Expected: 3245)
^{14}N-^{14}N: 1519; ^{15}N-^{15}N: 1465 (Expected: 1467)
^{14}N-^{11}B: 1421; ^{15}N-^{11}B: 1406 (Expected: 1401)
^{14}N-^{56}Fe: 639; ^{15}N-^{56}Fe: 618 (Expected: 621)

Figure 4-6 Tabulated ^{15}N-X vs. ^{14}N-X Stretches vs. Harmonic Oscillator Calculated Shifts

$Fe(depe)_2(\mu\text{-}N_2)Fe(^{i}Pr_2Tp)(BAr^F_4)$ (4):

$Fe(depe)_2N_2$ (1) (20.0 mg, 40.0 µmol), Fe(II)($^{i}Pr_2Tp$)Cl (22.2 mg, 40.0 µmol), and $NaBAr^F_4$ (35.4 mg, 40.0 mg) were combined in a scintillation vial. C_6H_5F (2 mL) was then added at room temperature and the mixture stirred for three minutes, generating a dark brown solution and a colorless precipitate. The mixture was filtered, and the filtrate evaporate under vacuum to afford $Fe(depe)_2(\mu\text{-}N_2)Fe(^{i}Pr_2Tp)(BAr^F_4)$ (4) as a dark brown/green powder (69.0 mg, 91% yield). A single crystal suitable for X-ray diffraction was prepared by layering pentane over a C6H5F solution of 4. A solution of 4 in C_6H_5F was used for transmission IR spectroscopy. ^{11}B-NMR (C_6D_6): -6.01; ^{31}P-NMR (C_6D_6): 80.34, 80.11. µeff (Evans Method): 4.77 (3.87 unpaired electrons; S=2). UV/Vis (C_6H_6): 441 (ε=2780), 902 (IVCT, ε=1680). Solvent-Dependent IVCT band peak position, absorption coefficient (ε), full width at half max (FWHM): C_6H_6: 910 nm, ε=1700 $M^{-1}cm^{-1}$, FWHM=3398 cm^{-1}; C_6H_5F: 914 nm, ε=993 $M^{-1}cm^{-1}$, FWHM=3276 cm^{-1}; tetrahydrofuran: 905 nm, ε=857 $M^{-1}cm^{-1}$, FWHM=2872 cm^{-1}. IR (C6H5F, cm^{-1}): 1824.

$Fe(I)(depe)_2(\mu\text{-}N_2)(BAr^F_4)$

This compound was prepared as reported in main text reference #9c (J. Am. Chem. Soc., 2016, 138 (41), pp 13521–13524) with minor modifications. $Fe(depe)_2N_2$ (1) (20.0 mg, 40.0 µmol) was combined with ferrocenium BAr^F_4 (41.0 mg, 40.0 µmol) at -80 °C in 1 mL diethyl ether. The

solution immediately became a light-yellow color. The solution was allowed to stir at room temperature for 1 hour, after which time the solution became deep blue. The solution was triturated with 15 mL pentane and allowed to stand. The supernatant was decanted, and the solid washed with pentane (3 x 15 mL). The solid was dried under vacuum for 1 hour, providing 42 mg of $Fe(I)(depe)_2(\mu\text{-}N_2)(BAr^F{}_4)$ as a light blue powder (78% yield). As this previously reported compound is S=1/2, the complex was NMR silent (although the $BAr^F{}_4$ anion could be identified by ^{19}F NMR). IR (KBr): 2074 cm^{-1}; IR (PhF): 2056 cm^{-1}. ^{19}F-NMR (PhF): -62.97. The EPR spectrum (295 K, PhF) closely matched the reported literature spectrum for 1^+ OTf^- (223 K, THF).

4.9.3 In-Situ Generation and Characterization of Fe-N_2-LA Adducts

$Fe(depe)_2(N_2)$ (10 µmol, 4.9 mg) and 10 µmol of a Lewis acid were combined in a small 2 mL vial equipped with a teflon lined septum (a gas chromatography sample vial). To this was added 0.5 mL solvent (Et_2O if $LA=M^+BAr^F{}_4^-$ (M= Na, K, Rb, Cs) or $LiB(C_6F_5)_4$; C_6H_5F if $LA=BR_3$ (R=2,6-F_2-Ph, 2,4,6-F_3-Ph, C_6F_5, OC_6F_5, or F)), and the vial shaken vigorously for 30 seconds to afford a homogeneous solution. The solution was then transferred via syringe into a transmission IR solution cell and IR spectra were immediately recorded.

4.9.4 Determination of Equilibrium Binding Constants for Fe-N_2-LA Adducts

General Procedure for $LA=BR_3$ in C_6H_5F (R=2,6-F_2-Ph, 2,4,6-F_3-Ph, C_6F_5, or OC_6F_5):

A C_6H_5F solution containing $Fe(depe)_2(N_2)$ (0.100 M) and diisopropyl ketone (0.100 M) (50.0 µL, 5.00 µmol) was added to a solution of Lewis acid (0.050M, 100 µL, 5.00 µmol) in a 2 mL vial equipped with a teflon lined septum (a gas chromatography sample vial) using a volumetric syringe. The vial was shaken vigorously for 30 seconds to afford a homogeneous solution. The solution was then transferred via syringe into a transmission IR solution cell and IR spectra were immediately recorded. Concentrations were evaluated based on the relative integration of $Fe(depe)_2(N_2)$ vs. the diisopropyl ketone internal standard, as compared to an IR spectrum taken of a 0.02 M stock of a 1:1 mixture of $Fe(depe)_2(N_2)$ and diisopropyl ketone (relative integrated IR absorption: 6.55).

General Procedure for $LA=M^+$ in Et_2O (M^+=[Li $B(C_6F_5)_4$, Na $BAr^F{}_4$, K $BAr^F{}_4$, Rb $BAr^F{}_4$, Cs $BAr^F{}_4$]):

A Et_2O solution containing $Fe(depe)_2(N_2)$ (40.0 mM) and diisopropyl ketone (40.0 mM) (250 µL, 10.0 µmol) was added to a solution of Lewis acid (40.0 mM, 250 µL, 10.0 µmol) in a 2

mL vial equipped with a teflon lined septum (a gas chromatography sample vial) using a volumetric syringe. The vial was shaken vigorously for 30 seconds to afford a homogeneous solution. The solution was then transferred via syringe into a transmission IR solution cell and IR spectra were immediately recorded. Concentrations were evaluated based on the relative integration of $Fe(depe)_2(N_2)$ vs. the diisopropyl ketone internal standard, as compared to an IR spectrum taken of a 0.02 M stock of a 1:1 mixture of $Fe(depe)_2(N_2)$ and diisopropyl ketone (relative integrated IR absorption: 8.56).

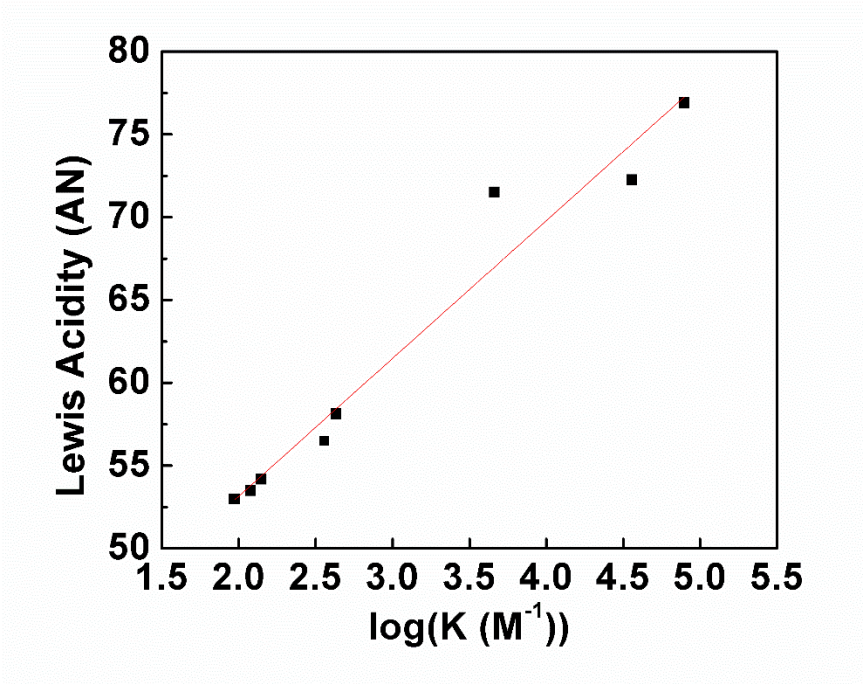

Figure 4-7 Binding Constant vs. Lewis Acidity

4.9.5 Electrochemical Analysis

This work was done in collaboration with James Shanahan.

Lewis acid adducts of **1** were prepared in fluorobenzene in situ via addition of a stock solution of each Lewis acid to an aliquot of a stock solution of **1** to yield a 30 mM of a dark brown stock solution of the adduct. The resulting adduct stock solutions were cooled in the dry ice acetonitrile bath prior to addition of aliquots of analyte to the electrolyte to a concentration of 4 mM **1-LA**. For measurements indicating excess LA, an appropriate amount of the LA stock solution was added to the cell containing the initial 1 eq adduct and gently swirled at low temperature for 1 min prior to additional data collection.

For measurement of **3**, solid HBArF (1 eq) was added to the cooled stock solution (30 mM) of **2** at -40 °C. An aliquot of the resulting solution was used without further purification for electrochemical analysis at a concentration of 4 mM assuming quantitative conversion of **2** to **3**.

For measurement of **4**, a 30 mM stock solution in fluorobenzene was prepared from the purified solid and added to the cell to yield a solution of 4 mM.

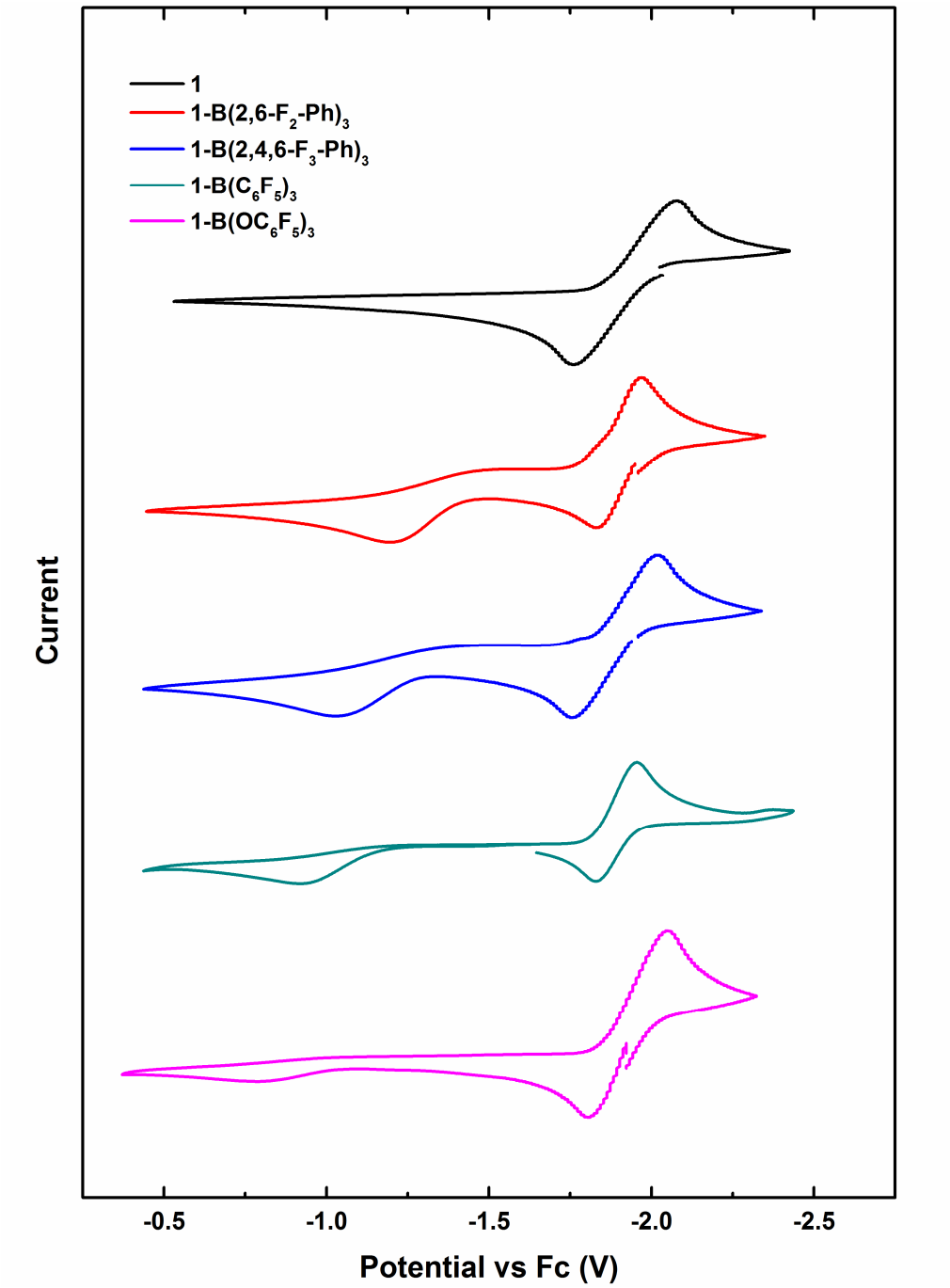

Figure 4-8 CV of **1** vs **1**-LA Adducts (Scan Rate 100 mV/s)

4.9.6 DFT Calculations

Calculations were performed with the Gaussian 09[166] suite of programs using the B3LYP functional,[167] the IEFPCM polarizable continuum solvent model for fluorobenzene,[168] and an ultrafine (150,974 point) integration grid for all atoms. All reported compounds underwent geometry optimization with the 6-31G(d,p) basis set,[169] followed by vibrational frequency calculations. These were used to verify that the structures were truly local energetic minima by the absence of imaginary vibrational modes and to provide entropies of formation at 25 °C. Enthalpies of formation and orbital energies were calculated with a further single-point energy calculation performed using the higher-level 6-311G(2d,p)(51) basis set. Due to significant hindered rotor effects in the molecules under investigation, zero point enthalpy corrections determined in the course of the calculation of vibrational modes with the 6-31G(d,p) basis set were then combined with these enthalpies of formation calculated using the 6-311++G(2d,p) basis set to provide the zero-point energy corrected enthalpy for each compound rather than using calculated free energies of formation. Natural bonding orbital analysis was performed using NBO version 3.1[170] and orbital mixing analysis was performed using AOMix version 6.46[171] using the 6-311G(2d,p) basis set. The Walsh analysis was performed by performing a relaxed potential energy surface scan on **1-BF$_3$** in which the N-N-B angle was varied from 120° to 180° in 6° increments with the 6-31G(d,p) basis set, followed by single point energy calculations with the 6-311g(2d,p) basis set to provide enthalpies of formation and orbital energies at each angle. Coordinates of the N_2-BF_3 unit in each of these relaxed fixed-angle geometries were then used to obtain enthalpies of formation and orbital energies for this fragment at each angle.

Compound	ΔH_{corr} (kcal/mol)	K(from ΔH_{corr}, kcal/mol)	υ_{NN} (calc, cm^{-1})	K(expt.)	υ_{NN} (expt.)	Acceptor Number (expt.)
$Fe(depe)_2(N_2)$	NA	NA	2076.5033	NA	1958	NA
$Fe(depe)_2(\mu\text{-}N_2)(B(Ph)_3)$	5.6	6.4E-04	1877	<1.0E-01	NA	60.01
$Fe(depe)_2(\mu\text{-}N_2)(B(4\text{-}F\text{-}Ph)_3)$	3.6	1.5E-02	1866	<1.0E-01	NA	62.51
$Fe(depe)_2(\mu\text{-}N_2)(B(2,6\text{-}F_2\text{-}Ph)_3)$	0.6	2.4E+01	1901	1.1E+03	1856	67.42
$Fe(depe)_2(\mu\text{-}N_2)(B(2,4,6\text{-}F_3\text{-}Ph)_3)$	-1.8	1.2E+03	1888	9.3E+03	1843	69.07
$Fe(depe)_2(\mu\text{-}N_2)(B(C_6F_5)_3)$	-11.6	2.1E+11	1854	2.1E+04	1809	79.36
$Fe(depe)_2(\mu\text{-}N_2)(B(OC_6F_5)_3)$	0.5	7.0E+01	1846	3.2E+00	1786	89.46
$Fe(depe)_2(\mu\text{-}N_2)(BF_3)$	-17.3	6.8E+15	1852	NA	1812	81.37

Figure 4-9 Corrected enthalpies of binding between Lewis acids (LA) and $Fe(depe)_2N_2$, Approximate calculated binding constants, calculated N-N vibrational frequency, and comparison with experimental values

Compound	Proximal Nitrogen Atom Charge	Terminal Nitrogen Atom Charge	NN π^* orbital population (e^-)
$Fe(depe)_2(N_2)$	0.108	-0.215	0.169
$Fe(depe)_2(\mu\text{-}N_2)(B(Ph)_3)$	0.113	-0.266	0.209
$Fe(depe)_2(\mu\text{-}N_2)(B(4\text{-}F\text{-}Ph)_3)$	0.107	-0.277	0.210
$Fe(depe)_2(\mu\text{-}N_2)(B(2,6\text{-}F_2\text{-}Ph)_3)$	0.118	-0.252	0.217
$Fe(depe)_2(\mu\text{-}N_2)(B(2,4,6\text{-}F_3\text{-}Ph)_3)$	0.112	-0.264	0.218
$Fe(depe)_2(\mu\text{-}N_2)(B(C_6F_5)_3)$	0.089	-0.296	0.222
$Fe(depe)_2(\mu\text{-}N_2)(B(OC_6F_5)_3)$	0.111	-0.369	0.228
$Fe(depe)_2(\mu\text{-}N_2)(BF_3)$	0.112	-0.377	0.220

Figure 4-10 Tabulated Natural Bonding Orbital Data (6-311++g(2d,p))

Compound	N_2 π* Energy	HOMO Energy
N_2	-0.717	NA
$Fe(depe)_2(N_2)$	-1.18	-3.73
$Fe(depe)_2(\mu\text{-}N_2)(B(Ph)_3)$	-3.89	-4.307
$Fe(depe)_2(\mu\text{-}N_2)(B(4\text{-}F\text{-}Ph)_3)$	-4.07	-4.385
$Fe(depe)_2(\mu\text{-}N_2)(B(2,6\text{-}F_2\text{-}Ph)_3)$	-4.09	-4.298
$Fe(depe)_2(\mu\text{-}N_2)(B(2,4,6\text{-}F_3\text{-}Ph)_3)$	-4.27	-4.38
$Fe(depe)_2(\mu\text{-}N_2)(B(C_6F_5)_3)$	-4.81	-4.597
$Fe(depe)_2(\mu\text{-}N_2)(B(OC_6F_5)_3)$	-5.24	-4.867
$Fe(depe)_2(\mu\text{-}N_2)(BF_3)$	-5.23	-4.758

Figure 4-11 Tabulated Molecular Orbital Energies (6-311g(2d,p))

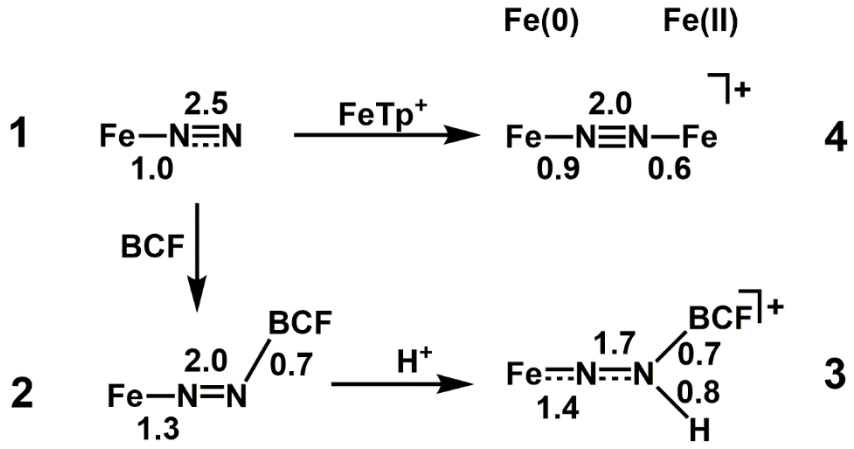

Figure 4-12 Wiberg bond indices (NBO, 6-311g(2d,p)) for **1-4**

N-N-B Angle	N_2-BF_3 Enthalpy	Fe(depe)$_2$$N_2$-$BF_3$ Enthalpy
120	-434.1535	-2715.0532
126	-434.1591	-2715.0531
132	-434.1636	-2715.0527
138	-434.1687	-2715.0513
144	-434.1733	-2715.0494
150	-434.1774	-2715.0472
156	-434.1809	-2715.0450
162	-434.1838	-2715.0431
168	-434.1859	-2715.0415
174	-434.1872	-2715.0405
180	-434.1874	-2715.0402

Figure 4-13 Walsh Analysis of **1-BF_3**; Tabulated Energies

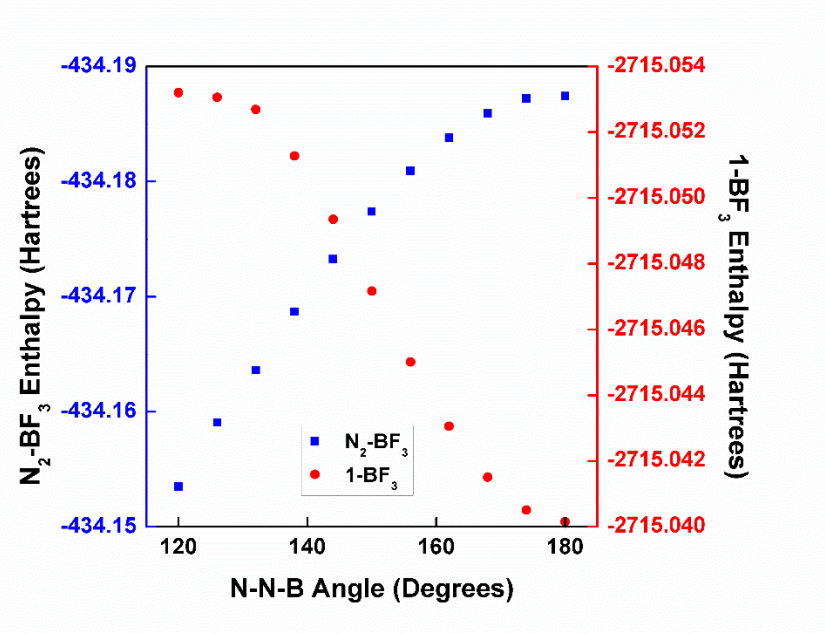

Figure 4-14 Free Energy of Fe(depe)$_2$$N_2$-$BF_3$ with varied N-N-B Angle vs. N_2-BF_3

Chapter 5. Recyclable Trifluoromethylation Reagents from Fluoroform

Portions of this chapter have been published:
Geri, J. B.; Szymczak, N. K.; Recyclable Trifluoromethylation Reagents from Fluoroform
J. Am. Chem. Soc. 2017, 139, 9811-9814.

5.1 Abstract

We present a strategy to rationally prepare CF_3^- transfer reagents at ambient temperature from HCF_3. We demonstrate that a highly reactive CF_3^- adduct can be synthesized from alkali metal hydride, HCF_3, and borazine Lewis acids in quantitative yield at room temperature. These nucleophilic reagents transfer CF_3^- to substrates without additional chemical activation, and after CF_3 transfer, the free borazine is quantitatively regenerated. These features enable syntheses of popular nucleophilic, radical, and electrophilic trifluoromethylation reagents with complete recycling of the borazine Lewis acid.

5.2 Introduction

The trifluoromethyl functional group is widely used in medicinal chemistry to enhance the bioavailability, lipophilicity, and resistance to oxidative degradation of drug molecules, and these properties have led to its inclusion in 60 approved drugs.[172] Fluoroform (HCF_3,< \$0.10/mole) is an attractive starting material for CF_3 installation reactions: it is nontoxic, widely available, and easily handled.[173] However, even though >0.5 million metric tons of HCF_3 are produced each year as a byproduct from PTFE manufacturing, it is not used as a CF_3 feedstock and is instead incinerated because of its high global warming potential.[174]

Unlike methane, which is widely used as a source of the $–CH_3$ group,[175] the use of HCF_3 as a $-CF_3$ feedstock has presented significant challenges. Although HCF_3 has a large C-H bond dissociation enthalpy (106 kcal/mol),[176] its weak acidity (pK_a = 28)[177] renders deprotonation strategies for C-H bond activation tractable.[173a,178] Unlike CH_3^-, which can be readily transferred to electrophilic substrates using organometallic reagents,[179] analogous $LiCF_3$ and $MgX(CF_3)$ are

unstable because they irreversibly eliminate F^- at -80 °C.[180] However, CF_3^- can be stabilized through the formation of a Lewis acid (LA)-CF_3 adduct; this strategy forms the basis of all nucleophilic trifluoromethylation reagents.[181] The key challenge that prevents the economic synthesis of LA-CF_3^- reagents from HCF_3 through deprotonation is poor compatibility between components of the reaction mixture. The Lewis acid and Brønsted base must coexist in solution prior to HCF_3 addition because the CF_3^- anion is extremely unstable. Furthermore, the strong base needed to deprotonate HCF_3 must not irreversibly react with the Lewis acid, and the Lewis acid itself must not promote CF_3^- defluorination (Figure **5-1**).

Two primary strategies have emerged to provide compatible pairs of Lewis acids and bases: the use of steric bulk to separate reactive Lewis acidic and basic centers,[8,182] and the use of Lewis pairs with mismatched strength between Lewis acidic and basic centers to enable *reversible* adduct formation.[68,183] Recently, steric control has been used to activate HCF_3 using a mixture of bulky bases (potassium bis(trimethylsilyl)amide (KHMDS) [71] or phosphazene superbases)[184] and Lewis acids such as $SiMe_3Cl$. The instability of the CF_3^- intermediate (-80 °C) requires the combination of KHMDS and electrophiles *prior* to addition of HCF_3, which presents an operational challenge. This strategy is limited by the expense of the required bases, cryogenic temperatures, and low generality.[173a]

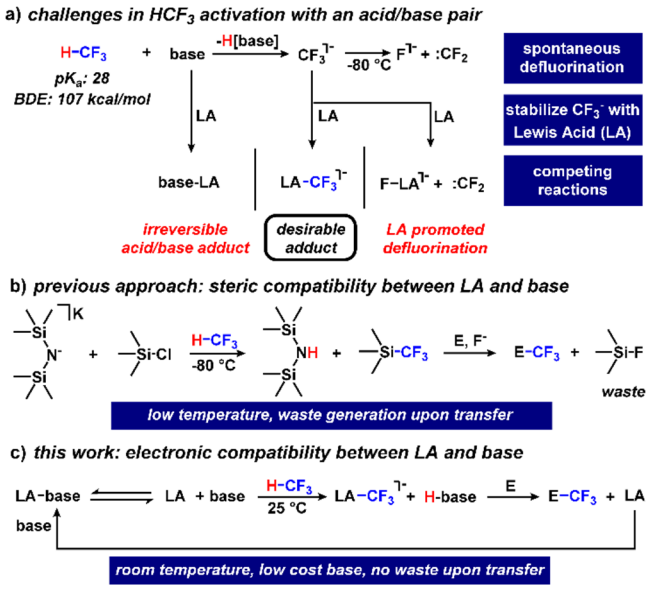

Figure 5-1 Challenges and solutions associated with HCF_3 activation

In contrast with the use of steric bulk at the base, we sought to design a system for room-temperature HCF_3 activation using neutral, *weak* Lewis acids to avoid irreversible reactions with

bases and provide optimal stabilization of CF_3^-. Importantly, we hypothesized that a precisely tuned Lewis acid could be readily recyclable, impart high CF_3^- nucleophilicity to a LA-CF_3 adduct, and prevent F^- elimination from CF_3^- at room temperature. This represents a distinct concept in HCF_3 activation: no systematic approach for the selection of Lewis acids capable of providing these three desirable properties has been reported.

We targeted low-cost alkali metal hydride derived bases (NaH: \$0.10/mole, KH: \$35/mole) for HCF_3 deprotonation, and boron-based Lewis acids. A widely used solvent, dimethyl sulfoxide (DMSO), reacts with alkali hydrides to produce the dimsyl anion ($DMSO^-$, $pK_a = 35$).[185] Due to the low expense of this strong, soluble base and its ability to deprotonate HCF_3, we selected it as an ideal basic partner.[186] Boron-based Lewis acids were targeted because they have a wide range of Lewis acidities,[187] and can easily prepared.

5.3 Computational Selection of Lewis Acids for Experimental Investigation

An appropriately selected Lewis acid must react *reversibly* with K[DMSO] in order to enable HCF_3 deprotonation, while subsequently providing sufficient Lewis acidity to capture and stabilize CF_3^-. In order to rationally select Lewis acids with a wide range of strengths for experimental evaluation, the CF_3^- affinity of a variety of cyclic and acyclic boron Lewis acids was assessed computationally using density functional theory (DFT). The ΔG of the reaction between CF_3^- and a given Lewis acid was calculated at the M062X/6-311++G(d,p) level.[169,188] The scale was set to zero relative to the known adduct between dimethylformamide and CF_3.[178a] The data were translated to provide predicted relative binding constants on a log scale (pK_{CF3}) as a unified metric of CF_3^- affinity. We used these data to select a set of 13 Lewis acids representing a 30 pK_{CF3} span for experimental evaluation in reactions between K[DMSO] , Lewis acids, and HCF_3 (Figure **5-2**).

5.4 Experimental Screening of Lewis Acids

Equimolar quantities of K[DMSO] and each Lewis acid were combined at room temperature in DMSO solvent at 0.1 M concentration. HCF_3 gas was added (1 atm), and the formation of B-CF_3 adducts was assessed by ^{19}F-NMR spectroscopy. Lewis acids with pK_{CF3} values above 11 exhibited *irreversible* coordination to $[DMSO]^-$, and did not react with HCF_3.

Lewis acids with pK_{CF3} values below 6 rapidly reacted with HCF_3, but were insufficiently Lewis acidic to stabilize the CF_3^- anion resulting from HCF_3 deprotonation (Figure **5-2**).[189]

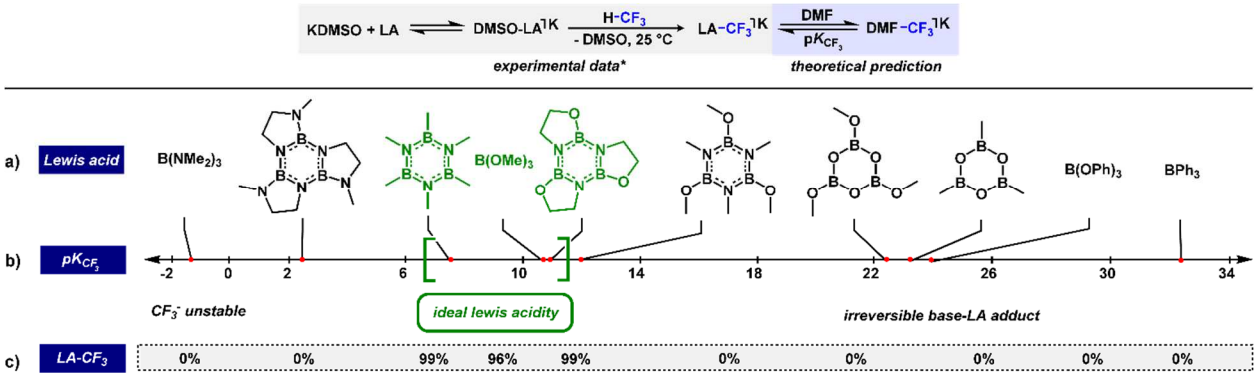

Figure 5-2 Development of LA-CF_3^- adducts from HCF_3. a) Lewis acids evaluated. b) Calculated pK_{CF3} values (M062X/6-311++G(d,p)). c) Experimental yield of LA-CF_3^- adduct (^{19}F-NMR)

Three Lewis acids with intermediate pK_{CF3} values between 6 and 11 productively reacted with HCF_3 to provide B-CF_3 species in quantitative yield (Figure **5-3**A). When either hexamethylborazine ($B_3N_3Me_6$), trimethyl borate ($B(OMe)_3$), or trisethyleneoxyborazine ($(BOC_2H_4N)_3$) were combined with one equiv. K[DMSO], followed by one equiv. HCF_3 in DMSO solvent, the B-CF_3 adducts were observed (**1**, **2**, and **3**) in quantitative conversion within 5 min at room temperature. These three Lewis acids are inexpensive; $B(OMe)_3$ is a commodity chemical with many industrial applications (<$1/mole),[190] and $B_3N_3Me_6$ and $(BOC_2H_4N)_3$ can be synthesized from cheap, simple starting materials. Importantly, **2** is currently an expensive CF_3^- reagent with reported applications in direct nucleophilic trifluoromethylation and copper-catalyzed cross-coupling.[191] Solutions of **1** and **3** are oxygen-stable, decomposed on exposure to moisture, and returned the free borazine Lewis acids upon thermal decomposition.

5.5 Synthesis and Characterization of Borazine-CF_3^- Adducts

To examine the mechanism of CF_3 adduct formation, the reaction between $B_3N_3Me_6$ and K[DMSO] was followed spectroscopically. The combination of equimolar amounts of K[DMSO] and $B_3N_3Me_6$ in DMSO afforded a homogeneous solution containing a single new species with C_s symmetry, as assessed by NMR spectroscopy. ^{1}H, ^{13}C, and ^{11}B-NMR spectra support the formation of a 1:1 Lewis pair between K[DMSO] and $B_3N_3Me_6$ at room temperature (**4**). The ^{11}B-NMR spectra exhibited a 2:1 set of resonances at 32.5 and -3.6 ppm. The resonance at -3.6 ppm is consistent with a tetrahedral boron center, while the broad resonance at 32.5 ppm ($\nu_{1/2}$ = 477 Hz)

is minimally shifted from the free $B_3N_3Me_6$ (35.5), consistent with two planar boron centers.[192] The reversibility of K[DMSO] adduct formation with $B_3N_3Me_6$ was examined by variable temperature NMR spectroscopy. At room temperature, the ^{1}H-NMR spectrum exhibited broad resonances at 0.04 and -0.44 ppm for the B-*CH*$_3$ resonances. These resonances sharpened as the temperature was lowered to 15 °C. As the temperature was raised, the resonances broadened and coalesced at 35 ºC; further increasing the temperature to 90 °C resulted in the appearance of resonances consistent with free $B_3N_3Me_6$. Upon cooling, **4** was cleanly regenerated. The coalescence temperature of 35 ºC was used to estimate a $\Delta G^{\ddagger} \approx 14$ kcal/mol.[193] These data are consistent with a dynamic and reversible exchange process between $[DMSO]^-$ and $B_3N_3Me_6$ at room temperature (Figure **5-3**B).

The addition of one equiv HCF_3 to **4** immediately (<1 minute) afforded **1** in 99% yield. NMR spectroscopy revealed a species similar to **4**, as assessed via ^{1}H, ^{11}B, ^{19}F and ^{13}C NMR spectroscopy. A new resonance at -65.7 ppm ($^2J_{10B\text{-}13C}$=210 was observed in the ^{19}F NMR spectrum, consistent with a B-CF_3 adduct. A new 2:1 set of resonances in the ^{11}B NMR spectrum at 33.1 and -5.7 ppm was observed along with two 2:1 sets of -CH_3 resonances in the ^{1}H and ^{13}C-NMR spectra, representing the desymmetrized N-CH_3 (^{1}H: 2.49, 2.45 ppm, ^{13}C: 34.73, 34.55 ppm) and B-CH_3 (^{1}H: 0.08, -0.35 ppm, ^{13}C: 4.31, 0.16 ppm) units. The sharp peaks exhibited by this complex in the ^{1}H, ^{13}C, and ^{19}F NMR spectra suggest that although **4** equilibrates with free K[DMSO], the formation of **1** is irreversible at room temperature.

Preparation of **1** in the less polar solvent tetrahydrofuran (THF) required adjustments to the base and the countercation. Potassium toluide (KTol) was selected as an inexpensive base that can be prepared on large scales and in high (>95%) yield from KO*t*Bu, BuLi, and toluene at room temperature.[194] The Lewis adduct between KTol, 18-crown-6,[195] and $B_3N_3Me_6$ (**5**) was characterized using NMR spectroscopy and X-ray crystallography. **5** possesses similar NMR spectra in comparison with **4** and **5**: C_s symmetry and diagnostic 2:1 sets of B-CH_3 and N-CH_3 resonances. The solid-state structure of **5** revealed a tetrahedral boron center, containing two distinct B-C bond lengths for the B-CH_3 and B-CH_2Ph bonds (1.590(4) Å and 1.775(5) Å, respectively). The B-CH_2Ph bond length is among the longest structurally characterized B-C bonds[196] and consistent with a weak B-CH_2Ph bond. Similar to **4**, variable temperature ^{1}H NMR spectra of **5** exhibited dynamic behavior with broadening of the B-CH_3 peaks at 25 °C, which indicate reversible dissociation of the toluide base.

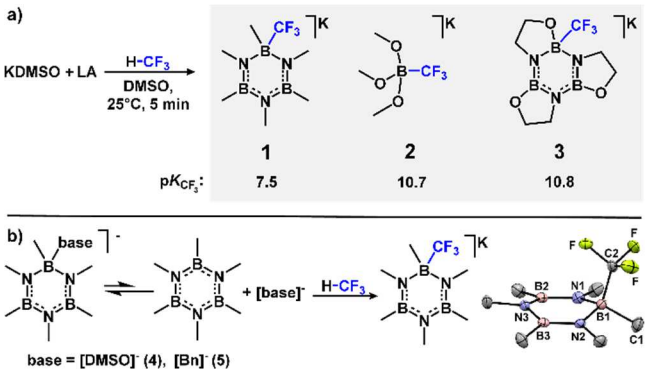

Figure 5-3 a) Synthesis of 1, 2, and 3 from HCF3. b) HCF_3 activation by $B_3N_3Me_6$/base.

Solutions of **1** were prepared in THF by the addition of one equiv HCF_3 to **5**. **1** was obtained as a weighable solid in 95% yield by evaporation of THF, and was structurally characterized by X-ray crystallography. A single crystal of **1** was grown through diffusion of pentane into a concentrated THF solution at -30 °C, enabling a structural analysis (Figure **5-3**B). The aromatic character of the borazine unit was disrupted by the inclusion of a tetrahedral boron center resulting from the formation of a new B-CF_3 bond (C1-B1-C2: 107.1(2)°), with elongation of the proximal B-N bond distances (B1-N1: 1.550(3) Å; B1-N2: 1.549(3) Å) vs. 1.44(3) in free borazine). The B1-C2 (*CF_3*) bond (1.656(4) Å) is longer than the B1-C1 (*CH_3*) bond (1.627(4) Å), consistent with a weaker B-CF_3 bond. DFT analyses augmented the structural data and revealed a larger binding enthalpy of CH_3^- to $B_3N_3Me_6$ than that of CF_3^- by 8.5 kcal/mol. These structural and calculated metrics indicate that CF_3^- transfer should be preferred over CH_3^- transfer to electrophilic substrates.

5.6 Preliminary Investigation of CF_3^- Transfer to Organic Electrophiles

Although $KB(OMe)_3CF_3$ (**2**) has been previously shown to facilitate nucleophilic CF_3^- transfer reactions, these proceed only under forcing reaction conditions.[197] Because nucleophilic CF_3^- transfer necessitates the cleavage of a B-CF_3 bond, we hypothesized that CF_3^- reagents stabilized by weaker Lewis acids may exhibit superior nucleophilicity. **1** has a pK_{CF3} value 3.2 units lower than **2**, indicating that $B_3N_3Me_6$ is a weaker Lewis acid than $B(OMe)_3$. The addition of $B(OMe)_3$ to **1** afforded **2** in 80% yield, which is consistent with the difference in the calculated CF_3^- affinity of $B_3N_3Me_6$ and $B(OMe)_3$ (Figure **5-4**b). When **1** was allowed to react with benzophenone, the corresponding trifluoromethylcarbinol was generated in 72% yield in 30 minutes at room temperature. In contrast, **2** provided only 2% yield under identical conditions; this implicates a higher nucleophilicity of **1** than **2** (Figure **5-4**b).

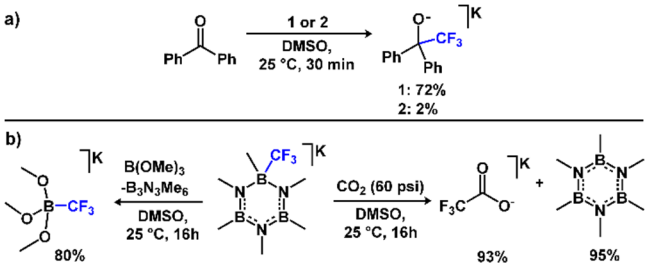

Figure 5-4 a) Relative reactivity of **1** and **2**. b) CF_3^- transfer between **1** and $B(OMe)_3$; synthesis of $CF_3CO_2^-$ from HCF_3 and subsequent recovery of $B_3N_3Me_6$.

The observation that $B_3N_3Me_6$ can be released upon thermal decomposition of **1** suggests that the free Lewis acid may be regenerated, recovered, and reused after CF_3^- transfer. As the simplest carbonyl-containing electrophile, CO_2 was selected as an initial substrate to test this hypothesis. The addition of 4 atm CO_2 to **1** in DMSO afforded trifluoroacetate ($CO_2CF_3^-$) in 93% isolated yield after 16h, concomitant with precipitation of $B_3N_3Me_6$ (Figure **5-4**b). $B_3N_3Me_6$ was recovered in 95% isolated yield by extraction into pentane; the recovery of the free Lewis acid after CF_3 transfer is a unique attribute of this system. Transformations with high atom economy using **1** should provide an economic and operational advantage[198] in comparison with $SiMe_3CF_3/CsF$[181a], $KB(OMe_3)CF_3$ or $DMF/KOtBu/HCF_3$,[186] which generate stoichiometric waste ($SiMe_3F$) or require low temperatures (-80 °C).

5.7 Synthesis of Existing CF_3^-, $CF_3\bullet$, and CF_3^+ Reagents

The high cost of trifluoromethylation reagents stems largely from their multi-step syntheses from CF_3Br or CF_3I.[181a,199] The regeneration of the $B_3N_3Me_6$ Lewis acid in the reactions noted above suggested that these popular reagents could be prepared from HCF_3 using $B_3N_3Me_6$ as a recyclable component, thereby reducing the reaction inputs to low cost base, HCF_3, and the direct precursor (Figure **5-5**). Reagents used to install the CF_3 group can be divided between their use for nucleophilic CF_3^-,[200] radical $CF_3\bullet$,[201] and electrophilic CF_3^+ transfer.[202] The most important of these is $SiMe_3CF_3$, the currently used precursor to almost all other trifluoromethylation reagents.[181a] We used the preparation of this compound to demonstrate the practical *in situ* recyclability of the Lewis acid on a large scale.

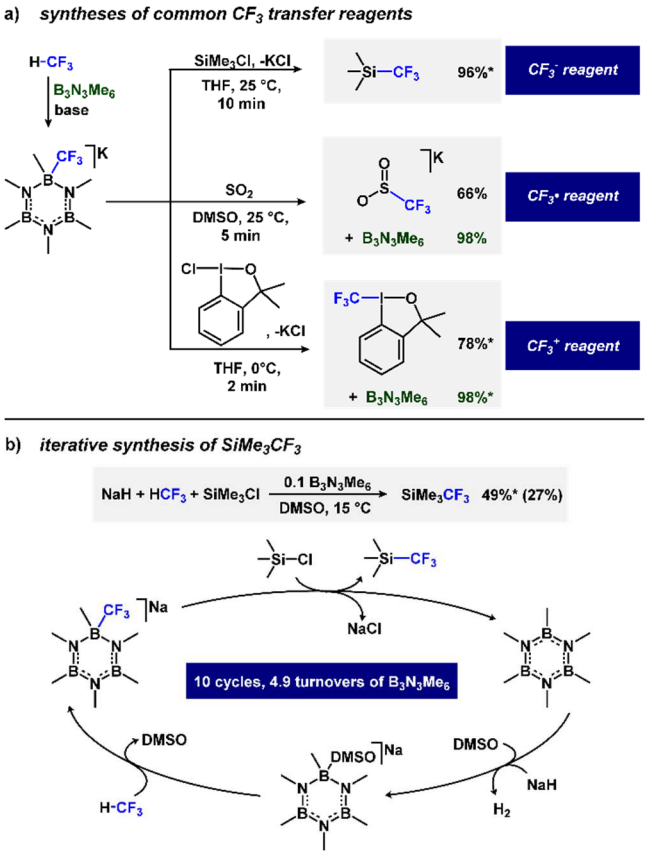

Figure 5-5 a) Synthesis of $SiMe_3CF_3$, KSO_2CF_3, and Togni I from HCF_3. b) Iterative synthesis of $SiMe_3CF_3$ with in-situ $B_3N_3Me_6$ recycling.

Through ten cycles of an iterative addition/distillation protocol, we achieved ~5 turnovers with respect to $B_3N_3Me_6$ to obtain 34 mmol $SiMe_3CF_3$ after distillation without the need for separation or purification of the borazine Lewis acid. The only consumed reagents used were low cost NaH, $SiMe_3Cl$, and HCF_3. The radical CF_3• reagent KSO_2CF_3[201] was also prepared in 66% isolated yield by treating SO_2 with **1** (98 % recovery of $B_3N_3Me_6$). Finally, the hypervalent iodonium-CF_3 reagent Togni I,[202] a widely used CF_3^+ reagent, was synthesized in 78% chemical yield and with 98% regeneration of $B_3N_3Me_6$ by treating 1-chloro-3,3-dimethyl-1,3-dihydro-1λ_3-benzo[*d*][1,2]iodaoxole with **1**. We expect that direct access to these well-established nucleophilic CF_3^-, radical CF_3•, and electrophilic CF_3^+ reagents from HCF_3 may reduce the cost and increase access to the CF_3 group in existing large-scale processes.

5.8 Conclusions

In summary, through a combined theoretical/experimental approach, we have developed a predictive design concept which led to the economic preparation of several trifluoromethylation

reagents from HCF_3. One of these, **1**, exhibited high nucleophilicity at room temperature. After CF_3^- transfer, the free Lewis acid was quantitatively regenerated. We exploited this property to present an iterative synthesis of $SiMe_3CF_3$ on a large scale from NaH, HCF_3, and $SiMe_3Cl$ as the only consumed reagents with repeated *in-situ* reuse of the Lewis acid. This methodology provides direct access to other common trifluoromethylating reagents from HCF_3, including $K(B(OMe)_3CF_3$, KSO_2CF_3, KCO_2CF_3, and Togni reagent I. Finally, we introduce borazines as a class of precisely tunable, weak Lewis acids for synthetic applications. The rational selection of compatible Lewis acids and bases for efficient nucleophilic trifluoromethylation using HCF_3 is a design strategy that may also be applied to other unstable anions to promote other difficult nucleophilic functionalizations.

5.9 Experimental Details

5.9.1 General Considerations

Hexamethylborazine,[203] (B,B',B'')trismethoxy-(N,N',N'')trimethylborazine,[204] tris-N-methylethyleneiminoborazine,[205] tris-N-methyl(1,3)propyleneiminoborazine,[205] 1-Chloro-1,3-dihydro-3,3-dimethyl-1,2-benziodoxole,[206] benzylpotassium,[207] dimsyl potassium,[185] dimsyl sodium,[208] were prepared according to literature procedures. DMSO, pentane, THF, benzene, acetonitrile, toluene, and DMF were purified using a Glass Contour solvent purification system through percolation through a Cu catalyst, molecular sieves, and alumina and finally stored over activated molecular sieves for a minimum of 48 hours. Xylene was distilled from molten sodium under nitrogen. All other reagents were used from commercial sources without further purification. Unless otherwise noted, all manipulations were performed under an inert nitrogen atmosphere.

NMR spectra were recorded on a Varian Vnmrs 700, Varian Vnmrs 500, or Varian MR400 spectrometer. ^1H, ^{13}C, ^{19}F, and ^{11}B shifts are reported in parts per million (ppm) relative to TMS, with the residual solvent peak used as an internal reference. ^{11}B and ^{19}F NMR spectra are referenced to fluorobenzene or, in spectra lacking internal standard, on a unified scale, where the single primary reference is the frequency of the residual solvent peak in the ^1H NMR spectrum. Peaks not listed in the peak assignment correspond to residual solvent.[209] Multiplicities are reported as follows: singlet (s), doublet (d), triplet (t), quartet (q), pentet (p), septet (sp), and multiplet (m). Mass spectra were obtained on an electrospray Agilent Q-TOF mass spectrometer or a Micromass AutoSpec Ultima Magnetic Sector Mass Spectrometer electron ionization mass

spectrometer. Crystals were mounted on a Rigaku AFC10K Saturn 944+ CCD-based X-ray diffractometer equipped with a low temperature device and Micromax-007HF Cu-target micro-focus rotating anode (λ = 1.54187 Å) operated at 1.2 kW power (40 kV, 30 mA). The X-ray intensities were measured at 85(1) K with the detector placed at a distance 42.00 mm from the crystal; the data were processed with CrystalClear 2.011 and corrected for absorption. The structures were solved and refined with the Olex2[164] software package and ShelXL.[165] NMR spectra were processed using MestReNova version 10.0.2. For the purpose of labeling atoms for spectral assignments, hydrogen atoms are labeled with Greek letters while carbon atoms are labeled with numbers. In spectra of *in-situ* reactions, HCF_3 and fluorobenzene (internal standard) appear at -78.52 and -113.15 ppm, respectively.

Calculations were performed with the Gaussian 09[210] suite of programs using the M062X functional,[188] the IEFPCM polarizable continuum solvent model for dimethylsulfoxide,[168] and an ultrafine (150,974 point) integration grid for all atoms. All reported compounds underwent geometry optimization with the 6-31G(d,p) basis set,[169] followed by vibrational frequency calculations. These were used to verify that the structures were truly local energetic minima by the absence of imaginary vibrational modes and to provide entropies of formation at 25 °C. Enthalpies of formation were calculated with a further single-point energy calculation performed using the higher-level 6-311++G(2d,p)[211] basis set. Entropies of formation determined in the course of the calculation of vibrational modes with the 6-31G(d,p) basis set were then combined with these enthalpies of formation calculated using the 6-311++G(2d,p) basis set to provide the Gibbs free energy for each compound.

5.9.2 Selection of Lewis Acid for Preparation of LA-CF_3 Reagents from HCF_3: Summary

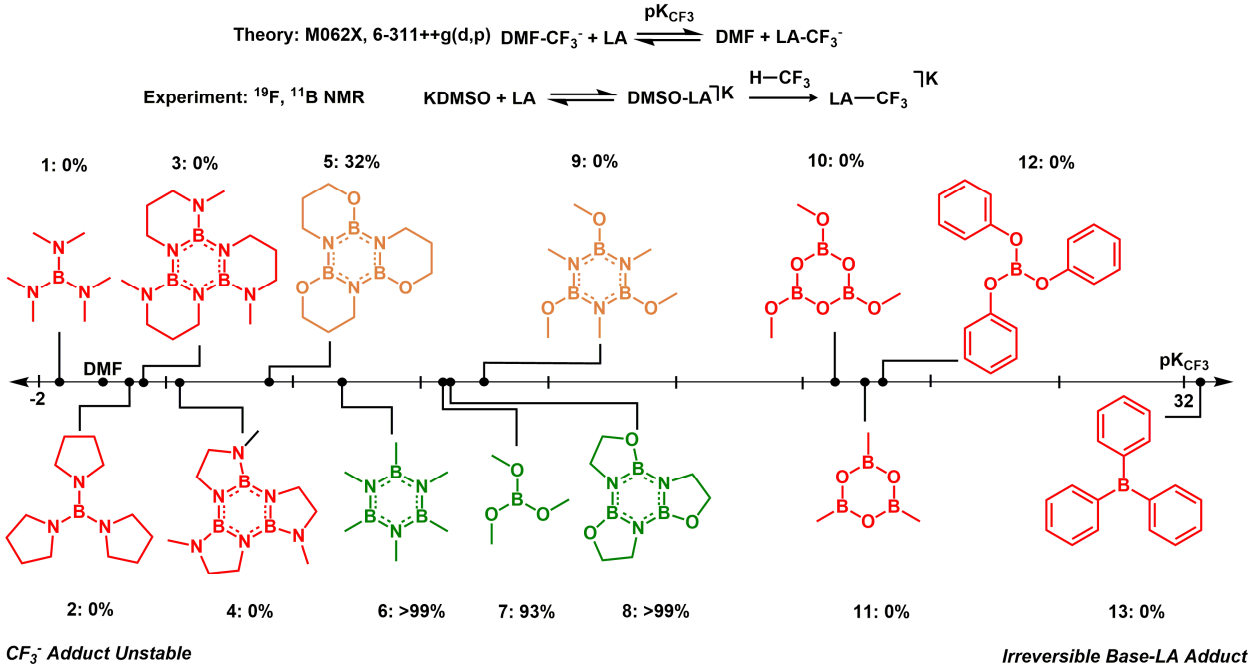

Figure 5-6 Summary of Lewis acid screening data: pK_{CF3} vs. yield of LA-CF_3 adducts

5.9.3 Computational Determination of pK_{CF3}:

The Gibbs free energies (G) of a set of Lewis acids and their complexes with CF_3^- were obtained, with dimethylformamide (DMF) used as a reference compound. The relative affinity of each Lewis acid for CF_3^- relative to DMF was calculated by first calculating the change in Gibbs free energy (ΔG) for a reaction of a free Lewis acid with the anionic DMF-CF_3^- adduct to produce a Lewis acid-CF_3 adduct and free DMF. The ΔG was then transformed into a pK_{CF3}.

Lewis Acid	ΔG	K	pK_{CF3}
DMF	0.00	0.00E+00	0.00
$B(NMe_2)_3$ (1)	1.63	4.95E-02	-1.31
$B(NCH_2H_4)_3$ (2)	-1.14	8.24E+00	0.92
$(BNMeC_3H_6N)_3$ (3)	-1.73	2.44E+01	1.39
$(BNMeC_2H_4N)_3$ (4)	-2.99	2.47E+02	2.39
$(BOC_3H_6N)_3$ (5)	-6.43	1.41E+05	5.15
$B_3N_3(Me)_6$ (6)	-9.37	3.14E+07	7.50
$B_3N_3Me_3(NMe_2)_3$	-9.92	8.72E+07	7.94
$B(OMe)_3$ (7)	-13.45	5.87E+10	10.77
$(BOC_2H_4N)_3$ (8)	-13.53	6.84E+10	10.84
$B_3N_3Me_3(OMe)_3$ (9)	-14.94	9.19E+11	11.96
$B_3O_3OMe_3$ (10)	-26.36	1.26E+21	21.10
$B_3O_3Me_3$ (11)	-27.27	6.76E+21	21.83
$BOPh_3$ (12)	-28.17	3.57E+22	22.55
BPh_3 (13)	-40.62	3.32E+32	32.52

Figure 5-7 Tabulated pK_{CF3} of Each Lewis Acid. ΔG is given in kcal/mol. K and pK_{CF3} are dimensionless.

5.9.4 Experimental Evaluation of Lewis Acid Reactions with KDMSO and HCF_3

Experimental: To 0.1 mmol of Lewis acid dissolved in 1.0 mL DMSO was added one equiv. dimsyl potassium (50 µL, 2.0 M stock) and fluorobenzene as an internal standard (9.0 µL, 0.095 mmol) in an 8 mL vial. The mixture was stirred for 10 minutes, and HCF_3 gas was sparged through the solution for 10 seconds. After 10 minutes, ^{19}F NMR spectra were obtained.

5.9.5 Preparation of Polycyclic Borazine Lewis Acids

Although these compounds have been previously prepared, we present alternative preparations from BH_3•SMe_2 with expanded characterization.[212]

Trisethyleneoxyborazine:

Ethanolamine (35g, 0.57 mol) was suspended in 400 mL toluene at room temperature in a 3-necked 1-liter flask equipped with a large 5 cm stirbar, valved sidearm leading to a nitrogen/vacuum manifold, a rubber septum, and a water-cooled reflux condenser topped with a distillation head with a connected water-jacketed condenser, receiving flask, and gas outlet leading to a nitrogen/vacuum manifold. Borane-dimethylsulfide (60 mL, 0.63 mol) was then added rapidly by syringe through the septum. ~40 mL of dimethylsulfide promptly distilled concomitant with gas evolution. After 30 minutes, gas evolution had largely ceased, leaving a sticky, white, foaming solid along the walls of the flask. The rubber septum was then replaced with a glass stopper against a positive flow of nitrogen. At this time, the reaction was heated to 110 °C and stirred, resulting in gas evolution. After 16 hours, the reaction was homogeneous with no gas evolution. The distillation head and reflux condenser were exchanged for a rubber septum against a positive flow of nitrogen, and a large cannula was used to transfer the hot solution through a Schlenk frit into a 1-liter Schlenk flask. The frit was then replaced with a rubber septum, and the hot solution was cooled to -20 °C for 16 hours to give large white crystals of the product. The supernatant was removed from the flask while still cold, via cannula, and the solid dried under vacuum to provide 21 g (54%) trisethyleneoxyborazine as a white, crystalline solid. Its melting point is somewhat higher than that found in the literature (literature m.p.: 205 °C).[212] ^{1}H-NMR (C_6D_6): 3.84 (2H, (t, $J_{1H\text{-}1H}$ = 7.6)), 3.15 (2H, (t, $J_{1H\text{-}1H}$=7.6)). ^{13}C-NMR: 68.04, 42.43. ^{11}B-NMR: 28.35. Melting point: 220 °C. HRMS (EI+): 207.1160 (M+: 207.1158).

Tris(1,3)propyleneoxyborazine:

1, 3-Propanolamine (0.630 mL, 8.25 mmol) was suspended in 10 mL xylene at room temperature in a 50 mL Schlenk flask equipped with a 1 cm stirbar, a valved sidearm leading to a nitrogen/vacuum manifold, and a water-cooled reflux condenser topped with a rubber septum connected to a nitrogen/vacuum manifold via a needle. BH_3-Dimethylsulfide (0.950 mL, 9.90 mmol) was then added rapidly by syringe through the septum. A small quantity of dimethylsulfide (<1 mL) promptly distilled off along with a voluminous quantity of H_2 gas. After 30 minutes, H_2 evolution had largely ceased, leaving a sticky, white, slightly foaming solid along the walls of the flask. At this time, the reaction was heated to 150 °C and stirred, giving a boiling solution with continuous evolution of H_2 gas. After two hours, H_2 evolution had slowed considerably and most of the white solid in the reaction had dissolved. After 56 hours, the reaction was homogeneous and H_2 evolution had ended. The reflux condenser was then replaced with a glass stopper and

solvent removed under vacuum. The solid residue was then sublimed to provide 307 mg (45%) tris(1,3)propyleneoxyborazine as a white, crystalline solid. Its spectroscopic characteristics match those reported in the literature (^{11}B-NMR: 24 ppm).[212b] ^{1}H-NMR (C_6D_6): 3.73 (2H, (t, $J_{1H\text{-}1H}$=5.3)), 3.21 (2H, (t, $J_{1H\text{-}1H}$=5.3)), 1.40 (2H, (p, $J_{1H\text{-}1H}$=5.6)). ^{13}C-NMR: 62.98, 38.25, 27.36. ^{11}B-NMR: 24.39. HRMS (EI+): 249.1628 (M+: 249.1627).

5.9.6 Preparation of Pure $B_3N_3Me_6$-Base Adducts

K(18-crown-6)($B_3N_3Me_6$)($CH_2C_6H_5$):

Hexamethylborazine (0.100 mmol, 16.4 mg) and 18-crown-6 (0.100 mmol, 26.4 mg) were dissolved in 0.50 mL THF-d_8 in an 8 mL vial. The vial was then chilled to -80 °C. To the cold solution was added benzylpotassium (0.100 mmol, 13.0 mg), and the resulting blood red solution quickly turned light purple. The cold solution was quickly transferred to a J-Young NMR tube, which had been pre-chilled to -80 °C. The tube was then placed in an NMR spectrometer probe which had been pre-chilled to -45 °C. NMR spectra were obtained at this temperature, and then the spectrometer was slowly warmed in 10 °C increments to 25 °C. At each temperature, following a 5-minute temperature equilibration, a ^{1}H NMR spectrum was recorded. The compound decomposed slowly at temperatures above 5 °C. Single crystals of this compound were obtained by vapor diffusion of pentane into a concentrated THF solution at -35 °C. ^{1}H-NMR (THF-d_8): 6.74 (δ, 2H, broad), 6.61 (ζ, 2H, broad), 6.46 (η, 1H, broad), 3.53 (τ, 24H, s), 2.50 (ß, 6H, s), 2.10 (γ, 3H, s), 1.45 (θ, 2H, s), -0.08 (ε, 6H, s), -0.36 (α, 3H, s). ^{13}C-NMR: 154.55 (10), 129.56 (7), 126.54 (6), 120.23 (8), 71.87 (9), 36.09 (2), 35.35 (4), 34.78 (5, q, $J_{11B\text{-}13C}$=175), 9.42 (1, q, $J_{11B\text{-}13C}$=224), 0.60 (1). ^{11}B-NMR: 31.68 (2B, broad), -1.65 (1B, sharp).

K($B_3N_3Me_6$)(CD_2SOCD_3):

Hexamethylborazine (0.100 mmol, 16.4 mg) and KDMSO-d_5 in DMSO-d_6 (0.100 mmol, 50.7 µL of 1.97 M stock solution) were dissolved in 0.50 mL DMSO-d_6 in a J-Young NMR tube. The NMR tube was then chilled to 15 °C in an NMR probe, and NMR spectra were recorded. The temperature in the probe was increased in 10 °C increments to 90 °C, with ^{1}H NMR spectra recorded at each temperature after a 5-minute equilibration. The two sets of B-Me resonances coalesced into a singlet at 35 °C, consistent with a dynamic exchange process at room temperature. ^{1}H-NMR (DMSO-d_6): 2.44 (ß, γ, 12H, broad), 0.04 (ε, 6H, broad), -0.44 (α, 3H, broad). ^{13}C-NMR: 34.51 (2, 4, broad), 10.34 (1, broad), -0.01 (3, broad). ^{11}B-NMR: 32.55 (2B, broad), -3.57 (1B, sharp).

5.9.7 Preparation of Pure $B_3N_3Me_6$-CF_3 Adducts from HCF_3

K(18-crown-6)($B_3N_3Me_6$)CF_3:

A J-Young NMR tube charged with 0.100 mmol K(18-crown-6)($B_3N_3Me_6$)($CH_2C_6H_5$) in 0.50 mL THF at -80 °C was charged with 14 psig HCF_3. The cold NMR tube was placed in a pre-cooled NMR spectrometer at -80 °C. ^{19}F NMR showed complete conversion to K(18-crown-6)($B_3N_3Me_6$)CF_3 within 10 minutes. The solvent was removed *in vacuo* and reconstituted in THF-d_8. Single crystals of this compound were obtained by vapor diffusion of pentane into a concentrated THF solution at -35 °C. ^{1}H-NMR (THF-d_8): 3.60 (τ, 24H, s), 2.59 (γ, 3H, s), 2.56 (ß, 6H, s), 0.12 (ε, 6H, s), -0.27 (α, 3H, s). ^{13}C-NMR: 70.13 (5), 34.02 (2), 33.88 (4), 3.41 (1, q, $J_{^{10B}-^{13C}}$=210), -1.20 (3) ^{11}B-NMR: 32.87 (2B, broad), -5.56 (1B, sharp). ^{19}F-NMR: -65.75 (q, $J_{^{10B}-^{13C}}$=19.1)

K($B_3N_3Me_6$)CF_3:

A J-Young tube charged with K($B_3N_3Me_6$)(CD_2SOCD_3) (0.100 mmol) was charged with 14 psig HCF_3. ^{1}H-NMR (DMSO-d_6): 2.49 (γ, 3H, s), 2.45 (ß, 6H, s), 0.08 (ε, 6H, broad), -0.35 (α, 3H, broad). ^{11}B-NMR: 33.06 (2B, broad), -5.68 (1B, sharp). ^{19}F-NMR: -64.46 (q, $J_{^{11B}-^{19F}}$=22.8). Due to ^{11}B/^{10}B-^{13}C and ^{19}F-^{13}C coupling in the trifluoromethyl group, the carbon atom in the CF_3 group was not directly detected in the ^{13}C NMR spectrum.

5.9.8 Preparation of LA-CF_3 Stock Solutions from HCF_3

K(18-crown-6)($B_3N_3Me_6$)CF_3(THF) in THF:

Hexamethylborazine (2.70 mmol, 0.443 g) and 18-crown-6 (2.70 mmol, 0.712 g) were dissolved in 11 mL THF in a 20 mL single-neck conical flask equipped with a large Teflon-coated magnetic stirbar. The vessel was then cooled to 0 °C for one hour with gentle stirring. Benzylpotassium (2.70 mmol, 0.350 g) was quickly added to this cold solution, and the initial deep red color of dissolved benzylpotassium quickly changed to light purple. The flask was then sealed with a belt-clamped septum. HCF_3 was added to the sealed vessel with a 60 mL syringe (3.3 mmol, 75 mL) and continuously stirred for 10 minutes. ^{19}F NMR showed >99% yield of K($B_3N_3Me_6CF_3$).

K($B_3N_3Me_6$)CF_3 in DMSO:

Hexamethylborazine (2.70 mmol, 0.443 g) was suspended in 13 mL DMSO in a 20 mL single-neck conical flask equipped with a large Teflon-coated magnetic stirbar, which was then sealed with a belt-clamped septum. Dimsyl potassium (1.80 M, 2.70 mmol, 1.50 mL) was then rapidly added via syringe, and the mixture was stirred for 30 minutes at 2000 rpm, which afforded

a homogeneous solution. HCF_3 was added to the sealed vessel with a 60 mL syringe (12.0 mmol, 297 mL) and continuously stirred for 10 minutes. ^{19}F NMR showed >99% yield of $K(BOCH_2CH_2N)_3CF_3$. The $t_{1/2}$ of this solution (^{19}F NMR, 25 °C): 17 days

$K(B(OMe)_3CF_3$ in DMSO:

$B(OMe)_3$ (5.00 mmol, 0.560 mL) was dissolved in 21.8 mL DMSO in a 100 mL single-neck round bottom flask equipped with a large Teflon-coated magnetic stirbar, which was then sealed and secured with a belt-clamped septum. Dimsyl potassium (1.93 M, 5.00 mmol, 2.59 mL) was then rapidly added via syringe, and the mixture was vigorously stirred for 15 seconds. HCF_3 was immediately added to the sealed vessel with a 60 mL syringe (6.00 mmol, 148 mL) and stirred rapidly for 10 minutes. The product was confirmed by comparison with an authentic sample dissolved in DMSO-d_6 (^{19}F-NMR: -65.41 (3F, s)). Yield: 96% by ^{19}F NMR. The $t_{1/2}$ of this solution (^{19}F NMR, 25 °C): >5 months

$K(BOCH_2CH_2N)_3CF_3$ (3) in DMSO:

Trisethyleneoxyborazine (10.5 mmol, 2.17 g) was suspended in 43 mL DMSO in a 100 mL single-neck round bottom flask equipped with a large Teflon-coated magnetic stirbar, which was then sealed with a belt-clamped septum. Dimsyl potassium (1.93 M, 10.0 mmol, 5.18 mL) was then rapidly added via syringe, and the mixture vigorously stirred for 30 minutes. HCF_3 was added to the sealed vessel with a 60 mL syringe (12.0 mmol, 297 mL) and continuously stirred for 10 minutes. ^{19}F NMR showed 99% yield of $K(BOCH_2CH_2N)_3CF_3$ (based on KDMSO). The $t_{1/2}$ of this solution (^{19}F NMR, 25 °C): >5 months

5.9.9 Nucleophilic Trifluoromethylation with LA-CF_3

To 0.1 mmol of benzophenone dissolved in 0.50 mL DMSO or THF was added one equivalent **1** (in THF or DMSO), **2**, or **3**. NMR spectra were recorded at 30-minute, 5-hour, 24 hour, and 72-hour time points to monitor conversion to diphenyltrifluoromethylcarbinol through integration against a 0.030 mmol fluorobenzene internal standard.

Synthesis of $KB(OMe)_3CF_3$ from 1

Experimental: Trimethyl borate (11.2 µL, 0.100 mmol) was placed in an NMR tube and dissolved in 0.50 mL DMSO. $K(B_3N_3Me_6CF_3)$ (0.50 mL 0.20 M stock in DMSO, 0.10 mmol) was then added and the NMR tube was vigorously shaken. ^{19}F NMR spectra were recorded 10 minutes after CF_3^- addition and the product peak integrated against 0.3 mmol fluorobenzene internal standard. The product was confirmed by comparison with an authentic sample prepared according

to literature methods[191] dissolved in DMSO-d_6 (^{19}F-NMR: -65.41 (3F, dd, $J_{11B\text{-}19F}$: 49, 24)): -65.47 (3F, dd, $J_{11B\text{-}19F}$: 49, 24). Yield: 80%.

Synthesis of Potassium Trifluoroacetate from 1

$K(B_3N_3Me_6)CF_3$ (2.00 mmol, 0.2 M stock in DMSO) was placed in a Fisher-Porter tube with a small stirbar. The vessel was charged with 60 psig carbon dioxide, and stirred. A pressure drop to 56 psig was observed along with the precipitation of copious white solid. The reaction was stirred at room temperature for 12 hours. After this time, the reaction mixture was extracted with pentane (3 x 10 mL). The combined pentane extracts were dried over anhydrous calcium chloride, then filtered and the solvent was removed under high vacuum to afford hexamethylborazine in 95% yield (314 mg, 1.91 mmol). ^{1}H-NMR ($CDCl_3$): 2.86 (α, 9H, s), 0.47 (ß, 9H, s). ^{13}C-NMR: 34.52, 0.03 (broad). ^{11}B-NMR: 36.52 (s). HRMS (ES+): 165.1781 (M+: 165.1780). The DMSO phase was removed by sublimation (0.1 mTorr). The white solid residue was extracted into water (5 mL), washed with dichloromethane (6 x 3 mL), and dried in a scintillation vial to give potassium trifluoroacetate as an off-white solid in 93% yield (285 mg, 1.86 mmol). ^{13}C[^{19}F]-NMR (D_2O): 162.90, 116.32. ^{19}F-NMR (D_2O): -75.40 (s). IR: 1671.2, 1607.3, 1428.1, 1387.3, 1202.7, 1174.4, 1118.5, 1022.7. 833.1. 801.5. 720.6.

5.9.10 Synthesis of Trifluoromethylation Reagents from 1

$SiMe_3CF_3$:

Hexamethylborazine (7.70 mmol, 1.26 g) and 15-crown-5 (7.70 mmol, 1.70 g) were suspended in 37 mL DMSO in a 500 mL Schlenk flask equipped with a large Teflon-coated magnetic stirbar, valved stopcock with independent vacuum adapter and a septum, and a valved sidearm. This sidearm was connected to a series of three 40 mL traps held at 0 °C, -80 °C, and -120 °C, and a large 1-liter trap held at -200 °C which were all connected to a vacuum manifold equipped with a digital manometer. The flask was held above a water bath equipped with a copper coil connected to a laboratory chiller, and held at 15 °C. For a visual representation, see photograph below.

The following operations were then carried out:

Step 1: NaDMSO (7.0 mmol, 1.7M, 4.2 mL) was added, and the reaction was stirred for 30 minutes at 25 °C to generate Na(15-crown-5)($B_3N_3Me_6$)DMSO. Step 2: The flask was lowered into the 15 °C water bath the mixture chilled for 5 minutes, and HCF_3 (220 mL, 1.20 equiv., 8.40 mmol) was then added to the reaction at 15 °C over the course of 5 minutes. The reaction was then

stirred for 5 minutes. Step 3: $SiMe_3Cl$ (7.60 mmol , 0.964 mL) was added to the reaction over the course of 1 minute as a neat liquid, then the reaction was stirred for four minutes. Step 4: The inert gases in the apparatus were withdrawn through the series of low temperature traps until a static vacuum of 0.070 mTorr or better was obtained. The volatiles were distilled under static vacuum with the reaction flask held at 15 °C for 30 minutes, then for a further hour with the reaction flask held at 25 °C. The reaction flask was then closed off from the series of traps and refilled with nitrogen.

Steps 1 through 4 were then repeated ten times. After the first cycle, the reaction was homogeneous. From the second cycle on, increasing amounts of NaCl precipitate accumulated and the reaction became dark brown in color. The contents of the -80 °C and -120 °C traps were then combined to give 8.22 g crude colorless oil. ^{1}H NMR analysis of the distillate showed that it was 65% $SiMe_3CF_3$ and 37% $(SiMe_3)_2O$, corresponding to 49% conversion of the limiting reagent NaDMSO used to $SiMe_3CF_3$. The mixture was then separated using two fractional distillations to provide 2.82 g of pure $SiMe_3CF_3$ (27% isolated yield, 22% lost to evaporation; purity 95%) as a colorless oil via fractional distillation (b.p.: 54 °C).). ^{1}H-NMR ($CDCl_3$): 0.26. ^{13}C-NMR: 131.56 (q, $J_{13C\text{-}19F}$=322), -5.38. ^{19}F-NMR: -66.81 (s). ^{29}Si-NMR: 4.10 (q, $J_{29Si\text{-}19F}$=38.1).

Figure 5-8 Photograph of Apparatus

KSO_2CF_3:

Hexamethylborazine (7.70 mmol, 1.26 g) was suspended in 37 mL DMSO in a 500 mL Schlenk flask. KDMSO (7.00 mmol, 2.0M) was then added, and the reaction was stirred for 30 minutes to generate $K(B_3N_3Me_6)$DMSO. HCF_3 (220 mL, 1.20 equiv., 8.40 mmol) was then added to the reaction at 25 °C over the course of 5 minutes. The reaction was then stirred for 5 minutes. SO_2 (220 mL, 1.20 equiv., 8.40 mmol) was then added to the reaction over the course of 1 minute, then stirred for four minutes. Hexamethylborazine was recovered from the reaction mixture by extraction with pentane in 98% yield (1.23g). The DMSO was then removed by vacuum distillation to provide KSO_2CF_3 in >95% yield with 20% contamination with DMSO. The resulting solid was dissolved in water (10 mL) and washed with CH_2Cl_2 (10 x 5 mL), ethyl acetate (1 x 5 mL), and hexane (1 x 5 mL). The resulting aqueous phase was evaporated to give 793 mg of KSO_2CF_3 (66%). ^{13}C-NMR (D_2O): 126.18 (q, $J_{13C\text{-}19F}$: 343). ^{19}F-NMR (D_2O): -75.40 (s). HRMS (ESI-): 132.9576 (M-K: 132.9566).

1-Trifluoromethyl-3,3-dimethyl-1,3-dihydro-1λ-benzo[d][1,2]iodaoxole

Hexamethylborazine (0.290 mmol, 47.7 mg) and 18-crown-6 (0.290 mmol, 76.6 mg) were dissolved in 1.5 mL THF in a 20 mL flask equipped with a Teflon-coated magnetic stirbar. The vessel was then allowed to cool to 0 °C in a glovebox cold-well for 30 minutes. Benzylpotassium (0.270 mmol, 35.2 mg) was then quickly added to this cold solution, and the initial deep red color of dissolved benzylpotassium quickly changed to a faint purple color. The homogeneous solution was stirred for 2 minutes, giving a homogeneous purple solution. The flask was then sealed with a tightly belt-clamped septum. Gaseous HCF_3 was added to the sealed vessel with a 30 mL syringe (0.32 mmol, 8.0 mL) and continuous efficient stirring. The colorless solution was stirred for 2 minutes, and brought to room temperature. 1 equivalent 1-chloro-3,3-dimethyl-1,3-dihydro-1λ-benzo[d][1,2]iodaoxole (0.27 mmol, 80 mg) was then added to the reaction mixture, and stirred at room temperature for 10 minutes; in this time, a white precipitate appeared. A 60 µL sample was removed for analysis by ^{19}F and ^{1}H NMR; conversion to 1-trifluoromethyl-3,3-dimethyl-1,3-dihydro-1λ-benzo[d][1,2]iodaoxole was 78%, while hexamethylborazine was regenerated (98%). The fluorine NMR spectra of the product matched literature spectra (^{19}F-NMR ($CDCl_3$): -40.1).[213] ^{19}F-NMR (THF): -41.32 (s).

5.9.11 Comments on Practical Aspects of Borazine Lewis Acid Synthesis:

Due their high thermal stability,[214] borazine Lewis acids can be easily prepared from the combination of commercially available and inexpensive amines (NH_3MeCl: \$6/mole from Merck) and boron halides or hydrides ($NaBH_4$: \$11/mole from Merck) at 150-250 °C in high yield. While some hexaalkylborazines are robust in water, and can be worked up on the bench, most borazines are not.[215] All borazine compounds can be readily hydrolyzed with strong aqueous acid or base, which can simplify purification of trifluoromethylation reactions. The most economic preparations of borazines proceed through one of two procedures:

Procedure 1: A two-step protocol allows the synthesis of widely varied C_3-symmetric borazines with individual substituents on nitrogen and boron. BCl_3, BH_3, or $NaBH_4$ are combined with alkylammonium or alkylamine substrates to produce a N,N,N-trialkyl-B,B,B-trichloro[216] or trihydroborazine[203a] through elimination of H_2 or HCl gas.[216] Next, the boron centers are functionalized with nucleophiles such as alkoxides, amines, alkyl anions, and thiolates.[203b,217]

Procedure 2: Polycyclic C_3-symmetric borazines can be prepared in one step from an appropriate aminoalcohol or diamine and BH_3[218] or $B(SEt)_3$[205] with elimination of H_2 or HSEt. Aminoalcohols can be used to construct borazines using $B(OiPr)_3$, which is lower cost than either BH_3 or $B(SEt)_3$.[219] For example, tris-ethyleneoxyborazine, can be readily prepared in an efficient and low-cost route from $B(OiPr)_3$ and ethanolamine by continuous removal of iPrOH by distillation.[220]

Chapter 6. Room-Temperature, Rapid, and Broad Scope Trifluoromethylation of Organic and Inorganic Electrophiles with Borazine-CF_3^- Adducts

Portions of this chapter have been published:

Geri, J. B.; Wolf, M. M. W., Szymczak, N. K.; Borazine-CF3- Adducts for Rapid, Room Temperature, and Broad Scope Trifluoromethylation

Angew. Chem. Int. Ed. 2018, 57, 1381.

6.1 Abstract

We present a strategy to use a fluoroform-derived borazine CF_3^- transfer reagent to effect rapid nucleophilic reactions in the absence of exogenous activator additives within minutes at room temperature. Inorganic electrophiles spanning 7 groups of the periodic table can be trifluoromethylated in high yield, including transition metals used for catalytic trifluoromethylation. Organic electrophiles included arenes and heteroarenes, enabling C-H, C-X (F, Cl), and C-NO_2 trifluoromethylation reactions.

6.2 Introduction

The trifluoromethyl (CF_3) group is an indispensable building block in organic synthesis.[221] As the smallest fluoroalkyl group, it dramatically increases the bioavailability and metabolic stability of drug candidates without altering their steric profile. Nucleophilic trifluoromethylation reactions are particularly attractive; however, the trifluoromethyl anion (CF_3^-) is highly unstable.[180] While CF_3^- can be generated for *in-situ* use, it undergoes irreversible F^- elimination at -80 °C. Lewis acids can be employed to stabilize CF_3^-, but stabilization comes at the cost of attenuated CF_3^- nucleophilicity.[222] As a result, currently used CF_3^- reagents present a more limited reactivity scope than analogous alkyl Grignard and organolithium reagents.

The most commonly used CF_3^- transfer reagent, $SiMe_3CF_3$, uses a cationic Lewis acid (LA, $SiMe_3^+$) to stabilize CF_3^-. $SiMe_3CF_3$ is typically activated by a Lewis base (Nuc; e.g. F^-) to form $SiMe_3(Nuc)(CF_3)^-$ which can release CF_3^-; however, this intermediate is unstable above -

60°C.[181a,223] Therefore low reaction temperatures or *in-situ* activation in the presence of substrate are used, but these conditions introduce operational challenges and/or decreased CF_3 transfer selectivity.[181a,223c] An alternative approach that does not require an activator is the use of neutral LAs to generate anionic LA-CF_3^- adducts.[191,224] Unfortunately, previously employed LAs are either too strong ($B(OMe)_3$,[224] BR_3[225]) or too weak (DMF),[181b] resulting in either low CF_3^- nucleophilicity[197] or low thermal stability.[181b,226] $B(OR)_3CF_3^-$ and DMF-CF_3^- also present reactive oxyanion nucleophiles which can engage in competing reactions with oxophilic electrophiles.[181b,224] A LA with optimal strength and no competing nucleophilic sites could enable the synthesis of potent and selective trifluoromethylation reagents.

We recently reported the preparation of LA-CF_3^- adducts from fluoroform (HCF_3; an industrial waste product), using electronically matched LA/Brønsted base pairs (Figure **6-1**).[72] A combined empirical/theoretical approach facilitated the construction of a CF_3^- affinity scale (pK_{CF3}) which identified hexamethylborazine ($B_3N_3Me_6$) as one of the weakest LAs capable of stabilizing CF_3^- at room temperature; the corresponding CF_3^- adduct, **2**, is highly nucleophilic. Unlike $SiMe_3CF_3/F^-$ (**1a**), $B(OMe)_3CF_3^-$ (**1b**), or DMF-CF_3^- (**1c**), **2** does not present competing nucleophilic centers, enabling reactions with hard electrophiles such as $SiMe_3Cl$, and the free Lewis acid is regenerated after CF_3^- transfer. In this chapter, we show that **2** is capable of rapid and highly general CF_3^- transfer to diverse transition metal, main group, and organic electrophiles.

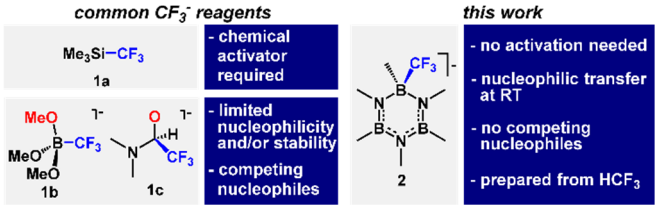

Figure 6-1 Previously reported CF_3^- sources and new borazine-CF_3^- reagents (E=electrophile).

6.3 Trifluoromethylation of Transition Metal Electrophiles

The reactivity profile for CF_3 transfer from a transition metal-CF_3 unit is dictated by the identity of the metal center.[227] Depending on the metal used, the CF_3 ligand can be used to form C-CF_3 bonds through direct nucleophilic transfer (Zn^{2+}),[228] radical substitution (Ag^+),[229] or reductive elimination (Cu^+,[230] Au^{3+},[231] Pd^{2+})[232]. We selected reactions with these metals to assess the transmetalation activity of **2**. Zn(TMEDA)$(Cl)_2$, $AgNO_3$, and Au(SiPr)Cl react with one equiv. **2** to afford M-CF_3 products (**3e**: 74%, **3c**: 44%, and **3d**: 15%) in under 10 minutes at 25 °C (Figure

6-2). While Ag, Au, and Zn –CF_3 complexes are useful CF_3 transfer reagents, only Cu and Pd complexes catalyze cross-coupling with CF_3^-.[191,223c] When treated with one equiv. **2** for 10 min, CuI and Pd(TMEDA)(*p*-tolyl)I reacted to afford $CuCF_3$ and $PdCF_3$ complexes in high yield (**3b**: 83% and **3a:** 98%). The obtained $CuCF_3$ reacts with (4-Ph)PhI to afford (4-Ph)PhCF_3 (66%).

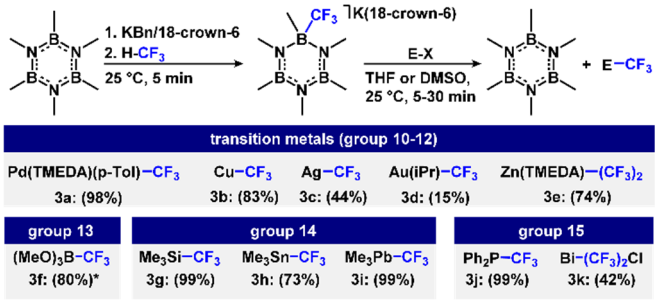

Figure 6-2 Reactions with inorganic electrophiles.

6.4 Trifluoromethylation of Main Group Inorganic Electrophiles

Main group electrophiles in groups 13-15 are challenging substrates for nucleophilic trifluoromethylation due to their high oxo/fluorophilicity.[233] **2** enabled the synthesis of $B(OMe)_3CF_3^-$, $SiMe_3CF_3$, $SnMe_3CF_3$,[234] and $PbMe_3CF_3$[235] from their corresponding halides in good to excellent yield (**3f**: 99%, **3g**: 96%, **3h**: 73%, and **3i**: 99% respectively) at room temperature. Group 15 halides were also trifluoromethylated by **2**; when PPh_2Cl and $BiCl_3$ were combined with **2**, PPh_2CF_3[236] (**3j**) and $Bi(CF_3)_2Cl$[237] (**3k**) were prepared in 99% and 42% yield.

SCF_3 and $SeCF_3$ are important functional groups in medicinal chemistry,[238] and SCF_3^-,[239] $SeCF_3^-$,[239] and $TeCF_3^-$[240] are useful synthons that must be prepared using **1a** at -60 °C. In contrast, **2** reacts with S, Se, and Te within 20 minutes at 25 °C to produce SCF_3^- (4c: 92%), $SeCF_3^-$ (4d: 61%), and $TeCF_3^-$ (4e: 97%); these anions were alkylated *in-situ* in 87% (**4f**), 68% (**4g**), and 59% (**4h**) combined yield. Additionally, dichalcogenides react with **2** to afford S- and Se-ethers (79% (**4a**), 69% (**4b**)). Because **2** is prepared from HCF_3, these reactions represent an economical route to R-SCF_3 and R-$SeCF_3$ moieties.

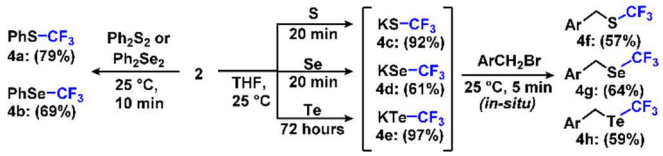

Figure 6-3 Reactions with organic and inorganic chalcogens.

6.5 Comparison with Previously Reported Reagents

We repeated the above reactions using anionic CF_3 transfer reagents: analogous to **2**, these single reagent precursors require no optimization of exogenous additives. **1b**-**c** transfer CF_3^- to inorganic electrophiles, but the reactions are conducted high temperature (**1b**)[191] or cryogenic conditions (**1c**).[191,226,239] Efficiency was compared at 25°C (0.1 M) and yield measured after 10 min.[241] **1b** only provided trace product in all reactions, and **1c** provided products in lower yield than **2** for all but 2 of 14 substrates (**3d** and **4d** (**2**: 15%, 61%; **1c**: 56%, 86%). We attribute the favorable reactivity profile of **2** in comparison with previously reported anionic CF_3^- precursors to the combination of a high rate of CF_3^- transfer and the absence of competing nucleophilic sites.

6.6 Raid Synthesis of Togni I from HCF_3 and its In-Situ Use

Rapid and broad scope synthetic procedures are essential for the preparation of molecules containing ^{18}F ($t_{1/2}$=120 minutes).[242] In principle, the electrophilic CF_3^+ transfer reagent Togni I (**5a**) would be particularly suited for these reactions.[202] The preparation of an ^{18}F isotopologue directly from HCF_3 is attractive, considering the availability of $HC^{19}F_2{}^{18}F$.[243] We used the *in-situ* generation of Togni I from HCF_3-derived **2** to showcase the speed with which HCF_3 can be transformed and delivered to trifluoromethylated substrates through an electrophilic reaction pathway (Figure **6-4**). Preparation of **2** from HCF_3, CF_3^- transfer to form Togni I, and addition of 1-thio-β-D-glucose tetraacetate afforded **5b** in 32 minutes (43% combined yield, Figure **6-4**). Rapid access to CF_3^+ sources from HCF_3 may enable future electrophilic radiotrifluoromethylations.

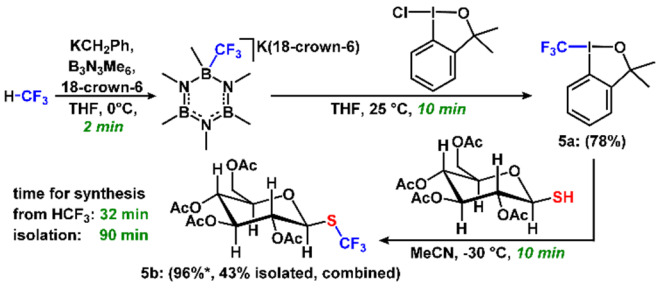

Figure 6-4 Rapid electrophilic trifluoromethylation from HCF_3.

6.7 Addition of CF_3^- to Carbonyl and Imine-Containing Compounds

We next explored the reactions between **2** and non-enolizable organic electrophiles (Figure **6-5**). CF_3^- addition reactions have been extensively studied with carbonyl substrates and were used to benchmark **2**. Substrates containing acyl chloride, isocyanate, aldehyde, ketone, ester, imine, and carbonate groups all afforded addition products in good yield (**6a**-**6k**: 29-87%). In contrast to reactions using **2**, **1b** provided <10% yield in all cases under identical conditions.

6.8 Nucleophilic Aromatic Substitution and Heteroaromatic Addition with CF_3^-

Nucleophilic aromatic addition and substitution (S_NAr) reactions offer unique, orthogonal reactivity patterns[227,244] in comparison with organometallic cross-coupling[227] and radical aromatic substitution.[244b] However, S_NAr reactions with CF_3^- are not well described.[245] We hypothesized that the high nucleophilicity of **2** would support S_NAr reactivity. Indeed, we found that **2** can be used for metal-free C-F and C-NO_2 aromatic trifluoromethylation (Figure **6-5**). **2** reacted with perfluorotoluene, 2-nitropyridine, and *p*-dinitrobenzene to afford **6l-n** in modest yield (27-42%). These reactions represent new general routes to Ar-CF_3 compounds.

Unsubstituted heteroarenes can form σ-complexes with strong nucleophiles, and subsequent oxidation/rearomatization can be an attractive C-H functionalization strategy.[246] Unsubstituted triazine, pyrimidine, and quinazoline compounds selectively reacted with **2** at the 4-position to furnish σ-adducts (Figure **6-5**), which were oxidized to CF_3-substituted products (**6o-q**). Notably, 5-bromo-2-chloropyrimidine afforded **6r** in 49% yield as the sole product. In 4-Cl substituted quinazolines or triazines, treatment with **2** afforded geminal bistrifluoromethylated amides (**6s-u**). The anionic σ-adducts were functionalized at the nitrogen atom by introducing an electrophile (e.g. H_2O, benzyl bromide) to trap and isolate dearomatized heterocyclic products. To demonstrate this selectivity, **6v** was prepared in 60% yield over three steps in one pot. These 4-selective trifluoromethylations of heteroarenes complement *meta*- selective radical C-H trifluoromethylations.[247]

6.9 Selective C-H Trifluoromethylation Reactions with Unsubstituted Quinolines

We hypothesized that **2** could enable selective addition reactions with pyridines if they were first activated by LAs. Using only the steric bulk of the activating LA to control selectivity,

quinoline-LA adducts reacted with **2** to afford σ-adducts at either the 2- (BF_3) or 4- ($B(C_6F_5)_3$) position. These reactions proceeded with high (85%; 93%) selectivity with commercially available LAs, in contrast with a previous method that relied on larger $B(C_6F_4CF_3)_3$ for 4- selective trifluoromethylation.[248] Oxidation of the σ-adducts afforded the C-H trifluoromethylated products (**6w**: 27%; **6x**: 61%). This methodology expands the scope of 2- selective trifluoromethylation reactions beyond pyridine N-oxides,[249] enabling the use of substrates containing oxidizable functionalities.[250] For example, **6y** (37%) contains an allylic thioether that would be oxidized under conditions required to obtain a quinoline N-oxide.[251] Overall, the broad scope reactivity profile provided by **2** showcases the utility of a highly nucleophilic reagent that does not require exogenous activators. [252]

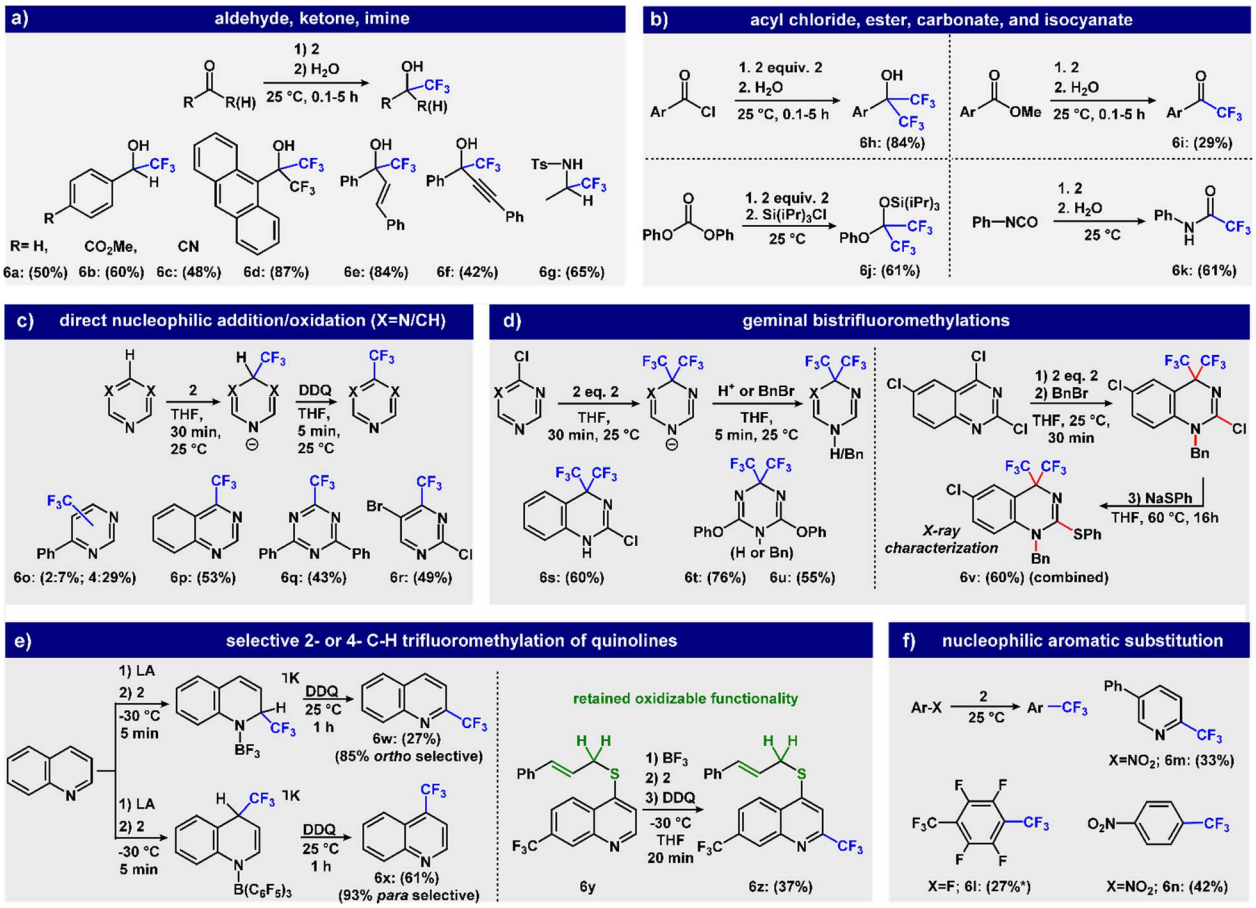

Figure 6-5 a) CF_3^- addition to C=O and C=N compounds. b) CF_3^- addition to acyl chloride, ester, carbonate, and isocycante compounds. c) Nucleophilic aromatic substitution. (*: yield determined by ^{19}F-NMR) d) Direct nucleophilic addition/oxidation. e) Geminal bistrifluoromethylations. f) Selective 2- or 4- C-H trifluoromethylation of quinolines.

6.10 Conclusions

In summary, we have demonstrated that a recyclable and fluoroform-derived CF_3^- reagent promotes rapid and broad-scope trifluoromethylation of transition metals, main group elements, and organic compounds at 25 °C. **2** is an excellent transmetalation reagent, rapidly trifluoromethylating 18 different elements in high yield. The reagents promote CF_3^- transfer reactions with diverse organic electrophiles including carbonyl/imine and (hetero)aromatic compounds. We anticipate that the newly discovered reagent will find numerous applications in organic synthesis.

6.11 Experimental Details

6.11.1 General Considerations

See Subchapter 5.9.

6.11.2 Reactions with Inorganic Electrophiles

To 0.100 mmol of substrate dissolved in 0.50 mL DMSO or THF was added 0.100 mmol K(18-crown-6)($B_3N_3Me_6$)CF_3 as a solution in matching solvent. Characterization of $B(OMe)_3CF_3^-$ is provided for in our previous manuscript.[253]

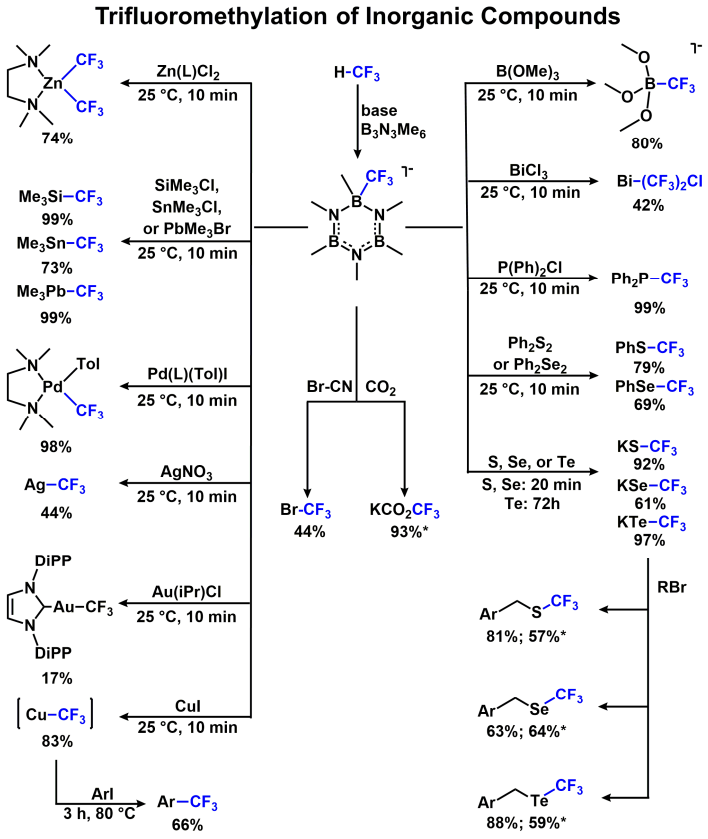

Figure 6-6 Summary of Reactions with Inorganic Electrophiles

$Pd(TMEDA)(Tol)CF_3$

Experimental: Pd(TMEDA)(Tol)I (Tol=$C_6H_4CH_3$) (22.0 mg, 0.0500 mmol) was placed in an NMR tube and dissolved in 1.5 mL THF. K(18-crown-6)($B_3N_3Me_6CF_3$)(THF) (0.250 mL 0.20 M stock in THF, 0.0500 mmol) was then added and the NMR tube and vigorously shaken. ^{19}F NMR spectra were recorded 10 minutes after CF_3^- addition and the product peak integrated against 0.030 mmol fluorobenzene internal standard. The product conformed to literature spectra of Pd(TMEDA)(Ph). ^{19}F NMR (literature (in $CDCl_3$): -21.14):[254] -20.18 (3F, s). Yield: 98%.

$CuCF_3$

Experimental: CuI (19.0 mg, 0.100 mmol) was placed in an NMR tube and dissolved in 0.50 mL DMSO. K($B_3N_3Me_6CF_3$) (0.50 mL 0.20 M stock in DMSO, 0.100 mmol) was then added and the NMR tube vigorously shaken. ^{19}F NMR spectra were recorded 10 minutes after CF_3^- addition and the product peak integrated against 0.030 mmol fluorobenzene internal standard. The product conformed to literature spectra of $CuCF_3$, in which a Schlenk equilibrium is observed. ^{19}F NMR (literature (in DMF): -28.8):[230] -29.24 (63%, s), -26.43 (19%, s). Yield: 83%.

Trifluoromethylbiphenyl

Experimental: Biphenyl iodide (28.0 mg, 0.100 mmol) was added to the solution of $CuCF_3$ prepared and the NMR tube vigorously shaken. The mixture was heated to 80 °C for 12h. ^{19}F NMR spectra were recorded and the product peak integrated against 0.030 mmol fluorobenzene internal standard. The product conformed to literature spectra of trifluoromethylbiphenyl. ^{19}F NMR (literature ($CDCl_3$): -62.4):[255] -61.07 (3F, s).Yield: 66%. HRMS (EI+): 222.0659 (M^+: 222.0656)

$AgCF_3$

Experimental: $AgNO_3$ (16.9 mg, 0.100 mmol) was placed in an NMR tube and dissolved in 0.50 mL DMSO. $K(B_3N_3Me_6CF_3)$ (0.50 mL 0.20 M stock in DMSO, 0.10 mmol) was then added and the NMR tube vigorously shaken. ^{19}F NMR spectra were recorded 10 minutes after CF_3^- addition and the product peak was integrated against 0.030 mmol fluorobenzene internal standard. The product conformed to literature spectra of $AgCF_3$. In literature reports of $AgCF_3$ compounds, the NMR shift varies between -20 and -30 and the coupling constant varies between 70 and 150 Hz depending on solvent and ancillary ligands.[256] ^{19}F NMR (literature in DMF): -23-26, $J_{109Ag\text{-}19F}$ = 100-125):[257] -23.50 (3F, (d, $J_{109Ag\text{-}19F}$ = 91.7). Yield: 44%.

$Au(iPr)CF_3$

Experimental: Au(iPr)Cl (iPr=1,3-bis(2,6-diisopropylphenyl)imidazol-2-ylidene) (31 mg, 0.050 mmol) was placed in an NMR tube and dissolved in 0.25 mL THF. K(18-crown-6)($B_3N_3Me_6CF_3$)(THF) (0.250 mL 0.20 M stock in THF, 0.0500 mmol) was then added and the NMR tube and vigorously shaken. ^{19}F NMR spectra were recorded 10 minutes after CF_3^- addition and the product peak integrated against 0.030 mmol fluorobenzene internal standard. The product conformed to literature spectra of $Au(iPr)CF_3$. ^{19}F NMR (literature (in CD_2Cl_2): -28.4):[258] -27.77 (3F, s). Yield: 15%.

$Zn(TMEDA)(CF_3)_2$

Experimental: $ZnCl_2$ (6.8 mg, 0.050 mmol) was placed in an NMR tube and dissolved in 0.5 mL THF. Tetramethylethylenediamine (TMEDA, 7.5 µL, 0.050 mmol) was then added and the homogeneous solution was allowed to stand for 10 minutes. K(18-crown-6)($B_3N_3Me_6CF_3$)(THF) (0.50 mL 0.20 M stock in THF, 0.10 mmol) was then added and the NMR tube vigorously shaken. ^{19}F NMR spectra were recorded 10 minutes after CF_3^- addition and the product peak integrated against 0.030 mmol fluorobenzene internal standard. The product

conformed to literature spectra of $Zn(TMEDA)(CF_3)_2$. ^{19}F NMR (literature (in $CDCl_3$): -40.5):[259] -40.0 (6F, s). Yield: 74%.

$SiMe_3CF_3$

Experimental: Trimethylsilyl chloride (10.8 mg, 0.100 mmol) was placed in an NMR tube and dissolved in 0.50 mL THF. $K(18\text{-crown-6})(B_3N_3Me_6CF_3)(THF)$ (0.50 mL 0.20 M stock in THF, 0.10 mmol) was then added and the NMR tube vigorously shaken. ^{19}F NMR spectra were recorded 10 minutes after CF_3^- addition and the product peak integrated against 0.30 mmol fluorobenzene internal standard. The product conformed to literature spectra of $SiMe_3CF_3$. ^{19}F NMR (literature ($CDCl_3$): -66.81):[253] -66.52 (3F, s). Yield: 99%.

$SnMe_3CF_3$

Experimental: Trimethyltin chloride (19.9 mg, 0.100 mmol) was placed in an NMR tube and dissolved in 0.50 mL THF. $K(18\text{-crown-6})(B_3N_3Me_6CF_3)(THF)$ (0.50 mL 0.20 M stock in THF, 0.10 mmol) was then added and the NMR tube vigorously shaken. ^{19}F NMR spectra were recorded 10 minutes after CF_3^- addition and the product peak integrated against 0.30 mmol fluorobenzene internal standard. The product conformed to literature spectra of $SnMe_3CF_3$. ^{19}F NMR (literature (neat liquid): -49.1, $J_{119Sn\text{-}19F}$: 133):[234] –50.33 (3F, s, (^{119}Sn satellites: $J_{119Sn\text{-}19F}$: 136). Yield: 73%.

$PbMe_3CF_3$

Experimental: Trimethyllead bromide (33.0 mg, 0.100 mmol) was placed in an NMR tube and dissolved in 0.50 mL THF. $K(18\text{-crown-6})(B_3N_3Me_6CF_3)(THF)$ (0.50 mL 0.20 M stock in THF, 0.10 mmol) was then added and the NMR tube vigorously shaken. ^{19}F NMR spectra were recorded 10 minutes after CF_3^- addition and the product peak integrated against 0.30 mmol fluorobenzene internal standard. The product conformed to literature spectra of $PbMe_3CF_3$. ^{19}F NMR (literature (neat liquid): -43.9):[235]–43.8 (3F, s). Yield: 99%.

$KB(OMe)_3CF_3$

Experimental: Trimethyl borate (11.2 μL, 0.100 mmol) was placed in an NMR tube and dissolved in 0.50 mL DMSO. $K(B_3N_3Me_6CF_3)$ (0.50 mL 0.20 M stock in DMSO, 0.10 mmol) was then added and the NMR tube was vigorously shaken. ^{19}F NMR spectra were recorded 10 minutes after CF_3^- addition and the product peak integrated against 0.3 mmol fluorobenzene internal standard. The product was confirmed by comparison with an authentic sample prepared according

to literature methods[191] dissolved in DMSO-d_6 (^{19}F-NMR: -65.41 (3F, dd, $J_{11B-19F}$: 49, 24)): -65.47 (3F, dd, $J_{11B-19F}$: 49, 24). Yield: 80%.

PPh_2CF_3

Experimental: Diphenylphosphine chloride (22.0 mg, 0.100 mmol) was placed in an NMR tube and dissolved in 0.50 mL THF. K(18-crown-6)($B_3N_3Me_6CF_3$)(THF) (0.50 mL 0.20 M stock in THF, 0.10 mmol) was then added and the NMR tube vigorously shaken. After five minutes, colorless crystals had formed, and the solution became yellow. ^{19}F NMR spectra were recorded 10 minutes after CF_3^- addition and the product peak integrated against 0.11 mmol fluorobenzene internal standard. The product conformed to literature spectra of PPh_2CF_3. ^{19}F NMR (literature (in $CDCl_3$): -55.3, $J_{31P-19F}$: 73):[236] -55.13 (3F, (d, $J_{31P-19F}$: 73.2). Yield: 99%.

$Bi(CF_3)_2Cl$

Experimental: Bismuth trichloride (10.5 mg, 0.033 mmol) was placed in an NMR tube and combined with 0.50 mL THF. K(18-crown-6)($B_3N_3Me_6CF_3$)(THF) (0.50 mL 0.20 M stock in THF, 0.10 mmol) was then added and the NMR tube vigorously shaken. After five minutes, colorless crystals had formed along with a black precipitate. ^{19}F NMR spectra were recorded 10 minutes after CF_3^- addition and the product peak integrated against 0.03 mmol fluorobenzene internal standard. The product conformed to literature spectra of $Bi(CF_3)_2Cl$. ^{19}F NMR (literature (in MeCN): -37.8):[237] -37.26. Yield: 42%.

$PhSCF_3$

Experimental: Diphenyldisulfide (21.8 mg, 0.100 mmol) was placed in an NMR tube and dissolved in 0.50 mL DMSO. K($B_3N_3Me_6CF_3$) (0.50 mL 0.20 M stock in DMSO, 0.10 mmol) was then added and the NMR tube vigorously shaken. ^{19}F NMR spectra were recorded 10 minutes after CF_3^- addition and the product peak integrated against 0.3 mmol fluorobenzene internal standard. The product conformed to literature spectra of $PhSCF_3$. ^{19}F NMR (literature (in $CDCl_3$): -42.7):[260] -42.33. Yield: 79%.

$PhSeCF_3$

Experimental: Diphenyldiselenide (31.2 mg, 0.100 mmol) was placed in an NMR tube and dissolved in 0.50 mL DMSO. K($B_3N_3Me_6CF_3$) (0.50 mL 0.20 M stock in DMSO, 0.10 mmol) was then added and the NMR tube vigorously shaken. ^{19}F NMR spectra were recorded 10 minutes after CF_3^- addition and the product peak integrated against 0.30 mmol fluorobenzene internal standard.

The product conformed to literature spectra of $PhSeCF_3$. ^{19}F NMR (literature (in $CDCl_3$): -36.6):[261] -36.21 (3F, s). Yield: 69%.

2-Naphthylmethyl trifluoromethyl sulfide:

Experimental: Finely powdered elemental sulfur (12.8 mg, 0.400 mmol) was stirred in 10 mL THF for one minute to give a light-yellow suspension. With vigorous stirring, K(18-crown-6)($B_3N_3Me_6CF_3$)(THF) (2.00 mL, 0.2 M in THF, 0.400 mmol) was added. The color immediately changed to light green, then after 30 seconds to a deep blue. After 20 minutes, the color disappeared to afford a homogeneous solution of K(18-crown-6)SCF_3, from which a 30 µL sample was removed for analysis by ^{19}F NMR spectroscopy (92% K(18-crown-6)SCF_3 *in-situ*). Bromomethyl naphthalene (0.400 mmol, 88.4 mg) was then added to the stirred solution. The solution was stirred for 30 minutes, and again sampled and analyzed by ^{19}F NMR spectroscopy (81% 2-Naphthylmethyl trifluoromethyl sulfide *in-situ*). The THF solvent was removed by rotary evaporation, and the reaction was quenched with 10 mL water and extracted with CH_2Cl_2 (5 x 2 mL), the CH_2Cl_2 extract was evaporated, and the crude solid was purified by flash silica chromatography. Chromatography conditions: 100% Hexane, 8 column volumes, 25 g SiO_2, flow rate 1 column volume per minute. 54.9 mg white solid (57% isolated). ^1H-NMR ($CDCl_3$): 7.86 (δ, 1H, (m, $J_{1H\text{-}1H}$=7.1, 2)), 7.85 (ε, 1H, m (overlap)), 7.83 (θ, 1H, m (overlap)), 7.80 (β, 1H, s), 7.52 (η, 1H, (m, $J_{1H\text{-}1H}$=7.1, 2)), 7.51 (ζ, 1H, (m, $J_{1H\text{-}1H}$=7.1, 2)), 7.47 (γ, 1H, (dd, $J_{1H\text{-}1H}$=8.4, 1.6)), 4.30 (α, 2H, s). ^{13}C-NMR: 133.28 (6), 132.85 (7), 132.34 (2), 130.64 (12, q, $J_{13C\text{-}19F}$=307), 128.79 (5), 127.92 (4), 127.77 (8), 127.74 (9), 126.51 (10), 126.49 (3), 126.37 (11), 34.58 (1, q, $J_{13C\text{-}19F}$=2.3). ^{19}F-NMR: -45.19 (s). HRMS (EI+): 242.0380 (M^+: 242.0377). Note: Use of superstoichiometric sulfur severely reduces the yield of the reaction. The solubility of K(18-crown-6)SCF_3 appears to be between 0.04 and 0.06 moles/L in 25 °C THF.

2-Naphthylmethyl trifluoromethyl selenide:

Experimental: 100 mesh grey elemental selenium (31.2 mg, 0.400 mmol) was stirred in 10 mL THF for one minute to give a light brown suspension. With vigorous stirring, K(18-crown-6)($B_3N_3Me_6CF_3$)(THF) (2.00 mL, 0.2 M in THF, 0.400 mmol) was added. The color immediately changed to a slightly darker brown. After 20 minutes, the reaction was slightly turbid. The amount of K(18-crown-6)$SeCF_3$ in solution was assessed through removal of a 30 µL sample, analyzed by ^{19}F NMR spectroscopy (61% K(18-crown-6)$SeCF_3$ *in-situ*). Bromomethyl naphthalene (88.4 mg, 0.400 mmol) was then added to the stirred solution. Within one minute a thick, white solid

precipitated. The solution was stirred for 30 minutes, and again sampled and analyzed by ^{19}F NMR spectroscopy (63% 2-naphthylmethyl trifluoromethyl selenide *in-situ*). The THF solvent was then removed by rotary evaporation, and the reaction was quenched with 10 mL water and extracted with CH_2Cl_2 (5 x 2 mL), the CH_2Cl_2 extract evaporated, and the crude solid was purified by flash silica chromatography. Chromatography conditions: 100% Hexane, 8 column volumes, 25 g SiO_2, flow rate 1 column volume per minute. 61.2 mg white solid (64% isolated). ^{1}H-NMR ($CDCl_3$): 7.85 (δ, 1H, (m, overlap)), 7.83 (ε, 1H, m (overlap)), 7.82 (θ, 1H, m (overlap)), 7.80 (β, 1H, s), 7.51 (η, 1H, (m, overlap)), 7.50 (ζ, 1H, (m, overlap)), 7.47 (γ, 1H, (dd, J_{1H-1H}=8.4, 1.8)), 4.43 (α, 2H, s). ^{13}C-NMR: 133.39 (6), 132.32 (7), 132.71 (2), 128.81 (5), 127.83 (4), 127.73 (8), 127.72 (9), 126.76 (10), 126.50 (3), 126.31 (11), 122.87 (12, q, $J_{13C-19F}$=331), 29.54 (1, q, $J_{13C-19F}$=1.6). ^{19}F-NMR: -34.35 (s). ^{77}Se-NMR: 505.92 (q, $J_{77Se-19F}$=13.5). HRMS (EI+): 289.9821 (M^+: 289.9822). Notes: Use of superstoichiometric selenium severely reduces the yield of the reaction.

2-Naphthylmethyl trifluoromethyl telluride:

Experimental: Elemental tellurium (51.0 mg, 0.400 mmol) was stirred in 10 mL THF for 10 minutes to give a suspension. With vigorous stirring, K(18-crown-6)($B_3N_3Me_6CF_3$)(THF) (2.00 mL, 0.2 M in THF, 0.400 mmol) was added. The color immediately changed to a light purple. After 72 hours, the reaction was slightly turbid and deep purple in color. The amount of K(18-crown-6)$TeCF_3$ in solution was assessed through removal of a 30 µL sample, analyzed by ^{19}F NMR spectroscopy (97% K(18-crown-6)$TeCF_3$ *in-situ;* ^{19}F NMR: 2.06; ^{125}Te NMR: 207.48 ($J_{125Te-19F}$=251.8). Bromomethyl naphthalene (88.4 mg, 0.400 mmol) was then added to the stirred solution. Within one minute a thick, white solid precipitated. The solution was stirred for 30 minutes, and again sampled and analyzed by ^{19}F NMR spectroscopy (88% 2-naphthylmethyl trifluoromethyl selenide *in-situ*). The THF solvent was then removed by rotary evaporation, and the reaction was quenched with 10 mL water and extracted with CH_2Cl_2 (5 x 2 mL), the CH_2Cl_2 extract evaporated, and the crude solid was purified by flash silica chromatography. Chromatography conditions: 100% Hexane, 8 column volumes, 25 g SiO_2, flow rate 1 column volume per minute. 80.1 mg white solid (59% isolated). ^{1}H-NMR ($CDCl_3$): 7.75 (4H, (m, overlap)), 7.45 (3H, m (overlap)), 4.69 (2H, s). ^{19}F-NMR: -27.28 (s). MS (EI+): 340.1 (M^+: 339.9719)

6.11.3 Nucleophilic Trifluoromethylation of Inorganic Compounds with LA-CF_3: Comparison between 2 and previously reported CF_3^- sources (1a-c)

Protocol for reactions with $KB(OMe)_3CF_3$:

To 0.100 mmol of substrate dissolved in 0.50 mL of THF was added 0.100 mmol $KB(OMe)_3CF_3$ as a solution in 0.50 mL THF. Yields were determined by ^{19}F NMR integration against fluorobenzene internal standard after 10 minutes at room temperature.

Protocol for reactions with $SiMe_3CF_3$/KF/18-crown-6:

To 0.100 mmol of substrate dissolved in 0.50 mL of THF was added 0.100 mmol of a 1:1 mixture of $SiMe_3CF_3$/18-crown-6 as a solution in in 0.5 mL THF. 0.10 mmol KF was then added as a solid, and the mixture vigorously shaken for 10 minutes at room temperature. Yields were determined by ^{19}F NMR integration against fluorobenzene internal standard.

Protocol for reactions with KDMF•CF_3:

To 0.100 mmol of substrate dissolved in 0.50 mL DMF was added 0.100 mmol KDMF•CF_3 as a solution in 0.50 mL DMF. Both solutions were chilled to -40 °C prior to combination, and the reaction mixtures were then rapidly warmed to room temperature (<1 minute) and allowed to react for 10 minutes. Yields were determined by ^{19}F NMR integration against fluorobenzene internal standard.

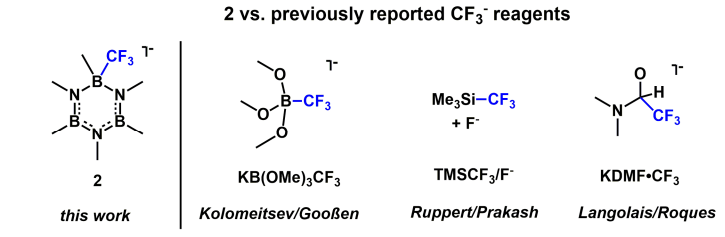

Table: Reactivity of CF_3^- Sources with Inorganic Electrophiles

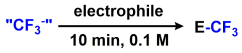

Electrophile	Product	CF_3^- Reagents			
		1	$KB(OMe)_3CF_3$	$TMSCF_3/F^-$	$KDMF•CF_3$
S	KS–CF_3	92%	0.0%	0.0%	5.2%
Se	KSe–CF_3	61%	0.0%	0.3%	86%
NCBr	Br-CF_3	44%	0.3%	2.2%	0.3%
PPh_2Cl	PPh_2-CF_3	99%	0.0%	0.0%	6.8%
$BiCl_3$	Bi-$(CF_3)_2Cl$	42%	0.0%	0.0%	0.0%
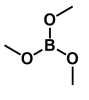	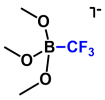	80%	--	0.0%	0.0%
Me_3SiCl	Me_3Si–CF_3	96%	0.2%	--	0%
Me_3SnCl	Me_3Sn–CF_3	73%	0.2%	47%	0%
Me_3PbBr	Me_3Pb–CF_3	99%	0.2%	32%	0%
	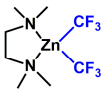	74%	0.1%	0.0%	0.0%
CuI	Cu–CF_3	83%	0.0%	0.0%	1.4%
$AgNO_3$	Ag–CF_3	44%	0.0%	7.8%	19%
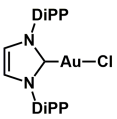	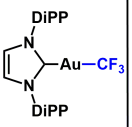	15%	0.0%	0.0%	56%
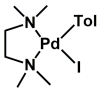	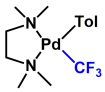	98%	0.1%	2.1%	63%

* Conditions: 1: 25 °C, THF; $KB(OMe)_3CF_3$: 25 °C, THF; $KDMF•CF_3$: -40 °C to 25 °C, DMF

Figure 6-7 Comparison between **2** and previous CF_3^- Reagents

6.11.4 Rapid Electrophilic Trifluoromethylation of Thiols using 2

1-Trifluoromethylthio-β-D-glucose tetraacetate

Step 1:

This procedure was reported in our manuscript describing the preparation of **2**.[253]

Hexamethylborazine (0.290 mmol, 47.7 mg) and 18-crown-6 (0.290 mmol, 76.6 mg) were dissolved in 1.5 mL THF in a 20 mL flask equipped with a Teflon-coated magnetic stirbar. The vessel was then allowed to cool to 0 °C in a glovebox cold-well for 30 minutes. Benzylpotassium (0.270 mmol, 35.2 mg) was then quickly added to this cold solution, and the initial deep red color of dissolved benzylpotassium quickly changed to a faint purple color. The homogeneous solution was stirred for 2 minutes, giving a homogeneous purple solution. The flask was then sealed with a tightly belt-clamped septum. Gaseous HCF_3 was added to the sealed vessel with a 30 mL syringe (0.32 mmol, 8.0 mL) and continuous efficient stirring. The colorless solution was stirred for 2 minutes, and brought to room temperature. 1 equivalent 1-chloro-3,3-dimethyl-1,3-dihydro-1λ-benzo[d][1,2]iodaoxole (0.27 mmol, 80 mg) was then added to the reaction mixture, and stirred at room temperature for 10 minutes; in this time, a white precipitate appeared. A 60 µL sample was removed for analysis by ^{19}F and ^{1}H NMR; conversion to 1-trifluoromethyl-3,3-dimethyl-1,3-dihydro-1λ-benzo[d][1,2]iodaoxole was 78%, while hexamethylborazine was regenerated (98%). The fluorine NMR spectra of the product matched literature spectra (^{19}F-NMR ($CDCl_3$): -40.1).[213] ^{19}F-NMR (THF): -41.32 (s).

Step 2:

The solvent was removed under vacuum (5 minutes), reconstituted in 1.5 mL acetonitrile, cooled to -30 °C (5 minutes), and a -30 °C solution of 1-thio-β-D-glucose tetraacetate (0.270 mmol, 100 mg) in 1.5 mL acetonitrile quickly added. The reaction was then immediately allowed to warm to room temperature and vigorously stirred for 10 minutes (synthesis time: 32 minutes). A 30 µL sample was removed for analysis by ^{19}F NMR spectroscopy, the reaction was opened to air, and the solvent was removed by rotary evaporation. The white solid was then suspended in 10 mL water, and the organic components extracted into dichloromethane (4 x 2 mL). The dichloromethane extract was then dried with magnesium sulfate, filtered, concentrated to 2 mL, and purified by flash chromatography. Chromatography conditions: 50 g SiO_2, 12%-100% ethyl acetate/hexanes over 10 column volumes, R_f: 0.58. The product is not UV active, so it was detected during elution by means of an attached evaporative light scattering detector (Biotage ELSD-A120; settings: nebulizer temperature: 40 °C, evaporation temperature: 60 °C, flow: 2.5). The fractions containing 1-trifluoromethylthio-β-D-glucose tetraacetate were combined and evaporated by rotary evaporation, then dried under high vacuum (50.4 mg, 43% combined yield from benzylpotassium). Time required for isolation: 90 minutes. ^{1}H-NMR ($CDCl_3$): 5.23 (1H, γ, (t, J_{1H-}

$_{1H}$=9.3)), 5.07 (1H, ε, (t, J_{1H-1H}=9.8)), 5.01 (1H, ß, (t, J_{1H-1H}=9.7)), 4.96 (1H, α, (d, J_{1H-1H}=10.3)), 4.26 (1H, τ, (dd, J_{1H-1H}=12.5, 5.3)), 4.10 (1H, τ, (dd, J_{1H-1H}=12.4, 2.2)), 3.77 (1H, ζ, (ddd, J_{1H-1H}=10.1, 5.3, 2.3)). ^{13}C-NMR: 170.49 (7), 169.90 (7), 169.25 (7), 129.33 (9, q, $J_{13C-19F}$=308), 81.43 (1, q, $J_{13C-19F}$=2.8), 76.24 (5), 73.32 (3), 69.22 (2), 67.76 (4), 61.67 (6), 20.56 (8), 20.47 (8), 20.44 (8). ^{19}F-NMR: -40.08 (s). HRMS (ESI+): 450.1045 (M+NH_4: 450.1040).

6.11.5 Nucleophilic Trifluoromethylation of Organic Compounds with LA-CF_3: Initial Condition Screening

To 0.1 mmol of substrate dissolved in 0.50 mL DMSO or THF was added one of the above stock solutions of the HCF_3 derived CF_3^- reagent. NMR spectra were recorded at 30-minute, 1 hour, 5 hour, and 24-hour time points to monitor conversion to trifluoromethylated product through integration against a 0.030 mmol fluorobenzene internal standard. In cases where anionic addition products were observed, confirmation of product identity was made through GCMS.

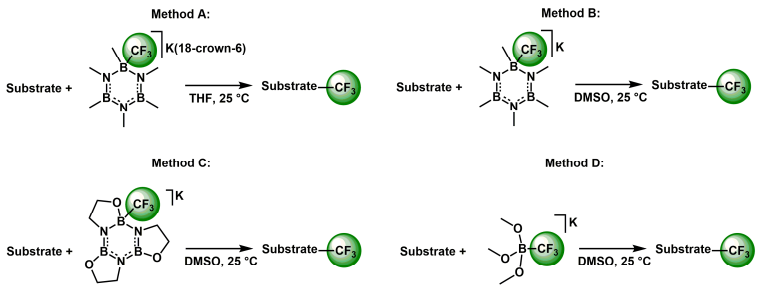

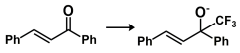

Method A: 30m: 19% 5h: 21% 72h: 20%
Method B: 30m: 58% 5h: 37% 24h: 6% 72h: 0%
Method C: 30m: 19% 5h: 17% 24h: 5% 72h: 0%
Method D: 30m: 3.5% 5h: 3.3% 24h: 1.7% 72h: 0%

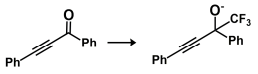

Method A: 30m: 75% 5h: 76% 72h: 77%
Method B: 30m: 4.6% 5h: 2.0% 72h: 0.4%
Method C: 30m: 9% 5h: 8% 24h: 7% 72h: 5%
Method D: 30m: 10% 5h: 12% 24h: 12% 72h: 12%

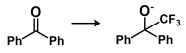

Method A: 30m: 100% 5h: 100% 24h: 101% 72h: 100%
Method B: 30m: 72% 5h: 87% 24h: 89% 72h: 93%
Method C: 30m: 39% 5h: 50% 24h: 36% 72h: 25%
Method D: 30m: 2.6% 5h: 5.5% 24h: 6.1% 72h: 17%

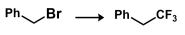

Method A: 30m: 12% 5h: 12% 72h: 12%
Method B: 30m: 2% 5h: 2% 24h: 2% 72h: 2%
Method C: 30m: 0% 5h: 0% 24h: 0% 72h: 0%
Method D: 30m: 0% 5h: 0% 24h: 0% 72h: 0%

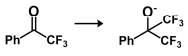

Method A: 30m: 100% 5h: 100% 24h: 100% 72h: 100%
Method B: 30m: 92% 5h: 100% 24h: 87% 72h: 90%
Method C: 30m: 100% 5h: 100% 24h: 100% 72h: 100%
Method D: 30m: 76% 5h: 119% 24h: 133% 72h: 130%

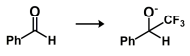

Method A: 30m: 85% 5h: 11% 24h: 0% 72h: 0%
Method B: 30m: 80% 5h: 71% 24h: 77% 72h: 75%
Method C: 30m: 95% 5h: 100% 24h: 100% 72h: 98%
Method D: 30m: 26% 5h: 76% 24h: 77% 72h: 81%

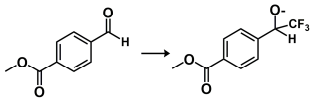

Method A: 30m: 25% 5h: 29% 24h: 26% 72h: 25%
Method B: 30m: 57% 5h: 0% 24h: 0% 72h : 0%
Method C: 30m: 93% 5h: 92% 24h: 92% 72h: 79%
Method D: 30m: 25% 5h: 72% 24h: 73% 72h: 73%

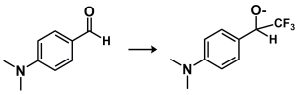

Method A: 30m: 88% 5h: 86% 24h: 80% 72h: 78%
Method B: 30m: 57% 5h: 32% 24h: 52% 72h: 53%
Method C: 30m: 56% 5h: 59% 24h: 51% 72h: 42%
Method D: 30m: 14% 5h: 56% 24h: 58% 72h: 59%

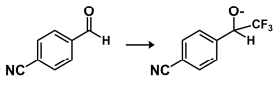

Method A: 30m: 32% 5h: 28% 24h: 23% 72h: 20%
Method B: 30m: 38% 5h: 0% 24h: 0% 72h: 0%
Method C: 30m: 88% 5h: 88% 24h: 84% 72h: 62%
Method D: 30m: 22% 5h: 51% 24h: 50% 72h: 49%

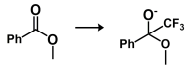

Method A: a) 30m: 5% 5h: 30% 72h: 83%
b) 30m: 64% 5h: 52% 72h: 20%
Method B: 30m: 0% 5h: 0% 24h: 0% 72h: 0%
Method C: 30m: 0% 5h: 0% 24h: 0% 72h: 0%
Method D: 30m: 0% 5h: 0% 24h: 0% 72h: 0%

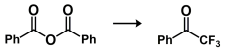

Method A: 30m: 54% 5h: 58% 24h: 58% 72h: 53%
Method B: 30m: 20% 5h: 25% 24h: 27% 72h: 27%
Method C: 30m: 39% 5h: 35% 24h: 41% 72h: 41%
Method D: 30m: 65% 5h: 37% 24h: 1% 72h: 0%

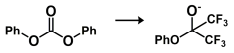

Method A: 30m: 98% 5h: 100% 24h: 100% 72h: 100%
Method B: 30m: 65% 5h: 62% 24h: 46% 72h: 32%
Method C: 30m: 50% 5h: 58% 24h: 61% 72h: 53%
Method D: 30m: 0% 5h: 36% 24h: 54% 72h: 62%

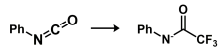

Method A: 30m:92% 5h: 96% 24h: 98% 72h: 96%
Method B: 30m: 16% 5h: 18% 24h: 18% 72h: 18%
Method C: 6% 5h: 8% 24h: 8% 72h: 8%
Method D: 30m: 0.7% 5h: 2.1% 24h: 5.0% 72h: 7.5%

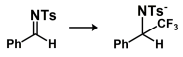

Method A: 30m: 99% 5h: 99% 72h: 99%
Method B: 30m: 95% 5h: 91% 24h: 96% 72h: 93%
Method C: 30m: 98% 5h: 100% 24h: 100% 72h: 98%
Method D: 30m: 22% 5h: 63% 24h: 85% 72h: 90%

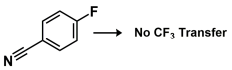

Method A: 30m: 0% 5h: 0% 24h: 0% 72h: 0%
Method B: 30m: 0% 5h: 0% 24h: 0% 72h: 0%
Method C: 30m: 0% 5h: 0% 24h: 0% 72h: 0%
Method D: 30m: 0% 5h: 0% 24h: 0% 72h: 0%

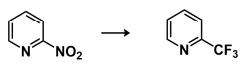

Method A: a) 30m: 21% 5h: 30% 72h: 32%
b) 30m: 21% 5h: 21% 72h: 31%
Method B: 30m: 0.1% 5h: 0% 24h: 0% 72h: 0%
Method C: 30m: 0% 5h: 0% 24h: 0% 72h: 0%
Method D: 30m: 0% 5h: 0% 24h: 0% 72h: 0%

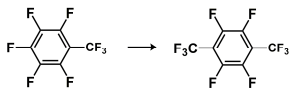

Method A: 30m: 30% 5h: 30% 72h: 30%
Method B: 30m: 25% 5h: 20% 6h: 20% 72h: 19%
Method C: 30m:15% 5h: 22% 6h: 17% 72h: 10%
Method D: 30m:14% 5h: 21% 24h: 19% 72h: 20%

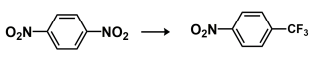

Method A: 30m: 41% 5h: 48% 24h: 54% 72h: 58%
Method B: 30m: 0.1% 5h: 0.7% 24h: 1.5% 72h: 1.5%
Method C: 30m: 15% 5h: 19% 24h: 24% 72h: 27%
Method D: 30m: 0.7% 5h: 2% 24h: 6% 72h: 9%

Figure 6-8 Condition Screening for Nucleophilic Trifluoromethylation of Organic Electrophiles

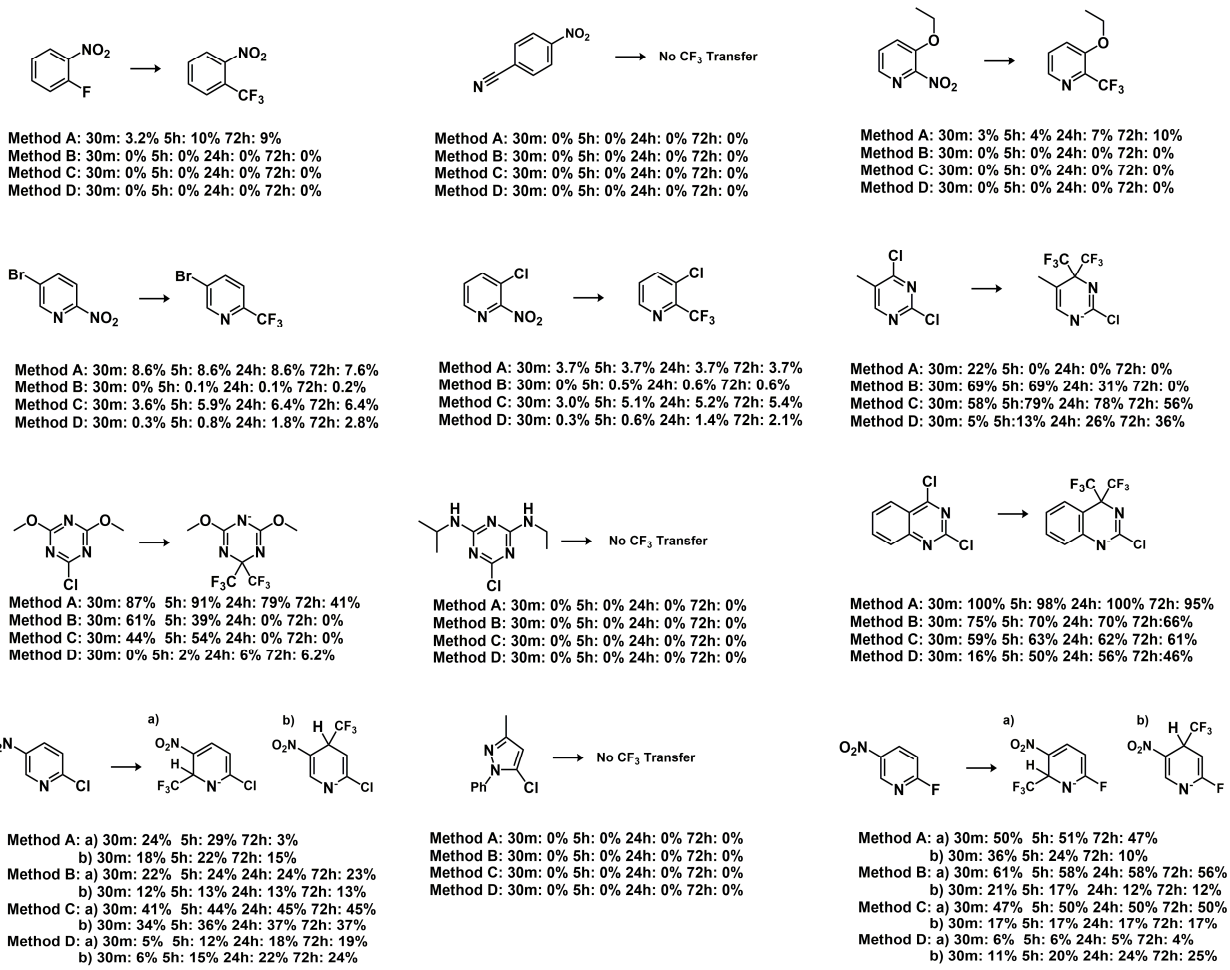

Figure 6-9 Optimization Table Contd.

6.11.6 Nucleophilic Trifluoromethylation of Organic Compounds with LA-CF_3: Isolated Compounds and Characterization

An appropriate quantity of a 0.2 M stock solution of K(LA-CF_3) was added to a 0.2 M solution of substrate in a 20 mL scintillation vial. The mixture was then stirred for the specified time (*vide infra*) then quenched by adding 15 mL of 5% aqueous HCl or saturated aqueous ammonium chloride. The product was then extracted into CH_2Cl_2 (5 x 3 mL CH_2Cl_2) and the organic phase dried with $MgSO_4$. The dried organic phase was then filtered, concentrated to 1 mL, then purified by silica chromatography using a Biotage Isolera automated flash chromatography apparatus. The collected fractions were concentrated by rotary evaporation and further dried under high vacuum to afford the pure products.

6.11.7 1,2 Addition Reactions with C=O and C=N compounds

1-Phenyl-1-trifluoromethylmethanol:

Substrate: Benzaldehyde. Conditions: Solvent: DMSO. LA: $K(BOCH_2CH_2N)_3CF_3$. 1.0 equivalents $K(LA\text{-}CF_3)$ used. 0.40 mmol substrate. Reaction time: 1 hour. Quench: 5% HCl. Chromatography conditions: 100% CH_2Cl_2, 9 column volumes, 10g SiO_2, flow rate: 1 column volume per minute. 62 mg colorless oil, 88%. Due to the volatile nature of the product it could not be dried under high vacuum. ^{1}H-NMR ($CDCl_3$): 7.46 (ß, 2H, m), 7.41 (α, γ, 3H, m), 4.98 (ε, 1H, (q, $J_{1H\text{-}19F}$=6.7)), 2.88 (ζ, 1H, s). ^{13}C-NMR: 133.92, 129.53, 128.60, 127.41, 124.22 (q, $J_{13C\text{-}19F}$=282), 72.79 (q, $J_{13C\text{-}19F}$=32). ^{19}F-NMR: -78.36 (d, $J_{19F\text{-}1H}$=6.7). HRMS (ESI-): 221.0435 (M+HCO_2: 221.0431).

Methyl 4-(trifluoro-1-ethanol)benzoate

Substrate: Methyl 4-formyl benzoate. Conditions: Solvent: DMSO. LA: $K(BOCH_2CH_2N)_3CF_3$. 1.0 equivalents $K(LA\text{-}CF_3)$ used. 0.40 mmol substrate. Reaction time: 1 hours. Quench: 5% HCl. Chromatography conditions: 0-100% hexane/ethyl acetate, 16 column volumes, 50 g SiO_2, flow rate 0.5 column volume per minute. 56 mg white solid, 60%. ^{1}H-NMR ($CDCl_3$): 8.00 (ß, 2H, (d, $J_{1H\text{-}1H}$=8.1)), 7.54 (γ, 2H, (d, $J_{1H\text{-}1H}$=7.9)), 5.08 (ε, 1H, (q, $J_{1H\text{-}19F}$=6.7)), 3.89 (α, 3H, s), 3.72 (ζ, 1H, s). ^{13}C-NMR: 167.00, 139.02, 130.83, 129.69, 127.51, 124.02 (q, $J_{13C\text{-}19F}$=282), 72.25 (q, $J_{13C\text{-}19F}$=32), 52.39. ^{19}F-NMR: -78.18 (d, $J_{19F\text{-}1H}$=6.7). HRMS (ESI-): 235.0573 (M-H: 235.0577).

4-(Trifluoro-1-ethanol)benzonitrile

Substrate: 4-formyl-benzonitrile. Conditions: Solvent: DMSO. LA: $K(BOCH_2CH_2N)_3CF_3$. 1.0 equivalent $K(LA\text{-}CF_3)$ used. 0.40 mmol substrate. Reaction time: 1 hours. Quench: 5% HCl. Chromatography conditions: 0-100% CH_2Cl_2/ethyl acetate, 8 column volumes, 10 g SiO_2, flow rate 1 column volume per minute. 39 mg white solid, 48%. ^{1}H-NMR ($CDCl_3$): 7.68 (ß, 2H, (d, $J_{1H\text{-}1H}$=8.2)), 7.63 (α, 2H, (d, $J_{1H\text{-}1H}$=8.1)), 5.11 (γ, 1H, (p, $J_{1H\text{-}19F}$=6.2)), 3.44 (ε, 1H, (d, $J_{1H\text{-}1H}$=4.6))). ^{13}C-NMR: 139.19, 132.28, 128.27, 123.78(q, $J_{13C\text{-}19F}$=282), 118.27, 112.94, 72.25 (q, $J_{13C\text{-}19F}$=32). ^{19}F-NMR: -78.18 (d, $J_{19F\text{-}1H}$=6.4). HRMS (ESI-): 200.0322 (M-H: 200.0329).

1-(Anthracen-9-yl)-1,1-bistrifluoromethylcarbinol

Substrate: Anthracen-9-yl trifluoromethyl ketone. Conditions: Solvent: THF. LA: K(18-crown-6)($B_3N_3Me_6CF_3$)(THF). 2.0 equivalents $K(LA\text{-}CF_3)$ used. 0.40 mmol substrate. Reaction

time: 1 hour. Quench: 5% HCl. Chromatography conditions: 0-100% hexane ethyl acetate, 16 column volumes, 25 g SiO_2, flow rate 1 column volume per minute. 120 mg yellow crystals, 87%. ^{1}H-NMR ($CDCl_3$): 9.02 (α, 1H, (d, J_{1H-1H}=9.3)), 8.55 (α, 1H, (d, J_{1H-1H}=9.3)), 8.51 (γ, 1H, s), 7.99 (ß, 2H, (t, J_{1H-1H}=9.5)), 7.59 (ß, 1H, (t, J_{1H-1H}=8.3)), 7.49 (α, ß, 3H, m), 3.98 (ε, 1H, s). ^{13}C-NMR: 134.06, 133.11, 132.46, 132.41, 131.38, 131.15, 129.39, 129.11, 127.34, 126.71, 125.98, 124.78, 124.61, 123.94(q, $J_{13C-19F}$=290), 121.94, 83.46(p, $J_{13C-19F}$=31). ^{19}F-NMR: -69.31 (s). HRMS (ES+): 344.0630 (M+: 344.0636).

1-(Trans)-phenylethenyl-1-phenyl-trifluoromethylcarbinol

Substrate: Trans-chalcone. Conditions: Solvent: THF. LA: K(18-crown-6)($B_3N_3Me_6CF_3$)(THF). 1.0 equivalents K(LA-CF_3) used. 0.80 mmol substrate. Reaction time: 10 minutes. Quench: 5% HCl. Chromatography conditions: 0-100% hexane ethyl acetate, 16 column volumes, 25 g SiO_2, flow rate 1 column volume per minute. 190 mg colorless oil, 84%. ^{1}H-NMR ($CDCl_3$): 7.69 (ß, 2H, (d, J_{1H-1H}=7.7)), 7.45 (ß, α, 5H, m), 7.38 (ß, 2 H, (t, J_{1H-1H}=7.4)), 7.33 (α, 1H, (t, J_{1H-1H}=7.3)), 6.91 (γ, 1H, (d, J_{1H-1H}=16.1)), 6.77 (γ, 1H, (d, J_{1H-1H}=16.1)), 2.79 (ε, 1H, s). ^{13}C-NMR: 137.40, 135.51, 133.58, 128.84, 128.76, 128.67, 128.41, 126.95, 126.84, 126.46, 125.08(q, $J_{13C-19F}$=286), 77.34(q, $J_{13C-19F}$=29). ^{19}F-NMR: -78.46 (s). HRMS (EI+): 278.0919(M+: 278.0918).

1-Phenylethynyl-1-phenyl-trifluoromethylcarbinol

Substrate: Diphenylpropynone. Conditions: Solvent: THF. LA: K(18-crown-6)($B_3N_3Me_6CF_3$)(THF). 1.0 equivalents K(LA-CF_3) used. 0.40 mmol substrate. Reaction time: 16 hours. Quench: saturated NH_4Cl. Chromatography conditions: 0-30% hexane ethyl acetate, 16 column volumes, 50 g SiO_2, flow rate 1 column volume per minute. 45 mg orange oil, 42%. ^{1}H-NMR ($CDCl_3$): 7.83 (ß, 2H, (d, J_{1H-1H}=4.8)), 7.56 (ß, 2H, (d, J_{1H-1H}=4.8)), 7.46 (α, ß, 3H, m), 7.42 (α, 1H, (p, J_{1H-1H}=7.4)), 7.37 (ß, 2H, (t, J_{1H-1H}=7.4)), 3.15 (ε, 1H, s). ^{13}C-NMR:135.26, 132.06, 129.55, 129.53, 128.47, 128.25, 127.19, 123.39(q, $J_{13C-19F}$=286), 120.93, 88.09, 84.40, 73.36(q, $J_{13C-19F}$=33). ^{19}F-NMR: -80.29 (s). HRMS (ESI-): 275.0683(M-H: 275.0684).

N-tosyl-1-trifluoromethyl-benzylamine

Substrate: N-tosylbenzaldimine. Conditions: Solvent: DMSO. LA: K($BOCH_2CH_2N)_3CF_3$. 1.0 equivalent K(LA-CF_3) used. 0.40 mmol substrate. Reaction time: 1 hours. Quench: saturated NH_4Cl. Chromatography conditions: 0-100% hexane/CH_2Cl_2, then 0-100% CH_2Cl_2/ethyl acetate, 16 column volumes, 25 g SiO_2, flow rate 1 column volume per minute. 86 mg white solid, 65%.

^{1}H-NMR ($CDCl_3$): 7.60 (ß, 2H, (d, $J_{1H\text{-}1H}$=8.2)), 7.18 (ß, α, 7H, m), 6.16 (ε, 1H, (d, $J_{1H\text{-}1H}$=9.1)), 4.91 (γ, 1H, (p, $J_{1H\text{-}19F}$=7.7)), 2.34 (η, 3H, s). ^{13}C-NMR: 143.74, 136.89, 131.79, 129.46, 129.19, 128.74, 127.76, 126.92, 123.89(q, $J_{13C\text{-}19F}$=282), 59.18(q, $J_{13C\text{-}19F}$=32), 21.43. ^{19}F-NMR: -74.02 (d, $J_{19F\text{-}1H}$=7.4). HRMS (ESI-): 328.0624(M-H: 328.0625).

1,1-bistrifluoromethyl-1-(4-phenyl)phenyl-methanol:

Substrate: Biphenyl-4-carbonyl chloride. Conditions: Solvent: THF. LA: K(18-crown-6)($B_3N_3Me_6CF_3$)(THF). 2.2 equivalents K(LA-CF_3) used. 0.40 mmol substrate. Reaction time: 16 hours. Quench: 5% HCl. Chromatography conditions: 0-20% Hexane/Ethyl acetate, 8 column volumes, 25 g SiO_2, flow rate 1 column volume per minute. 107 mg white solid, 84%. ^{1}H-NMR ($CDCl_3$): 7.82 (ε, 2H, (d, $J_{1H\text{-}1H}$=8.1)), 7.71 (δ, 2H, (d, $J_{1H\text{-}1H}$=8.2)), 7.64 (γ, 2H, (d, $J_{1H\text{-}1H}$=7.8)), 7.49 (ß, 2H, (t, $J_{1H\text{-}1H}$=7.5)), 7.41 (α, 1H, (t, $J_{1H\text{-}1H}$=7.3)), 3.38 (ζ, 1H, s). ^{13}C-NMR:143.16, 139.88, 128.90, 128.06, 127.94, 127.30, 127.20, 126.94, 122.65(q, $J_{13C\text{-}19F}$=288), 77.18 (p, $J_{13C\text{-}19F}$=30.3) (overlap with $CDCl_3$). ^{19}F-NMR: -75.58 (s). HRMS (ES+): 320.0636 (M-$C_3H_7^+$: 320.0636).

Trifluoromethyl-(4-phenyl)phenyl Ketone:

Substrate: Methyl biphenyl-4-carboxylate. Conditions: Solvent: THF. LA: K(18-crown-6)($B_3N_3Me_6CF_3$)(THF). 1.0 equivalents K(LA-CF_3) used. 0.40 mmol substrate. Reaction time: 30 minutes. Quench: 5% HCl. Chromatography conditions: 0-100% Hexane/Ethyl acetate, 8 column volumes, 25 g SiO_2, flow rate 1 column volume per minute. 29 mg white solid, 29%. ^{1}H-NMR ($CDCl_3$): 8.17 (ε, 2H, (d, $J_{1H\text{-}1H}$=8.0)), 7.78 (δ, 2H, (d, $J_{1H\text{-}1H}$=8.4)), 7.66 (γ, 2H, (d, $J_{1H\text{-}1H}$=7.1)), 7.51 (ß, 2H, (t, $J_{1H\text{-}1H}$=7.6)), 7.45 (α, 1H, (t, $J_{1H\text{-}1H}$=7.4)). ^{13}C-NMR: 180.07 (q, $J_{13C\text{-}19F}$=35.0), 148.21, 139.11, 130.72, 129.11, 128.89, 128.56, 127.63, 127.34, 116.76 (q, $J_{13C\text{-}19F}$=291),. ^{19}F-NMR: -71.35 (s). HRMS (ES+): 250.0611 (M^+: 250.0605).

Triisopropylsilyl Hexafluoro-2-phenoxypropan-2-ol

Substrate: Diphenylcarbonate. Conditions: Solvent: THF. LA: K(18-crown-6)($B_3N_3Me_6CF_3$)(THF). 2.0 equivalents K(LA-CF_3) used. 0.40 mmol substrate. Reaction time: 30 minutes. Quench: 2.0 equivalents triisopropylsilyl chloride were added, then the reaction stirred for 16 hours at 25 °C. The reaction mixture was then quenched with 10 mL water. Chromatography conditions: 100% Hexane, 4 column volumes, 100 g SiO_2, flow rate 0.5 column volume per minute; chromatography was repeated six times to remove triisopropylsilyl phenol. 102 mg colorless oil, 61%. Boiling point: 65 °C at 0.080 Torr. ^{1}H-NMR ($CDCl_3$): 7.32 (ß, 2H, (t, $J_{1H\text{-}1H}$=8.4)), 7.19 (α, 3H, m), 1.14 (γ, 3H, m), 1.05 (ε, 18H, (d, $J_{1H\text{-}1H}$=7.2)). ^{13}C-NMR:151.46,

129.07, 125.80, 123.58, 120.73(q, $J_{13C\text{-}19F}$=293), 95.20 (p, $J_{13C\text{-}19F}$=32.8), 17.43, 13.07. ^{19}F-NMR: -76.97 (s). HRMS (ES+): 373.1061 (M-$C_3H_7^+$: 373.1059).

Phenyl trifluoroacetamide

Substrate: Phenyl isocyanate. Conditions: Solvent: THF. LA: K(18-crown-6)($B_3N_3Me_6CF_3$)(THF). 1.0 equivalents K(LA-CF_3) used. 0.80 mmol substrate. Reaction time: 1 hour. Quench: 5% HCl. Chromatography conditions: 10-50% hexane/CH_2Cl_2, 8 column volumes, 25 g SiO_2, flow rate 1 column volume per minute. 91 mg white solid, 61%. ^{1}H-NMR ($CDCl_3$): 8.03 (ε, 1H, s), 7.54 (γ, 2H, (d, $J_{1H\text{-}1H}$=7.7)), 7.46 (ß, 2H, (t, $J_{1H\text{-}1H}$=8.0), 7.23 (α, 1H, (t, $J_{1H\text{-}1H}$=7.4)). ^{13}C-NMR: 154.87(q, $J_{13C\text{-}19F}$=37), 135.04, 129.33, 126.39, 120.56, 115.72(q, $J_{13C\text{-}19F}$=288). ^{19}F-NMR: -75.80 (s). HRMS (ES+): 189.0401 (M+: 189.0401).

6.11.8 Nucleophilic Aromatic Substitution

Perfluoro-*p*-xylene

Substrate: Perfluorotoluene. Conditions: Solvent: THF. LA: K(18-crown-6)($B_3N_3Me_6CF_3$)(THF). 1.0 equivalents K(LA-CF_3) used. 0.10 mmol substrate. Reaction time: 10 min. Quench: water. Characterized *in-situ*; yield determined by ^{19}F-NMR spectroscopy and integrated against 0.030 mmol fluorobenzene. The product spectrum closely matched the literature chemical shifts and ^{19}F-^{19}F coupling constants. Because of highly complex coupling, spin simulation in MestReNova was performed using the literature coupling constants to provide comparison with the experimental *in-situ* spectrum. (Literature ^{19}F-NMR (solvent not specified): -57.6 ($J_{19F\text{-}19F}$ = 22.7 (α-(β/ζ), ω-(ε/γ)), 0.4 (α-(ε/γ), ω-(β/ζ)), -138.9 ($J_{19F\text{-}19F}$=18.6 (β-ε, ζ-γ), 13.2 (β-γ, ζ-ε))).[262] Chemical yield: 27%. *In-Situ* ^{19}F-NMR: -56.46 (α, ω 6F, m), -139.38 (β, ε, γ, ζ, 4F, m)

1-Trifluoromethyl-4-nitrobenzene

Substrate: 1,4-Dinitrobenzene. Conditions: Solvent: THF. LA: K(18-crown-6)($B_3N_3Me_6CF_3$)(THF). 1.0 equivalents K(LA-CF_3) used. 0.40 mmol substrate. Reaction time: 2 hour. Quench: water. Chromatography conditions: 0-100% Hexane/CH_2Cl_2, 8 column volumes, 25 g SiO_2, flow rate 1 column volume per minute. 64 mg white solid, 42%. ^{1}H-NMR ($CDCl_3$): 8.34 (α, 2H, (d, $J_{1H\text{-}1H}$=8.4)), 7.84 (α, 2H, (d, $J_{1H\text{-}1H}$=8.5)). ^{13}C-NMR: 150.00, 136.06 (q, $J_{13C\text{-}19F}$=33), 126.77 (q, $J_{13C\text{-}19F}$=3), 124.07, 122.94(q, $J_{13C\text{-}19F}$=273), 73.36(q, $J_{13C\text{-}19F}$=33). ^{19}F-NMR: -63.19 (s). HRMS (ES+): 191.0195 (M+: 191.0194).

5-Phenyl-2-Trifluoromethylpyridine:

Substrate: 5-Phenyl-2-nitropyridine. Conditions: Solvent: THF. LA: K(18-crown-6)($B_3N_3Me_6CF_3$)(THF). 1.0 equivalents K(LA-CF_3) used. 0.40 mmol substrate. Reaction time: 2 hours. Quench: 10 mL water. Chromatography conditions: 0-30% Hexane/Ethyl acetate, 8 column volumes, 25 g SiO_2, flow rate 1 column volume per minute. 30 mg white solid, 33%. ^{1}H-NMR ($CDCl_3$): 8.94 (α, 1H, s), 8.04 (ß, 1H, (d, J_{1H-1H}=8.1)), 7.76 (ß, 1H, (d, J_{1H-1H}=8.1)), 7.60 (γ, 2H, (d, J_{1H-1H}=8.1)), 7.53 (δ, 2H, (t, J_{1H-1H}=8.1)), 7.46 (ε, 1H, (t, J_{1H-1H}=6.8)). ^{13}C-NMR: 148.46, 146.77 (q, $J_{13C-19F}$=34.7), 139.48, 136.35, 135.48, 129.32, 129.00, 127.33, 121.69 (q, $J_{13C-19F}$=273), 120.43 (q, $J_{13C-19F}$=2.7). ^{19}F-NMR: -71.38 (s). HRMS (ESI+): 224.0679 (M+H: 224.0682).

6-Phenyl-(2-/4-)trifluoromethylpyrimidine:

6-Phenylpyrimidine (93.7 mg, 0.600 mmol) was dissolved in 3 mL THF. K(18-crown-6)($B_3N_3Me_6CF_3$)(THF) (3.00 mL, 0.2 M in THF, 0.600 mmol) was then added. After 72 hours, 2,3-dichloro-5,6-dicyano-1,4-benzoquinone (135 mg, 0.600 mmol) was added and the mixture stirred for five minutes. NMR spectra showed a mixture of two trifluoromethylated products. The reaction mixture was quenched with water. The aqueous phase was extracted with CH_2Cl_2 (5 x 2 mL), the CH_2Cl_2 extract was dried and concentrated, and the crude oil was purified by flash silica chromatography. Chromatography conditions: 0-40% Hexane/DCM, 12 column volumes, 25 g SiO_2, flow rate 1 column volume per minute. Chromatography afforded separated -2 and -4 substituted products. 6-Phenyl-2-trifluoromethylpyrimidine: 9.2 mg white solid, 7%. ^{1}H-NMR ($CDCl_3$): 8.91 (ß, 1H, (d, J_{1H-1H}=5.3)), 8.17 (γ, 2H, (dd, J_{1H-1H}=8.1, 1.4)), 7.88 (α, 1H, (d, J_{1H-1H}=5.3)), 7.57 (ε, 1H, m), 7.55 (δ, 2H, m) ^{13}C-NMR: 165.28, 158.30, 157.05 (q, $J_{13C-19F}$=36.5), 135.04, 132.04, 129.22, 127.45, 119.63 (q, $J_{13C-19F}$=275), 118.23 ^{19}F-NMR: -70.65 (s). HRMS (ESI+): 225.0635 (M+H: 225.0640). 6-Phenyl-4-trifluoromethylpyrimidine: 39.5 mg white solid, 29%. ^{1}H-NMR ($CDCl_3$): 9.39 (α, 1H, s), 8.15 (γ, 2H, (d, J_{1H-1H}=6.9)), 8.03 (ß, 1H, s), 7.58 (ε, 1H, m), 7.55 (δ, 2H, m) ^{13}C-NMR: 166.51, 159.40, 156.16 (q, $J_{13C-19F}$=36.0), 135.34, 132.10, 129.26, 127.40, 120.66 (q, $J_{13C-19F}$=275), 112.54 ^{19}F-NMR: -73.70 (s). HRMS (ESI+): 225.0635 (M+H: 225.0640).

4-Trifluoromethylquinazoline:

Quinazoline (78 mg, 0.600 mmol) was dissolved in 3 mL THF. K(18-crown-6)($B_3N_3Me_6CF_3$)(THF) (3.00 mL, 0.2 M in THF, 0.600 mmol) was then added. After 1 hour, 2,3-dichloro-5,6-dicyano-1,4-benzoquinone (135 mg, 0.600 mmol) was added and the mixture stirred for one hour. NMR spectra showed a single product. The reaction mixture was quenched with

water. The aqueous phase was extracted with CH_2Cl_2 (5 x 2 mL), the CH_2Cl_2 extract was dried and concentrated, and the crude oil was purified by flash silica chromatography. Chromatography conditions: 0-20% Hexane/Ethyl Acetate, 16 column volumes, 25 g SiO_2, flow rate 1 column volume per minute. 4-Trifluoromethylquinazoline: 64.0 mg yellow oil, 53%. ^{1}H-NMR ($CDCl_3$): 9.44 (α, 1H, s), 8.25 (ß, 1H, (d, J_{1H-1H}=8.5)), 8.18 (ε, 1H, (d, J_{1H-1H}=8.5)), 8.03 (δ, 1H, (t, J_{1H-1H}=8.3)), 7.55 (γ, 1H, (t, J_{1H-1H}=7.7)). ^{13}C-NMR: 154.57 (q, $J_{13C-19F}$=34.9), 153.50, 151.86, 134.88, 129.50, 129.40, 124.27 (q, $J_{13C-19F}$=2.7), 121.24 (q, $J_{13C-19F}$=277), 120.28^{19}F-NMR: -64.55 (s). HRMS (ESI+): 199.0478 (M+H: 199.0483).

4-Trifluoromethyl-5-bromo-2-chloro-pyrimidine:

5-Bromo-2-chloro-pyrimidine (154 mg, 0.800 mmol) was dissolved in 4 mL THF. K(18-crown-6)($B_3N_3Me_6CF_3$)(THF) (4.00 mL, 0.2 M in THF, 0.800 mmol) was then added. After 5 minutes, 2,3-dichloro-5,6-dicyano-1,4-benzoquinone (135 mg, 0.600 mmol) was added and the mixture stirred for one hour. NMR spectra showed a single product. The reaction mixture was quenched with water. The aqueous phase was extracted with CH_2Cl_2 (5 x 2 mL), the CH_2Cl_2 extract was dried and concentrated, and the crude oil was purified by flash silica chromatography. Chromatography conditions: 0-20% Hexane/DCM, 12 column volumes, 25 g SiO_2, flow rate 1 column volume per minute. 4-Trifluoromethyl-5-bromo-2-chloro-pyrimidine: 102.3 mg colorless oil, 49%. ^{1}H-NMR ($CDCl_3$): 8.94 (α, 1H, s). ^{13}C-NMR: 164.56, 159.61, 155.21 (q, $J_{13C-19F}$=36.7), 119.28 (q, $J_{13C-19F}$=277), 115.35 ^{19}F-NMR: -68.22 (s). HRMS (EI+): 259.8966 (M+: 259.8964).

4-Trifluoromethyl-2-6-diphenyltriazine:

2-6-Diphenyltriazine[263] (0.4 mg, 0.800 mmol) was dissolved in 2 mL THF. K(18-crown-6)($B_3N_3Me_6CF_3$)(THF) (4.00 mL, 0.2 M in THF, 0.800 mmol) was then added. After 5 minutes, 2,3-dichloro-5,6-dicyano-1,4-benzoquinone (135 mg, 0.600 mmol) was added and the mixture stirred for one hour. NMR spectra showed a single product. The reaction mixture was quenched with water. The aqueous phase was extracted with CH_2Cl_2 (5 x 2 mL), the CH_2Cl_2 extract was dried and concentrated, and the crude oil was purified by flash silica chromatography. Chromatography conditions: 2-15% Hexane/DCM, 8 column volumes, 25 g SiO_2, flow rate 1 column volume per minute. 4-Trifluoromethyl-5-bromo-2-chloro-pyrimidine: 52.5 mg white solid, 43%. ^{1}H-NMR ($CDCl_3$): 8.69 (α, 4H, (d, J_{1H-1H}=8.4)), 7.66 (γ, 2H, (t, J_{1H-1H}=7.3)), 7.58 (ß, 4H, (t, J_{1H-1H}=7.7)). ^{13}C-NMR: 173.07, 165.19 (q, $J_{13C-19F}$=37.7), 134.43, 133.73, 129.41, 128.90, 119.07 (q, $J_{13C-19F}$=277) ^{19}F-NMR: -72.28 (s). HRMS (ESI+): 302.0897 (M+H: 302.0905).

4,4-Bistrifluoromethyl-2-chloro-3-hydroquinazoline

Substrate: Dichloroquinazoline. Conditions: Solvent: THF. LA: K(18-crown-6)($B_3N_3Me_6CF_3$)(THF). 1.5 equivalents K(LA-CF_3) used. 0.80 mmol substrate. Reaction time: 30 minutes. Quench: 10 mL 5% NaOH, then brought to pH 7 with glacial acetic acid. Chromatography conditions: 0-100% hexane/ethyl acetate, 16 column volumes, 25 g SiO_2, flow rate 1 column volume per minute.146 mg light yellow solid, 60%. ^{1}H-NMR ($CDCl_3$): 8.22 (η, 1H, s), 7.58 (α, 1H, (d, J_{1H-1H}=8.0)), 7.41 (ε, 1H, (t, J_{1H-1H}=7.7), 7.22 (ß, 1H, (t, J_{1H-1H}=7.7)), 6.88 (ζ, 1H, (d, J_{1H-1H}=8.0)). ^{13}C-NMR: 145.84 (3), 135.58 (4), 131.34 (6), 128.19 (8), 125.66 (7), 122.42(1, q, $J_{13C-19F}$=288), 115.09 (5), 108.67 (9), 73.36(2, p, $J_{13C-19F}$=29). ^{19}F-NMR: -73.73 (s). HRMS (ESI+): 303.0114 (M+H: 303.0124).

The trifluoromethyl groups were assigned based on crosspeaks in 2D NMR experiments and a septet for carbon #2 in the ^{13}C NMR spectrum. HSQC was used to identify the carbon atoms associated with hydrogen atoms α, ß, ε, and ζ. ^{19}F-^{13}C HMBC was then used to identify one bond coupling with carbon 1, two bond coupling with carbon 2, four bond coupling with carbon 3, and four bond coupling with carbon 8. Carbon 3 was assigned based on its lack of long-range coupling with any protons and high shift. The positions of carbons 9 and 4 were assigned based on their long-range coupling with hydrogen atoms α, ß, ε, and ζ. The position of carbon 8 was based on its proximity to the ^{19}F group. Finally, the position of acidic hydrogen η and confirmation of the assignment was obtained through single-crystal X-Ray diffraction. A single crystal was obtained by allowing a concentrated solution of 4,4-Bistrifluoromethyl-2-chloro-3-hydroquinazoline in chloroform to slowly evaporate.

2,4-Phenoxy-6,6-bistrifluoromethyl-3-hydro-triazine

Substrate: 2,4-diphenoxy-6-chlorotriazine. Solvent: THF. Conditions: LA: K(18-crown-6)($B_3N_3Me_6CF_3$)(THF). 2.0 equivalents K(LA-CF_3) used. 0.40 mmol substrate. Reaction time: 2 hour. Quench: water. Chromatography conditions: 0-50% Hexane/Ethyl acetate, 8 column volumes, 25 g SiO_2, flow rate 1 column volume per minute. 123 mg white solid, 76%. ^{1}H-NMR (DMSO-d_6): 12.36 (ε, 1H, s), 7.84 (ß, 2H, (t, 4H, (t, J_{1H-1H}=7.8)), 7.27 (α, 2H, (t, J_{1H-1H}=7.3)), 7.21 (γ, 4H, (d, J_{1H-1H}=8.0)). ^{13}C-NMR (DMSO-d_6): 155.74, 151.04, 130.12, 126.60, 122.09(q, $J_{13C-19F}$=288), 121.63, 81.02 (p, $J_{13C-19F}$=29.5). ^{19}F-NMR: -79.44 (s). HRMS (ES+): 403.0759 (M+: 403.0755).

2,4-Phenoxy-6,6-bistrifluoromethyl-3-benzyl-triazine

Substrate: 2,4-diphenoxy-6-chlorotriazine. Conditions: Solvent: THF. LA: K(18-crown-6)($B_3N_3Me_6CF_3$)(THF). 2.0 equivalents K(LA-CF_3) used. 0.40 mmol substrate. Reaction time: 30 minutes. Quench: 1 equiv. benzyl bromide was added under nitrogen, then the reaction stirred for 16 hours at 25 °C. The reaction mixture was then quenched with 10 mL water. Chromatography conditions: 0-100% Hexane/Ethyl acetate, 16 column volumes, 25 g SiO_2, flow rate 1 column volume per minute. 108 mg white solid, 55%. ^{1}H-NMR ($CDCl_3$): 7.37 (α, 10H, m), 7.24 (ε, 2H, (t, $J_{1H\text{-}1H}$=7.4)), 7.11 (γ, 3H, m), 5.21 (ß, 2H, s). ^{13}C-NMR: 153.07, 151.25, 136.53, 129.33, 128.92, 127.95, 126.86, 126.02, 121.59(q, $J_{13C\text{-}19F}$=288), 121.11, 78.83(p, $J_{13C\text{-}19F}$=30.3), 46.00. ^{19}F-NMR: -80.41 (s). HRMS (ES+): 493.1229 (M+: 493.1225).

1-benzyl-6-chloro-2-(phenylthio)-4,4-bis(trifluoromethyl)-1,4-dihydroquinazoline:

Substrate: Trichloroquinazoline. Experimental: Trichloroquinazoline (0.400 mmol, 93.4 mg) was combined with 2 equivalents K(18-crown-6)($B_3N_3Me_6CF_3$)(THF) (0.800 mmol, 4.00 mL, 0.2M solution in THF) and stirred for 30 minutes at 25 °C. One equivalent benzyl bromide (0.400 mmol, 68.4 mg) was then added, and the mixture stirred at 70 °C for 24 hours. The reaction was then cooled to 25 °C, and 1 equivalent sodium thiophenolate (0.400 mmol, 52.8 mg) was added. The reaction was then heated to 70 °C and stirred for 24 hours. The THF solvent was then removed by rotary evaporation, and the crude solid purified by flash chromatography (conditions: 25g SiO_2 column, 0-50% CH_2Cl_2/Hexane over 16 column volumes at a flow rate of 1 column volume per minute) to afford 120 mg of white solid (60%). ^{1}H-NMR ($CDCl_3$): 7.55 (η, 2H, overlap), 7.54 (1H, α, overlap), 7.41 (5H, χ, τ, ζ, overlap), 7.34 (1H, σ, (t, $J_{1H\text{-}1H}$=7.4)), 7.28 (2H, ε, (d, $J_{1H\text{-}1H}$=7.7)), 7.24 (1H, (d(d), ($J_{1H\text{-}1H}$=8.8, 2.1)), 6.75 (1H, γ, (d, $J_{1H\text{-}1H}$=9.0)), 5.27 (2H, δ, s). ^{13}C-NMR: 158.99, 136.80, 135.69, 134.95, 130.81, 129.48, 129.37, 129.21, 128.73, 128.08, 127.93, 125.76, 122.46 (q, $J_{13C\text{-}19F}$=288), 115.67, 113.23, 66.80(p, $J_{13C\text{-}19F}$=28.7), 50.36. ^{19}F-NMR: -73.92 (s). HRMS (ESI+): 501.0619 (M+H: 501.0621). A single crystal was obtained for X-Ray diffraction by allowing a concentrated solution in chloroform to slowly evaporate.

6.11.9 Selective C-H Trifluoromethylation of Quinolines

4-Trifluoromethylquinoline:

Experimental: Quinoline (51.6 mg, 0.400 mmol) was dissolved in 2 mL THF along with $B(C_6F_5)_3$ (204 mg, 0.400 mmol). This was cooled to -30 °C, and combined with K(18-crown-6)($B_3N_3Me_6CF_3$)(THF) (2.00 mL, 0.2 M in THF, 0.400 mmol) with stirring. The reaction was allowed to warm to room temperature over 30 minutes, NMR spectra recorded, and then 2,3-

dichloro-5,6-dicyano-1,4-benzoquinone (181 mg, 0.800 mmol) was added. *In-situ* NMR spectra showed conversion to the dearomatized *para*, rather than the *ortho*, intermediate in 93% selectivity. The reaction was stirred for 1 hour at room temperature, and the reaction mixture quenched with water. The aqueous phase was extracted with CH_2Cl_2 (5 x 2 mL), the CH_2Cl_2 extract was dried and concentrated, and the crude oil was purified by flash silica chromatography. Chromatography conditions: 0-80% Hexane/Ethyl acetate, 16 column volumes, 50 g SiO_2, flow rate 1 column volume per minute. 50.2 mg colorless oil, 65%. ^{1}H-NMR ($CDCl_3$): 9.05 (ß, 1H, (d, J_{1H-1H}=4.2)), 8.24 (γ, 1H, (d, J_{1H-1H}=8.5)), 8.17 (γ, 1H, (d, J_{1H-1H}=8.5)), 7.83 (ε, 1H, (t, J_{1H-1H}=7.2)), 7.72 (ε, α, 2H, m (overlap)). ^{13}C-NMR: 149.53, 148.94, 134.28 (q, $J_{13C-19F}$=31.8), 130.41, 130.21, 128.32, 124.03 (q, $J_{13C-19F}$=2.2), 123.40 (q, $J_{13C-19F}$=274.7), 122.95, 117.93 (q, $J_{13C-19F}$=5.3). ^{19}F-NMR: -61.46 (s). HRMS (ESI+): 198.0523 (M+H: 198.0525).

2-Trifluoromethylquinoline:

Experimental: Quinoline (51.6 mg, 0.400 mmol) was dissolved in 2 mL THF along with BF_3 (204 mg, 0.400 mmol). This was cooled to -30 °C, and combined with K(18-crown-6)($B_3N_3Me_6CF_3$)(THF) (2.00 mL, 0.2 M in THF, 0.400 mmol) with stirring. The reaction was allowed to warm to room temperature over 30 minutes, and then 2,3-dichloro-5,6-dicyano-1,4-benzoquinone (181 mg, 0.800 mmol) was added. *In-situ* NMR spectra showed conversion to the dearomatized *ortho*, rather than the *para*, intermediate in 85% selectivity. The reaction was stirred for 1 hour at room temperature, and the reaction mixture was quenched with water. The aqueous phase was extracted with CH_2Cl_2 (5 x 2 mL), the CH_2Cl_2 extract dried and concentrated, and the crude oil purified by flash silica chromatography. Chromatography conditions: 0-80% Hexane/Ethyl acetate, 16 column volumes, 50 g SiO_2, flow rate 1 column volume per minute. 21.6 mg white solid, 27%. ^{1}H-NMR ($CDCl_3$): 8.36 (α, 1H, (d, J_{1H-1H}=8.5)), 8.24 (α, 1H, (d, J_{1H-1H}=8.5)), 7.91 (ß, 1H, (d, J_{1H-1H}=8.2)), 7.82 (γ, 1H, (t, J_{1H-1H}=7.6)), 7.75 (ß, 1H, (d, J_{1H-1H}=8.5)), 7.65 (γ, 1H, (t, J_{1H-1H}=7.6)). ^{13}C-NMR: 147.89 (q, $J_{13C-19F}$=34.6), 147.14, 138.10, 130.79, 130.08, 128.83, 128.57, 127.66, 121.55 (q, $J_{13C-19F}$=275), 116.75. ^{19}F-NMR: -67.13 (s). HRMS (ESI+): 198.0522 ($M+H^+$: 198.0525).

4-(Cinnamylthio)-2,7-bis(trifluoromethyl)quinoline:

Experimental: 4-(thio)-7-trifluoromethylquinoline (229 mg, 1.00 mmol) was dissolved in 10 mL THF and combined with KOtBu (112 mg, 1.00 mmol). After stirring for 5 minutes, cinnamyl bromide was added (197 mg, 1.00 mmol). After five additional minutes, the reaction

solvent was evaporated, 10 mL water added, and the product extracted with CH_2Cl_2 (5 x 2 mL). The CH_2Cl_2 extract was then dried and concentrated, and the crude oil purified by flash silica chromatography. Chromatography conditions: 5-40% Hexane/Ethyl Acetate, 16 column volumes, 100 g SiO_2, flow rate 1 column volume per minute. 280 mg white solid, 81%. ^{1}H-NMR (CD_3OD): 8.75 (δ, 1H, (d, J_{1H-1H}=4.9)), 8.37 (γ, 1H, (d, J_{1H-1H}=8.8)), 8.27 (ß, 1H, s), 7.81 (π, 1H, (d, J_{1H-1H}=8.8)), 7.63 (α, 1H, (d, J_{1H-1H}=4.9)), 7.38 (ν, 2H, (d, J_{1H-1H}=7.7)), 7.28 (ξ, 2H, (t, J_{1H-1H}=7.3)), 7.21 (ζ, 1H, (t J_{1H-1H}=7.4)), 6.77 (μ, 1H, (d, J_{1H-1H}=15.7)), 6.40 (τ, 1H, (dt, J_{1H-1H}=15.7, 7.0)), 4.09 (ε, 2H, (d, J_{1H-1H}=7.0)). ^{19}F-NMR: -63.11 (2, s), -67.98 (1, s). HRMS (ESI+): 346.0872 ($M+H^+$: 346.0877).

4-(Cinnamylthio)-2,7-bis(trifluoromethyl)quinoline:

Experimental: 4-(Cinnamylthio)-2,7-bis(trifluoromethyl)quinoline (204 mg, 0.600 mmol) was dissolved in 0.75 mL THF along with BF_3 (74 μL, 0.600 mmol). This was cooled to -30 °C, and combined with K(18-crown-6)($B_3N_3Me_6CF_3$)(THF) (3.00 mL, 0.2 M in THF, 0.600 mmol) with stirring. The reaction was allowed to warm to room temperature over 10 minutes, and then 2,3-dichloro-5,6-dicyano-1,4-benzoquinone (181 mg, 0.800 mmol) was added. After 10 minutes, the solvent was evaporated, and the reaction quenched with 5% NaOH solution in water. The aqueous phase was extracted with CH_2Cl_2 (5 x 2 mL), the CH_2Cl_2 extract dried and concentrated, and the crude oil purified by flash silica chromatography. Chromatography conditions: 0-20% Hexane/DCM, 12 column volumes, 25 g SiO_2, flow rate 1 column volume per minute. 91.9 mg white solid, 37%. ^{1}H-NMR ($CDCl_3$): 8.50 (ß, 1H, s), 8.29 (γ, 1H, (d, J_{1H-1H}=8.8)), 7.82 (π, 1H, (d, J_{1H-1H}=8.8)), 7.65 (α, 1H, s), 7.36 (ν, 2H, (d, J_{1H-1H}=7.5)), 7.32 (ξ, 2H, (t, J_{1H-1H}=7.6)), 7.27 (ζ, 1H, (t J_{1H-1H}=7.6)), 6.79 (μ, 1H, (d, J_{1H-1H}=15.7)), 6.28 (τ, 1H, (dt, J_{1H-1H}=15.5, 7.1)), 4.04 (ε, 2H, (d, J_{1H-1H}=7.0)). ^{13}C-NMR: 150.86, 148.22 (q, $J_{13C-19F}$=34.7), 145.49, 135.77, 135.59, 132.79 (q, $J_{13C-19F}$=33.1), 128.63 (m), 128.61 (m), 128.53 (m), 128.46 (m), 126.62, 124.92 (d, $J_{13C-19F}$=24.9), 123.85 (d, $J_{13C-19F}$=22), 123.43 (q, $J_{13C-19F}$=273), 121.40, 121.23 (q, $J_{13C-19F}$=276), 113.18 (q, $J_{13C-19F}$=35.2), 34.36.^{19}F-NMR: -63.11 (2, s), -67.98 (1, s). HRMS (ESI+): 414.0742 ($M+H^+$: 414.0751).

Chapter 7. The Difluoromethyl Group as a Masked Nucleophile

7.1 Abstract

Benzylic difluoromethylene (Ar-CF_2-R) linkages have shown significant potential as metabolically-resistant replacements for benzylic linkages and can be used as bioisosteres in place of ketone, cyclopropyl, and dimethylmethylene groups in medicinal chemistry. However, a current lack of synthetic methodologies and reagents capable of constructing such linkages has limited their use. We present a strategy in which common aryl difluoromethyl groups ($ArCF_2H$) can be transformed into reactive nucleophilic aryl difluoromethanide ($ArCF_2^-$) transfer reagents which react with electrophiles in under five minutes at room temperature. This methodology is highly general in both electrophile and (hetero)aryl difluoromethanide nucleophile, enabling a new and highly robust retrosynthetic disconnection at the C-C bond of aryl difluoromethylene linkages between organic fragments, and we anticipate that it will find diverse applications in the synthesis of fluorinated medicinally active compounds.

7.2 Introduction

Benzylic methylene linkages (Ar-CH_2-R) are common motifs in medicinal chemistry, with over 1000 drug candidates and commercial pharmaceuticals featuring this functional.[264] However, these linkages are metabolically unstable because their C-H bonds (90 kcal/mol) are readily cleaved by p450 enzymes in the liver. Even less stable are doubly benzylic Ar-CH_2-Ar groups (C-H bond: 82 kcal/mol),[265] of which only 33 clinical examples are known. Their low stability can render promising lead compounds useless in the clinic, so replacement of the CH_2 group with structurally similar but metabolically stable linkages is an attractive strategy for structure-activity relationship (SAR) optimization. Difluoromethylene (R-CF_2-R) linkages present similar steric profiles to methylene linkages, yet are metabolically robust and exhibit enhanced lipophilicity. This feature was exploited in the preparation of RWJ-445167, a thrombin inhibitor, in which a problematic benzylic linkage led to a short biological half-life.[266] Replacement of the Ar-CH_2-R

linkage with a Ar-CF_2-R linkage improved lipophilicity, bioavailability, and eliminated the principal mode of metabolic degradation.[267]

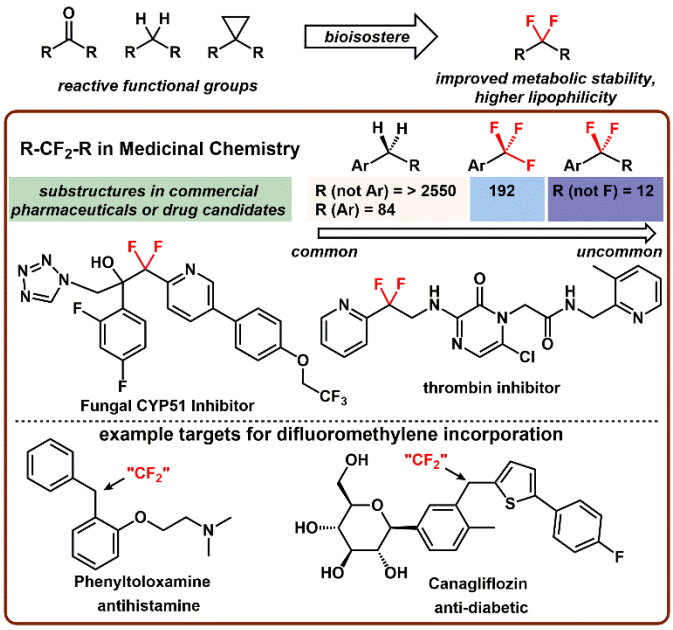

Figure 7-1 The CF_2 linkage in medicinal chemistry

Compared with commercial pharmaceuticals containing Ar-F or CF_3 units (764), only *five* feature singly benzylic ArCF_2-R and *zero* feature doubly benzylic Ar-CF_2-Ar units because of a lack of synthetic tools. Existing methodologies require reagents that are toxic, explosive, and of highly limited scope.[268] The most common retrosynthetic disconnection is at the C-F bonds of the CF_2 unit through ketone deoxyfluorination using trifluorosulfuranes,[269] dithioketal fluorination using bromonium fluoride,[270] radical fluorination of C-H bonds,[271] or nucleophilic fluorination of dichloromethylene (CCl_2).[272] However, each of these strategies carry significant disadvantages, and cannot be safely used at scale.

Unlike alcohols and aldehydes, ketones which are not activated by ring strain (e. g. fluorenone) do not react with typical deoxyfluorination reagents such as diethylaminotrifluorosulfurane (DAST). Under forcing conditions, α-deprotonation of aliphatic ketones forms vinyl fluorides, and the required temperatures generate highly explosive diaminodifluorosulfuranes byproducts. Bromonium fluoride dethiofluorination similarly promotes the formation of vinyl fluorides, but reaction mixtures also become contaminated by radical bromination side products. Nucleophilic fluorination of dichloromethylene units requires harsh radical chlorination conditions to synthesize the precursors. Finally, radical C-H fluorination

requires use of harsh F• sources which can lead to fluorination of other C-H bonds. In the thrombin inhibitor example noted above, significant effort was expended to avoid explosive deoxyfluorination reagents and ultimately the drug was prepared in a lengthy linear synthesis using bromodifluoroacetate.[273]

A more desirable disconnection is at the RCF_2-R carbon-carbon bond, as it would enable more convergent synthetic approaches. Electrophilic approaches to C-CF_2R bonds are limited to largely unavailable RCF_2Br starting materials. Recently, sulfone-based reagents and Ar-CF_3 starting materials have been used as precursors to RCF_2• species through radical coupling (Baran)[274] or photocatalytic methodologies (König).[275] However, these routes are limited in scope due to the harsh photoreductants required to cleave C-F bonds in trifluoromethyl groups and the restriction of redox active sulfone based approaches to the generation of aliphatic difluoromethyl radicals.

The instability of RCF_2^- groups to loss of fluoride renders straightforward approaches to nucleophilic RCF_2^- transfer such as deprotonation of R-CF_2H groups impractical. More attractive is nucleophilic substitution of fluorine atoms in $SiMe_3CF_3$ to generate $SiMe_3CF_2R$ reagents,[268d,276] but this is of limited scope due to either a lack of available starting materials or competing loss of CF_3^- from hypervalent silicate intermediates. Insertion of difluorocarbene into Zn-C bonds can be used to prepare RCF_2Zn reagents, but this method is limited to the preparation of R-CH_2-CF_2-Zn.[268e-g,268j] Due to the limitations of these methodologies, most molecules containing Ar-CF_2-R linkages are constructed outwards from an existing Ar-CF_2-R group in a linear synthetic approach. The current lack of convergent retrosynthetic disconnections at $ArCF_2$-R bonds, and especially a lack of nucleophilic or electrophilic approaches, has rendered these linkages largely inaccessible to medicinal chemists.

The low stability of fluoroalkyl anions is the root cause of slow progress in the development of nucleophilic fluoroalkylation methods. Our group has pioneered a new Lewis acid capture/release strategy to stabilize CF_3^-, the least stable fluoroalkyl group.[72] We discovered that hexamethylborazine ($B_3N_3Me_6$) is a Lewis acid that imparts unique stability to CF_3^- and facilitates rapid transfer of CF_3 to 13 elements, including organic and inorganic electrophiles, without competing side-reactions. This approach enabled new nucleophilic aromatic substitution reactions with (hetero)arenes exhibiting distinct selectivity in comparison with Pd- and Cu- catalyzed cross-coupling.[277] In this work, we expand this chemical strategy beyond CF_3^- and develop analogous

reagents derived from deprotonation of common difluoromethylated (hetero)arenes which are capable of constructing currently inaccessible R-CF_2-R linkages.

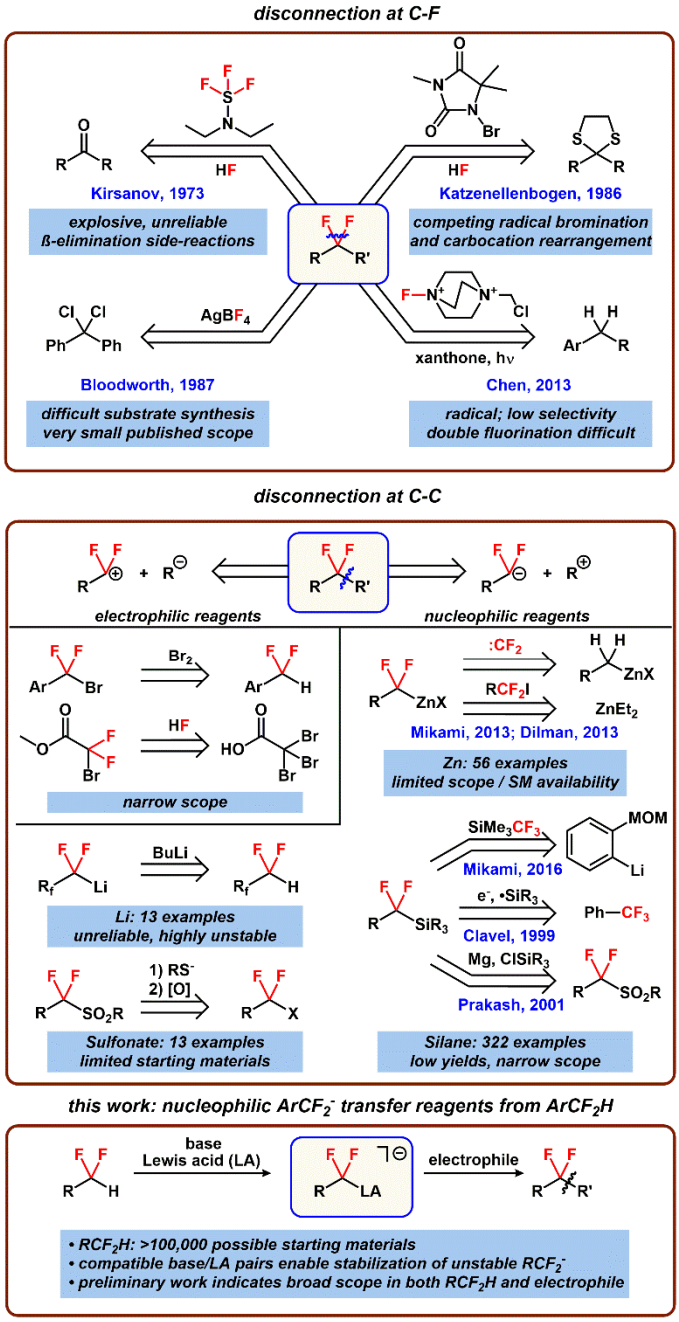

Figure 7-2 Approaches for preparing R-CF_2-R linkages

7.3 Deprotonation of $PhCF_2H$ and Capture of $PhCF_2^-$ Anion

In our previous work, we discovered that hexamethylborazine ($B_3N_3Me_6$) is a weak Lewis acid that does not form irreversible adducts with strong bases (KCH_2Ph, KDMSO), permitting deprotonation of HCF_3 with concomitant *in-situ* capture of CF_3^-. The $B_3N_3Me_6$-stabilized CF_3^- anion is highly nucleophilic, transferring to a wide variety of electrophiles including carbonyl, imine, and activated heteroarenes. Mechanistic studies indicated that the reactions proceed through dissociative mechanisms, and the $B_3N_3Me_6$ Lewis acid could be recovered and recycled *in-situ*. We suspected that similar systems of strong bases and weak Lewis acids could be used for the deprotonation of qualitatively similar RCF_2H groups, stabilization of otherwise unavailable RCF_2^- synthons, and RCF_2^- transfer to electrophiles. Based on the demonstrated utility of difluorobenzylic linkages in medicinal chemistry, we focused our efforts on the preparation of $ArCF_2^-$ reagents.

While pK_a measurements for $ArCF_2$-H bonds are unavailable, we anticipated that KCH_2Ph would be capable of deprotonating HCF_2Ph (difluoromethylbenzene). We previously reported that KCH_2Ph forms a reversible adduct with $B_3N_3Me_6$, and hypothesized that the equilibrium quantity of free $PhCH_2^-$ would be capable of deprotonating difluoromethylbenzene and that the highly unstable $PhCF_2^-$ anion generated in this reaction could be captured by $B_3N_3Me_6$ *in-situ*. When we added $PhCF_2H$ to an equimolar combination of $B_3N_3Me_6$, KCH_2Ph (pK_a: ~41), and 18-crown-6 in THF at 0 °C, we immediately observed quantitative formation of the expected [K(18-crown-6)][$PhCF_2$-$B_3N_3Me_6$] (**1**) adduct. Similar reactions carried out using $KCHPh_2$ (pK_a: ~32) and $KC(Me)Ph_2$ (pK_a: ~35) did not afford detectable quantities of CF_2Ph^--containing products (<0.1%), establishing that the solution pK_a of $PhCF_2$-H falls between 35-41. Addition of lithium salts to this adduct resulted in its rapid decomposition, reflecting the previously observed instability of fluoroalkyl anions in the presence of fluorophilic alkali cations.

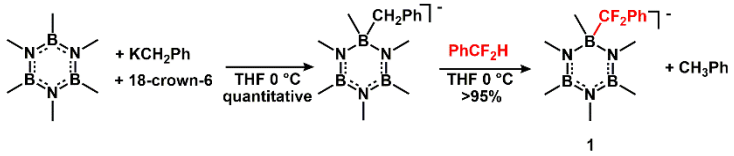

Figure 7-3 Preparation of $PhCF_2$-$B_3N_3Me_6^-$

7.4 Difluorobenzylation of Organic Electrophiles

We used **1** as a model nucleophilic $ArCF_2^-$ synthon to explore the scope in electrophile for nucleophilic difluoromethylarylation. **1** reacted with a wide variety of electrophiles, including benzaldehyde, benzoyl chloride, methyl benzoate, chalcone, phenyl isocyanate, and N-tosylbenzimine in 1,2-addition reactions. Notably, acetophenone reacted in 11% yield, suggesting that reactions with enolizable ketones were possible with **1**. This contrasts the reactivity of $B_3N_3Me_6$-CF_3^- with acetophenone and other enolizable ketones, which does not form C-CF_3 bonds and results exclusively in formation of undesired enolates. Previous methods to aryldifluoromethyl ketones, carbinols, and amines relied exclusively on difluorobromoacetate as an electrophilic difluoromethylene synthon; this approach enables highly convergent approaches to difluoromethylene linkages akin to Grignard addition reactions.

Compounds containing thiodifluoromethylene linkages (R-S-CF_2-R) are exceptionally difficult to access in organic synthesis, but are especially promising as metabolically stable analogues to unstable benzylic thioethers. One largely unused approach to such compounds is nucleophilic substitution of simple disulfide starting materials using aryl difluoromethanide synthons. Upon addition of **1** to diphenyldisulfide, 43% conversion to the difluorobenzyl thioether was observed.

In addition to reactions with carbonyl, disulfide, and imine containing compounds, **1** is capable of $PhCF_2^-$ transfer to arene electrophiles. **1** can carry out the first nucleophilic aromatic substitutions performed using difluorobenzyl anion equivalents in reactions with dinitrobenzene (38%) and 2-nitropyridine (8%), albeit in low to moderate yield, generating diaryl difluoromethylene products (Ar-CF_2-Ar). Such species are extremely difficult to synthesize using current methodologies, but represent the most desirable targets in medicinal chemistry due to their potential to replace metabolically unstable diarylmethanes. An alternative approach to direct nucleophilic aromatic substitution is dearomative nucleophilic addition to Lewis acid activated heterocycles, followed by C-H oxidation with DDQ. **1** can promote 4- selective difluorobenzylation in reactions with the $B(C_6F_5)_3$-pyridine (96%) and $B(C_6F_5)_3$-quinazoline (71%).

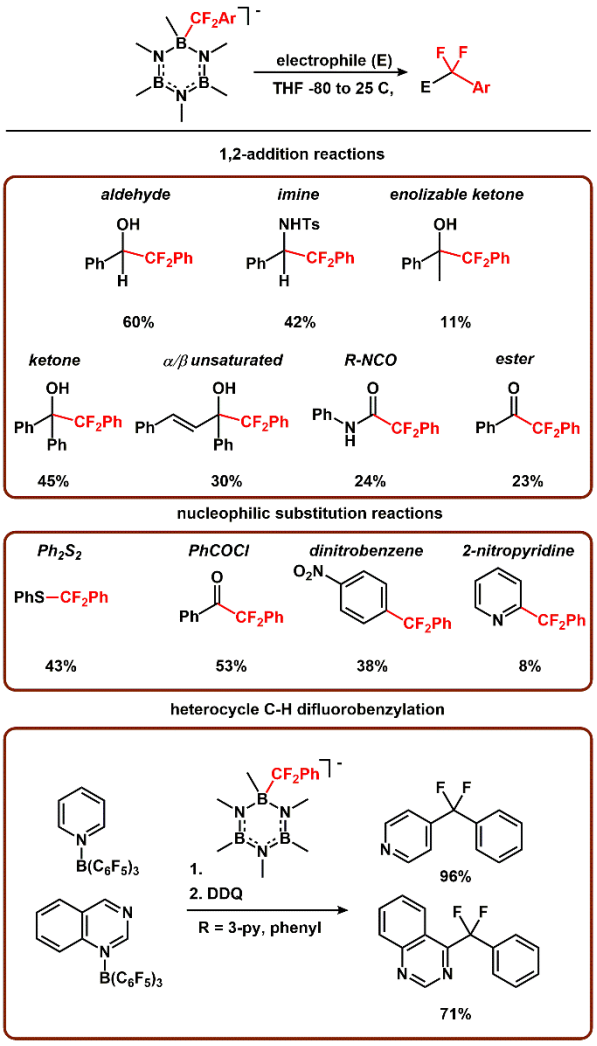

Figure 7-4 Reactivity of $PhCF_2$-$B_3N_3Me_6$ with electrophiles

7.5 K(iPr)$_2$ as a Base for PhCF$_2$H Deprotonation

We anticipated that the high nucleophilicity of KCH_2Ph would present complications in deprotonating more electrophilic heteroaryl and haloaryl-substituted difluoromethyl groups, so we explored the use of less nucleophilic bases for $ArCF_2H$ deprotonation. The desired bulky base would need to possess a pK_a value greater than 35, be free of fluorophilic lithium and sodium countercations, and be stable as a THF solution.

Potassium diisopropylamide ($KN(iPr)_2$, pK_a > 41)[278] appears to satisfy these criteria, but had been previously described as highly unstable in contact with ethereal solvents and $HNiPr_2$ was the only known solvent in which it could be used. We found that in $HN(iPr)_2$, no reaction was observed between $KN(iPr)_2$ and a mixture of $B_3N_3Me_6$, $PhCF_2H$, and 18-crown-6, likely due to

the basicity-attenuating effect of hydrogen bonds in solution. We found that $KN(iPr)_2$ could form stable solutions in THF at -80 °C at high concentration (up to 1.0 M), providing an unattenuated source of dissolved KDA. Addition of this solution to a combination of $B_3N_3Me_6$, $PhCF_2H$, and 18-crown-6 in THF at -80 afforded **2** in quantitative yield. The order of addition was found to greatly impact the success of the reaction, due to the instability of $PhCF_2^-$ in the absence of $B_3N_3Me_6$ and of $KN(iPr)_2$ in the presence of 18-crown-6. The steric bulk of $KN(iPr)_2$ permitted an expansion of the reaction scope to Lewis acids beyond $B_3N_3Me_6$, facilitating preparation of the $K(18\text{-crown-6})^+$ salts of $PhCF_2(B(OMe)_3)^-$ (71%), $PhCF_2(BO_3Me_3)^-$ (53%), and $PhCF_2((BOCH_2CH_2N)_3)^-$ (20%).

Previous work by Collum et. al. with $NaN(iPr)_2$[279] suggested that tertiary amines such as NMe_2Et could be used to prepare concentrated and highly stable solutions of heavy alkali diisopropylamide. While $KN(iPr)_2$ is highly insoluble in NMe_2Et, we found that solutions of modest concentration (0.5 M) could be prepared in tetramethylethylenediamine which could be handled at room temperature. Addition of 20% NMe_2Et by volume allowed the handling of such solutions at -80 °C. However, the use of tetramethylethylenediamine/NMe_2Et as a solvent system for $PhCF_2H$ deprotonation provided less than 20% yield of **1**.

7.6 Broad-Scope Preparation of Nucleophilic $ArCF_2^-$ Reagents

A wide variety of difluoromethyl (hetero)arenes react with $KN(iPr)_2/B_3N_3Me_6$/18-crown-6 in THF at -80 °C to form stabilized aryldifluoromethanide transfer reagents. The reagents were prepared and characterized at -80 °C using variable temperature ^{11}B and ^{19}F NMR spectroscopy. We began by studying the selectivity of $-CF_2H$ deprotonation in the presence of aryl bromides, which can promote *o*-metalation / benzyne formation. Difluoromethylbenzene with 2-, 3-, and 4-bromide substituents could all be used in high-yielding preparations of $B_3N_3Me_6/ArCF_2^-$ adducts (67%, 93%, and 99% chemical yield). This is in contrast to previously reported electrogeneration of CF_2Ph^- equivalents through cathodic reduction of trifluorotoluene in the presence of $SiMe_3Cl$ or reductive photocatalytic $ArCF_3$ fragmentation into $ArCF_2$ radical, which require such highly reducing potentials that Ar-Br fragmentation would dominate.

Difluoromethyl heteroarenes can also be deprotonated to reveal difluoromethanide adducts. In addition to the more facile deprotonation of 2- and 4- difluoromethylpyridine (83%, 98% chemical yield), unactivated 3- difluoromethylpyridine can also be deprotonated in high yield

(91%). 7-Difluoromethylquinoline can also be deprotonated in modest yield (26%), despite its enhanced electrophilicity in the N-heterocycle. Beyond six-membered N-heterocycles, difluoromethylated five-membered heterocycles can also be deprotonated. 2-Difluoromethyl benzofuran, N-benzyl 2-difluoromethyl benzimidazole, 1-difluoromethyl-4-(1-methyl-4-pyrazolyl)benzene, and 2-difluoromethyl-5-(tert-butylacetylenyl)-thiophene can all be deprotonated in moderate to quantitative yield (65%, 94%, 95%, and 98%). An important limitation of this method is that substrates containing alternative C-H bonds in optimal positions for substrate-directed C-H deprotonation can react with $K(iPr)_2$ through undesired pathways. For example, 1-(4-fluorophenyl)-3-difluoromethyl-4-phenyl pyrazole is deprotonated by $K(iPr)_2/B_3N_3Me_6$ exclusively at the single pyrazolyl C-H bond, rather than through deprotonation of the -CF_2H group. Notably, O-CF_2H groups did not react with $K(iPr)_2/B_3N_3Me_6$, suggesting that their pK_a is greater than 41.

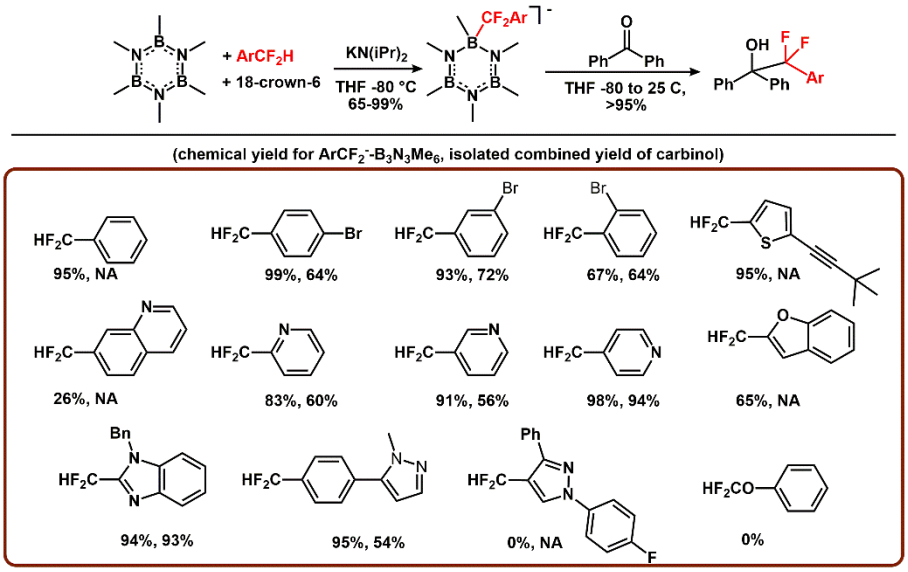

Figure 7-5 Scope in $ArCF_2H$

The relative reactivity of **1** and functionalized (hetero)aryl difluoromethanide reagents was explored in reactions with benzophenone as a model electrophile. The reactions proceed in high isolated yield (54-94%), with chemical yields ranging from 65% to 95%. Notably, all substituted (hetero)aryl reagents reacted completely with benzophenone at room temperature within 5 minutes, while **1** requires four days at room temperature.

We evaluated the robustness of our nucleophilic difluoromethylarylation methodology by coupling four representative electrophiles with four different difluoromethyl arenes in all 16

possible combinations. We selected 4-bromo-1-difluoromethylbenzene, 3-difluoromethylpyridine, 1-benzyl-2-difluoromethylbenzimidazole, and 2-difluoromethyl-5-tertbutylacetylenylthiophene as representative nucleophiles including a variety of heterocycles and substituents. Benzaldehyde, N-tosylbenzimine, diphenyldisulfide, and pyridine-$B(C_6F_5)_3$ were selected as representative examples of carbonyl addition, imine addition, disulfide nucleophilic substitution, and 4-selective C-H difluoromethylarylation of heterocycles. The moderate to high isolated yields observed across the series of reactions (41% to 87%, with an average yield of 62%) suggest that our methodology is highly generalizable.

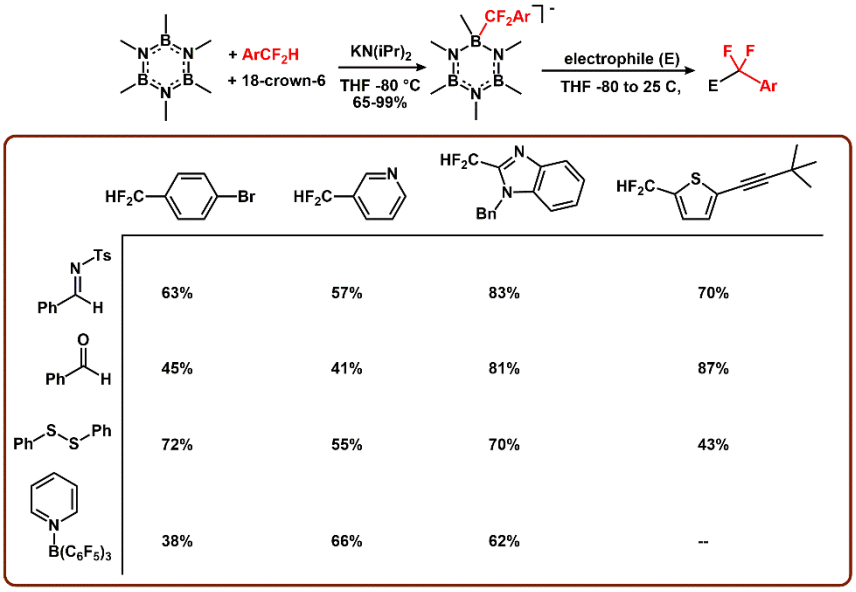

Figure 7-6 Robustness screen for nucleophilic addition of $ArCF_2^-$ synthons to electrophiles

7.7 Conclusions

In conclusion, we have developed a general and robust approach for the conversion of difluoromethyl (hetero)arenes into stabilized, structurally diverse, and previously inaccessible $ArCF_2^-$ transfer reagents. The reagents are highly reactive, transferring $ArCF_2^-$ to a wide variety of organic electrophiles including aldehydes, ketones, isocyanates, activated heteroarenes, nitroarenes, disulfides, imines, and esters. The methodologies used for both $ArCF_2H$ deprotonation and $ArCF_2^-$ transfer are highly robust, providing high yields of difluoromethylene-linked products through a wide array of possible nucleophile / electrophile combinations. We anticipate that this work will enable applications of difluoromethylene linkages in medicinal chemistry.

7.8 Difluoromethyl anion transfer reagents generated from difluoromethane

In addition to reactions using difluoromethyl arenes as precursors to RCF_2^- synthons, we explored the use of difluoromethane (CF_2H_2) as a source of CF_2H^-. Of all difluoromethylene containing functional groups, the difluoromethyl (RCF_2) group is the most commonly used and has found applications in numerous small-molecule pharmaceuticals.[280] This work began as a natural extension of our work with HCF_3, but proved to be significantly more challenging due to the high affinity of CF_2H^- for Lewis acids in combination with its extreme basicity. We began by constructing a CF_2H^- affinity scale as we had previously built for CF_3^-; however, the high nucleophilicity of CF_2H^- necessitated the design of weaker Lewis acids than had previously been employed for CF_3^-, due to an expected reduction in the rate of CF_2H^- dissociation from Lewis acids vs. CF_3^-. To this end, we prepared a variety of B-N containing heterocycles,[281] and several strained organotin species, which we had hypothesized would enable the preparation of stable LA-CF_2H^- adducts. Upon treating a mixture of the Lewis acid, CH_2F_2, and 18-crown-6 with $KN(iPr)_2$ at -80 °C in THF, we observed the formation of several stable boron-CF_2H^- adducts, the first reported compounds containing a B-CF_2H bond, in high yield. No organotin Lewis acids reacted to produce hypervalent Sn-CF_2H adducts, and several Lewis acids we expected to work well did not (B-N naphthalene appears to form an organic radical anion through single-electron transfer, for example). In addition, dimethylformamide furnished the corresponding -ate complex with CF_2H^- in quantitative yield. A and C were characterized through X-Ray crystallography.

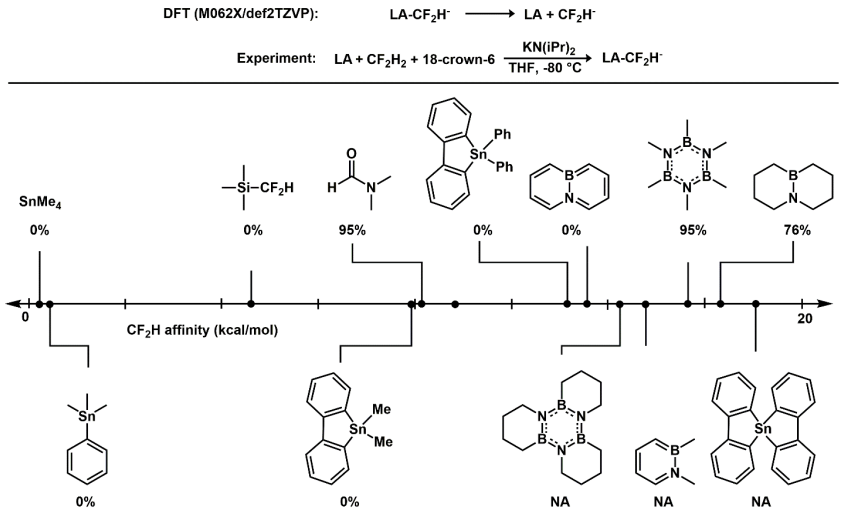

Figure 7-7 CF_2H^- affinity of select Lewis acids, and preparation of LA-CF_2H^- adducts.

We used this methodology to prepare three LA-CF_2H^- adducts on a multigram scale (A, B, and C), and isolated them as free-flowing, stable, crystalline solids. Notably, none of these reagents promoted CF_2H^- transfer to any organic electrophile, including benzaldehyde, dinitrobenzene, $SiMe_3Cl$, benzophenone, or benzyl bromide. Indeed, benzyl bromide reacted at the *nitrogen* center of the Lewis acid -ate complexes, rather than through CF_2H^- transfer; aqueous workup led to quantitative generation of benzylic amines. The adduct with dimethylformamide did not undergo any productive reactions, although it was possible to extend its synthesis to -N,N dibutyl formamide (and the anionic adduct could be oxidized using DDQ to difluoromethyl amides in low yield (~30%). Attempts to directly difluoromethylate other electrophiles using $KN(iPr)_2$ / CH_2F_2, such as pyridine N-oxide, quinoline, benzonitrile, quinazoline, and methyl benzoate, were unsuccessful.

However, it was possible to transfer CF_2H^- to Pd(II) and Cu(I) complexes in medium to high yield. When B is combined with copper iodide and iodobenzene at 100 °C in DMF, $PhCF_2H$ was observed in 43% yield after 16 hours. This reaction likely proceeds through an unstable $CuCF_2H$ complex.[282] In addition, Pd(TMEDA)PhI reacts with C to provide Pd(TMEDA)$PhCF_2H$ in quantitative yield after being heated in THF at 70 C °C for 30 minutes. Curiously, these reactions were selective in that C did not react with CuI and B did not react with Pd(TMEDA)PhI under analogous reaction conditions. Additionally, A (prepared from hexamethylborazine) did not transfer CF_2H^- to any tested substrates and appeared to generate Pd(0) or Cu(0) metal upon mixing with Pd(II) or Cu(I) complexes through electrochemical reduction. These results suggest that B-CF_2H^- adducts may serve as useful difluoromethylating reagents in catalysis, but that the reactivity of such adducts cannot be easily predicted using CF_2H^- affinity as a guide.

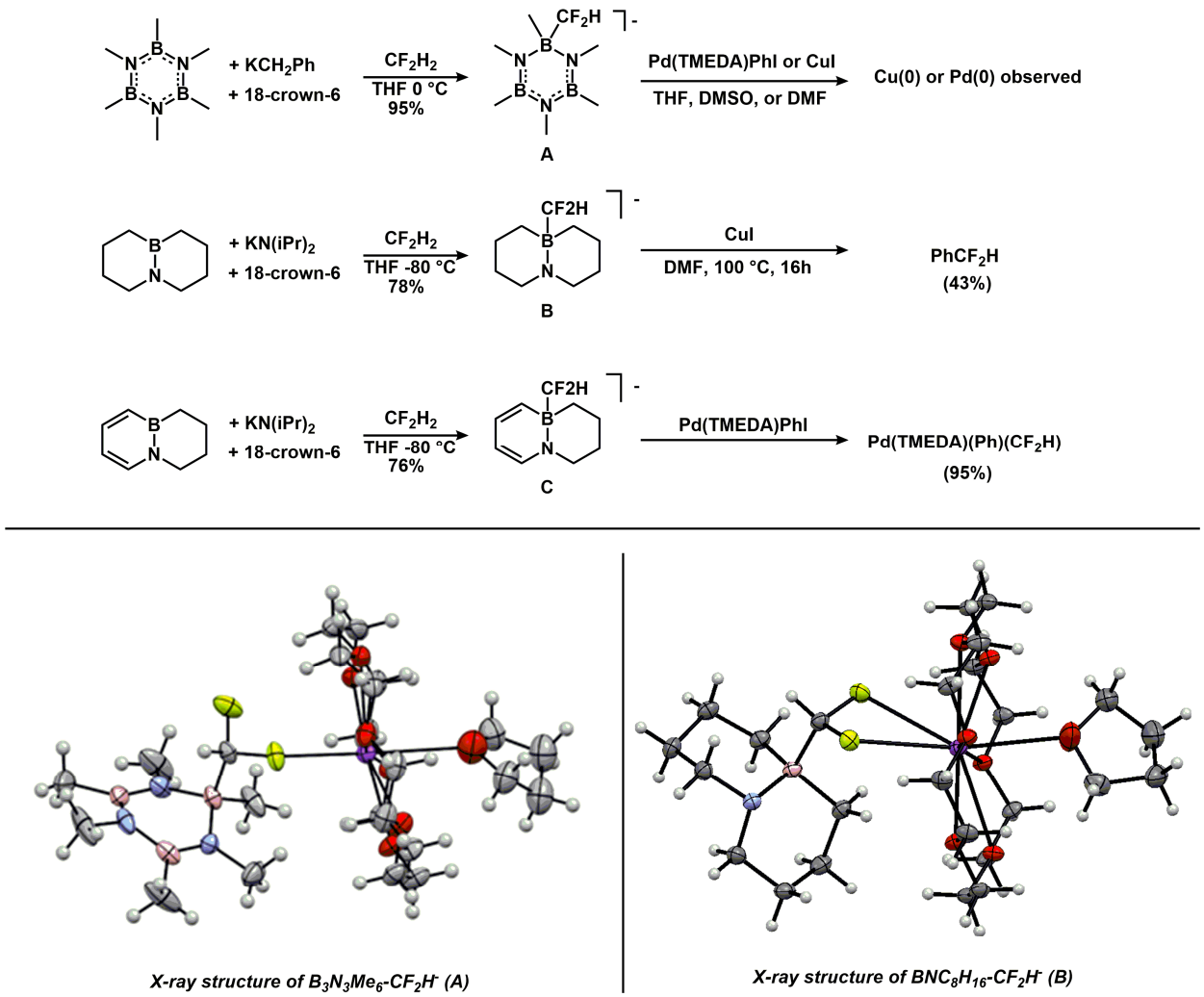

Figure 7-8 Preparation of B-CF_2H adducts A, B, and C and their reactivity with inorganic electrophiles.

We hypothesize that this idiosyncratic reactivity is due to varied steric bulk affecting the ability of A, B, and C to promote transmetalation to Pd and Cu centers through associative mechanisms. Two key pieces of evidence support this hypothesis: C reacts with Pd(TMEDA)PhI while A does not, despite it having a significantly higher CF_2H^- affinity, and B does not react with Pd(TMEDA)PhI despite having a lower CF_2H^- affinity than C. We suggest that the lower steric bulk of B and C, enabled by the low profile of their chair-configured cyclohexyl substructures, enables pre-coordination of the reagent with a Pd or Cu center through the nitrogen atom of the B-N heterocycle. We know that this nitrogen atom has nucleophilic character, because it can be functionalized using benzyl bromide as an electrophile. After pre-coordination, CF_2H^- transfer can

proceed through an associative mechanism. In contrast, A cannot engage in pre-coordination due to its increased steric bulk.

Future efforts to design boron-based difluoromethylation reagents should focus on developing Lewis acids with minimal steric bulk and nucleophilic metal-directing functional groups. In the author's opinion, designing Lewis acids with low CF_2H^- affinity is an intractable approach to designing difluoromethylation reagents due to the extremely high nucleophilicity and instability of "naked" CF_2H^-. Notably, this anion is capable of deprotonating THF. Even $SiMe_3CF_2H$, which can act as a weak Lewis acid to form $SiMe_3(CF_2H)_2^-$, does not easily give up the CF_2H^- anion and is extremely unstable.[283] Our preliminary results in this area suggest that a "window" of ideal Lewis acidity capable of supporting both stable CF_2H^- units and facilitating dissociative CF_2H^- transfer to organic electrophiles may not exist.

7.9 Experimental Details

7.9.1 Synthesis of [K(18-crown-6)][$B_3N_3Me_6(CF_2H)$] (A)

[K(18-crown-6)][$B_3N_3Me_6(CH_2Ph)$] (2.0 mmol, 10 mL 0.20 M stock in THF) was prepared at 0 °C as previously reported. To this solution was added CF_2H_2 (58 mL gas, 2.2 mmol), and the reaction mixture stirred for 15 minutes at room temperature. PhF (0.4 mmol) was added as an internal standard, and the mixture analyzed by NMR spectroscopy. A single crystal was obtained by slow diffusion of pentane into the THF solution at -30 °C. To obtain a solid, the solution was poured into 100 mL pentane and stirred at room temperature for 15 minutes. The suspension was filtered and washed with pentane to provide the title compound as a white solid in 95% yield. ^{19}F NMR: -130.1.

7.9.2 Synthesis of [K(18-crown-6)][$BNC_8H_{16}(CF_2H)$] (B)

Potassium diisopropylamide (0.967 g, 6.95 mmol) was dissolved in 10 mL THF at -80 °C and allowed to stand for one minute. BNC_8H_{16} (B-N decalin) (1.0 g, 7.23 mmol) was added to this mixture. CH_2F_2 (361 mL, 13.9 mmol) was then added, followed by a solution of 18-crown-6 (1.908 g, 7.23 mmol) in 10 mL THF. The reaction mixture was allowed to warm to room temperature, stirred for ten minutes, and then poured into 200 mL pentane. The suspended white

solid was then filtered, washed with ether (200 mL) and pentane (200 mL) and then dried under vacuo to afford 2.83 grams (78% yield) of crystalline solid. ^{19}F NMR: -122.51.

7.9.3 Synthesis of [K(18-crown-6)][BNC$_8$H$_{12}$(CF$_2$H)] (C)

This compound was prepared as noted above in 7.9.2 on a 7 mmol scale. Yield: 78%. ^{19}F NMR: -126.83.

7.9.4 Synthesis of [K(18-crown-6)][B$_3$N$_3$Me$_6$(CF$_2$Ph)]

[K(18-crown-6)][B$_3$N$_3$Me$_6$(CH$_2$Ph)] (2.0 mmol, 10 mL 0.20 M stock in THF) was prepared at 0 °C as previously reported. To this solution was added PhCF$_2$H (247 μL, 2.2 mmol), and the reaction mixture stirred for 15 minutes at room temperature. PhF (0.4 mmol) was added as an internal standard, and the mixture analyzed by NMR spectroscopy. A single crystal was obtained by slow diffusion of pentane into the THF solution at -30 °C. To obtain a solid, the solution was poured into 100 mL pentane and stirred at room temperature for 15 minutes. The suspension was filtered and washed with pentane to provide the title compound as a white solid in quantitative yield.

7.9.5 Difluoromethylarylation Reagents: In-Situ Characterization

General Protocol: Potassium diisopropylamide (41.8 mg, 0.30 mmol) was dissolved in 5 mL THF at -80 °C and allowed to stand for one minute. [Important: KDA is unstable in THF at room temperature, so must be weighed into an empty vessel, the vessel and solid KDA precooled to -80 °C, and dissolved in THF precooled to -80 °C.] Separately, hexamethylborazine (54.12 mg, 0.33 mmol), 18-crown-6 (79.2 mg, 0.30 mmol), and ArCF$_2$H (0.33 mmol) were dissolved in 10 mL THF and the solution cooled to -80 °C. The solution of KDA was then rapidly added to the solution of hexamethylborazine, 18-crown-6, and ArCF$_2$H, and the mixture allowed to stand for five minutes. 0.060 mmol PhF was then added as an internal standard, and the solutions were analyzed by NMR spectroscopy at -80 °C. [Important: the concentration of generated reagent should not exceed 20 mM during synthesis, or reduced yields are observed in many cases.]

(2-Bromophenyl)difluoromethanide hexamethylborazine adduct:

0.3 mmol scale. Yield (^{19}F NMR): 67%. ^{11}B NMR: -5.27. ^{19}F NMR: -105.48.

(3-Bromophenyl) difluoromethanide hexamethylborazine adduct:

0.3 mmol scale. Yield (^{19}F NMR): 93%. ^{11}B NMR: -5.46. ^{19}F NMR: -110.23.

(4-Bromophenyl) difluoromethanide hexamethylborazine adduct:

0.3 mmol scale. Yield (^{19}F NMR): 99%. ^{11}B NMR: -5.47, 34.90. ^{19}F NMR: -110.57.

(2-Pyridyl) difluoromethanide hexamethylborazine adduct:

0.3 mmol scale. Yield (^{19}F NMR): 83%. ^{11}B NMR: -4.32. ^{19}F NMR: -112.02.

(3-Pyridyl) difluoromethanide hexamethylborazine adduct:

0.3 mmol scale. Yield (^{19}F NMR): 91%. ^{11}B NMR: -4.41, 35.95. ^{19}F NMR: -110.05.

(4-Pyridyl) difluoromethanide hexamethylborazine adduct:

0.3 mmol scale. Yield (^{19}F NMR): 98%. ^{11}B NMR: -4.33. ^{19}F NMR: -111.55.

(1-Benzyl-1H-benzo[d]imidazol-2-yl) difluoromethanide hexamethylborazine adduct:

0.3 mmol scale. Yield (^{19}F NMR): 94%. ^{11}B NMR: -4.20, 35.33. ^{19}F NMR: -106.83.

(4-(1-methyl-1H-pyrazol-5-yl) difluoromethanide hexamethylborazine adduct:

0.3 mmol scale. Yield (^{19}F NMR): 95%. ^{11}B NMR: -4.43. ^{19}F NMR: -108.89.

7.9.6 Difluoromethylarylation of Organic Electrophiles: Initial Screening

General protocol: 0.05 mmol $ArCF_2^-$ reagent in 1.0 mL THF was combined with 0.05 mmol electrophile dissolved in 0.5 mL THF at -80 °C. Reaction progress was measured after 10 minutes at room temperature by ^{19}F-NMR spectroscopy, measuring the quantity of $R\text{-}CF_2Ar$ generated.

	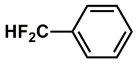	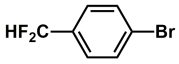	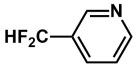	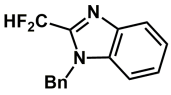	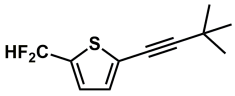
	60%	62%	91%	72%	86%
	11%	44%	7%	30%	46%
	45%	59%	75%	100%	61%
	53%	77%	12%	31%	16%
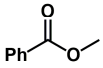	23%	50%	60%	90%	90%
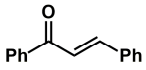	30%	77%	62%	68%	60%
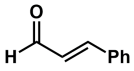	--	0%	0%	--	--
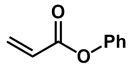	--	0%	0%	--	--
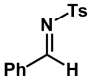	42%	82%	92%	82%	90%
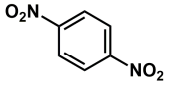	38%	27%	34%	16%	24%
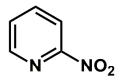	8%	18%	20%	36%	14%
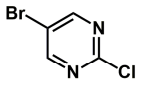	56%	72%	76%	86%	85%
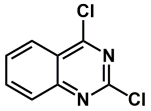	0%	--	--	--	--
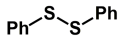	43%	88%	98%	73%	98%
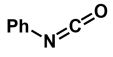	24%	32%	39%	63%	66%

Figure 7-9 Initial Screening: $ArCF_2^-$ Transfer

7.9.7 Difluoromethylarylation of Organic Electrophiles: Reactions with Ph_2CO

General protocol: The ~0.020 M, THF solution obtained from a 0.30 mmol scale preparation of $ArCF_2^-$ reagent was combined with Ph_2CO (54.6 mg, 0.30 mmol) dissolved in 3.0 mL THF at -80 °C. The reaction mixture was then allowed to warm to room temperature and allowed to stand for 10 minutes. The solution was poured into saturated NH_4Cl in H_2O (50 mL) and the organics extracted into DCM (3 x 50 mL). The organic extract was dried with $MgSO_4$, filtered, concentrated onto 3 grams of silica gel, and purified by flash chromatography as specified.

(2-(3-pyridyl)-2,2-difluoro-1-phenylethanol):

0.30 mmol substrate, 1 equiv. reagent. Chromatography conditions: 10% to 60% ethyl acetate / hexanes over 12 column volumes, 50 g SiO_2, flow rate 0.5 column volumes per minute. 55.9 mg white solid, 60%. ^{1}H-NMR ($CDCl_3$): 8.43 (ξ, 1H, (d, J_{1H-1H}=4.6)), 7.80 (ß, 1H, (t, J_{1H-1H}=7.8)), 7.75 (ρ, 1H, (d, J_{1H-1H}=7.8)), 7.57 (ε, 4H, (d, J_{1H-1H}=7.8)), 7.30 (α, 1H, (dd, J_{1H-1H}=7.5, 5.0)), 7.26 (δ, 4H, (t, J_{1H-1H}=7.7)), 7.24 (θ, 1H, s), 7.22 (ζ, 2H, (t, J_{1H-1H}=7.0)). ^{13}C-NMR: 155.03 (t, $J_{13C-19F}$=29.7), 147.87, 141.49, 137.87, 127.90 (t, $J_{13C-19F}$=2.3), 127.67, 127.47, 124.90, 121.32 (t, $J_{13C-19F}$=4.2), 116.97 (t, $J_{13C-19F}$=252.6), 81.32 (t, $J_{13C-19F}$=24.3). ^{19}F-NMR: -104.19 (2F, s). HRMS (ESI+): 294.1092 (M-OH: 294.1094).

(2-(3-pyridyl)-2,2-difluoro-1-phenylethanol):

0.30 mmol substrate, 1 equiv. reagent. Chromatography conditions: 10% to 60% ethyl acetate / hexanes over 12 column volumes, 50 g SiO_2, flow rate 0.5 column volumes per minute. 52.3 mg white solid, 56%. ^{1}H-NMR ($CDCl_3$): 8.46 (α, 1H, (d, J_{1H-1H}=4.5)), 8.29 (ξ, 1H, s), 7.43 (ε, 4H, (d, J_{1H-1H}=6.0)), 7.29 (ρ, 1H, overlap), 7.28 (δ, 4H, (t, J_{1H-1H}=6.6)), 7.26 (α, 2H, (t, J_{1H-1H}=6.6)), 7.09 (ß, 1H, (dd, J_{1H-1H}=8.4, 4.9)), 3.46 (θ, 1H, s). ^{13}C-NMR: 150.30, 148.36 (t, $J_{13C-19F}$=6.7), 141.15, 135.03 (t, $J_{13C-19F}$=6.3), 130.41 (t, $J_{13C-19F}$=26.8), 128.05, 127.98 (t, $J_{13C-19F}$=2.2), 127.90, 122.54 (t, $J_{13C-19F}$=256.5), 121.82, 80.60 (t, $J_{13C-19F}$=28.0). ^{19}F-NMR:-102.72 (2F, s). HRMS (ESI+): 312.1198 (M+H: 312.1200).

(2-(3-pyridyl)-2,2-difluoro-1-phenylethanol):

0.30 mmol substrate, 1 equiv. reagent. Chromatography conditions: 20% to 100% ethyl acetate / hexanes over 12 column volumes, 50 g SiO_2, flow rate 0.5 column volumes per minute. 87.7 mg white solid, 94%. ^{1}H-NMR ($CDCl_3$): 8.38 (α, 2H, (d, J_{1H-1H}=5.4)), 7.43 (ε, 4H, (d, J_{1H-1H}=7.0)), 7.27 (δ, 4H, overlap), 7.26 (ζ, 2H, overlap), 6.96 (ß, 2H, (d, J_{1H-1H}=5.5)), 3.81 (θ, 1H, s). ^{13}C-NMR: 148.60, 142.84 (t, $J_{13C-19F}$=27.6), 141.08, 128.04, 127.95 (t, $J_{13C-19F}$=2.2), 127.90,

122.14 (t, $J_{13C\text{-}19F}$=256.5), 121.96 (t, $J_{13C\text{-}19F}$=6.1), 80.42 (t, $J_{13C\text{-}19F}$=27.3). ^{19}F-NMR: -101.3 (2F, s). HRMS (ESI+): 312.1197 (M+H: 312.1200).

(2-(4-bromophenyl)-2,2-difluoro-1-phenylethanol):

0.30 mmol substrate, 1 equiv. reagent. Chromatography conditions: 1% to 20% ethyl acetate / hexanes over 10 column volumes, 50 g SiO_2, flow rate 0.5 column volumes per minute. 52.5 mg colorless oil, 45%. ^{1}H-NMR ($CDCl_3$): 7.61 (ε, 4H, (d, $J_{1H\text{-}1H}$=7.8)), 7.55 (α, 1H, (d, $J_{1H\text{-}1H}$=7.5)), 7.51 (σ, 1H, (t, $J_{1H\text{-}1H}$=7.8)), 7.37 (δ, 4H, (t, $J_{1H\text{-}1H}$=7.4)), 7.34 (ζ, 2H, (t, $J_{1H\text{-}1H}$=7.2)), 7.16 (τ, 1H, (d, $J_{1H\text{-}1H}$=8.1)), 7.10 (ß, 1H, (t, $J_{1H\text{-}1H}$=7.5)), 1.30 (θ, 1H, s).^{13}C-NMR: 159.47 (t, $J_{13C\text{-}19F}$=8.0), 137.60 (t, $J_{13C\text{-}19F}$=2.0), 133.68 (t, $J_{13C\text{-}19F}$=1.8), 128.25, 128.04, 127.16 (t, $J_{13C\text{-}19F}$=1.6), 126.01 (t, $J_{13C\text{-}19F}$=254.4), 124.27, 122.16 (t, $J_{13C\text{-}19F}$=1.8), 121.61 (t, $J_{13C\text{-}19F}$=26.4), 111.66, 93.06 (t, $J_{13C\text{-}19F}$=24.4). ^{19}F-NMR: -89.66 (2F, s). HRMS (ES+): 308.1026 (M-HBr: 308.1013).

(2-(4-bromophenyl)-2,2-difluoro-1-phenylethanol):

0.30 mmol substrate, 1 equiv. reagent. Chromatography conditions: 0% to 10% ethyl acetate / hexanes over 12 column volumes, 50 g SiO_2, flow rate 0.5 column volumes per minute. 84.0 mg colorless oil, 72%. ^{1}H-NMR ($CDCl_3$): 7.46 (σ, 1H, (d, $J_{1H\text{-}1H}$=7.1)), 7.45 (ε, 4H, (d, $J_{1H\text{-}1H}$=11.2)), 7.30 (δ, 4H, overlap), 7.29 (ζ, 2H, m), 7.24 (τ, 1H, s), 7.06 (ß, 1H, (t, $J_{1H\text{-}1H}$=7.9)), 6.97 (α, 1H, (d, $J_{1H\text{-}1H}$=7.8)), 2.81 (θ, 1H, s).^{13}C-NMR: 141.20, 136.38 (t, $J_{13C\text{-}19F}$=26.8), 132.62, 130.75 (t, $J_{13C\text{-}19F}$=6.7), 128.01, 128.00, 127.86, 126.08 (t, $J_{13C\text{-}19F}$=6.5), 122.51 (t, $J_{13C\text{-}19F}$=256.9), 121.13, 80.83 (t, $J_{13C\text{-}19F}$=28.4). ^{19}F-NMR: -101.79 (2F, s). HRMS (ESI+): 183.0806, 204.9470 (M-OH: 294.9934). (M-$BrPhCF_2$: 183.0810; M-Ph_2CO: 204.9464).

(2-(4-bromophenyl)-2,2-difluoro-1-phenylethanol):

0.30 mmol substrate, 1 equiv. reagent. Chromatography conditions: 0% to 18% ethyl acetate / hexanes over 12 column volumes, 50 g SiO_2, flow rate 0.5 column volumes per minute. 74.7 mg white solid, 64%. ^{1}H-NMR ($CDCl_3$): 7.44 (ε, 6H, (d, $J_{1H\text{-}1H}$=6.7)), 7.34 (α, 2H, (d, $J_{1H\text{-}1H}$=8.4)), 7.28 (δ, 4H, overlap), 7.27 (ζ, 2H, overlap), 6.94 (ß, 2H, (d, $J_{1H\text{-}1H}$=8.3)), 2.78 (θ, 1H, s)).^{13}C-NMR: 141.28, 133.41 (t, $J_{13C\text{-}19F}$=26.7), 130.25, 129.13 (t, $J_{13C\text{-}19F}$=6.5), 127.97, 127.94, 127.86, 124.19 (t, $J_{13C\text{-}19F}$=1.9), 122.99 (t, $J_{13C\text{-}19F}$=256.5), 80.77 (t, $J_{13C\text{-}19F}$=28.6). ^{19}F-NMR: -101.67 (2F, s) HRMS (ESI+): 183.0617, 204.9467 (M-$BrPhCF_2$: 183.0810; M-Ph_2CO: 204.9464).

(2-(3-pyridyl)-2,2-difluoro-1-phenylethanol):

0.30 mmol substrate, 1 equiv. reagent. Chromatography conditions: 0% to 100% ethyl acetate / hexanes over 15 column volumes, 50 g SiO_2, flow rate 0.5 column volumes per minute.

A fraction eluting at 8 CV was further purified by reverse phase chromatography: 0-100% MeCN/H_2O over 20 CV, 25g Biotage SNAP Ultra C18, 1 CV/min. 63.2 mg white solid, 54%. ^{1}H-NMR ($CDCl_3$):7.47 (ε, 4H, overlap), 7.47 (τ, 1H, overlap), 7.28 (δ, 4H, overlap), 7.27 (ζ, 2H, overlap), 7.24 (α, 2H, (d, J_{1H-1H}=8.0)), 7.15 (β, 2H, (d, J_{1H-1H}=8.0)), 6.29 (σ, 1H, (d, J_{1H-1H}=4.0)), 3.82 (ξ, 3H, s), 3.32 (θ, 1H, s). ^{13}C-NMR: 142.78, 141.50, 138.52, 134.58 (t, $J_{13C-19F}$=26.5), 131.75, 128.05 (t, $J_{13C-19F}$=2.1), 127.87, 127.81 (t, $J_{13C-19F}$=6.4), 127.78, 127.25, 123.12 (t, $J_{13C-19F}$=256.4), 106.22, 80.86 (t, $J_{13C-19F}$=28.6), 37.46. ^{19}F-NMR: -101.57 (2F, s). HRMS (ESI+): 391.1619 (M+H: 391.1622).

(2-(1-benzyl-1H-benzo[d]imidazol-2-yl)-2,2-difluoro-1-phenylethanol):

0.30 mmol substrate, 1 equiv. reagent. Chromatography conditions: 1% to 20% ethyl acetate / hexanes over 10 column volumes, 100 g SiO_2, flow rate 0.25 column volumes per minute. 122.9 mg white solid, 93%. ^{1}H-NMR ($CDCl_3$): 7.70 (θ, 1H, (dd, J_{1H-1H}=7.0, 2.3)), 7.53 (ω, 4H, (d, J_{1H-1H}=7.3)), 7.34 (ß, 2H, overlap), 7.32 (α, 1H, overlap), 7.31 (ε, 1H, overlap), 7.30 (ι, 1H, overlap), 7.27 (τ, 1H, overlap), 7.26 (δ, 2H, overlap), 7.25 (σ, 4H, overlap), 7.14 (μ, 1H, s), 7.10 (γ, 2H, (d, J_{1H-1H}=7.3)), 5.64 (ζ, 2H, s). ^{13}C-NMR: 146.14 (t, $J_{13C-19F}$=30.8), 141.39, 140.46, 135.72, 134.94, 128.88, 127.93, 127.91, 127.90, 127.72, 127.62, 126.22, 124.90, 123.44, 120.94, 117.14 (t, $J_{13C-19F}$=249.9), 110.86, 81.19 (t, $J_{13C-19F}$=23.3), 48.55 (t, $J_{13C-19F}$=4.2). ^{19}F-NMR: 96.11 (2F, s, broad). HRMS (ESI+): 441.1776 (M+H: 441.1778).

7.9.8 Difluoromethylarylation of Organic Electrophiles: Robustness Screen

Protocol A: The ~0.020 M, THF solution obtained from a 0.30 mmol scale preparation of $ArCF_2^-$ reagent was combined with electrophile (0.30 mmol) dissolved in 3.0 mL THF at -80 °C. The reaction mixture was then allowed to warm to room temperature and allowed to stand for 10 minutes. The solution was poured into saturated NH_4Cl in H_2O (50 mL) and the organics extracted into DCM (3 x 50 mL). The organic extract was dried with $MgSO_4$, filtered, concentrated onto 3 grams of silica gel, and purified by flash chromatography as specified.

Protocol B: The ~0.020 M, THF solution obtained from a 0.30 mmol scale preparation of $ArCF_2^-$ reagent was combined with pyridine-$B(C_6F_5)_3$ (0.30 mmol) dissolved in 3.0 mL THF at -80 °C. The reaction was allowed to stand for 2 hours at room temperature. DDQ (68.1 mg, 0.30 mmol) was then added, and the reaction mixture stirred for ten minutes. Tetramethylammonium fluoride (41.9 mg, 0.45 mmol) was then added, and the reaction mixture stirred for 1 hour at 60 °C. The reaction mixture was then poured into saturated $NaHCO_3$ in H_2O (50 mL) and the organics

extracted into DCM (3 x 50 mL). The organic extract was dried with $MgSO_4$, filtered, concentrated onto 3 grams of silica gel, and purified by flash chromatography as specified.

(4-Bromophenyl)difluoromethyl phenyl sulfide:

Protocol A used. Substrate: Diphenyl disulfide. 0.30 mmol substrate, 1 equiv. reagent. Chromatography conditions: 100% Hexane, 8 column volumes, 100 g SiO_2, flow rate 0.25 column volume per minute, repeated 5 times to remove Ph_2S_2. 68.4 mg white solid, 72%. ^{1}H-NMR ($CDCl_3$): 7.61 (γ, 2H, (d, J_{1H-1H}=7.2)), 7.55 (α, 2H, (d, J_{1H-1H}=8.5)), 7.44 (ε, 1H, (t, J_{1H-1H}=7.4)), 7.43 (ß, 2H, (d, J_{1H-1H}=8.3)), 7.38 (δ, 2H, (t, J_{1H-1H}=7.5)). ^{13}C-NMR: 136.41, 134.96 (t, $J_{13C-19F}$=25.6), 131.58, 130.08, 128.08, 127.23 (t, $J_{13C-19F}$=278.8), 127.12 (t, $J_{13C-19F}$=4.5), 127.02, 125.10. ^{19}F-NMR: -72.03 (s). HRMS (ES+): 313.9576 (M: 313.9576).

(3-Pyridyl)difluoromethyl phenyl sulfide:

Protocol A used. Substrate: Diphenyl disulfide. 0.30 mmol substrate, 1 equiv. reagent. Chromatography conditions: 12% to 100% ethyl acetate/hexanes over 12 column volumes, 50 g SiO_2, flow rate 0.50 column volumes per minute. 39.0 mg white solid, 55%. ^{1}H-NMR ($CDCl_3$): 8.78 (α, 1H, (d, J_{1H-1H}=1.5)), 8.68 (β, 1H, (d, J_{1H-1H}=3.9)), 7.83 (ε, 1H, (d, J_{1H-1H}=8.0)), 7.59 (δ, 2H, (d, J_{1H-1H}=7.2)), 7.44 (ω, 1H, (t, J_{1H-1H}=7.4)), 7.37 (π, 2H, (t, J_{1H-1H}=7.6)), 7.33 (γ, 1H, (dd, J_{1H-1H}=7.9, 4.9)). ^{13}C-NMR: 151.64, 146.86 (t, $J_{13C-19F}$=4.8), 136.51, 133.09 (t, $J_{13C-19F}$=4.4), 131.93 (t, $J_{13C-19F}$=25.7), 130.27, 129.16, 126.65 (t, $J_{13C-19F}$=278.6), 126.57, 122.96. ^{19}F-NMR: -76.47 (s). HRMS (ESI+): 238.0498 (M+H: 238.0496).

1-Benzyl-2-(difluoro(phenylthio)methyl)-1H-benzo[d]imidazole:

Protocol A used. Substrate: Diphenyl disulfide. 0.30 mmol substrate, 1 equiv. reagent. Chromatography conditions: 5% to 40% ethyl acetate/hexanes over 12 column volumes, 50 g SiO_2, flow rate 0.50 column volumes per minute. 76.5 mg white solid, 70%. ^{1}H-NMR ($CDCl_3$): 7.90 (α, 1H, (d, J_{1H-1H}=8.0)), 7.70 (θ, 2H, (d, J_{1H-1H}=7.2)), 7.47 (ζ, 1H, (t, J_{1H-1H}=7.4)), 7.40 (ψ, 2H, (t, J_{1H-1H}=7.6)), 7.33 (ß, 1H, (t, J_{1H-1H}=7.1)), 7.30 (γ, 1H, overlap), 7.29 (ω, 2H, overlap), 7.26 (σ, 1H, overlap), 7.24 (ε, 1H, (d, J_{1H-1H}=8.0)), 7.10 (π, 2H, (d, J_{1H-1H}=7.1)), 5.60 (δ, 2H, s). ^{13}C-NMR: 145.34 (t, $J_{13C-19F}$=29.8), 141.42, 137.00, 135.88, 135.50, 130.44, 129.19, 128.83, 127.91, 126.32, 125.31, 124.94, 123.88 (t, $J_{13C-19F}$=275), 123.39, 121.41, 111.02, 48.57. ^{19}F-NMR: -68.11 (s). HRMS (ESI+): 367.1074 (M+H: 367.1075).

2-(Difluoro(phenylthio)methyl)-5-(3,3-dimethylbut-1-yn-1-yl)thiophene:

Protocol A used. Substrate: Diphenyl disulfide. 0.30 mmol substrate, 1 equiv. reagent. Chromatography conditions: 100% hexanes over 12 column volumes, 100 g SiO_2, flow rate 1.0 column volumes per minute. 42.0 mg colorless oil, 43%. ^{1}H-NMR ($CDCl_3$): 7.63 (γ, 2H, (d, J_{1H-1H}=7.2)), 7.43 (ζ, 1H, (t, J_{1H-1H}=7.4)), 7.38 (ε, 2H, (t, J_{1H-1H}=7.5)), 7.10 (δ, 1H, (d, J_{1H-1H}=3.8)), 6.96 (ß, 1H, (d, J_{1H-1H}=3.8)), 1.31 (α, 9H, s). ^{13}C-NMR: 137.09 (t, $J_{13C-19F}$=30.3), 136.25, 130.38, 130.08, 129.07, 127.62, 127.35 (t, $J_{13C-19F}$=4.4), 127.08, 124.77 (t, $J_{13C-19F}$=276), 104.52, 71.42, 30.67, 28.30. ^{19}F-NMR: -62.80 (s). HRMS (ESI+): 303.0673 (M-F: 303.0677).

N-(2-(5-(3,3-dimethylbut-1-yn-1-yl)thiophen-2-yl)-2,2-difluoro-1-phenylethyl)-4-methylbenzenesulfonamide:

Protocol A used. Substrate: *N*-tosyl benzaldimine. 0.30 mmol substrate, 1 equiv. reagent. Chromatography conditions: 0 to 40% ethyl acetate / hexanes over 16 column volumes, 50 g SiO_2, flow rate 0.5 column volumes per minute. 99.1 mg white solid, 70%. ^{1}H-NMR ($CDCl_3$): 7.50 (θ, 2H, (d, J_{1H-1H}=8.2)), 7.20 (ε, 1H, (t, J_{1H-1H}=7.3)), 7.14 (δ, 2H, (t, J_{1H-1H}=7.6)), 7.06 (ω, 2H, (d, J_{1H-1H}=7.6)), 7.04 (ζ, 2H, (d, J_{1H-1H}=7.6)), 6.85 (β, 1H, (d, J_{1H-1H}=3.6)), 6.81 (γ, 1H, (d, J_{1H-1H}=3.7)), 5.83 (τ, 1H, (d, J_{1H-1H}=9.3)), 4.91 (σ, 1H, (q, J_{1H-19F}=11.6)), 2.33 (ψ, 3H, s), 1.29 (α, 9H, s). ^{13}C-NMR: 143.31, 137.00, 134.70 (t, $J_{13C-19F}$=30.8), 133.35, 130.41, 129.28, 128.55, 128.30, 128.29, 127.63 (t, $J_{13C-19F}$=6.0), 127.24, 126.95, 118.67 (t, $J_{13C-19F}$=249), 104.18, 71.39, 63.20 (t, $J_{13C-19F}$=29.8), 30.68, 28.26, 21.48. ^{19}F-NMR: -92.88 (m). HRMS (ESI+): 454.1300 (M-F: 454.1311).

N-(2-(1-benzyl-1H-benzo[d]imidazol-2-yl)-2,2-difluoro-1-phenylethyl)-4-methylbenzenesulfonamide:

Protocol A used. Substrate: *N*-tosyl benzaldimine. 0.30 mmol substrate, 1 equiv. reagent. Chromatography conditions: 7 to 60% ethyl acetate / hexanes over 12 column volumes, 50 g SiO_2, flow rate 0.5 column volumes per minute. 129.3 mg white solid, 83%. ^{1}H-NMR ($CDCl_3$): 7.83 (χ, 1H, (d, J_{1H-1H}=8.1)), 7.61 (θ, 2H, (d, J_{1H-1H}=8.2)), 7.49 (τ, 1H, (d, J_{1H-1H}=9.2)), 7.34 (ϖ, 2H, (overlap)), 7.33 (γ, 1H, (overlap)), 7.27 (ß, 1H, (t, J_{1H-1H}=7.5)), 7.20 (ν, 1H, (overlap)), 7.19 (ε, 1H, (overlap)), 7.16 (δ, 2H, (overlap)), 7.15 (α, 1H, (overlap)), 7.13 (ξ, 2H, (overlap)), 7.08 (ω, 2H, (d, J_{1H-1H}=8.1)), 6.85 (ζ, 2H, (d, J_{1H-1H}=6.9)), 5.31 (ρ, 2H, (q, J_{1H-1H}=16.6)), 5.29 (σ, 1H, (q, J_{1H-19F}=8.1))), 2.3 (ψ, 3H, s). ^{13}C-NMR: 144.27 (t, $J_{13C-19F}$=30.5), 143.01, 141.04, 137.76, 135.36, 135.07, 133.52 (d, $J_{13C-19F}$=4.8), 129.21, 129.04, 128.76, 128.42, 128.12, 127.79, 126.97, 126.14, 124.86, 123.41, 121.03, 116.47 (dd, $J_{13C-19F}$=249.6, 244.5), 110.90, 62.70 (t, $J_{13C-19F}$=27.7), 48.40

(d, $J_{13C\text{-}19F}$=6.7), 21.43. ^{19}F-NMR: -87.94 (dd, $J_{1H\text{-}19F,\ 19F\text{-}19F}$=9.3, 275.4)), -87.94 (dd, $J_{1H\text{-}19F,\ 19F\text{-}19F}$=9.9, 275.4)). HRMS (ESI+): 518.1703 (M+H: 518.1709).

N-(2-(4-bromophenyl)-2,2-difluoro-1-phenylethyl)-4-methylbenzenesulfonamide:

Protocol A used. Substrate: *N*-tosyl benzaldimine. 0.30 mmol substrate, 1 equiv. reagent. Chromatography conditions: 0% to 25% ethyl acetate / hexanes over 12 column volumes, 50 g SiO_2, flow rate 0.5 column volumes per minute. 89.0 mg white solid, 63%. ^{1}H-NMR ($CDCl_3$): 7.45 (θ, 2H, (d, $J_{1H\text{-}1H}$=8.1)), 7.37 (α, 2H, (d, $J_{1H\text{-}1H}$=8.3)), 7.20 (ε, 1H, (t, $J_{1H\text{-}1H}$=7.3)), 7.14 (δ, 2H, (t, $J_{1H\text{-}1H}$=7.6)), 7.06 (ω, 2H, (d, $J_{1H\text{-}1H}$=8.0)), 7.04 (ß, 2H, (d, $J_{1H\text{-}1H}$=8.4)), 6.99 (ζ, 2H, (d, $J_{1H\text{-}1H}$=7.6)), 5.58 (τ, 1H, (d, $J_{1H\text{-}19F}$=9.1)), 4.83 (σ, 1H, m), 2.34 (ψ, 3H, s). ^{13}C-NMR: 143.39, 137.02, 133.44, 132.86 (t, $J_{13C\text{-}19F}$=26.3), 131.36, 129.30, 128.56, 128.29, 128.24, 127.54 (t, $J_{13C\text{-}19F}$=6.0), 126.85, 124.82 (t, $J_{13C\text{-}19F}$=1.8), 120.22 (t, $J_{13C\text{-}19F}$=250.4), 63.06 (t, $J_{13C\text{-}19F}$=29.3), 21.50. ^{19}F-NMR: -103.81 (dd, $J_{1H\text{-}19F,\ 19F\text{-}19F}$=11.9, 247.3)). HRMS (ESI+): 294.9934 (M-NTs: 294.9905).

N-(2-(3-pyridyl)-2,2-difluoro-1-phenylethyl)-4-methylbenzenesulfonamide:

Protocol A used. Substrate: *N*-tosyl benzaldimine. 0.30 mmol substrate, 1 equiv. reagent. Chromatography conditions: 15% to 100% ethyl acetate / hexanes over 15 column volumes, 50 g SiO_2, flow rate 0.5 column volumes per minute. 40.2 mg white solid, 57%. ^{1}H-NMR ($CDCl_3$): 8.60 (ρ, 1H, (d, $J_{1H\text{-}1H}$=4.7)), 8.43 (ξ, 1H, s), 7.51 (ß, 1H, (d, $J_{1H\text{-}1H}$=7.9)), 7.48 (θ, 2H, (d, $J_{1H\text{-}1H}$=8.0)), 7.20 (α, 1H, (t, $J_{1H\text{-}1H}$=5.3)), 7.19 (ε, 1H, (t, $J_{1H\text{-}1H}$=7.4)), 7.11 (δ, 2H, (t, $J_{1H\text{-}1H}$=7.5)), 7.05 (ω, 2H, (d, $J_{1H\text{-}1H}$=7.9)), 6.97 (ζ, 2H, (d, $J_{1H\text{-}1H}$=7.6)), 6.22 (τ, 1H, (d, $J_{1H\text{-}1H}$=9.2)), 4.89 (σ, 1H, (q, $J_{1H\text{-}19F}$=12.1)), 2.31 (ψ, 3H, s). ^{13}C-NMR: 151.23, 147.19 (t, $J_{13C\text{-}19F}$=6.4), 143.38, 137.11, 133.92 (t, $J_{13C\text{-}19F}$=5.7), 133.07, 129.97, 129.33 (t, $J_{13C\text{-}19F}$=26.2), 128.69, 128.39, 128.26, 126.88, 122.89, 119.80 (t, $J_{13C\text{-}19F}$=250.6), 63.20 (t, $J_{13C\text{-}19F}$=28.8), 21.42. ^{19}F-NMR: -103.36 (dd, $J_{1H\text{-}19F,\ 19F\text{-}19F}$=11.3, 251.7)), -105.18 (dd, $J_{1H\text{-}19F,\ 19F\text{-}19F}$=12.8, 251.8)). HRMS (ESI+): 236.0883 (M+H: 236.0887).

(2-(3-pyridyl)-2,2-difluoro-1-phenylethanol):

Protocol A used. Substrate: benzaldehyde. 0.30 mmol substrate, 1 equiv. reagent. Chromatography conditions: 20% to 100% ethyl acetate / hexanes over 15 column volumes, 50 g SiO_2, flow rate 0.5 column volumes per minute. 47.7 mg white solid, 41%. ^{1}H-NMR ($CDCl_3$): 8.59 (α, 1H, (d, $J_{1H\text{-}1H}$=4.0)), 8.45 (ξ, 1H, s), 7.50 (ρ, 1H, (d, $J_{1H\text{-}1H}$=7.9)), 7.31 (ζ, 1H, (t, $J_{1H\text{-}1H}$=7.2)), 7.28 (δ, 2H, (t, $J_{1H\text{-}1H}$=7.4)), 7.24 (β, 1H, (dd, $J_{1H\text{-}1H}$=7.5, 5.2)), 7.19 (ε, 2H, (d, $J_{1H\text{-}1H}$=7.5)), 5.13 (τ, 1H, (t, $J_{1H\text{-}1H}$=9.1)), 3.41 (θ, 1H, (s, broad)). ^{13}C-NMR: 150.83, 147.61 (t, $J_{13C\text{-}}$

$_{19F}$=6.5), 135.51 (d, $J_{13C\text{-}19F}$=3.9), 134.48 (t, $J_{13C\text{-}19F}$=5.9), 129.62 (t, $J_{13C\text{-}19F}$=26.3), 128.93, 128.15, 127.60, 122.56, 120.35 (t, $J_{13C\text{-}19F}$=248.6), 76.55 (dd, $J_{13C\text{-}19F}$=31.8, 29.8). ^{19}F-NMR: -105.5 (dd, $J_{1H\text{-}19F,\ 19F\text{-}19F}$=9.2, 255.0)), -107.15 (dd, $J_{1H\text{-}19F,\ 19F\text{-}19F}$=8.6, 255.1)). HRMS (ESI+): 389.1127 (M+H: 389.1135).

(2-(4-bromophenyl)-2,2-difluoro-1-phenylethanol):

Protocol A used. Substrate: benzaldehyde. 0.30 mmol substrate, 1 equiv. reagent. Chromatography conditions: 2% to 15% ethyl acetate / hexanes over 15 column volumes, 50 g SiO_2, flow rate 0.5 column volumes per minute. 42.1 mg white solid, 45%. ^{1}H-NMR ($CDCl_3$): 7.45 (ß, 2H, (d, $J_{1H\text{-}1H}$=8.2)), 7.32 (ζ, 1H, (t, $J_{1H\text{-}1H}$=7.3)), 7.28 (δ, 2H, (t, $J_{1H\text{-}1H}$=7.4)), 7.18 (ε, 2H, (d, $J_{1H\text{-}1H}$=7.5)), 7.09 (α, 2H, (d, $J_{1H\text{-}1H}$=8.2)), 5.07 (τ, 1H, (t, $J_{1H\text{-}19F}$=31.1)), 2.54 (θ, 1H, s).^{13}C-NMR: 135.47 (t, $J_{13C\text{-}19F}$=2.1), 132.59 (t, $J_{13C\text{-}19F}$=26.5), 131.06 (t, $J_{13C\text{-}19F}$=0.3), 128.84, 128.12 (t, $J_{13C\text{-}19F}$=6.2), 128.09, 127.66, 124.56 (t, $J_{13C\text{-}19F}$=2.0), 120.86 (t, $J_{13C\text{-}19F}$=248.6), 76.60 (t, $J_{13C\text{-}19F}$=31.1). ^{19}F-NMR: -109.46 (dd, $J_{1H\text{-}19F,\ 19F\text{-}19F}$=9.7, 248.4)), -110.34 (dd, $J_{1H\text{-}19F,\ 19F\text{-}19F}$=8.9, 248.4)). HRMS (ESI+): 294.9926 (M-OH: 294.9934).

(2-(5-(3,3-dimethylbut-1-yn-1-yl)thiophen-2-yl)-2,2-difluoro-1-phenylethanol):

Protocol A used. Substrate: benzaldehyde. 0.30 mmol substrate, 1 equiv. reagent. Chromatography conditions: 2% to 15% ethyl acetate / hexanes over 15 column volumes, 50 g SiO_2, flow rate 0.5 column volumes per minute. 83.5 mg white solid, 87%. ^{1}H-NMR ($CDCl_3$): 7.33 (ζ, 1H, (m, overlap)), 7.32 (δ, 2H, (m, overlap)), 7.30 (ε, 2H, (m, overlap)), 6.93 (ß, 1H, (d, $J_{1H\text{-}1H}$=3.2)), 6.82 (γ, 1H, (d, $J_{1H\text{-}1H}$=3.8)), 5.10 (τ, 1H, (td, $J_{1H\text{-}1H,\ 1H\text{-}19F}$=3.2, 9.3)), 2.64 (θ, 1H, (d, $J_{1H\text{-}1H}$=2.7)), 1.30 (α, 9H, s).^{13}C-NMR: 135.32 (d, $J_{13C\text{-}19F}$=2.7), 134.29 (t, $J_{13C\text{-}19F}$=30.9), 130.21, 128.87, 128.14, 127.67, 127.54 (t, $J_{13C\text{-}19F}$=5.8), 127.03 (t, $J_{13C\text{-}19F}$=1.7), 119.52 (t, $J_{13C\text{-}19F}$=247.2), 103.98, 76.63 (t, $J_{13C\text{-}19F}$=31.3), 71.51, 30.70, 28.27. ^{19}F-NMR: -97.82 (dd, $J_{1H\text{-}19F,\ 19F\text{-}19F}$=8.6, 256.0)), -93.69 (dd, $J_{1H\text{-}19F,\ 19F\text{-}19F}$=9.7, 256.4)). HRMS (ESI+): 303.1020 (M-OH: 303.1019).

(2-(1-benzyl-1H-benzo[d]imidazol-2-yl)-2,2-difluoro-1-phenylethanol):

Protocol A used. Substrate: benzaldehyde. 0.30 mmol substrate, 1 equiv. reagent. Chromatography conditions: 5% to 40% ethyl acetate / hexanes over 15 column volumes, 100 g SiO_2, flow rate 0.25 column volumes per minute. 88.5 mg white solid, 81%. ^{1}H-NMR ($CDCl_3$): 7.86 (θ, 1H, (d, $J_{1H\text{-}1H}$=6.9)), 7.58 (ω, 2H, (d, $J_{1H\text{-}1H}$=7.1)), 7.41 (σ, 2H, (t, $J_{1H\text{-}1H}$=6.5)), 7.40 (δ, 1H, (t, $J_{1H\text{-}1H}$=6.4)), 7.36 (τ, 1H, (t, $J_{1H\text{-}1H}$=7.6)), 7.32 (ι, 1H, (t, $J_{1H\text{-}1H}$=7.6)), 7.29 (α, 1H, overlap), 7.28 (ß, 2H, (t, $J_{1H\text{-}1H}$=7.8)), 7.26 (ε, 1H, (d, $J_{1H\text{-}1H}$=6.9)), 7.10 (γ, 2H, (d, $J_{1H\text{-}1H}$=6.4)), 5.68 (π, 1H,

(d, $J_{1H\text{-}19F}$=20.9)), 5.56 (μ, 1H, (d, $J_{1H\text{-}1H}$=2.7)), 5.54 (ζ, 2H, s). ^{13}C-NMR: 146.24 (t, $J_{13C\text{-}19F}$=30.9), 140.82, 135.39, 135.23, 234.37, 128.84, 128.60, 128.08, 127.95, 126.47, 125.03, 123.57, 120.80, 115.91 (dd, $J_{13C\text{-}19F}$=249.7, 241.7), 111.23, 74.71 (dd, $J_{13C\text{-}19F}$=28.6, 23.0), 48.51. ^{19}F-NMR: -101.17 (d, $J_{1H\text{-}19F,\ 19F\text{-}19F}$=285.1)), -114.02 (dd, $J_{1H\text{-}19F,\ 19F\text{-}19F}$=20.9, 285.2)). HRMS (ESI+): 365.1460 (M+H: 365.1465).

1-benzyl-2-(difluoro(pyridin-4-yl)methyl)-1H-benzo[d]imidazole:

Protocol B used. Substrate: pyridine-B(C_6F_5)$_3$. 0.30 mmol substrate, 1 equiv. reagent. Chromatography conditions: 10% to 100% ethyl acetate / hexanes over 18 column volumes, 50 g SiO_2, flow rate 0.5 column volumes per minute. 62.4 mg white solid, 62%. ^{1}H-NMR ($CDCl_3$): 8.76 (σ, 2H, (d, $J_{1H\text{-}1H}$=5.3)), 7.81 (θ, 1H, (d, $J_{1H\text{-}1H}$=5.2)), 7.53 (μ, 2H, (d, $J_{1H\text{-}1H}$=5.3)), 7.31 (ι, 1H, (overlap)), 7.30 (τ, 1H, (overlap)), 7.29 (ß, 2H, (overlap)), 7.28 (α, 1H, (overlap)), 7.27 (ε, 1H, (overlap)), 7.09 (γ, 2H, (d, $J_{1H\text{-}1H}$=7.6)), 5.64 (ζ, 2H, s). ^{13}C-NMR: 150.21, 146.00 (t, $J_{13C\text{-}19F}$=32.2), 142.55 (t, $J_{13C\text{-}19F}$=27.0), 141.50, 136.03, 135.55, 128.88, 127.99, 126.27, 125.07, 123.30, 121.43, 120.55 (t, $J_{13C\text{-}19F}$=5.4), 116.39 (t, $J_{13C\text{-}19F}$=240.7), 110.91, 48.59 (t, $J_{13C\text{-}19F}$=3.4). ^{19}F-NMR: -94.18 (2F, s). HRMS (ESI+): 336.1310 (M+H: 336.1312).

(2-(1-benzyl-1H-benzo[d]imidazol-2-yl)-2,2-difluoro-1-phenylethanol):

Protocol B used. Substrate: pyridine-B(C_6F_5)$_3$. 0.30 mmol substrate, 1 equiv. reagent. Chromatography conditions: 1-10% MeOH / DCM over 18 column volumes, 50 g SiO_2, flow rate 0.5 column volumes per minute. A fraction eluting at 15 CV was then repurified using reverse-phase chromatography: 0-100% H_2O / MeCN over 12 CV, 25g Biotage SNAP Ultra C18, 1 CV/min. Finally, the product was extracted into hexanes from 5% KOH (3 x 5 mL) and evaporated. 41.0 mg colorless oil, 66%. ^{1}H-NMR ($CDCl_3$): 8.75 (σ, 2H, (d, $J_{1H\text{-}1H}$=5.2)), 8.74 (α, 1H, s), 8.72 (ß, 1H, (d, $J_{1H\text{-}1H}$=4.2)), 7.80 (ε, 1H, (d, $J_{1H\text{-}1H}$=7.9)), 7.42 (μ, 2H, (d, $J_{1H\text{-}1H}$=5.0)), 7.39 (γ, 1H, (dd, $J_{1H\text{-}1H}$=8.1, 5.0)). ^{13}C-NMR: 151.71, 150.58, 147.10 (t, $J_{13C\text{-}19F}$=5.9), 144.58 (t, $J_{13C\text{-}19F}$=29.5), 133.29 (t, $J_{13C\text{-}19F}$=5.3), 132.13 (t, $J_{13C\text{-}19F}$=28.3), 123.36, 119.90 (t, $J_{13C\text{-}19F}$=5.3), 118.49 (t, $J_{13C\text{-}19F}$=243.8). ^{19}F-NMR: -93.79 (2F, s). HRMS (ESI+): 207.0729 (M+H: 207.0734).

(2-(1-benzyl-1H-benzo[d]imidazol-2-yl)-2,2-difluoro-1-phenylethanol):

Protocol B used. Substrate: benzaldehyde. 0.30 mmol substrate, 1 equiv. reagent. Chromatography conditions: 10-100% ethyl acetate / hexanes over 18 column volumes, 50 g SiO_2, flow rate 0.5 column volumes per minute. A fraction eluting at 8 CV was then repurified using reverse-phase chromatography: 0-100% H_2O / MeCN over 12 CV, 25g Biotage SNAP Ultra C18,

1 CV/min. 32.4 mg white solid, 38%. ^{1}H-NMR ($CDCl_3$): 8.72 (σ, 2H, (d, $J_{1H\text{-}1H}$=5.0)), 7.58 (ß, 2H, (ß, $J_{1H\text{-}1H}$=8.2)), 7.39 (μ, 2H, (d, $J_{1H\text{-}1H}$=5.0)), 7.36 (α, 2H, (d, $J_{1H\text{-}1H}$=8.2)). ^{13}C-NMR: 150.43, 145.13 (t, $J_{13C\text{-}19F}$=29.8), 135.19 (t, $J_{13C\text{-}19F}$=28.2), 131.97, 127.28 (t, $J_{13C\text{-}19F}$=5.6), 125.02, 119.97 (t, $J_{13C\text{-}19F}$=5.3), 118.96 (t, $J_{13C\text{-}19F}$=243.3). ^{19}F-NMR: -94.61 (2F, s). HRMS (ESI+): 283.9883 (M+H: 283.9886).

Chapter 8. Summary and Future Outlook

8.1 Summary

In this work, frustrated Lewis pairs were used as a conceptual framework to design several tailored systems for the heterolysis or polarization of H_2, HBPin, N_2, and HCF_2R which rely on unconventional Lewis acids (borazine) and/or Lewis bases (pendent oxyanions, Fe(0) centers, Brønsted superbases). The use of a single conceptual approach to advance knowledge in such different areas of chemistry (catalyst design, bioinorganic chemistry, organic methodology) underlines the broad utility of FLP concepts in bond heterolysis.

In Chapter 2, a rationally designed hydroboration catalyst was developed that exploits metal/ligand cooperativity between a Ru(II) center and an aryloxide base appended to an auxiliary bispyridylisoindolinate ligand to heterolyze B-H and H-H bonds and transfer hydride and borinium cation equivalents to nitriles and carbonyl compounds. At the time of publication, the reported catalyst represented the state of the art in nitrile hydroboration, selectively reducing nitriles in the presence of esters and benzylic ethers. Mechanistic studies showed that pendent aryloxide bases in the secondary coordination sphere facilitate B-H and H-H bond heterolysis, and the presence of several pendent base functional groups allowed us to study the impact of modulated ligand charge on catalytic activity through the preparation of complexes in four different protonation states. We found that sequential deprotonation of the complex leads to a dramatic increase in catalytic rate (100x increase per deprotonation), demonstrating "proton-switchable" reactivity. In Chapter 3, bispyridylisoindolinate ligands and terpyridine ligands were used to explore the impact of steric bulk, bite angle, and overall ligand charge on reversible CO_2 hydrogenation. In contrast to our

observations in nitrile hydroboration, we found that more *cationic* ligand frameworks maximized activity for both CO_2 hydrogenation and formic acid dehydrogenation.

In Chapter 4, we used low-valent Fe(0) center and simple alkali and triorganoborane Lewis acids as an unconventional FLP to synergistically activate N_2. We hypothesized that hydrogen bond donors in the secondary sphere of the FeMoCo active site in nitrogenase were responsible for facile and selective protonation of N_2. Because hydrogen bond donors are normally highly acidic and can be susceptible to reductive deprotonation or X-H oxidative addition by reduced metal centers, we used redox-inert organoboranes and alkali cations as electrophilic surrogates to model the impact of hydrogen bond donors on the electronic structure and reactivity of a Fe-N_2 unit. Combining these simple Lewis acids with $Fe(depe)_2N_2$ led to immediate formation of $Fe(depe)_2N_2$-LA adducts, which exhibited elongated and weakened N-N bonds. DFT analysis showed that the Lewis acids localized electron density at the terminal nitrogen atom and anodically shifted the redox potential of the Fe(0) unit to nearly the same redox potential as nitrogenase itself. Addition of acid led to selective protonation at the terminal nitrogen atom, as predicted.

In Chapters 5 and 6, hexamethylborazine was used in concert with powerful bases to generate useful and recyclable fluoroalkylation reagents. In these reactions, weakly Lewis acidic borazines do not irreversibly react with highly nucleophilic, inexpensive bases such as KDMSO and KCH_2Ph, and reversibly capture otherwise unstable CF_3^- generated from deprotonation of the industrial waste byproduct HCF_3 to form stable, yet highly reactive, nucleophilic trifluoromethylation reagents. Using this system, we were able to economically prepare nucleophilic, electrophilic, and radical trifluoromethylation reagents and directly trifluoromethylate over sixty organic and inorganic electrophiles.

In Chapter 7, we expanded the scope of this system to difluoromethyl arenes in place of HCF_3 gas. Previous methods for the preparation of nucleophilic difluoromethylaryl anions are limited to electrolytic or photocatalytic defluorination of trifluoromethyl arenes, which is incompatible with many common functional groups that are susceptible to reductive cleavage such as aryl halides. The limited scope and difficulty of previous approaches limited the range of

available nucleophilic $ArCF_2^-$ synthons in organic chemistry to CF_2-$C_6H_5^-$ and polytrifluoromethylated heteroarenes. Using hexamethylborazine and potassium diisopropylamide as an unconventional FLP, we demonstrated the first deprotonation reactions of difluoromethylarenes and were able to generate twelve different heteroaryl and aryl difluoromethanide transfer reagents, which can be used in highly robust and conjugative coupling reactions with organic electrophiles including aldehydes, ketones, disulfides, imines, isocyanates, and Lewis-acid activated pyridine, quinoline, pyrimidine, and quinoxaline heterocycles. Many products of these reactions are first-in-class structures, and the methodology promises to introduce the difluoromethylene linkage as a novel building block in medicinal chemistry.

8.2 Future Outlook

Cooperative catalysts in which reactive Lewis acids (hydrogen bond donors, boranes, or alkali cations) are covalently appended to a metal complex with an open coordination site are highly promising, if sometimes synthetically challenging, platforms for bond reorganization in organic substrates. However, in the author's opinion, their utility has been limited by their envisioned applications, rather than their true potential. Metal-ligand cooperativity has been most extensively used to mediate E-H bond heterolysis in hydrofunctionalization reactions of polar substrates (hydroboration, hydrosilation, etc.), but these transformations are well-established, and many non-catalytic approaches are more practical. Other uses typically relate to small-molecule bond activations (O_2, N_2, etc.) or C1 transformations (conversion of CO_2 into CO).

It would be better to use the unique power of these systems in bond heterolysis and substrate engagement/positioning to facilitate reactions of greater use in expanding the scope of organic chemistry. Specifically, pendent Lewis acids could be used to facilitate difficult C-F bond oxidative additions by facilitating charge build-up at the fluorine atom. Pendent Lewis acids would be expected to significantly change the energy landscape of any reaction involving oxidative addition, but could also facilitate new transformations by reversibly abstracting anionic ligands generated during oxidative addition to reveal a previously unavailable coordination site.

Alternatively, appended Lewis bases could be used to facilitate more difficult C-H bond deprotonations to generate nucleophilic carbanionic equivalents without requiring a net oxidation state change at the metal center. By careful positioning of the appended base, C-H bond activations could be better controlled, or hydrogen bond donors in the substrate could be used as directing groups through interactions with hydrogen bond accepting Lewis bases attached to a catalyst's ancillary ligand.

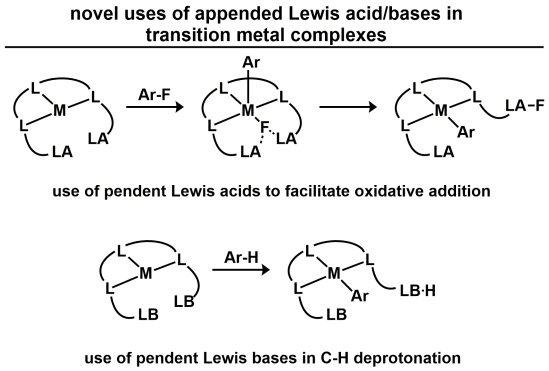

Figure 8-1 New reactions enabled by pendent functionality in metal complexes

Our discovery of superbase / weak Lewis acid systems for 1-H fluoroalkane deprotonation, fluoroalkyl anion capture, and fluoroalkyl anion transfer has many straightforward applications in nucleophilic reactions using unstable anions. Straightforward future directions in this area include the preparation of nucleophilic reagents for difluoromethylation, pentafluoroethylation, and the installation of more exotic functional groups such as perfluorocyclopropyl, perfluoroisopropyl, and perfluorotert-butyl fragments. In addition, it should be possible to easily extend our work in difluorobenzyl anion transfer to more general RCF_2^- fragments in which R could be an alkyl group, a heteroatom, an alkyne, or an alkene. These efforts may require some fine-tuning of the Lewis acid, either weakening it to accelerate RCF_2^- release or strengthening it to enhance reagent stability. Lastly, other unstable anions beyond perfluoroalkyl groups may become accessible using our FLP approach to bond activation. For example, it may be possible to generate stable nucleophilic SF_5^- transfer reagents from SF_4, a weak Lewis acid, and tetramethylammonium fluoride. This could

enable reactions such as pentafluorosulfonylation of aldehydes to generate pentafluorosulfonyl carbinols, which are currently inaccessible organic molecules due to the ease with which SF_4 itself can deoxyfluorinate alcohols.

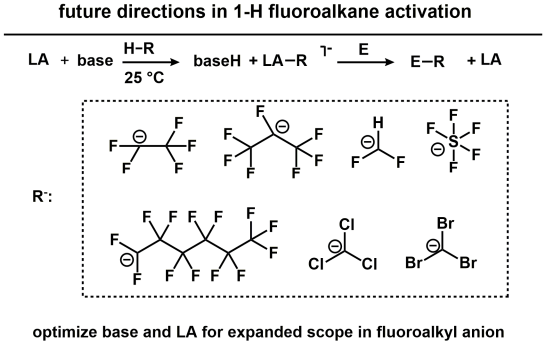

Figure 8-2 Expanded scope in stabilized fluoroalkyl anions

Polar approaches to bond formation using electrophiles and nucleophiles is fundamental to much of organic chemistry. The FLP approach to bond heterolysis enables new classes of polar bond forming reactions by enabling access to new types of nucleophiles and electrophiles, increasing chemical diversity by introducing new functional groups and selectivity types to the synthetic chemist's toolkit. As it is extended to Lewis acids and bases with increasing reactivity, new and previously unexpected types of organic transformations will be uncovered. Ongoing work in the Szymczak lab is focused on using this approach to explore new chemical space, develop approaches that increase structural diversity in organic compounds, and invent economic processes for upgrading energy-relevant biofeedstocks.

Bibliography

(1) Huheey, J. E. *Inorganic chemistry: principles of structure and reactivity*; Harper & Row: New York, 1978.

(2) Yoshikai, N.; Nakamura, E. *Chemical Reviews* **2012**, *112*, 2339.

(3) Clark, J. H. *Chemical Reviews* **1980**, *80*, 429.

(4) Stephan, D. W. *Science* **2016**, *354*, 1248.

(5) (a) Lane, C. F. *Aldrichimica Acta* **1973**, *6*, 51; (b) Staubitz, A.; Robertson, A. P. M.; Sloan, M. E.; Manners, I. *Chemical Reviews* **2010**, *110*, 4023.

(6) Stephan, D. W. *Organic & Biomolecular Chemistry* **2008**, *6*, 1535.

(7) Weicker, S. A.; Stephan, D. W. *Bulletin of the Chemical Society of Japan* **2015**, *88*, 1003.

(8) Stephan, D. W. *Journal of the American Chemical Society* **2015**, *137*, 10018.

(9) (a) Hedberg, C.; Wiley-VCH Verlag GmbH & Co. KGaA: 2008, p 109; (b) Morris, R. H.; Wiley-VCH Verlag GmbH & Co. KGaA: 2007; Vol. 1, p 45.

(10) Lapointe, D.; Fagnou, K. *Chemistry Letters* **2010**, *39*, 1118.

(11) Amatore, C.; Jutand, A.; Le Duc, G. *Chemistry – A European Journal* **2011**, *17*, 2492.

(12) Crabtree, R. H. *Chemical Reviews* **2016**, *116*, 8750.

(13) Pandey, K. K. *Coordination Chemistry Reviews* **2009**, *253*, 37.

(14) Schubert, U. In *Advances in Organometallic Chemistry*; Stone, F. G. A., West, R., Eds.; Academic Press: 1990; Vol. 30, p 151.

(15) Brookhart, M.; Green, M. L. H.; Parkin, G. *Proceedings of the National Academy of Sciences* **2007**, *104*, 6908.

(16) Hartley Frank, R. *Angewandte Chemie International Edition in English* **2003**, *11*, 596.

(17) Greene, C.; Grudzien, P. K.; York, J. T. *Journal of Organometallic Chemistry* **2017**, *851*, 122.

(18) (a) Jones, A. C. In *Homogeneous Gold Catalysis*; Slaughter, L. M., Ed.; Springer International Publishing: Cham, 2015, p 133; (b) York, J. T. *The Journal of Physical Chemistry A* **2016**, *120*, 6064.

(19) Morris, R. H. *Chemical Reviews* **2016**, *116*, 8588.

(20) Connelly, S. J.; Wiedner, E. S.; Appel, A. M. *Dalton Transactions* **2015**, *44*, 5933.

(21) Pons, V.; Conway, S. L. J.; Green, M. L. H.; Green, J. C.; Herbert, B. J.; Heinekey, D. M. *Inorganic Chemistry* **2004**, *43*, 3475.

(22) Matthews, S. L.; Pons, V.; Heinekey, D. M. *Journal of the American Chemical Society* **2005**, *127*, 850.

(23) Noyori, R.; Ohkuma, T. *Angewandte Chemie International Edition* **2001**, *40*, 40.

(24) (a) Tseng, K.-N. T.; Kampf, J. W.; Szymczak, N. K. *Organometallics* **2013**, *32*, 2046; (b) Moore, C. M.; Dahl, E. W.; Szymczak, N. K. *Current Opinion in Chemical Biology* **2015**, *25*, 9; (c) Tseng, K.-N. T.; Kampf, J. W.; Szymczak, N. K. *ACS Catalysis* **2015**, *5*, 5468; (d) Tseng, K.-N. T.; Rizzi, A. M.; Szymczak, N. K. *Journal of the American Chemical Society* **2013**, *135*, 16352; (e) Moore, C. M.; Szymczak, N. K. *Chemical Communications* **2013**, *49*, 400; (f) Dahl, E. W.; Louis-Goff, T.; Szymczak, N. K. *Chemical Communications* **2017**, *53*, 2287.

(25) Wiedner, E. S.; Chambers, M. B.; Pitman, C. L.; Bullock, R. M.; Miller, A. J. M.; Appel, A. M. *Chemical Reviews* **2016**, *116*, 8655.

(26) Tseng, K.-N. T.; Rizzi, A. M.; Szymczak, N. K. *Journal of the American Chemical Society* **2013**, *135*, 16352.

(27) Hale, L. V. A.; Malakar, T.; Tseng, K.-N. T.; Zimmerman, P. M.; Paul, A.; Szymczak, N. K. *ACS Catalysis* **2016**, *6*, 4799.

(28) Dub, P. A.; Henson, N. J.; Martin, R. L.; Gordon, J. C. *Journal of the American Chemical Society* **2014**, *136*, 3505.

(29) (a) Noyori, R.; Hashiguchi, S. *Accounts of Chemical Research* **1997**, *30*, 97; (b) Maire, P.; Büttner, T.; Breher, F.; Le Floch, P.; Grützmacher, H. *Angewandte Chemie International Edition* **2005**, *44*, 6318.

(30) Kim, Y.-E.; Oh, S.; Kim, S.; Kim, O.; Kim, J.; Han, S. W.; Lee, Y. *Journal of the American Chemical Society* **2015**, *137*, 4280.

(31) Lilio, A. M.; Reineke, M. H.; Moore, C. E.; Rheingold, A. L.; Takase, M. K.; Kubiak, C. P. *Journal of the American Chemical Society* **2015**, *137*, 8251.

(32) (a) Roberts, C. C.; Matías, D. M.; Goldfogel, M. J.; Meek, S. J. *Journal of the American Chemical Society* **2015**, *137*, 6488; (b) Burford, R. J.; Piers, W. E.; Parvez, M. *Organometallics* **2012**, *31*, 2949.

(33) (a) Onishi, N.; Xu, S.; Manaka, Y.; Suna, Y.; Wang, W.-H.; Muckerman, J. T.; Fujita, E.; Himeda, Y. *Inorganic Chemistry* **2015**, *54*, 5114; (b) Wang, W.-H.; Muckerman, J. T.; Fujita, E.; Himeda, Y. *New Journal of Chemistry* **2013**, *37*, 1860; (c) Koren-Selfridge, L.; Londino, H. N.; Vellucci, J. K.; Simmons, B. J.; Casey, C. P.; Clark, T. B. *Organometallics* **2009**, *28*, 2085; (d) Shvo, Y.; Czarkie, D.; Rahamim, Y.; Chodosh, D. F. *Journal of the American Chemical Society* **1986**, *108*, 7400; (e) Terrade, F. G.; Lutz, M.; van der Vlugt, J. I.; Reek, J. N. H. *European Journal of Inorganic Chemistry* **2014**, *2014*, 1826; (f) Gunanathan, C.; Milstein, D. *Accounts of Chemical Research* **2011**, *44*, 588.

(34) Khusnutdinova Julia, R.; Milstein, D. *Angewandte Chemie International Edition* **2015**, *54*, 12236.

(35) Lubitz, W.; Ogata, H.; Rüdiger, O.; Reijerse, E. *Chemical Reviews* **2014**, *114*, 4081.

(36) Yang, X.; Hall, M. B. *Journal of the American Chemical Society* **2009**, *131*, 10901.

(37) (a) Moore, C. M.; Quist, D. A.; Kampf, J. W.; Szymczak, N. K. *Inorganic Chemistry* **2014**, *53*, 3278; (b) Moore, C. M.; Szymczak, N. K. *Chemical Science* **2015**, *6*, 3373; (c) Moore, C. M.; Szymczak, N. K. *Chemical Communications* **2015**, *51*, 5490; (d) Moore, C. M.; Bark, B.; Szymczak, N. K. *ACS Catalysis* **2016**, *6*, 1981.

(38) (a) Fujita, K.-i.; Tanino, N.; Yamaguchi, R. *Organic Letters* **2006**, *9*, 109; (b) Hull, J. F.; Himeda, Y.; Wang, W.-H.; Hashiguchi, B.; Periana, R.; Szalda, D. J.; Muckerman, J. T.; Fujita, E. *Nat Chem* **2012**, *4*, 383.

(39) Wang, W.-H.; Muckerman, J. T.; Fujita, E.; Himeda, Y. *ACS Catalysis* **2013**, *3*, 856.

(40) Kelson, E. P.; Phengsy, P. P. *Journal of the Chemical Society, Dalton Transactions* **2000**, 4023.

(41) Nieto, I.; Livings, M. S.; Sacci, J. B.; Reuther, L. E.; Zeller, M.; Papish, E. T. *Organometallics* **2011**, *30*, 6339.

(42) Araki, K.; Kuwata, S.; Ikariya, T. *Organometallics* **2008**, *27*, 2176.

(43) Balaraman, E.; Khaskin, E.; Leitus, G.; Milstein, D. *Nature Chemistry* **2013**, *5*, 122.

(44) Werkmeister, S.; Junge, K.; Beller, M. *Organic Process Research & Development* **2014**, *18*, 289.

(45) Filonenko, G. A.; van Putten, R.; Schulpen, E. N.; Hensen, E. J. M.; Pidko, E. A. *ChemCatChem* **2014**, *6*, 1526.

(46) Geri, J. B.; Szymczak, N. K. *Journal of the American Chemical Society* **2015**, *137*, 12808.

(47) (a) Bauer, J.; Braunschweig, H.; Dewhurst, R. D. *Chemical Reviews* **2012**, *112*, 4329; (b) Karunananda, M. K.; Mankad, N. P. *ACS Catalysis* **2017**, *7*, 6110.

(48) Bauer, J.; Braunschweig, H.; Dewhurst Rian, D.; Radacki, K. *Chemistry* **?** *A European Journal* **2013**, *19*, 8797.

(49) Karunananda, M. K.; Mankad, N. P. *Organometallics* **2017**, *36*, 220.

(50) Hallnemo, G.; Olsson, T.; Ullenius, C. *Journal of Organometallic Chemistry* **1984**, *265*, c22.

(51) Horwitz, C. P.; Shriver, D. F. In *Advances in Organometallic Chemistry*; Stone, F. G. A., West, R., Eds.; Academic Press: 1984; Vol. 23, p 219.

(52) Butts, S. B.; Strauss, S. H.; Holt, E. M.; Stimson, R. E.; Alcock, N. W.; Shriver, D. F. *Journal of the American Chemical Society* **1980**, *102*, 5093.

(53) (a) Lee, Y.; Mankad, N. P.; Peters, J. C. *Nature Chemistry* **2010**, *2*, 558; (b) Chatt, J.; Dilworth, J. R.; Leigh, G. J.; Richards, R. L. *Journal of the Chemical Society D: Chemical Communications* **1970**, 955.

(54) Simonneau, A.; Turrel, R.; Vendier, L.; Etienne, M. *Angewandte Chemie International Edition* **2017**, *56*, 12268.

(55) Chatt, J.; Crabtree, R. H.; Jeffery, E. A.; Richards, R. L. *Journal of the Chemical Society, Dalton Transactions* **1973**, 1167.

(56) Yandulov, D. V.; Schrock, R. R. *Science* **2003**, *301*, 76.

(57) Connor, G. P.; Holland, P. L. *Catal. Today* **2016**, DOI: 10.1016/j.cattod.2016.08.014.

(58) (a) Zhao, M.; Wang, H.-B.; Ji, L.-N.; Mao, Z.-W. *Chemical Society Reviews* **2013**, *42*, 8360; (b) Spatzal, T.; Perez, K. A.; Einsle, O.; Howard, J. B.; Rees, D. C. *Science* **2014**, *345*, 1620.

(59) Miller, A. J. M.; Labinger, J. A.; Bercaw, J. E. *Journal of the American Chemical Society* **2008**, *130*, 11874.

(60) Tutusaus, O.; Ni, C.; Szymczak, N. K. *Journal of the American Chemical Society* **2013**, *135*, 3403.

(61) Kiernicki, J. J.; Zeller, M.; Szymczak, N. K. *Journal of the American Chemical Society* **2017**, *139*, 18194.

(62) (a) Geri, J. B.; Shanahan, J. P.; Szymczak, N. K. *Journal of the American Chemical Society* **2017**, *139*, 5952; (b) Melen Rebecca, L. *Angewandte Chemie International Edition* **2017**, *57*, 880.

(63) Brown, H. C.; Schlesinger, H. I.; Cardon, S. Z. *Journal of the American Chemical Society* **1942**, *64*, 325.

(64) Wittig, G.; Benz, E. *Chemische Berichte* **2006**, *92*, 1999.

(65) Welch, G. C.; Juan, R. R. S.; Masuda, J. D.; Stephan, D. W. *Science* **2006**, *314*, 1124.

(66) Spies, P.; Erker, G.; Kehr, G.; Bergander, K.; Frohlich, R.; Grimme, S.; Stephan, D. W. *Chemical Communications* **2007**, 5072.

(67) Hounjet Lindsay, J.; Bannwarth, C.; Garon Christian, N.; Caputo Christopher, B.; Grimme, S.; Stephan Douglas, W. *Angewandte Chemie International Edition* **2013**, *52*, 7492.

(68) Mahdi, T.; Stephan, D. W. *Journal of the American Chemical Society* **2014**, *136*, 15809.

(69) Xu, B. H.; Kehr, G.; Fröhlich, R.; Wibbeling, B.; Schirmer, B.; Grimme, S.; Erker, G. *Angewandte Chemie* **2011**, *123*, 7321.

(70) (a) Ueno, M.; Hori, C.; Suzawa, K.; Ebisawa, M.; Kondo, Y. *European Journal of Organic Chemistry* **2005**, *2005*, 1965; (b) Okusu, S.; Hirano, K.; Tokunaga, E.; Shibata, N. *ChemistryOpen* **2015**, *4*, 581.

(71) Prakash, G. K. S.; Jog, P. V.; Batamack, P. T. D.; Olah, G. A. *Science* **2012**, *338*, 1324.

(72) Geri, J. B.; Szymczak, N. K. *Journal of the American Chemical Society* **2017**, *139*, 9811.

(73) (a) Lancaster, K. In *Molecular Electronic Structures of Transition Metal Complexes I*; Mingos, D. M. P., Day, P., Dahl, J. P., Eds.; Springer Berlin Heidelberg: 2012; Vol. 142, p 119; (b) Natale, D.; Mareque-Rivas, J. C. *Chemical Communications* **2008**, 425.

(74) (a) Nair, S. K.; Christianson, D. W. *Journal of the American Chemical Society* **1991**, *113*, 9455; (b) Machczynski, M. C.; Gray, H. B.; Richards, J. H. *Journal of Inorganic Biochemistry* **2002**, *88*, 375.

(75) (a) Ringenberg, M. R.; Rauchfuss, T. B. *European Journal of Inorganic Chemistry* **2012**, *2012*, 490; (b) Ghosh, S.; Dey, A.; Sun, Y.; Scholes, C. P.; Solomon, E. I. *Journal of the American Chemical Society* **2008**, *131*, 277; (c) Dixon, N. A.; McQuarters, A. B.; Kraus, J. S.; Soffer, J. B.; Lehnert, N.; Schweitzer-Stenner, R.; Papish, E. T. *Chemical Communications* **2013**, *49*, 5571; (d) Lin, I.-J.; Gebel, E. B.; Machonkin, T. E.; Westler, W. M.; Markley, J. L. *Proceedings of the National Academy of Sciences of the United States of America* **2005**, *102*, 14581.

(76) Hashiguchi, B. G.; Young, K. J. H.; Yousufuddin, M.; Goddard, W. A.; Periana, R. A. *Journal of the American Chemical Society* **2010**, *132*, 12542.

(77) (a) Eisenstein, O.; Crabtree, R. H. *New Journal of Chemistry* **2013**, *37*, 21; (b) Clapham, S. E.; Hadzovic, A.; Morris, R. H. *Coordination Chemistry Reviews* **2004**, *248*, 2201.

(78) (a) Watanabe, M.; Murata, K.; Ikariya, T. *Journal of the American Chemical Society* **2003**, *125*, 7508; (b) Anaby, A.; Butschke, B.; Ben-David, Y.; Shimon, L. J. W.; Leitus, G.; Feller, M.; Milstein, D. *Organometallics* **2014**, *33*, 3716; (c) Bolaño, T.; Esteruelas, M. A.; Gay, M. P.; Oñate, E.; Pastor, I. M.; Yus, M. *Organometallics* **2015**, *34*, 3902.

(79) The only example of a transition metal hydrofunctionali-zation catalyst with three isolable protonation states did not include a comparison of catalytic activity between all three protonation states. See: Toda, T.; Kuwata, S.; Ikariya, T. Chemistry – A European Journal 2014, 20, 9539.

(80) Himeda, Y.; Onozawa-Komatsuzaki, N.; Sugihara, H.; Kasuga, K. *Journal of Photochemistry and Photobiology A: Chemistry* **2006**, *182*, 306.

(81) Moore, C. M.; Szymczak, N. K. *Dalton Transactions* **2012**, *41*, 7886.

(82) (a) Stahl, T.; Müther, K.; Ohki, Y.; Tatsumi, K.; Oestreich, M. *Journal of the American Chemical Society* **2013**, *135*, 10978; (b) Lu, Z.; Williams, T. J. *Chemical Communications* **2014**, *50*, 5391.

(83) For recent examples of catalytic non-cooperative polar bond hydroborations, see: (a) Arrowsmith, M.; Hadlington, T. J.; Hill, M. S.; Kociok-Köhn, G. Chem. Commun. 2012, 48, 4567;

(b) Hadlington, T. J.; Hermann, M.; Frenking, G.; Jones, C. J. Am. Chem. Soc. 2014, 136, 3028; (c) Chong, C. C.; Kinjo, R. ACS Catalysis 2015, 5, 3238;

(84) Westcott, S. A.; Baker, R. T. In *Modern Reduction Methods*; Andersson, P. G., Munslow, I. J., Eds.; Wiley-VCH Verlag GmbH & Co. KGaA: 2008, p 297.

(85) (a) Min Jung Chae, J. I. S., Duk Keun An *Bulletin of the Korean Chemical Society* **2007**, *28*, 2517; (b) Haddenham, D.; Pasumansky, L.; DeSoto, J.; Eagon, S.; Singaram, B. *The Journal of Organic Chemistry* **2009**, *74*, 1964.

(86) Although NaBH4 in carboxylic acid media provides some selectivity for nitriles, the acidic conditions are not compatible with many substrates. See: W. Gribble, G. Chemical Society Reviews 1998, 27, 395.

(87) Jeon, Y. T.; Yang, W.; Qiao, J. X.; Li, L.; Ruel, R.; Thibeault, C.; Hiebert, S.; Wang, T. C.; Wang, Y.; Liu, Y.; Clark, C. G.; Wong, H. S.; Zhu, J.; Wu, D.-R.; Sun, D.; Chen, B.-C.; Mathur, A.; Chacko, S. A.; Malley, M.; Chen, X.-Q.; Shen, H.; Huang, C. S.; Schumacher, W. A.; Bostwick, J. S.; Stewart, A. B.; Price, L. A.; Hua, J.; Li, D.; Levesque, P. C.; Seiffert, D. A.; Rehfuss, R.; Wexler, R. R.; Lam, P. Y. S. *Bioorganic & Medicinal Chemistry Letters* **2014**, *24*, 1294.

(88) (a) Eisenberger, P.; Bailey, A. M.; Crudden, C. M. *Journal of the American Chemical Society* **2012**, *134*, 17384; (b) Khalimon, A. Y.; Farha, P.; Kuzmina, L. G.; Nikonov, G. I. *Chemical Communications* **2011**, *48*, 455.

(89) Takaoka, A.; Mendiratta, A.; Peters, J. C. *Organometallics* **2009**, *28*, 3744.

(90) Steiner, T. *Angewandte Chemie International Edition* **2002**, *41*, 48.

(91) Desrosiers, P. J.; Cai, L.; Lin, Z.; Richards, R.; Halpern, J. *Journal of the American Chemical Society* **1991**, *113*, 4173.

(92) Collectively, the 1:2 integration of the hydride to OH protons as well as the absence of any other low-T1 resonances are not consistent witha Ru-(H2) intermediate under these conditions.

(93) (a) Jarek, R. L.; Flesher, R. J.; Shin, S. K. *Journal of Chemical Education* **1997**, *74*, 978; (b) Henry, R. M.; Shoemaker, R. K.; DuBois, D. L.; DuBois, M. R. *Journal of the American Chemical Society* **2006**, *128*, 3002; (c) Hulley, E. B.; Helm, M. L.; Bullock, R. M. *Chemical Science* **2014**.

(94) In many recent reports (See ref. 25), low temperature exchange rates have been scaled to 293K through speculative estimates of activation entropy, which may lead to inflated extrapolated rates. Adopting similar treatment, our rate at 293K is 1.9x 10^5 s-1 rather than 520 s-1. The large

negative entropy value in 5 may reflect of a loss of electronic entropy and symmetry in the transition state for hydride protonation.

(95) (a) Liu, T.; Wang, X.; Hoffmann, C.; DuBois, D. L.; Bullock, R. M. *Angewandte Chemie International Edition* **2014**, *53*, 5300; (b) Hulley, E. B.; Welch, K. D.; Appel, A. M.; DuBois, D. L.; Bullock, R. M. *Journal of the American Chemical Society* **2013**, *135*, 11736.

(96) Curtis, C. J.; Miedaner, A.; Ciancanelli, R.; Ellis, W. W.; Noll, B. C.; Rakowski DuBois, M.; DuBois, D. L. *Inorganic Chemistry* **2002**, *42*, 216.

(97) There is one previously reported bifurcated intramolecular hydrogen bond in a metal complex, with a long H-H contact of 1.8Å. Park, S.; Ramachandran, R.; Lough, A. J.; Morris, R. H. J. Chem. Soc., Chem. Commun. 1994, 2201.

(98) (a) Lee, D.-H.; P. Patel, B.; H. Crabtree, R.; Clot, E.; Eisenstein, O. *Chemical Communications* **1999**, 297; (b) Wessel, J.; Lee, J. C.; Peris, E.; Yap, G. P. A.; Fortin, J. B.; Ricci, J. S.; Sini, G.; Albinati, A.; Koetzle, T. F.; Eisenstein, O.; Rheingold, A. L.; Crabtree, R. H. *Angewandte Chemie International Edition in English* **1995**, *34*, 2507.

(99) Custelcean, R.; Jackson, J. E. *Chemical Reviews* **2001**, *101*, 1963.

(100) (a) Carroll, M. E.; Barton, B. E.; Rauchfuss, T. B.; Carroll, P. J. *Journal of the American Chemical Society* **2012**, *134*, 18843; (b) Huynh, M. T.; Wang, W.; Rauchfuss, T. B.; Hammes-Schiffer, S. *Inorganic Chemistry* **2014**, *53*, 10301.

(101) Filinchuk, Y.; Chernyshov, D.; Cerny, R. *The Journal of Physical Chemistry C* **2008**, *112*, 10579.

(102) Gunanathan, C.; Hölscher, M.; Pan, F.; Leitner, W. *Journal of the American Chemical Society* **2012**, *134*, 14349.

(103) Nöth, H.; Wrackmeyer, B. In *Nuclear Magnetic Resonance Spectroscopy of Boron Compounds*; Nöth, H., Wrackmeyer, B., Eds.; Springer Berlin Heidelberg: 1978; Vol. 14, p 109.

(104) Initial turnover frequency was calculated by determining the initial reaction rate through line fitting of product concentration during the first 10% of reaction progress, then dividing the reaction rate by the catalyst concentration. For a discussion of the merits of using initial TOF, see reference: Kozuch, S.; Martin, J. M. L. ACS Catalysis 2012, 2, 2787.

(105) (a) Arrowsmith, M.; Hadlington, T. J.; Hill, M. S.; Kociok-Köhn, G. *Chemical Communications* **2012**, *48*, 4567; (b) Hadlington, T. J.; Hermann, M.; Frenking, G.; Jones, C.

Journal of the American Chemical Society **2014**, *136*, 3028; (c) Oluyadi, A. A.; Ma, S.; Muhoro, C. N. *Organometallics* **2013**, *32*, 70.

(106) Under the same reaction conditions (25 °C, C6D6), H2 (100 psi) and NaBH4 did not react with benzonitrile to form benzylamine.

(107) (a) Arrowsmith, M.; Hill, M. S.; Hadlington, T.; Kociok-Köhn, G.; Weetman, C. *Organometallics* **2011**, *30*, 5556; (b) Mukherjee, D.; Ellern, A.; Sadow, A. D. *Chemical Science* **2014**, *5*, 959.

(108) (a) Widegren, J. A.; Finke, R. G. *Journal of Molecular Catalysis A: Chemical* **2003**, *198*, 317; (b) Crabtree, R. H. *Chemical Reviews* **2012**, *112*, 1536.

(109) Due to the pKa difference between 1 and 2, the same concentration of catalyst was used to compare the catalytic activity of 1 and 7.

(110) Query, I. P.; Squier, P. A.; Larson, E. M.; Isley, N. A.; Clark, T. B. *The Journal of Organic Chemistry* **2011**, *76*, 6452.

(111) We note these orders are defined at the high substrate concentrations used during the initial portion of catalysis. At low concentrations (<0.5 and <0.2 M for HBpin and PhCN, respectively), there is a positive correlation between concentration and the initial rate.

(112) 11 is proposed to engage in an equilibrium reaction prior to the turnover limiting step. Other reactions in the catalytic cycle likely also participate in equilibrium reactions with substrates, consistent with the observed saturation kinetics in HBpin and PhCN at high concentrations.

(113) While an inner sphere pathway is also possible, the high concentration of coordinatively saturated 11 in solution, in addition to the minimal activity observed for 7 in the presence of 9, suggest an outer sphere pathway may be more likely.

(114) Compounds containing heteroatom-boron bonds have gained recent interest as organic synthons. See: Hirner, J. J.; Faizi, D. J.; Blum, S. A. J. Am. Chem. Soc. 2014, 136, 4740.; Chong, E.; Blum, S. A. J. Am. Chem. Soc. 2015, 137, 10144.

(115) The diborylamine products react with benzaldehyde to form imines in the absence of a desiccant via the generation of BPin2O. For examples with PhCH2N(BCat)2, see Khalimon, A. Y.; Farha, P.; Kuzmina, L. G.; Nikonov, G. I. Chem. Commun. 2011, 48, 455.

(116) (a) Zou, X.; Zhang, Y. *Chemical Society Reviews* **2015**, *44*, 5148; (b) Blakemore, J. D.; Crabtree, R. H.; Brudvig, G. W. *Chemical Reviews* **2015**, *115*, 12974; (c) Walter, M. G.; Warren,

E. L.; McKone, J. R.; Boettcher, S. W.; Mi, Q.; Santori, E. A.; Lewis, N. S. *Chemical Reviews* **2010**, *110*, 6446.

(117) Lubitz, W.; Tumas, W. *Chemical Reviews* **2007**, *107*, 3900.

(118) (a) Wang, W.-H.; Himeda, Y.; Muckerman, J. T.; Manbeck, G. F.; Fujita, E. *Chemical Reviews* **2015**, *115*, 12936; (b) Czaun, M.; Kothandaraman, J.; Goeppert, A.; Yang, B.; Greenberg, S.; May, R. B.; Olah, G. A.; Prakash, G. K. S. *ACS Catalysis* **2016**, *6*, 7475.

(119) (a) Iguchi, M.; Himeda, Y.; Manaka, Y.; Matsuoka, K.; Kawanami, H. *ChemCatChem* **2016**, *8*, 886; (b) Rohmann, K.; Kothe, J.; Haenel, M. W.; Englert, U.; Hölscher, M.; Leitner, W. *Angewandte Chemie International Edition* **2016**, *55*, 8966.

(120) Mellmann, D.; Sponholz, P.; Junge, H.; Beller, M. *Chemical Society Reviews* **2016**, *45*, 3954.

(121) Wang, W.-H.; Feng, X.; Bao, M. In *Transformation of Carbon Dioxide to Formic Acid and Methanol*; Springer Singapore: Singapore, 2018, p 7.

(122) (a) Sordakis, K.; Tang, C.; Vogt, L. K.; Junge, H.; Dyson, P. J.; Beller, M.; Laurenczy, G. *Chemical Reviews* **2017**; (b) Bernskoetter, W. H.; Hazari, N. *Accounts of Chemical Research* **2017**, *50*, 1049.

(123) Hull, J. F.; Himeda, Y.; Wang, W.-H.; Hashiguchi, B.; Periana, R.; Szalda, D. J.; Muckerman, J. T.; Fujita, E. *Nature Chemistry* **2012**, *4*, 383.

(124) (a) Papp, G.; Csorba, J.; Laurenczy, G.; Joó, F. *Angewandte Chemie International Edition* **2011**, *50*, 10433; (b) Boddien, A.; Gärtner, F.; Federsel, C.; Sponholz, P.; Mellmann, D.; Jackstell, R.; Junge, H.; Beller, M. *Angewandte Chemie International Edition* **2011**, *50*, 6411; (c) Hsu, S.-F.; Rommel, S.; Eversfield, P.; Muller, K.; Klemm, E.; Thiel, W. R.; Plietker, B. *Angewandte Chemie International Edition* **2014**, *53*, 7074; (d) Kothandaraman, J.; Czaun, M.; Goeppert, A.; Haiges, R.; Jones, J.-P.; May, R. B.; Prakash, G. K. S.; Olah, G. A. *ChemSusChem* **2015**, *8*, 1442.

(125) Ono, T.; Qu, S.; Gimbert-Suriñach, C.; Johnson, M. A.; Marell, D. J.; Benet-Buchholz, J.; Cramer, C. J.; Llobet, A. *ACS Catalysis* **2017**, *7*, 5932.

(126) Gan, W.; Snelders, D. J. M.; Dyson, P. J.; Laurenczy, G. *ChemCatChem* **2013**, *5*, 1126.

(127) Sharma, S.; Singh, S. K.; Chandra, M.; Pandey, D. S. *Journal of Inorganic Biochemistry* **2005**, *99*, 458.

(128) (a) Crossland, J. L.; Tyler, D. R. *Coord. Chem. Rev.* **2010**, *254*, 1883; (b) Hazari, N. *Chem Soc Rev* **2010**, *39*, 4044.

(129) (a) Hoffman, B. M.; Lukoyanov, D.; Yang, Z. Y.; Dean, D. R.; Seefeldt, L. C. *Chem. Rev.* **2014**, *114*, 4041; (b) Hoffman, B. M.; Lukoyanov, D.; Dean, D. R.; Seefeldt, L. C. *Acc. Chem. Res.* **2013**, *46*, 587; (c) Howard, J. B.; Rees, D. C. *P Natl Acad Sci USA* **2006**, *103*, 17088; (d) Dance, I. *Chem Commun* **2013**, *49*, 10893.

(130) (a) Coric, I.; Mercado, B. Q.; Bill, E.; Vinyard, D. J.; Holland, P. L. *Nature* **2015**, *526*, 96; (b) Rittle, J.; Peters, J. C. *P Natl Acad Sci USA* **2013**, *110*, 15898; (c) Arashiba, K.; Miyake, Y.; Nishibayashi, Y. *Nat. Chem.* **2011**, *3*, 120.

(131) Braaksma, A.; Haaker, H.; Grande, H. J.; Veeger, C. *European Journal of Biochemistry* **1982**, *121*, 483.

(132) (a) Dance, I. *Dalton Trans.* **2012**, *41*, 7647; (b) Dos Santos, P. C.; Igarashi, R. Y.; Lee, H. I.; Hoffman, B. M.; Seefeldt, L. C.; Dean, D. R. *Acc. Chem. Res.* **2005**, *38*, 208.

(133) (a) Creutz, S. E.; Peters, J. C. *Chem. Sci.* **2017**, DOI:10.1039/C6SC04805F; (b) Bhattacharya, P.; Prokopchuk, D. E.; Mock, M. T. *Coord. Chem. Rev.* **2017**, *334*, 67.

(134) (a) Kim, C. H.; Newton, W. E.; Dean, D. R. *Biochemistry-Us* **1995**, *34*, 2798; (b) Yang, Z. Y.; Dean, D. R.; Seefeldt, L. C. *J Biol Chem* **2011**, *286*, 19417.

(135) (a) Borovik, A. S. *Acc. Chem. Res.* **2005**, *38*, 54; (b) Neu, H. M.; Baglia, R. A.; Goldberg, D. P. *Acc. Chem. Res.* **2015**, *48*, 2754.

(136) (a) Komiya, S.; Akita, M.; Yoza, A.; Kasuga, N.; Fukuoka, A.; Kai, Y. *J Chem Soc Chem Comm* **1993**, 787; (b) Perthuisot, C.; Jones, W. D. *New J Chem* **1994**, *18*, 621; (c) Hill, P. J.; Doyle, L. R.; Crawford, A. D.; Myers, W. K.; Ashley, A. E. *J. Am. Chem. Soc.* **2016**, *138*, 13521.

(137) Field, L. D.; Hazari, N.; Li, H. L. *Inorg. Chem.* **2015**, *54*, 4768.

(138) Sivaev, I. B.; Bregadze, V. I. *Coord. Chem. Rev.* **2014**, *270–271*, 75.

(139) Field, L. D.; Hazari, N.; Li, H. L.; Luck, I. J. *Magn Reson Chem* **2003**, *41*, 709.

(140) The increased Dd for the N2 unit upon functionalization is similar to, but less than, that observed for H+ (Dd 176 Mo(HIPTN3N)(N2H)) or SiR3+ (Dd 147.8-157.3 (SiPi-Pr3)Fe(N2SiR3)) see: Yandulov, D. V.; Schrock, R. R. J. Am. Chem. Soc. 2002, 124, 6252. and Lee, Y.; Mankad, N. P.; Peters, J. C. Nat. Chem. 2010, 2, 558.

(141) W-NN-BR2 units were reported see: Ishino, H.; Ishii, Y.; Hidai, M. Chem. Lett. 1998, 677.

(142) Similarly bent angles in an M-NN(R) unit have been previously reported for cationic R groups. See references 12 and 3b.

(143) McWilliams, S. F.; Rodgers, K. R.; Lukat-Rodgers, G.; Mercado, B. Q.; Grubel, K.; Holland, P. L. *Inorg. Chem.* **2016**, *55*, 2960.

(144) The acceptor number was derived from the shift of the 31P resonance of O=P(Et)3 upon coordination of the Lewis acid. See Beckett, M. A.; Strickland, G. C.; Holland, J. R.; Varma, K. S.; Polymer, 1996, 37, 4629-4631.

(145) Weaker boron Lewis acids, such as BPh3, do not coordinate even through the Lewis acidity is within the observed range. This is presumably due to the larger reorganization energy required of boron, vs. alkali metal, Lewis acids.

(146) However, 2 rapidly decomposes in the presence of most non-coordinating electrolyte anions (PF6, SbF6, ClO4, BF4, CB11H12). A variable-temperature NMR experiment showed that mixtures of 2 and the highly robust electrolyte N(Bu)4+ B(3,5-(CF3)2-C6H3)4- (TBA BArF24) in fluorobenzene are unstable at temperatures above -10 °C, but that this decomposition is prevented at -45 °C.

(147) This is similar to the reported value of the Fe(0/I) couple in THF (0.1 M [nBu4N][OTf], -1.95 V); see reference 8c.

(148) LA interactions to facilitate hydride insertion into Ru-N2 compounds has been computationally investigated. See Holscher, M.; Leitner, W. Eur. J. Inorg. Chem. 2014, 35, 6126-6133.

(149) (a) Bancroft, G. M.; Mays, M. J.; Prater, B. E. *J Chem Soc Chem Comm* **1969**, 585; (b) Buys, I. E.; Field, L. D.; Hambley, T. W.; Mcqueen, A. E. D. *Acta Crystallogr C* **1993**, *49*, 1056.

(150) Doyle, L. R.; Hill, P. J.; Wildgoose, G. G.; Ashley, A. E. *Dalton Trans.* **2016**, *45*, 7550.

(151) (a) Rittle, J.; Peters, J. C. *J. Am. Chem. Soc.* **2017**, DOI: 10.1021/jacs.6b12861; (b) Rittle, J.; Peters, J. C. *J. Am. Chem. Soc.* **2016**, *138*, 4243.

(152) As suggested by irreversible electrochemical oxidation of 2, catalytic reduction of N2 to NH3 or N2H4 by 1 was not enhanced in the presence of B(C6F5)3.

(153) (a) O'Donoghue, M. B.; Zanetti, N. C.; Davis, W. M.; Schrock, R. R. *J. Am. Chem. Soc.* **1997**, *119*, 2753; (b) Field, L. D.; Guest, R. W.; Turner, P. *Inorg. Chem.* **2010**, *49*, 9086; (c) Zhang, Q. F.; Chim, J. L. C.; Lai, W.; Wong, W. T.; Leung, W. H. *Inorg. Chem.* **2001**, *40*, 2470.

(154) (a) Betley, T. A.; Peters, J. C. *Journal of the American Chemical Society* **2004**, *126*, 6252; (b) McSkimming, A.; Harman, W. H. *J. Am. Chem. Soc.* **2015**, *137*, 8940; (c) Yu, R. P.; Darmon, J. M.; Hoyt, J. M.; Margulieux, G. W.; Turner, Z. R.; Chirik, P. J. *Acs Catalysis* **2012**, *2*, 1760; (d) Smith, J. M.; Lachicotte, R. J.; Pittard, K. A.; Cundari, T. R.; Lukat-Rodgers, G.; Rodgers, K. R.; Holland, P. L. *J. Am. Chem. Soc.* **2001**, *123*, 9222; (e) McWilliams, S. F.; Holland, P. L. *Acc. Chem. Res.* **2015**, *48*, 2059.

(155) D'Alessandro, D. M.; Keene, F. R. *Chemical Society Reviews* **2006**, *35*, 424.

(156) Masami, I.; Hironobu, A.; Hideno, F.; Nobumasa, K.; Yoshihiko, M.-o. *Bulletin of the Chemical Society of Japan* **1996**, *69*, 1937.

(157) Hirano, M.; Akita, M.; Morikita, T.; Kubo, H.; Fukuoka, A.; Komiya, S. *Journal of the Chemical Society, Dalton Transactions* **1997**, 3453.

(158) Yakelis, N. A.; Bergman, R. G. *Organometallics* **2005**, *24*, 3579.

(159) Mon, I.; Jose, D. A.; Vidal-Ferran, A. *Chemistry – A European Journal* **2013**, *19*, 2720.

(160) Brookhart, M.; Grant, B.; Volpe, A. F. *Organometallics* **1992**, *11*, 3920.

(161) Nicasio, J. A.; Steinberg, S.; Inés, B.; Alcarazo, M. *Chemistry – A European Journal* **2013**, *19*, 11016.

(162) Naumann, D.; Butler, H.; Gnann, R. *Zeitschrift für anorganische und allgemeine Chemie* **1992**, *618*, 74.

(163) Ono, T.; Ohta, M.; Sada, K. *ACS Macro Letters* **2012**, *1*, 1270.

(164) Dolomanov, O. V.; Bourhis, L. J.; Gildea, R. J.; Howard, J. A. K.; Puschmann, H. *Journal of Applied Crystallography* **2009**, *42*, 339.

(165) Sheldrick, G. *Acta Crystallographica Section A* **2008**, *64*, 112.

(166) Gaussian 09, Revision A.02, M. J. Frisch, G. W. Trucks, H. B. Schlegel, G. E. Scuseria, M. A. Robb, J. R. Cheeseman, G. Scalmani, V. Barone, G. A. Petersson, H. Nakatsuji, X. Li, M. Caricato, A. Marenich, J. Bloino, B. G. Janesko, R. Gomperts, B. Mennucci, H. P. Hratchian, J. V. Ortiz, A. F. Izmaylov, J. L. Sonnenberg, D. Williams-Young, F. Ding, F. Lipparini, F. Egidi, J. Goings, B. Peng, A. Petrone, T. Henderson, D. Ranasinghe, V. G. Zakrzewski, J. Gao, N. Rega, G. Zheng, W. Liang, M. Hada, M. Ehara, K. Toyota, R. Fukuda, J. Hasegawa, M. Ishida, T. Nakajima, Y. Honda, O. Kitao, H. Nakai, T. Vreven, K. Throssell, J. A. Montgomery, Jr., J. E. Peralta, F. Ogliaro, M. Bearpark, J. J. Heyd, E. Brothers, K. N. Kudin, V. N. Staroverov, T. Keith,

R. Kobayashi, J. Normand, K. Raghavachari, A. Rendell, J. C. Burant, S. S. Iyengar, J. Tomasi, M. Cossi, J. M. Millam, M. Klene, C. Adamo, R. Cammi, J. W. Ochterski, R. L. Martin, K. Morokuma, O. Farkas, J. B. Foresman, and D. J. Fox, Gaussian, Inc., Wallingford CT, 2016.

(167) Stephens, P. J.; Devlin, F. J.; Chabalowski, C. F.; Frisch, M. J. *The Journal of Physical Chemistry* **1994**, *98*, 11623.

(168) Scalmani, G.; Frisch, M. J. *The Journal of Chemical Physics* **2010**, *132*, 114110.

(169) Rassolov, V. A.; Ratner, M. A.; Pople, J. A.; Redfern, P. C.; Curtiss, L. A. *Journal of Computational Chemistry* **2001**, *22*, 976.

(170) NBO Version 3.1, E. D. Glendening, A. E. Reed, J. E. Carpenter, and F. Weinhold.

(171) S. I. Gorelsky, AOMix: Program for Molecular Orbital Analysis, http://www.sg-chem.net/, version 6.46, 2015; S. I. Gorelsky, A. B. P. Lever, J. Organomet. Chem. 2001, 635, 187-196.

(172) Wishart, D. S.; Knox, C.; Guo, A. C.; Shrivastava, S.; Hassanali, M.; Stothard, P.; Chang, Z.; Woolsey, J. *Nucleic Acids Research* **2006**, *34*, D668.

(173) (a) Grushin, V. V. *Chimica Oggi-Chemistry Today* **2014**, *32*, 81; (b) Henne, A. L. *Journal of the American Chemical Society* **1937**, *59*, 1200.

(174) McCulloch, A.; Lindley, A. A. *Atmospheric Environment* **2007**, *41*, 1560.

(175) Olsbye, U. *Angewandte Chemie International Edition* **2016**, *55*, 7294.

(176) Amphlett, J. C.; Coomber, J. W.; Whittle, E. *The Journal of Physical Chemistry* **1966**, *70*, 593.

(177) Symons, E. A.; Clermont, M. J. *Journal of the American Chemical Society* **1981**, *103*, 3127.

(178) (a) Russell, J.; Roques, N. *Tetrahedron* **1998**, *54*, 13771; (b) Zanardi, A.; Novikov, M. A.; Martin, E.; Benet-Buchholz, J.; Grushin, V. V. *Journal of the American Chemical Society* **2011**, *133*, 20901.

(179) Grignard, V. *Compt. rend* **1900**, *130*, 1322.

(180) (a) Lishchynskyi, A.; Miloserdov, F. M.; Martin, E.; Benet-Buchholz, J.; Escudero-Adán, E. C.; Konovalov, A. I.; Grushin, V. V. *Angewandte Chemie International Edition* **2015**, *54*, 15289; (b) Prakash, G. K. S.; Wang, F.; Zhang, Z.; Haiges, R.; Rahm, M.; Christe, K. O.; Mathew, T.; Olah, G. A. *Angewandte Chemie International Edition* **2014**, *53*, 11575.

(181) (a) Liu, X.; Xu, C.; Wang, M.; Liu, Q. *Chemical Reviews* **2015**, *115*, 683; (b) Langlois, B. R.; Billard, T.; Roussel, S. *Journal of Fluorine Chemistry* **2005**, *126*, 173.

(182) (a) Erős, G.; Nagy, K.; Mehdi, H.; Pápai, I.; Nagy, P.; Király, P.; Tárkányi, G.; Soós, T. *Chemistry – A European Journal* **2012**, *18*, 574; (b) Stephan, D. W.; Erker, G. *Angewandte Chemie International Edition* **2015**, *54*, 6400.

(183) Scott, D. J.; Fuchter, M. J.; Ashley, A. E. *Journal of the American Chemical Society* **2014**, *136*, 15813.

(184) Kawai, H.; Yuan, Z.; Tokunaga, E.; Shibata, N. *Organic & Biomolecular Chemistry* **2013**, *11*, 1446.

(185) Brown, C. A. *The Journal of Organic Chemistry* **1974**, *39*, 3913.

(186) Folléas, B.; Marek, I.; Normant, J.-F.; Jalmes, L. S. *Tetrahedron Letters* **1998**, *39*, 2973.

(187) Sivaev, I. B.; Bregadze, V. I. *Coordination Chemistry Reviews* **2014**, *270–271*, 75.

(188) Zhao, Y.; Truhlar, D. G. *Theoretical Chemistry Accounts* **2008**, *120*, 215.

(189) See SI for details

(190) Banfi, L.; Narisano, E.; Riva, R.; Matteson, D. S. In *Encyclopedia of Reagents for Organic Synthesis*; John Wiley & Sons, Ltd: 2001.

(191) Knauber, T.; Arikan, F.; Röschenthaler, G.-V.; Gooßen, L. J. *Chemistry – A European Journal* **2011**, *17*, 2689.

(192) Kennedy, J. D. In *Multinuclear NMR*; Springer: 1987, p 221.

(193) Jackman, L. *Dynamic nuclear magnetic resonance spectroscopy*; Elsevier, 2012.

(194) Lochmann, L.; Trekoval, J. *Journal of Organometallic Chemistry* **1987**, *326*, 1.

(195) 18-crown-6 was added to improve the stability of 1 in THF, due to the previously observed sensitivity of CF3- species towards alkali metal cations. Prakash, G. K. S.; Jog, P. V.; Batamack, P. T. D.; Olah, G. A. Science 2012, 338, 1324.

(196) Cambridge crystallographic database search (CSD version 5.38, updated November 2016)

(197) Levin, V. V.; Dilman, A. D.; Belyakov, P. A.; Struchkova, M. I.; Tartakovsky, V. A. T*etrahedron Letters* 2**011,** 5*2,* 281.

(198) Trost, B. M. A*ngewandte Chemie International Edition in English* 1**995,** 3*4,* 259.

(199) Burton, D. J.; Qui, W.; Sánchez-Roselló, M.; del Pozo Losada, C.; Luis Aceña, J. In E*ncyclopedia of Reagents for Organic Synthesis;* John Wiley & Sons, Ltd: 2001.

(200) Krishnamurti, R.; Bellew, D. R.; Prakash, G. K. S. T*he Journal of Organic Chemistry* 1**991,** 5*6,* 984.

(201) Zhang, C. A*dvanced Synthesis & Catalysis* 2**014,** 3*56,* 2895.

(202) Charpentier, J., Natalja Früh, and Antonio Togni. C*hemical Reviews* 2**014,** 1*15,* 650.

(203) (a) Bonham, J.; Drago, R. S.; Spielvogel, B. F.; Phillips, J. A.; Payet, C. R. In I*norganic Syntheses;* John Wiley & Sons, Inc.: 2007, p 8; (b) Smalley, J. H.; Stafiej, S. F. J*ournal of the American Chemical Society* 1**959,** 8*1,* 582.

(204) Bradley, M. J.; Ryschkewitsch, G. E.; Sisler, H. H. J*ournal of the American Chemical Society* 1**959,** 8*1,* 2635.

(205) Haworth, D. T.; Kiel, G. Y. L.; Todd, L. J.; Baize, M. W. In I*norganic Syntheses;* John Wiley & Sons, Inc.: 2007, p 57.

(206) Matoušek, V.; Pietrasiak, E.; Schwenk, R.; Togni, A. T*he Journal of Organic Chemistry* 2**013,** 7*8,* 6763.

(207) Bailey, P. J.; Coxall, R. A.; Dick, C. M.; Fabre, S.; Henderson, L. C.; Herber, C.; Liddle, S. T.; Loroño-González, D.; Parkin, A.; Parsons, S. C*hemistry – A European Journal* 2**003,** 9*,* 4820.

(208) Corey, E. J.; Chaykovsky, M. J*ournal of the American Chemical Society* 1**962,** 8*4,* 866.

(209) Fulmer, G. R.; Miller, A. J. M.; Sherden, N. H.; Gottlieb, H. E.; Nudelman, A.; Stoltz, B. M.; Bercaw, J. E.; Goldberg, K. I. O*rganometallics* 2**010,** 2*9,* 2176.

(210) Frisch, M. J.; Trucks, G. W.; Schlegel, H. B.; Scuseria, G. E.; Robb, M. A.; Cheeseman, J. R.; Scalmani, G.; Barone, V.; Mennucci, B.; Petersson, G. A.; Nakatsuji, H.; Caricato, M.; Li, X.; Hratchian, H. P.; Izmaylov, A. F.; Bloino, J.; Zheng, G.; Sonnenberg, J. L.; Hada, M.; Ehara, M.; Toyota, K.; Fukuda, R.; Hasegawa, J.; Ishida, M.; Nakajima, T.; Honda, Y.; Kitao, O.; Nakai, H.; Vreven, T.; Montgomery Jr., J. A.; Peralta, J. E.; Ogliaro, F.; Bearpark, M. J.; Heyd, J.; Brothers, E. N.; Kudin, K. N.; Staroverov, V. N.; Kobayashi, R.; Normand, J.; Raghavachari, K.; Rendell, A. P.; Burant, J. C.; Iyengar, S. S.; Tomasi, J.; Cossi, M.; Rega, N.; Millam, N. J.; Klene, M.; Knox, J. E.; Cross, J. B.; Bakken, V.; Adamo, C.; Jaramillo, J.; Gomperts, R.; Stratmann, R. E.; Yazyev, O.; Austin, A. J.; Cammi, R.; Pomelli, C.; Ochterski, J. W.; Martin, R. L.; Morokuma,

K.; Zakrzewski, V. G.; Voth, G. A.; Salvador, P.; Dannenberg, J. J.; Dapprich, S.; Daniels, A. D.; Farkas, Ö.; Foresman, J. B.; Ortiz, J. V.; Cioslowski, J.; Fox, D. J.; Gaussian, Inc.: Wallingford, CT, USA, 2009.

(211) McLean, A. D.; Chandler, G. S. T*he Journal of Chemical Physics* 1**980,** 7*2,* 5639.

(212) (a) Elmar-Manfred, H.; Hans, N.; Google Patents: 1967; (b) Cragg, R. H.; Weston, A. F. J*ournal of the Chemical Society, Dalton Transactions* 1**975,** 1761.

(213) Eisenberger, P.; Gischig, S.; Togni, A. C*hemistry – A European Journal* 2**006,** 1*2,* 2579.

(214) Newsom, H. C.; English, W. D.; McCloskey, A. L.; Woods, W. G. J*ournal of the American Chemical Society* 1**961,** 8*3,* 4134.

(215) Atkinson, I. B.; Blundell, D. C.; Clapp, D. B. J*ournal of Inorganic and Nuclear Chemistry* 1**972,** 3*4,* 3037.

(216) Butcher, I. M.; Gerrard, W. J*ournal of Inorganic and Nuclear Chemistry* 1**965,** 2*7,* 823.

(217) Niedenzu, K.; Harrelson, D. H.; Dawson, J. W. C*hemische Berichte* 1**961,** 9*4,* 671.

(218) Stepanenko, V.; Ortiz-Marciales, M.; Barnes, C. E.; Garcia, C. T*etrahedron Letters* 2**006,** 4*7,* 7603.

(219) Brotherton, R. J.; Steinberg, H. T*he Journal of Organic Chemistry* 1**961,** 2*6,* 4632.

(220) Robert J. Brotherton, G. W. W., Howard Steinberg; Corporation, U. S. B. C., Ed.; United States Borax & Chemical Corporation: United States, 1962.

(221) Purser, S.; Moore, P. R.; Swallow, S.; Gouverneur, V. C*hemical Society Reviews* 2**008,** 3*7,* 320.

(222) Billard, T.; Bruns, S.; Langlois, B. R. O*rganic Letters* 2**000,** 2*,* 2101.

(223) (a) Prakash, G. K. S.; Krishnamurti, R.; Olah, G. A. J*ournal of the American Chemical Society* 1**989,** 1*11,* 393; (b) Maggiarosa, N.; Tyrra, W.; Naumann, D.; Kirij, N. V.; Yagupolskii, Y. L. A*ngewandte Chemie International Edition* 1**999,** 3*8,* 2252; (c) Cho, E. J.; Senecal, T. D.; Kinzel, T.; Zhang, Y.; Watson, D. A.; Buchwald, S. L. S*cience* 2**010,** 3*28,* 1679.

(224) Kolomeitsev, A. A.; Kadyrov, A. A.; Szczepkowska-Sztolcman, J.; Milewska, M.; Koroniak, H.; Bissky, G.; Barten, J. A.; Röschenthaler, G.-V. T*etrahedron Letters* 2**003,** 4*4,* 8273.

(225) (a) Bardin Vadim, V.; Frohn, H.-J. In M*ain Group Metal Chemistry* 2002; Vol. 25, p 589; (b) Sprenger, J. A. P.; Schäfer, M.; Ignatiev, N.; Finze, M. J*ournal of Fluorine Chemistry* 2**015,** 1*74,* 30.

(226) Folléas, B. t.; Marek, I.; Normant, J.-F.; Saint-Jalmes, L. T*etrahedron* 2**000,** 5*6,* 275.

(227) Tomashenko, O. A.; Grushin, V. V. C*hemical Reviews* 2**011,** 1*11,* 4475.

(228) Aikawa, K.; Toya, W.; Nakamura, Y.; Mikami, K. O*rganic Letters* 2**015,** 1*7,* 4996.

(229) Ye, Y.; Lee, S. H.; Sanford, M. S. O*rganic Letters* 2**011,** 1*3,* 5464.

(230) Wiemers, D. M.; Burton, D. J. J*ournal of the American Chemical Society* 1**986,** 1*08,* 832.

(231) Levin, M. D.; Chen, T. Q.; Neubig, M. E.; Hong, C. M.; Theulier, C. A.; Kobylianskii, I. J.; Janabi, M.; O'Neil, J. P.; Toste, F. D. S*cience* 2**017,** 3*56,* 1272.

(232) Bakhmutov, V. I.; Bozoglian, F.; Gómez, K.; González, G.; Grushin, V. V.; Macgregor, S. A.; Martin, E.; Miloserdov, F. M.; Novikov, M. A.; Panetier, J. A.; Romashov, L. V. O*rganometallics* 2**012,** 3*1,* 1315.

(233) Kepp, K. P. I*norganic Chemistry* 2**016,** 5*5,* 9461.

(234) Eujen, R.; Jahn, N.; Thurmann, U. J*ournal of Organometallic Chemistry* 1**994,** 4*65,* 153.

(235) Eujen, R.; Patorra, A. J*ournal of Organometallic Chemistry* 1**992,** 4*38,* 57.

(236) Panne, P.; Naumann, D.; Hoge, B. J*ournal of Fluorine Chemistry* 2**001,** 1*12,* 283.

(237) Naumann, D.; Tyrra, W. J*ournal of Organometallic Chemistry* 1**987,** 3*34,* 323.

(238) Xu, X.-H.; Matsuzaki, K.; Shibata, N. C*hemical Reviews* 2**015,** 1*15,* 731.

(239) Tyrra, W.; Naumann, D.; Hoge, B.; Yagupolskii, Y. L. J*ournal of Fluorine Chemistry* 2**003,** 1*19,* 101.

(240) Jean-Pierre Bégué, D. B.-D. B*ioorganic and Medicinal Chemistry of Fluorine;* Wiley, 2008.

(241) 1a was activated with F- in the presence of substrate, 1b was used exactly as 2, and 1c was prepared and combined with substrates at -40 °C, then warmed to 25 °C and allowed to react for 10 minutes (See SI).

(242) Jacobson, O.; Kiesewetter, D. O.; Chen, X. B*ioconjugate Chemistry* 2**015,** 2*6,* 1.

(243) van der Born, D.; Herscheid, J. D. M.; Orru, R. V. A.; Vugts, D. J. C*hemical Communications* 2**013,** 4*9,* 4018.

(244) (a) Vladislav, M. V. R*ussian Chemical Reviews* 2**003,** 7*2,* 681; (b) Studer, A. A*ngewandte Chemie International Edition* 2**012,** 5*1,* 8950.

(245) Aromatic substitution of -NO2 and -F have been described, but the publications lack experimental details or product characterization. a) Bardin, V. V.; Kolomeitsev, A. A.; Furin, G. G.; Yagupol'skii, Y. L. Bulletin of the Academy of Sciences of the USSR, Division of chemical science 1990, 39, 1539. b) Bellew, D. Studies in organofluorine chemistry. Ph.D, University of Southern California, 1991.

(246) (a) Saczewski, J.; Paluchowska, A.; Klenc, J.; Raux, E.; Barnes, S.; Sullivan, S.; Duszynska, B.; Bojarski, A. J.; Strekowski, L. J*ournal of Heterocyclic Chemistry* 2**009,** 4*6,* 1259; (b) Yamanaka, H.; Ohba, S.; Konno, S. H*eterocycles* 1**987,** 2*6,* 2853.

(247) Nagib, D. A.; MacMillan, D. W. C. N*ature* 2**011,** 4*80,* 224.

(248) Nagase, M.; Kuninobu, Y.; Kanai, M. J*ournal of the American Chemical Society* 2**016,** 1*38,* 6103.

(249) Nishida, T.; Ida, H.; Kuninobu, Y.; Kanai, M. N*at Commun* 2**014,** 5.

(250) A. R. Katritzky, N. J. L. H*eterocycles* 1**992,** 3*3.*

(251) Wang, Y.; Yin, H.; Tang, X.; Wu, Y.; Meng, Q.; Gao, Z. T*he Journal of Organic Chemistry* 2**016,** 8*1,* 7042.

(252) 2 is comparable or better than 1a/activator for the described reactions with arenes (see SI).We note that reactions using 1a require screening various base additive to ensure compatibility and solubility: with 2, these are not required.

(253) Geri, J. B. S., N. K. J*ournal of the American Chemical Society* 2**017**

(254) Ball, N. D.; Gary, J. B.; Ye, Y.; Sanford, M. S. J*ournal of the American Chemical Society* 2**011,** 1*33,* 7577.

(255) Li, X.; Zhao, J.; Zhang, L.; Hu, M.; Wang, L.; Hu, J. O*rganic Letters* 2**015,** 1*7,* 298.

(256) (a) Klabunde, K. J. J*ournal of Fluorine Chemistry* 1**976,** 7*,* 95; (b) Naumann, D.; Wessel, W.; Hahn, J.; Tyrra, W. J*ournal of Organometallic Chemistry* 1**997,** 5*47,* 79; (c) Guerra, M. A.; Bierschenk, T. R.; Lagow, R. J. J*ournal of Organometallic Chemistry* 1**986,** 3*07,* C58.

(257) Ivashkin, P.; Lemonnier, G.; Cousin, J.; Grégoire, V.; Labar, D.; Jubault, P.; Pannecoucke, X. C*hemistry – A European Journal* 2**014,** *20,* 9514.

(258) Blaya, M.; Bautista, D.; Gil-Rubio, J.; Vicente, J. O*rganometallics* 2**014,** *33,* 6358.

(259) Aikawa, K.; Nakamura, Y.; Yokota, Y.; Toya, W.; Mikami, K. C*hemistry – A European Journal* 2**015,** *21,* 96.

(260) Betterley, N. M.; Surawatanawong, P.; Prabpai, S.; Kongsaeree, P.; Kuhakarn, C.; Pohmakotr, M.; Reutrakul, V. O*rganic Letters* 2**013,** *15,* 5666.

(261) Pooput, C.; Dolbier, W. R.; Médebielle, M. T*he Journal of Organic Chemistry* 2**006,** *71,* 3564.

(262) Ayanbadejo, F. A. M. S*pectrochimica Acta Part A: Molecular Spectroscopy* 1**969,** *25,* 1009.

(263) Wessig, P.; Schwarz, J. M*onatshefte für Chemie / Chemical Monthly* 1**995,** *126,* 99.

(264) Drugbank (http://www.drugbank.ca/). Accessed 1/30/2018.

(265) Zhang, X.-M.; Bordwell, F. G. J*ournal of the American Chemical Society* 1**992,** *114,* 9787.

(266) Maryanoff, B. E.; McComsey, D. F.; Costanzo, M. J.; Yabut, S. C.; Lu, T.; Player, M. R.; Giardino, E. C.; Damiano, B. P. C*hemical Biology & Drug Design* 2**006,** *68,* 29.

(267) Lee, L.; Kreutter, K. D.; Pan, W.; Crysler, C.; Spurlino, J.; Player, M. R.; Tomczuk, B.; Lu, T. B*ioorganic & Medicinal Chemistry Letters* 2**007,** *17,* 6266.

(268) (a) Fawcett, F. S.; Coffman, D. D.; Tullock, C. W. J*ournal of the American Chemical Society* 1**962,** *84,* 4275; (b) Zeng, X.; Wei, X.; Song, J. J.; Sarvestani, M.; Fandrick, D. R.; Qu, B.; Rodríguez, S.; Sieber, J. D.; Desrosiers, J.-N.; Yee, N. K.; Roschangar, F.; Senanayake, C. H. A*sian Journal of Organic Chemistry* 2**015,** *4,* 1262; (c) Hagooly, Y.; Rozen, S. O*rganic Letters* 2**012,** *14,* 1114; (d) Aikawa, K.; Maruyama, K.; Nitta, J.; Hashimoto, R.; Mikami, K. O*rganic Letters* 2**016,** *18,* 3354; (e) Levin, V. V.; Zemtsov, A. A.; Struchkova, M. I.; Dilman, A. D. O*rganic Letters* 2**013,** *15,* 917; (f) Smirnov, V. O.; Maslov, A. S.; Levin, V. V.; Struchkova, M. I.; Dilman, A. D. R*uss. Chem. Bull.* 2**014,** *63,* 2564; (g) Kondratyev, N. S.; Levin, V. V.; Zemtsov, A. A.; Struchkova, M. I.; Dilman, A. D. J*ournal of Fluorine Chemistry* 2**015,** *176,* 89; (h) Levin, V. V.; Zemtsov, A. A.; Struchkova, M. I.; Dilman, A. D. J*ournal of Fluorine Chemistry* 2**015,** *171,* 97; (i) Zemtsov, A. A.; Kondratyev, N. S.; Levin, V. V.; Struchkova, M. I.; Dilman, A. D. R*uss. Chem. Bull.* 2**016,** *65,* 2760; (j) Ashirbaev, S. S.; Levin, V. V.; Struchkova, M. I.; Dilman, A. D. J*ournal of Fluorine Chemistry* 2**016,** *191,* 143; (k) Ashirbaev, S. S.; Levin, V. V.; Struchkova, M. I.; Dilman, A. D. J. *Org. Chem.* 2**018,** *83,* 478.

(269) Markovskij, L. N.; Pashinnik, V. E.; Kirsanov, A. V. S*ynthesis* 1**973,** 1*973,* 787.

(270) Sondej, S. C.; Katzenellenbogen, J. A. T*he Journal of Organic Chemistry* 1**986,** 5*1,* 3508.

(271) Xia, J.-B.; Zhu, C.; Chen, C. J*ournal of the American Chemical Society* 2**013,** 1*35,* 17494.

(272) Bloodworth, A. J.; Bowyer, K. J.; Mitchell, J. C. T*etrahedron Letters* 1**987,** 2*8,* 5347.

(273) Ashwood, M. S.; Alabaster, R. J.; Cottrell, I. F.; Cowden, C. J.; Davies, A. J.; Dolling, U. H.; Emerson, K. M.; Gibb, A. D.; Hands, D.; Wallace, D. J.; Wilson, R. D. O*rg. Process Res. Dev.* 2**004,** 8*,* 192.

(274) Merchant, R. R.; Edwards, J. T.; Qin, T.; Kruszyk, M. M.; Bi, C.; Che, G.; Bao, D.-H.; Qiao, W.; Sun, L.; Collins, M. R.; Fadeyi, O. O.; Gallego, G. M.; Mousseau, J. J.; Nuhant, P.; Baran, P. S. S*cience* 2**018.**

(275) Chen, K.; Berg, N.; Gschwind, R.; König, B. J*ournal of the American Chemical Society* 2**017,** 1*39,* 18444.

(276) (a) Guidotti, J.; Metz, F.; Tordeux, M.; Wakselman, C. S*ynlett* 2**004,** 2*004,* 1759; (b) Clavel, P.; Léger-Lambert, M. P.; Biran, C.; Serein-Spirau, F.; Bordeau, M.; Roques, N.; Marzouk, H. S*ynthesis* 1**999,** 1*999,* 829.

(277) Geri Jacob, B.; Wade Wolfe Michael, M.; Szymczak Nathaniel, K. A*ngewandte Chemie International Edition* 2**018,** 5*7,* 1381.

(278) Lochmann, L.; Trekoval, J. J*ournal of Organometallic Chemistry* 1**979,** 1*79,* 123.

(279) Algera, R. F.; Ma, Y.; Collum, D. B. J*ournal of the American Chemical Society* 2**017,** 1*39,* 7921.

(280) Yerien Damian, E.; Barata-Vallejo, S.; Postigo, A. C*hemistry – A European Journal* 2**017,** 2*3,* 14676.

(281) Rohr, A. D.; Kampf, J. W.; Ashe, A. J. O*rganometallics* 2**014,** 3*3,* 1318.

(282) Fier, P. S.; Hartwig, J. F. J*ournal of the American Chemical Society* 2**012,** 1*34,* 5524.

(283) Chen, D.; Ni, C.; Zhao, Y.; Cai, X.; Li, X.; Xiao, P.; Hu, J. A*ngewandte Chemie International Edition* 2**016,** 5*5,* 12632.